Università degli Studi di Roma
"La Sapienza"
Scuola di Ingegneria Aerospaziale

Modellazione Strutturale per l'Analisi ed il Controllo Aerotermoelastico

Structural Modeling for Aerothermoelastic Analysis and Control

Tesi di Dottorato in Ingegneria Aerospaziale

Doctoral Thesis in Aerospace Engineering

Dottorando

Candidate

Gian Mario Polli

<table>
<tr><td>Coordinatore</td><td>Relatore</td></tr>
<tr><td>Chair</td><td>Advisor</td></tr>
<tr><td>Prof. Carlo Buongiorno</td><td>Prof. Franco Mastroddi</td></tr>
</table>

Anno Accademico 2003/2004

XVII Ciclo

ἄστερες μὲν ἀμφῐ́ κάλαν Σελάνναν
ἂψ απυκρύπτοισι φάεννον εἶδος,
ὀππότα πλήθοισα μάλιστα λάμπη
γᾶν επῐ́ παῖσαν

Saffo
(fr. 4 D, 34 LP)

Aknowledgments

I entered the University with the aim at proving my worth, determined to end quickly and with the maximum grade. Obtained the title, I discovered to not know what to do with it. The idea to switch from university to industry, from study to work, without taking a rest, did not attract me so much. Thus, the suggestion of Prof. Mastroddi to try the exam for the doctoral program seemed to me the most honorable loophole. Reading these lines, Prof. Mastroddi may remain disappointed understanding how miserable were my motivations and how badly misplaced was his credit on me. Therefore, Prof. Franco Mastroddi is the first I owe to thank if I am now concluding this journey enthusiast and proud to have completed it. Always careful in going along my wishes (often difficult to be interpreted by myself too), he was the one who blew patiently on the tepid embers of my enthusiasm; thanks to his presence, constant and at the same time discreet, this three years have been of study and personal growth as in the real essence of the doctorate.

I am also indebted to Prof. Liviu Librescu, co-advisor of the thesis, for having welcome me during my stay in Blacksburg at the Virginia Tech. He was not only a good teacher, from whose teaching and collaboration I derived an important part of this thesis, but also a wonderful person who has followed and directed my activity during my stay and after my departure.

I am deeply indebted also to the other co-advisor of the thesis: Prof. Luigi Morino. Once, in occasion of one of our first meetings, he told me that he did not want to give me a fish but rather to teach me to fish. I may not say if I become a good fisher, nonetheless, now, I like very much fishing; going to fish with Prof. Morino is what taught to me to love this sport. Dear Prof. Morino, the fruit of our fishing are in these pages and it is with the greatest gratitude that I am honored to invite you to this fish dinner.

Finally, I wish to thank Prof. Alessandro Agneni, who has followed me since the times of the

master's thesis. Always ironic, but also always helpful with me and with the people closest to me, he has inspired a part of this thesis.

I would like to thank also Giuliano, trusty lunch mate, perfect scout leader for the outdoors excursions, but also careful and firm judge during the preparation of scientific presentations. Thanks to Matteo for his jokes and powerpoint presentations, and for the results of some applications obtained with him and contained in this thesis. Many thanks to Pier who helped me during my stay in Blacksurg, thanks Davo, Ilhan and Mark who helped me to utmost profit the wonderful sport grounds of Virginia Tech.

Finally, I wish to thank my family that has been always close to me and that I overlooked so much lately.

If all the people mentioned before may be considered as stars that have lightened my way in the darkest moments, or that have represented a reference point for my endeavours, now I wish to thank the one to whom this thesis is dedicated and that with her contagious enthusiasm for research and her optimism for life, has changed me so much. Thanks to lighten my way Selanna, my Moon.

Contents

29th May 2005

List of Figures

Chapter 1

Overview

1.1 Motivations

The novel technological challenges in the aerospace industry, such as, to mention a couple, morphing aircrafts and the new generation of re-usable launch vehicles, request a refinement of the available mathematical models and of the methodologies of analysis to guarantee a better predictive capability during the design phase, and, eventually, during the operative life (see for an extensive review of these problems Ref. [85]). In particular, with reference to the realization and development of shape controllable vehicles (also known as morphing aircrafts), it is apparent the necessity for the designers of mathematical models of the aircraft (meant, in the most absolute generality, as a deformable body immersed in a fluid and, thus, subject to the most different aeroelastic and aerothermoelastic interaction phenomena) that be at a time phenomenologically dependable and easy to implement, and that, therefore, guarantee a high predictive capability of all the possible configurations undertaken by the aircraft, and of the power necessary to let it undertake them by means of some actuation mechanism. As, on the other hand, the goal of these systems is the maximization of the aerodynamic efficiency, the reduction of weight and, thus, the abatement of the operative costs, morphing aircrafts will be supplied of suitable control systems that permit them to reach their goals in all the operative conditions. These control systems would be more easily implemented if a dependable mathematical model of the structure and of the aeroelastic, thermo-elastic and piezo-elastic (if this control be done by means of piezoelectric materials) interaction phenomena be available, eliminating the model uncertainties that usually pain the development of effective control systems.[†] Similar considerations are valid also with respect to the new generation of re-usable launch vehicles, where, in particular, safety reasons impose more severe design constraint, that could be better respected if efficient mathematical model, capable to predict the operative boundaries and to assure an efficient structural optimization during the design phase, would be available. Obviously, the previous considerations are common to any engineering discipline, nonetheless, it is with

---

[†] The interested reader could refer to [61] for a presentation of control theory in presence and in absence of dependable mathematical models underlying the phenomena to be controlled.

explicit reference to the aerospace field that, this thesis has the ambitious goal to face some of the problems presented. In particular, this thesis deals with the development of a mathematical model for micro-structured continuum bodies, which are the natural setting when dealing with materials having preferential directions,[§] and faces three distinct problems of aerospace interest, in the framework of the previous considerations, that are: (i) a simple microstructured piezoelectric shell model with material fibers, inclined with respect to the normal, made of piezoelectric material, immersed in a matrix, and actuated by means of a voltage, different for each fiber, applied at their edges; (ii) the aero-thermo-elastic analysis of a swept composite wing, made of pyrolitic graphite material, impacted by a laser beam; (iii) the multi-modal aeroelastic vibrations suppression of aircraft wings by means of piezo-electric devices passively shunted.

1.2   State of the Art

In order to describe the state of the art in the structural modeling of advanced aerospace applications, one would necessitate of a thesis itself. On the base of this consideration, in this section, the attention will be limited only to few papers and authors who have mostly inspired the present work, postponing a more complete reference to the existing literature, at the presentation and discussion of the various issues in the main body of the thesis.

As it was anticipated in the previous Section the thesis deals with structural modeling for the analysis and control of aerospace systems; thus, it could appear strange to quote as a first source of inspiration a paper published on 1996 with the title "Smart biological systems as models for engineered structures" (Ref.[103]). Actually, this paper provides a number of interesting examples of biological structures featuring multifunctionality, hierarchical organization and adaptability, which could be modeled (*i.e.*, mathematically represented) with some of the considerations developed in this thesis. On the other hand, engineering reproductions of these smart biological systems could be efficiently employed in the design of advanced aerospace systems. Finally, note that, among the keywords included by Srinivasan in his paper, "smart structures" and "multifunctionality" deserve a special mention, indeed, they could be easily included as keywords for a project of morphing aircrafts too.

With this goal in mind in this thesis it is developed a theory for micro-structured continuum bodies which has found a relevant source of inspiration in the papers of Naghdi (Refs. [79, 80, 50, 81]), Epstein (Ref. [36]), Simo (Refs. [97, 98, 100, 101, 102]), Rubin (Ref. [94]), and more recently Wempner (Ref. [117]) and Di Carlo et al. (Ref. [33]). All these authors have elaborated theories of shell-like and rod-like bodies which regarded them as continua with special shape and partitionability

---

[§] To mention a couple of situations where materials manifest in preferential directions, consider the case of piezoelectric materials, where the polarization direction plays a crucial role in their electro-mechanical behavior, or the case of pyrolitic graphite materials that have a direction of transverse isotropy which bestow them interesting properties in the thermal protection, for instance, of aerospace structures. Incidentally, let us observe that the previous examples have been both considered in the applications of this thesis.

and thus worthy of a special, coherent, kinematics. In particular, the work of Simo constitutes, in the author's opinion, the most comprehensive treatment of "geometrically exact" shells and rods models, because, starting from a rigorous formulation of these models (often referred to as Cosserat-type models), he arrives to a consistent implementation and numerical validation of the derived equations. This same approach, to be compared to the more classical approach, for instance, of Ciarlet (Refs. [24, 26, 25]), consisting of an asymptotic expansion of the displacement field, has been considered in the developments. In particular, this thesis presents a novel exact formulations for the equilibrium equations of a shell-like body, whose material fibers, or directors, are free to distend and rotate.[¶] The purpose of this investigation is directed towards the actuation of the thickness distension feature of piezoelectric shells for the control of the sound radiated from the surfaces of the shells themselves (Refs. [73, 74, 86, 83]). Furthermore, although the extensibility of the fibers of shells is an issue widely studied and reported (see, for instance, Refs. [79, 101, 33]), to the author's best knowledge, this problem has not yet been solved using material coordinates in the deformed configuration and using a variational approach. These isssues are important, the first for the practical utilization of the formulation, the second to insure the optimality of the model. Specifically, in the first Part of the thesis it is shown how the use of material (convected) coordinates, virtual displacements, proper internal constraints, and suitable stress resultant definitions, allows one to formulate a generalization of the Reissner-Mindlin model as a novel one that consists of the Kirchhoff-Love model plus an additional vector equation describing the difference between the two models, in particular the equilibrium equation in the fiber direction. The solution of the governing equations, in terms of integral stress resultants, in the present configuration, enables one to deal with finite deformations of the shell and to implement a control procedure for the sound radiated by the shell, using a piezoelectric actuation mechanism. Finally, it is to be emphasized that the formulation utilized facilitates the implementation in the case in which the fibers are placed in an arbitrary direction. Illustrative examples show the usefulness of the proposed approach.

Regarding the applications considered in the second part, one may observe that they find their natural setting in three different fields of the engineering community: (i) the field of electro-elastic models in continuum mechanics; (ii) aeroelasticity and aero-thermo-elasticity; (iii) smart structures and passive damping control theory.

With respect to the first field, the work of Podio-Guidugli (Refs. [83, 88]) and Vidoli (Refs. [113, 114]) represent the closest references. The latter, in particular, was the first to emphasize the importance of considering piezoelectric plate problems in which the polarization direction is not coincident with the thickness direction. In the same framework, a natural source of comparison is represented by Ref. [92]. In this paper, however, the attention is mostly directed towards the determination of the minimum number of terms needed to represent the electric potential in respect of the constitutive equations. Moreover, because the application presented in Chapter 6 is intended

---

[¶] Note that, however, drill rotations (*i.e.*, rotations about the director) are not permitted in the model being, as it was observed in Ref. [97], irrelevant in shells, in sharp contrast with the theory of rods.

to demonstrate the potentiality of the proposed model for micro-structured continua, the reader should refer to Ref. [85] for a review of the most recent advances in the aerospace field with respect, in particular, to the realization of morphing structures.

With respect to the second field, the paper of Achenbach (Ref. [13]), where a coupled thermo-elastic formulation is presented, and the works of Librescu (Refs. [66, 58, 60]), where the composite swept wing model was first developed, consitutes the pricipal source of inspiration.

Finally, with respect to the third field, the fundamental paper of N.W. Hagood and A. von Flotow [55], that has set the bases for the modeling of passively controlled structures with piezoelectric patches, deserves a special mention. Several advances have been carried out since that paper from other investigators in that field, both from an experimental and mathematical point of view. In particular, in Ref. [72], to the author's best knowledge, for the first time this passive technique has been employed to damp the aeroelastic vibrations and to enhance the aeroelastic stability. The introduction in the analysis of more modes to be controlled has led to the consideration of different multi-modal control strategies (see, for instance, Refs. [31, 118, 57, 6]), one of which is presented and discussed in Chapter 8 with reference to an aeroelastic problem.

1.3   (Micro-) Structure of the Thesis

As it was observed in the first Section, the thesis has been divided into two parts: one theoretical, the other mostly applicative. It is in this sense that one may talk of micro-structure of the thesis, prefiguring the meaning of one of the main concept faced in this work: the "micro-structure of continuum bodies". Without reporting the formal physical and mathematical definition of micro-structure within the theory of continuum mechanics, which will be introduced and discussed extensively later in the main body of the thesis, let us observe that if one thinks of the first part of the thesis as a space ("support space" using the terminology of micro-structured continuum mechanics), whereabout the main issues of "the structural modeling for aerothermoelastic analysis and control" are presented and developed (in terms of equilibrium equations and limits of validity), and to the second part as a complementary space ("fiber space" in continuum mechanics), with respect to the thesis itself (the "body" in continuum theory), where those issues are applied (integrated one should say in the theory of continuum mechanics), one gets a first perception of what it is meant for micro-structured continuum bodies. In particular, as it is apparent from these considerations the idea of micro-structure is so general that it can be applied to a variety of cases and situations that makes this treatment particularly general.

Even if the definiton of micro-structured continuum bodies suggested before is quite general, it is not so far from the physical-mathematical definition that has been introduced for the first time by Duhem (Ref.[34]), subsequentely developed by E. and F. Cosserats (Ref.[27]) in one, two and three dimensions some years later, and that was finally employed by Germain in his theory of continuum mechanics (Ref.[43]). As a partial proof of the validity and generality of the direct (micro-structure)

approach, it can be observed that this theory has stimulated the production of an extensive literature (see for instance Refs. [79, 52, 80, 97, 98, 100, 101, 102, 81, 82, 51, 94, 117, 33]), sometimes also heavily criticized (see for instance Ref. [96]). On the other hand, it should be noted that in this thesis some concepts of micro-structure theory are employed, in particular for the setting of the kinematic descriptors, without renouncing to the Cauchy's three-dimensional theory in the deduction of the balance equations. In this sense, as it was observed in the previous section, the same approach of [33] is adopted regarding rods and shells as *three-dimensional bodies with special shape and partitionability, whose deformations are restricted to be, in some precise sense, "rod-like" and "shell-like"*.

Entering in the details of the thesis, the first Part ("Micro-Structured Continua") starts with the presentation of a shell model that constitutes a point of departure for the subsequent enhancements, giving the opportunity to introduce some classical concepts and ideas that will be developed in the framework of micro-structured continuum theories and tensor analysis on manifolds. The consideration of a single-director theory[‖] (elsewhere known as first-order theory) will be an issue common to all the formulations presented; nonetheless, the formulation may be easily extended to the consideration of multi-director theories[**] (see for instance Refs. [80, 62]). Another issue, common to all the models presented, will be the derivation of the equilibrium equations from the Virtual Work Principle. Moreover, in the derivation it is shown how the use of the Virtual Work Principle, proper internal constraints, and suitable stress resultant definitions, allows one, in the framework of the Reissner-Mindlin (RM) kinematical assumptions, to reduce the system of (dynamic) equilibrium equations to one formally equivalent to that obtainable in the framework of the Kirchhoff-Love (KL) hypotheses, with three additional equations describing the equilibrium in the fiber direction. From the author's point of view this is a very important aspect; indeed, in practical applications the difference between the RM and the KL formulations is small. Thus, it is convenient to recast the RM equations into a format that emphasizes this feature. This is important not only from a conceptual point of view (to show how the RM equations reduce in the limit to the KL equations), but also from a computational point of view, because the resulting equations isolate the "big contribution" (KL, of order zero) from the "small contribution" (RM equations of order one).

This goal is achieved in all the formulations presented, by exploiting in full the potentialities of the Virtual Work approach, specifically, the arbitrariness of the virtual displacement from the deformed configuration of the shell. Indeed, the virtual displacements $\delta\mathbf{u}_{(1)}$, representing the tangential displacement on the upper and lower surfaces, even in the context of the Reissner-Mindlin hypotheses, can be expressed as the sum of the displacement due to the Kirchhoff-Love assumption and of an

---

[‖] Actually, the definition of the director associated to a continuum with micro-structure is only *in fieri* in the first approach, but it will be a relevant issue in the subsequent developments.

[**] It is worth noting that even if the so-called "higher-order theories" for rods and shells and the multi-director theories of Cosserat's bodies are, for some aspects, equivalent, nonetheless, they should be considered distinctly. Indeed, while the latter belongs to the category of *direct* theories, the first should be referred to the category of *deductive* theories (see, for instance, Ref. [33]).

29th May 2005

arbitrary additional displacement.

$$\delta\mathbf{u}_{(1)} = \delta\mathbf{u}_{(1)}\big|_{KL} + \delta\mathbf{u}_{(1)}\big|_{RM}$$

where $\delta\mathbf{u}_{(1)}\big|_{KL}$ is specified imposing the KL constraints[¶] to the motion of the director.

In particular, in Chapter 2 the shell equilibrium equations are derived from the Virtual Work Principle assuming that the position $(\mathbf{x})$ of a generic material point of the shell in a 3D Euclidean reference frame at a generic instant of time be a function of the position $(\mathbf{p})$ of the corresponding material point on the middle surface and of the distance (η), measured along the normal $(\mathbf{n})$, to the middle surface.[‡] As a matter of fact, it can be noted that the previous representation does not make use of material (or convective) coordinates. Indeed, as η is an arc-length, *i.e.*, a measure of the distance from the mid-surface, a material point, identified in a generic configuration at time (t_1) by the triple of co-ordinates $\{\xi^1, \xi^2, \eta\}$, will be identified in a different istant of time (t_2) by $\left\{\hat{\xi}^1, \hat{\xi}^2, \hat{\eta}\right\}$ (with $\xi^\alpha \neq \hat{\xi}^\alpha$ and $\eta \neq \hat{\eta}$ in general).[§] Let us note that, in the particular case of the Kirchhoff-Love model a fiber initially normal remain normal after the deformation without distension and so $\{\xi^1, \xi^2, \eta\}$ would be material coordinates. On the other hand, if the fiber elongation would be permitted, even in the framework of the first Kirchhoff-Love kinematical hypothesis, $\{\xi^1, \xi^2, \eta\}$ would not be material coordinates anymore. Indeed, a material point on the upper surface would be identified at time t_1 by $(\xi^1, \xi^2, h(\xi^1, \xi^2, t_1))$ and at time t_2 by $(\xi^1, \xi^2, h(\xi^1, \xi^2, t_2))$ being $h(\xi^1, \xi^2, t_1) \neq h(\xi^1, \xi^2, t_2)$.

To overcome the shortcomings indicated before, two other levels of approximation have been considered, but only the last is reported in this thesis.[‖] In particular, as an intermediate step, the following representation of the shell geometry has been considered

$$\mathbf{x}\left(\xi^1, \xi^2, \zeta, t\right) = \mathbf{p}\left(\xi^1, \xi^2, t\right) + \zeta\, h\left(\xi^1, \xi^2, t\right)\, \mathbf{n}\left(\xi^1, \xi^2, t\right) \qquad \zeta \in [-1, 1]$$

where $\mathbf{p}$ is a map representing the mid-surface, $\mathbf{n}$ is the normal to the mid-surface in the point of coordinates $\{\xi^1, \xi^2\}$, finally, ζ, replacing η, is a measure of the distance from the mid-surface

---

[¶] Classically (see for instance Ref. [106]) the KL constraints are identified by the two following conditions:

(*i*) Points [..] lying initially on a normal-to-the-middle plane [..] remain on the normal-to-the-middle surface after deformation.

(*ii*) The normal stresses in the direction transverse to the plate can be disregarded.

Nonetheless, in order to retain this decomposition of the virtual displacements also in the new formulations presented, a revised version of the previous constraints will be introduced and will be discussed in the following chapters.

[‡] To measure, the importance and actuality of the formulation presented, especially with regard to the computational efficiency, the reader is referred to Ref. [63] that constitutes a very recent apport to the finite element modeling of shell, starting from the consideration of classical shell theory.

[§] What the author is meaining, in other terms, is that the normal does not remain normal during the motion; thus, the material points lying on the normal to the mid-surface at (ξ^1, ξ^2) at a certain time, will be crossed by another normal (*i.e.*, a normal originated by another point on the mid-surface) in an other istant of time.

[‖] A complete record of all the developments considered is contained in Ref. [90] using a tensorially invariant approach, whereas in the present thesis also a co-ordinate free (or absolute) notation is employed.

parametrized with respect to the current thickness (h) of the shell. This formulation is characterized by the fact that, in the framework of the KL model (not within the more general RM kinematical hypotheses), $\{\xi^\alpha, \zeta\}$ are material co-ordinates (and the upper and lower surfaces are co-ordinate surfaces) even if the shell experiences thickness stretching.

The last step in the present derivation is the consideration of the following map for the representation of the shell geometry

$$\mathbf{x}\left(\xi^1, \xi^2, \zeta, t\right) = \mathbf{p}\left(\xi^1, \xi^2, t\right) + \zeta\,\mathbf{q}\left(\xi^1, \xi^2, t\right) = \mathbf{p}\left(\xi^1, \xi^2, t\right) + \zeta\,\hbar\left(\xi^1, \xi^2, t\right)\,\mathbf{m}\left(\xi^1, \xi^2, t\right)$$

where $\mathbf{q}$ is the director, *i.e.*, a deformable vector field attached to every point of the material surface (see Ref. [50]), whose current length is $\hbar$ (distinct from the current thickness h) and whose associated unit vector is $\mathbf{m}$. With the previous representation map any deformation of the body is exactly accomplished in the KL and in the RM framework.[‡‡] Nonetheless, it should be observed that, although the previous representation is always valid for a shell-like structure in its reference (undeformed) configuration (or, in a certain instant of time $\hat{t}$), it restricts the material fiber of the shell to remain straight. Even if characterized by this limitation, this model enables one to deal with finite deformations, whereas the use of material convected coordinates is particularly indicated for the solution of dynamical problems, for example, by means of a incremental numerical approach (see Ref.[75, 76, 64, 97, 98]).

In an attempt to simplify the equilibrium equations, and their derivation from the Virtual Work Principle, three distinct approaches in the development of the present model for thin shells are followed.[†] These approaches have been identified by the following acronyms (borrowed from Ref. [97]):

1. SNF = Surface Natural Frame

2. SMF = Surface Mixed Frame

3. SCF = Surface Convected frame

[‡‡] It is now opportune to report an extract of a review paper on shells, written by Prof. Simmonds (Ref. [96]), that constitutes one of the most significative attacks to Cosserat theories in the current literature. In his critical review of shells' theory Simmonds questions: *Cosserat Theory. Who need it? I defy anyone to show me a physical phenomenon in shells which cannot be explained in a simpler, more straight-forward way by conventional shell theory (properly formulated and properly applied).* And later *Why introduce surface or shell coordinates unnecessarily? The reference configuration of a general shell can be described simply as a 1-parameter family of smooth, non-intersecting surfaces, characterized by a (thickness-like) parameter L, (a foliation). Thus, we may visualize a shell in its reference configuration as looking like a curved cake, made of layers of different ingredients of variable thicknesses.* We do not need to answer to Simmonds in defense of a formulation that has been applied several times in the past, nonetheless, we would like to point out that, at least for the analysis of a piezoelectric shell with material fiber inclined with respect to the normal, considered in the applications, the Cosserat model represents the most natural framework.

[†] In which sense the shell must be considered thin will be clarified later, for the moment observe that the present modeling is limited to one-director Cosserat surfaces, thus the it is assumed that the relative deformations of the layers are linear with respect to the deformations of the surface.

29th May 2005

The first approach consists in the projection of the virtual displacement on the surface natural frame which is a local frame (*i.e.*, a frame associated to each material point on the mid-surface) composed of the tangential vectors to the material lines on the mid-surface (in general not orthogonal to each other), and of the normal to the mid-surface. This approach is apparently the most natural yielding to the simplest system of equilibrium equations in the framework of RM kinematical hypotheses. On the other hand, it will be shown that the consideration of a revised version of the KL material constraint (*i.e.*, no shear is permitted along the material fiber (or director) and the fiber does not stretch), complicates so much the formulation and the expression of the final equilibrium equations, that another approach to follow seems mandatory. The second approach serves, indeed, to overcome these difficulties. In particular, in this case the virtual displacement are still projected along the surface natural frame, but the displacement in the normal direction is then expressed as a combination of the displacement along the fiber direction and of the in-plane displacement. In this case it will be shown that the equilibrium equations in the RM hypotheses are very complicated, but they simplify substantially when the revised KL constraints are introduced. Finally, the third approach starts directly with the decomposition of the virtual displacements (and of the gradient) in the fiber direction and in the in-plane direction. This approach, in particular, makes use of the layer basis vectors (covariant and contravariant) evaluated on the mid-surface (*i.e.*, for $\zeta = 0$), besides, as the contravariant vectors $\overset{\circ}{\mathbf{g}}{}^{1}$ and $\overset{\circ}{\mathbf{g}}{}^{2}$ identifies a plane orthogonal to the fiber $\mathbf{g}_3$, they represent the natural frame for the derivation of the equilibrium equations when the revised KL constraints are considered. In particular, the final expression of the equilibrium equations, their derivation and the relation between the resultant shear terms[§] will be put in comparison with those obtainable in the simplest classical case considered in Chapter 2, and, at this regard, it will be shown that the third approach is the one that best fits the consideration of the classical model both in the RM and the revised KL frameworks.

The analysis will be carried out starting with the consideration of the displacement gradient in the three approaches, then the equilibrium equations for the RM and for the revised KL model will be obtained. A different, but equivalent, approach will also presented in the appendix. We have called it the divergence approach, to be compared to the gradient approach chosen in the main body of the thesis. In particular in the appendix it will be shown that the two approaches for the derivation of the equilibrium equations from the Virtual Work Principle are completely equivalent.

*   *   *

Going to the second Part of the thesis (the so-called "fiber-space" or space for applications), it can be observed that it is mainly composed of applications useful to illustrate and apply some of the concepts developed in the first Part, and to face problems of interest for the aerospace field. In particular, three different problems have been considered: (i) the case of a microstructured

---

[§] It is worth recalling that in the classical KL model the shear terms can be let vanish in the equilibrium equations. This property is still valid also in the refined models here presented, however, according to the approach employed, the relation that permit them to vanish can be more or less intricate.

piezoelectric shell with material fibers, inclined with respect to the normal, made of piezoelectric material, immersed in a matrix, and actuated by means of a voltage, different for each fiber, applied at their edges; (ii) the aero-thermo-elastic analysis of a swept composite wing impacted by a laser beam; (iii) the multi-modal aeroelastic vibrations suppression of aircraft wings by means of piezoelectric devices passively shunted.

In particular, the first application is directed to the implementation of the shell's equilibrium equations, assuming that the co-ordinate ξ^2 is immaterial, in the sense that the external loads, the boundary conditions, the constitutive relations, and, thus, the equilibrium equations do not depend on this in-plane co-ordinate. Obviously, this assumption is made in order to simplify the formulation. The main characteristic of this problem is, however, the consideration of a special material assumption. Indeed, it will be assumed that the material fiber, in terms of which the geometry of the shell is described, are made of piezoelectric material polarized in the fiber direction. Moreover, consistently with the derivation of the first part of the thesis, it will be assumed that these fiber be inclined with respect to the normal and actuated, exploiting the electro-strictive effect (or converse piezoelectric effect), by means of the application of a voltage at the edges of each fiber. The problem will be solved numerically using a finite difference procedure applied to the equilibrium equations in terms of displacements. A complete derivation of the equilibrium equations in terms of displacements will be also reported with reference to this particular problem.

The second application presented regards the analysis of the aero-thermo-elastic response of an aircraft swept wing impacted by a laser beam. In particular, the equilibrium equations for the wing structure will be derived from the Virtual Work Principle modelling the wing as a plate-like body with appropriate internal constraints, and including warping effects, in the hypothesis of linearized kinematics and small displacements from a reference configuration. As a matter of fact, observe that this model was first introduced by Librescu in Ref. [66] and subsequently developed in Refs. [104, 60, 47] for the aeroelastic tailoring of aircraft swept wings. Moreover, a closed form solution will be found for the aeroelastic response of the wing, exposed to a time-dependent thermal field. The thermal field will be supposed generated by a laser beam impacting the upper surface of the wing, and, within this context, an uncoupled thermo-elastic model will be adopted. In particular, the expression of the thermal field, acting on the system as an external input, will be obtained using the Green's function method performed for the particular case under consideration. Moreover, it will be shown, as this excitation may be described as dependent on the internal status of the system (*i.e.*, the Lagrangean variables chosen for the model) in an equivalent way to what is normally done in aeroelasticity to model the aerodynamic feedback from the elastic variables. Although considered in a linearized context, the structural model of the wing will incorporate several non-classical effect such as the transverse shear effects, the anisotropy of the constituent materials, as well as the sweep angle. For computational purposes, and towards highlighting the effects of a number of physical and geometrical parameters, the case of a rectangular single-layered swept wing composed of a transversely isotropic material will be considered. Having in view its exceptional features in

the thermal protection of aerospace structures[38, 84], the pyrolitic graphite, that features thermo-mechanical transversely isotropic properties, will be considered. Moreover, it will be supposed that the wing is immersed in a subsonic incompressible flow whose speed is below the flutter critical speed of the system. Finally, the solution of the problem will be obtained analytically in a double Laplace transform domain, where both the space and time co-ordinates are converted to their Laplace variable space counterparts. Within this approach, the problem will be reduced to the solution of an algebraic problem in the transformed kinematical unknowns.

The third problem regards the implementation of a passive technique for the suppression of aeroelastic vibrations. In particular, this problem will be presented with respect to a multi-modal passive piezoelectric approach consisting in shunting the piezoelectric patches, bonded to the structure, to an electrical circuit tuned on the aeroelastic frequency of vibrations. This will be done with respect to any flight condition,¶ enabling one to damp the aeroelastic response in all the flight range and, eventually, to increase the flutter stability margin. The point of view adopted is substantially systematic, in the sense that the piezoelectric coupling will be integrated in a state-space representation of the aeroelastic system (constructed on the basis of the approximated natural modes of the structure) without entering in the details of the structural model and of the finite element procedure employed to arrive at the state-space representation. Nonetheless, it is worth noting that this technique is quite general being applicable to any type of structure experiencing a fluid-structure interaction phenomenon unless a suitable number of piezoelectric patches are bonded to the structure itself and are shunted by an electrical circuit. Finally, note that the state-space representation, in terms of the modal co-ordinates, permits to recognize a number of coupling effects between the structural, aerodynamical, and piezoelectrical degrees of freedom, and, in particular, to analyze how the vibration energy flows in the piezoelectric systems, and how the aeroelastic systems evolve under the effect of the piezoelectric coupling.

At conclusion of this introduction, it is worth noting that each of the applications presented is characterized by a high degree of multidisciplinarity. Indeed, all the applications deal with the interaction of a structural system (solid mechanics) with non-stationary aerodynamics (fluid-structure interaction) and in presence of electrical loads (active/passive piezoelectricity) or thermal loads (thermoelasticity). It is also worth noting that, for the sake of simplicity, both the electro-elastic and the thermo-elastic coupling have been limited to be unidirectional. Indeed, it has been assumed that the electrical field, in one case, and the thermal field, in the other case, are completely assigned by the (electrical and thermal) boundary conditions and are not dependent on the current deformation of the body. In particular, with respect to the piezoelectric coupling, it is apparent that this is a very strong and restrictive assumption because it excludes *a priori* the induced potential in the formulation of the problem. Indeed, as it is reported in Ref. [92] *when both mechanical and electrical loads are applied to the piezoelectric plate, it is thought that a more complicated variation*

¶ In particular, in the numerical simulations the flight speed, flight Mach number and flight altitude will be varied.

of the electric potential through the thickness would enhance the electro-mechanical coupling . As a matter of fact, let us observe that the consideration of the induced potential for the derivation of refined models of piezoelectric plates and shells has been extensively studied in the current literature but yet a tangible estimate of its importance has not been found. The interested reader could refer to the following papers for a review of the state of the art in this field [40, 39, 91, 83, 88, 92]. On the other hand, the negligence of the effect of the current deformation on the temperature field, even if considered in the theoretical developments of the second application, is traditionally assumed in the current literature (see for instance Ref.[17]). However, it deserves to be mentioned the case of a thermoelastic problem where the bi-directional coupling has been considered (Ref.[13]), and that has inspired the formulation, and the solution, of the problem presented in Chapter 7.

Part I

Micro-Structured Continua

Chapter 2

A point of departure

Following the example of Marsden in Ref.[69], the first part of this thesis starts with an introductory chapter, providing a quick survey of a few standard topics in shell theory, from a classical point of view. Similarly to Ref. [69], one of the first tasks faced in the following chapters is to repeat this material in the framework of tensor analysis on manifolds with reference to micro-structured continuum bodies. Moreover, the basic idea, underlying the formal decomposition of the problem in Kirchhoff-Love + Reissner-Mindlin (see Section 1.3), is here for the first time introduced and employed to derive the equilibrium equations and the related boundary conditions. However, in the present chapter the formulation is limited to the consideration of the proper kinematical hypotheses underlying the Kirchhoff-Love and Reissner-Mindlin models, whereas in the following chapters this approach will be extended to the consideration of a revised version of the hypotheses underlying these models. Furthermore, whilst in the present chapter the derivation of the equilibrium equations from the Virtual Work Principle starts with an appropriate expression of the divergence of the stress tensor, in the following the analysis will adopt another point of view emphasizing the role of the gradient of the virtual displacement field (see Appendix B for a comparison of the two approaches). Finally, let us observe that, although the following chapters contain some dependence on the present one, the reader with a background on shell theory may read it rapidly and go forward to the following ones.

2.1   Introduction

In this chapter the equilibrium equations of a thin shell are derived from the Principle of Virtual Work. The starting idea is to represent the geometry of the shell in the present (deformed) configuration at time t by the following decomposition:

$$\mathbf{x}\left(\xi^1, \xi^2, \eta, t\right) = \mathbf{p}\left(\xi^1, \xi^2, t\right) + \eta\,\mathbf{n}\left(\xi^1, \xi^2, t\right) \tag{2.1}$$

The previous equation states that the position $(\mathbf{x})$ of a generic material point (ξ^1, ξ^2, η, t) of the shell in a 3D Euclidean reference frame at the time t is a function of the position $(\mathbf{p})$ of the corresponding material point on the middle surface and of the distance (η), measured along the normal $(\mathbf{n})$, to the middle surface.

It is worth noting that the previous representation does not make use of material or convective coordinates, but it is performed at each instant of time. Indeed, as η is an arc-length, that is a measure of the distance along the normal to the middle surface, a material point identified in a generic configuration at time (t_1) by (ξ^1, ξ^2, η) will be identified in a different instant of time (t_2) by $\left(\hat{\xi}^1, \hat{\xi}^2, \hat{\eta}\right)$. Let us note that, in the particular case of the Kirchhoff-Love model a fiber initially normal remain normal after the deformation without distension and so (ξ^1, ξ^2, η) would be material coordinates. If the fiber elongation would be permitted, even in the frame of other Kirchhoff-Love assumptions, the previuos one would not be material coordinates anymore, indeed, a material point on the upper surface would be identified at time t_1 by $(\xi^1, \xi^2, h(\xi^1, \xi^2, t_1))$ and at time t_2 by $(\xi^1, \xi^2, h(\xi^1, \xi^2, t_2))$ being $h(\xi^1, \xi^2, t_1) \neq h(\xi^1, \xi^2, t_2)$. Moreover, note that the upper and lower surfaces are not coordinate surfaces being the thickness variable along the middle surface (*i.e.*, $h = h(\xi^1, \xi^2, t)$), whereas, in the new formulation in which η is replaced by ζ, and which is presented and discussed in the succeeding chapters, the upper and lower surfaces are coordinate surfaces. Finally, note that if the material points in the layer would be mapped by a vector $\mathbf{m}$ $(\mathbf{m} = \mathbf{m}(\xi^1, \xi^2, t) = \mathbf{n} + \mathbf{l})$ instead of by the normal in a generic instant of time, the coordinates ξ^1, ξ^2, η would be material coordinates within both the assumptions of the Kirchhoff-Love and Reissner-Mindlin models provided that no fiber elongation be permitted.

2.2   Surface geometry

Let the geometry of a surface $\mathcal{S}$ be described by:

$$\mathbf{x} = \mathbf{p}\left(\xi^1, \xi^2\right) \tag{2.2}$$

The covariant base vectors on $\mathcal{S}$ are defined by[†]

$$\mathbf{a}_\alpha := \frac{\partial \mathbf{p}}{\partial \xi^\alpha} \tag{2.3}$$

Their derivative is given by (first Weingarten and Gauss formula, see [53], p. 37, Eq. 1.13.47.a):

$$\frac{\partial \mathbf{a}_\alpha}{\partial \xi^\beta} = \frac{\partial^2 \mathbf{p}}{\partial \xi^\alpha \partial \xi^\beta} = \Gamma^\gamma_{\alpha\beta}\, \mathbf{a}_\gamma + b_{\alpha\beta}\, \mathbf{n} \tag{2.4}$$

[†] Henceforth, Greek indices span from 1 to 2, Latin indices span from 1 to 3. Also the Einstein convention on repeated indices is adopted.

where, by definition, the surface Christoffel symbols $\Gamma^\gamma_{\alpha\beta}$ are given by:

$$\Gamma^\gamma_{\alpha\beta} := \frac{\partial^2 \mathbf{p}}{\partial \xi^\alpha \partial \xi^\beta} \cdot \mathbf{a}^\gamma \qquad (2.5)$$

and the covariant components of the second metric tensor:

$$b_{\alpha\beta} := \frac{\partial^2 \mathbf{p}}{\partial \xi^\alpha \partial \xi^\beta} \cdot \mathbf{n} \qquad (2.6)$$

Let $\mathbf{n}$ be the surface unit normal. Hence, $\mathbf{n} \cdot \mathbf{a}_\beta = 0, \quad \mathbf{n} \cdot \mathbf{n} = 1$. Differentiating these with respect to ξ^α one obtains

$$\frac{\partial \mathbf{n}}{\partial \xi^\alpha} \cdot \mathbf{a}_\beta = -\mathbf{n} \cdot \frac{\partial \mathbf{a}_\beta}{\partial \xi^\alpha} = -b_{\alpha\beta} \qquad (2.7)$$

and

$$\frac{\partial \mathbf{n}}{\partial \xi^\alpha} \cdot \mathbf{n} = 0 \qquad (2.8)$$

Hence (second formula of Weingarten and Gauss, [53], p. 37, Eq. 1.13.47.c):

$$\frac{\partial \mathbf{n}}{\partial \xi^\alpha} = -b_{\alpha\beta}\mathbf{a}^\beta = -b^\beta_\alpha \mathbf{a}_\beta \qquad (2.9)$$

Also recall that the contravariant base vectors $\mathbf{a}^\beta$ are defined by

$$\mathbf{a}_\alpha \cdot \mathbf{a}^\beta = \delta^\beta_\alpha \qquad (2.10)$$

and

$$\mathbf{a}^\beta \cdot \mathbf{n} = 0 \qquad (2.11)$$

Hence one has

$$\mathbf{a}^1 = \frac{\mathbf{a}_2 \times \mathbf{n}}{\sqrt{a}} \qquad (2.12)$$

$$\mathbf{a}^2 = \frac{\mathbf{n} \times \mathbf{a}_1}{\sqrt{a}} \qquad (2.13)$$

$$\mathbf{n} = \frac{\mathbf{a}_1 \times \mathbf{a}_2}{\sqrt{a}} \qquad (2.14)$$

where

$$\sqrt{a} = \mathbf{a}_1 \times \mathbf{a}_2 \cdot \mathbf{n} = \|\mathbf{a}_1 \times \mathbf{a}_2\| \qquad (2.15)$$

2.2.1 Layer geometry

Let us consider a layer of non-uniform thickness $h = h\left(\xi^1, \xi^2\right)$. Let its geometry be defined by:

$$\mathbf{x} = \mathbf{p}\left(\xi^1, \xi^2\right) + \eta \, \mathbf{n}\left(\xi^1, \xi^2\right) =: \hat{\mathbf{x}}\left(\xi^1, \xi^2, \eta\right) \qquad [\eta \in (-h, h)] \qquad (2.16)$$

One identifies ξ^3 with η. This is usual in the classical approach (see for instance [53], p. 373). Hence the layer base vectors are defined by

$$\mathbf{g}_\alpha := \frac{\partial \hat{\mathbf{x}}}{\partial \xi^\alpha} = \frac{\partial \mathbf{p}}{\partial \xi^\alpha} + \eta \, \frac{\partial \mathbf{n}}{\partial \xi^\alpha} = \left(\delta_\alpha^\beta - \eta \, b_\alpha^\beta\right) \mathbf{a}_\beta \qquad (2.17)$$

Also,

$$\mathbf{g}_3 := \frac{\partial \hat{\mathbf{x}}}{\partial \eta} = \mathbf{n} \qquad (2.18)$$

Note that

$$\mathbf{g}_\alpha \cdot \mathbf{g}_3 = 0 \qquad\qquad \mathbf{g}_3 \cdot \mathbf{g}_3 = 1 \qquad (2.19)$$

For further utilization it is convenient to express the layer base vectors $\mathbf{g}_1$, $\mathbf{g}_2$, $\mathbf{g}_3$ in terms of the surface base vectors $\mathbf{a}_1$, $\mathbf{a}_2$, $\mathbf{n}$, as:

$$\mathbf{g}_k = \mathcal{T}_k^\beta \, \mathbf{a}_\beta + \mathcal{T}_k^3 \, \mathbf{n} \qquad (2.20)$$

where, using Eqs. (2.17), (2.18) and (2.19), one has

$$\mathcal{T}_\alpha^\beta := \mathbf{g}_\alpha \cdot \mathbf{a}^\beta = \delta_\alpha^\beta - \eta \, b_\alpha^\beta \qquad (2.21)$$

$$\mathcal{T}_\alpha^3 := \mathbf{g}_\alpha \cdot \mathbf{n} = 0 \qquad (2.22)$$

$$\mathcal{T}_3^\alpha := \mathbf{g}_3 \cdot \mathbf{a}_\alpha = 0 \qquad (2.23)$$

$$\mathcal{T}_3^3 := \mathbf{g}_3 \cdot \mathbf{n} = 1 \qquad (2.24)$$

Also recall that the contravariant base vectors are defined by

$$\mathbf{g}_h \cdot \mathbf{g}^k = \delta_h^k \qquad (2.25)$$

i.e.,

$$\mathbf{g}^1 = \frac{\mathbf{g}_2 \times \mathbf{g}_3}{\sqrt{g}} \tag{2.26}$$

$$\mathbf{g}^2 = \frac{\mathbf{g}_3 \times \mathbf{g}_1}{\sqrt{g}} \tag{2.27}$$

$$\mathbf{g}^3 = \frac{\mathbf{g}_1 \times \mathbf{g}_2}{\sqrt{g}} \tag{2.28}$$

with

$$\sqrt{g} = \mathbf{g}_1 \times \mathbf{g}_2 \cdot \mathbf{g}_3 \tag{2.29}$$

2.2.2   Upper and lower surface geometry

The upper (or lower) surface $\mathcal{S}^{(u)}$ is given by the mapping

$$\mathbf{x} = \mathbf{x}^{(u)} \left(\xi^1, \xi^2 \right) := \hat{\mathbf{x}} \left(\xi^1, \xi^2, \eta^{(u)} \left(\xi^1, \xi^2 \right) \right) \tag{2.30}$$

where the superscript (u) stands for upper. Since $\eta^{(u)}$ is not constant (but function of ξ^1 and ξ^2) the upper surface is not a coordinate-surface. The base vectors on the upper surface are given by

$$\mathbf{a}_\alpha^{(u)} = \frac{\partial \mathbf{x}^{(u)}}{\partial \xi^\alpha} = \frac{\partial \mathbf{x}}{\partial \xi^\alpha} + \frac{\partial \mathbf{x}}{\partial \eta^{(u)}} \frac{\partial \eta^{(u)}}{\partial \xi^\alpha} = \mathbf{g}_\alpha^{(u)} + \eta_{/\alpha}^{(u)} \mathbf{g}_3 \tag{2.31}$$

where

$$\eta_{/\alpha}^{(u)} = \frac{\partial \eta^{(u)}}{\partial \xi^\alpha}. \tag{2.32}$$

The metric tensor on $\mathcal{S}^{(u)}$ is given by (see Eq. (2.19))

$$a_{\alpha\beta}^{(u)} = \mathbf{a}_\alpha^{(u)} \cdot \mathbf{a}_\beta^{(u)} = g_{\alpha\beta}^{(u)} + \eta_{/\alpha}^{(u)} \, \eta_{/\beta}^{(u)} \tag{2.33}$$

The area of an outer-surface element, $dS^{(u)}$, is given by

$$dS^{(u)} = \| d\xi^1 \mathbf{a}_1^{(u)} \times d\xi^2 \mathbf{a}_2^{(u)} \| = \sqrt{a^{(u)}} \, d\xi^1 \, d\xi^2 \tag{2.34}$$

with

$$a^{(u)} = \| \mathbf{a}_1^{(u)} \times \mathbf{a}_2^{(u)} \|^2 = \| a_{\alpha\beta}^{(u)} \| \tag{2.35}$$

The unit normal to the upper surface is defined by

$$\mathbf{n}^{(u)} = \frac{\mathbf{a}_1^{(u)} \times \mathbf{a}_2^{(u)}}{\|\mathbf{a}_1^{(u)} \times \mathbf{a}_2^{(u)}\|} = \frac{\mathbf{a}_1^{(u)} \times \mathbf{a}_2^{(u)}}{\sqrt{a^{(u)}}} \tag{2.36}$$

Using Eq. (2.31) and Eq. (2.26) yields

$$\mathbf{a}_1^{(u)} \times \mathbf{a}_2^{(u)} = \left(\mathbf{g}_1^{(u)} + \eta_{/1}^{(u)} \mathbf{g}_3 \right) \times \left(\mathbf{g}_2^{(u)} + \eta_{/2}^{(u)} \mathbf{g}_3 \right) = \sqrt{g^{(u)}} \left(\mathbf{g}^{3(u)} - \eta_{/\alpha}^{(u)} \mathbf{g}^{\alpha(u)} \right) \tag{2.37}$$

Thus, the outwardly directed normal to $\mathcal{S}^{(u)}$ is given by

$$\mathbf{n}^{(u)} = \sqrt{\frac{g^{(u)}}{a^{(u)}}} \left(\mathbf{g}^{3(u)} - \eta_{/\alpha}^{(u)} \mathbf{g}^{\alpha(u)} \right). \tag{2.38}$$

or

$$n_\alpha^{(u)} = -\eta_{/\alpha}^{(u)} \sqrt{\frac{g^{(u)}}{a^{(u)}}} \qquad\qquad n_3^{(u)} = \sqrt{\frac{g^{(u)}}{a^{(u)}}} \tag{2.39}$$

Equations (2.30)-(2.39) with superscript (l) instead of (u) hold for the lower surface except for a change in sign for $\mathbf{n}^{(l)}$ which is defined to be also outwardly directed

$$\mathbf{n}^{(l)} = -\frac{\mathbf{a}_1^{(l)} \times \mathbf{a}_2^{(l)}}{\sqrt{a^{(l)}}} = -\sqrt{\frac{g^{(l)}}{a^{(l)}}} \left(\mathbf{g}^{3(l)} - \eta_{/\alpha}^{(l)} \mathbf{g}^{\alpha(l)} \right) \tag{2.40}$$

or

$$n_\alpha^{(l)} = \eta_{/\alpha}^{(l)} \sqrt{\frac{g^{(l)}}{a^{(l)}}} \qquad\qquad n_3^{(l)} = -\sqrt{\frac{g^{(l)}}{a^{(l)}}} \tag{2.41}$$

2.2.3 Lateral surface geometry

Let $\xi^\alpha = \xi^\alpha(\gamma)$ describe the boundary contour of $\mathcal{S}$ (covered counter clockwise with respect to $\mathbf{n}$ for increasing γ) with γ being an arclength. Moreover, assume that the lateral surface $\mathcal{S}_C$ of the shell is given in the form

$$\mathbf{x} = \mathbf{x}_C(\gamma, \eta) := \hat{\mathbf{x}}[\xi^\alpha(\gamma), \eta] = \mathbf{p}[\xi^\alpha(\gamma)] + \eta\, \mathbf{n}[\xi^\alpha(\gamma)] \tag{2.42}$$

in other words surface $\mathcal{S}_C$ is composed of lines normal to $\mathcal{S}$.

Note that γ is an arclength only for $\eta = 0$. Thus, the base vectors are

$$\frac{\partial \mathbf{x}_C}{\partial \gamma} = \frac{\partial \mathbf{x}}{\partial \xi^\alpha} \frac{d\xi^\alpha}{d\gamma} = t^\alpha \mathbf{g}_\alpha = \mathbf{t} \tag{2.43}$$

$$\frac{\partial \mathbf{x}_C}{\partial \eta} = \mathbf{n} \tag{2.44}$$

with $t^\alpha = d\xi^\alpha/d\gamma$ and $\mathbf{t} = t^\alpha \mathbf{g}_\alpha$ tangent to the curve $\mathbf{x}(\gamma) = \mathbf{x}(\xi^1(\gamma), \xi^2(\gamma), \eta)$. Note that t^α is independent of η but $\mathbf{t}$ is a unit vector only for $\eta = 0$.

The outward unit normal to the lateral surface is

$$\mathbf{n}_C = \frac{1}{\sqrt{a_C}} \frac{\partial \mathbf{x}_C}{\partial \gamma} \times \frac{\partial \mathbf{x}_C}{\partial \eta} = \frac{1}{\sqrt{a_C}} \mathbf{t} \times \mathbf{n} = \frac{1}{\sqrt{a_C}} t^\gamma \mathbf{g}_\gamma \times \mathbf{n} \tag{2.45}$$

with

$$\sqrt{a_C} = \left\| \mathbf{t} \times \mathbf{n} \right\|. \tag{2.46}$$

Note that $a_C = 1$ for $\eta = 0$.

For later reference, let us introduce the vector $\boldsymbol{\nu} = \sqrt{a/g} \, \mathbf{t} \times \mathbf{n} = \sqrt{a/g} \, \sqrt{a_C} \, \mathbf{n}_C$. Note that $\boldsymbol{\nu} \cdot \mathbf{n} = 0$. Hence $\boldsymbol{\nu} = \nu^\alpha \mathbf{g}_\alpha$ with

$$\nu_\alpha = \boldsymbol{\nu} \cdot \mathbf{g}_\alpha = \sqrt{\frac{a}{g}} \, t^\beta \, \mathbf{g}_\beta \times \mathbf{n} \cdot \mathbf{g}_\alpha = \sqrt{\frac{a}{g}} t^\beta \, \mathbf{g}_\alpha \times \mathbf{g}_\beta \cdot \mathbf{n} = \begin{cases} \sqrt{a} \, t^2 & \text{for} \quad \alpha = 1 \\ -\sqrt{a} \, t^1 & \text{for} \quad \alpha = 2 \end{cases} \tag{2.47}$$

Note that ν_α are independent of η, whereas $\boldsymbol{\nu}$ is a function of η. Again, $\boldsymbol{\nu}$ is a unit vector for $\eta = 0$, and coincides with $\mathbf{n}_C$.

2.3 Virtual work for a shell

In this section the equilibrium equations of a shell[†] are developed starting from the virtual work theorem in the form

$$-\iiint_\mathcal{V} \mathbf{T} : \delta\mathbf{E} \, d\mathcal{V} + \iiint_\mathcal{V} \mathbf{f} \cdot \delta\mathbf{u} \, d\mathcal{V} + \oiint_\mathcal{S} \mathbf{t}_A \cdot \delta\mathbf{u} \, d\mathcal{S} = 0 \tag{2.48}$$

where $\mathbf{t}_A$ is the applied external surface force, $\mathbf{f}$ is the external volume force, and $\delta\mathbf{u}$ is a virtual displacement compatible with the geometric boundary conditions, whereas $\delta\mathbf{E}$ has components

$$\delta\varepsilon_{ij} = \frac{1}{2} \left(\delta u_{i/j} + \delta u_{j/i} \right) \tag{2.49}$$

Recalling that $\mathbf{T}$ is symmetric, Eq. (2.48) can be rewritten as

$$\delta W = \iiint_\mathcal{V} \left(\text{Div}\,\mathbf{T} + \mathbf{f} \right) \cdot \delta\mathbf{u} \, d\mathcal{V} + \oiint_\mathcal{S} \left(\mathbf{t}_A - \mathbf{t} \right) \cdot \delta\mathbf{u} \, d\mathcal{S} = 0 \tag{2.50}$$

where $\mathbf{t} = \mathbf{T}\mathbf{n}$.

In the following it will be useful to set $S = S_U \bigcup S_L \bigcup S_C$ (see Fig. (2.1)), and treat separately the

---

[†] Note that, in Eq. (2.48), the inertial forces have been neglected. Nonetheless, they could be included, via d'Alembert principle, substituting $\mathbf{f}$ with $\mathbf{f} - \rho\,\mathbf{a}$, where ρ is the volume mass density and $\mathbf{a}$ the material acceleration.
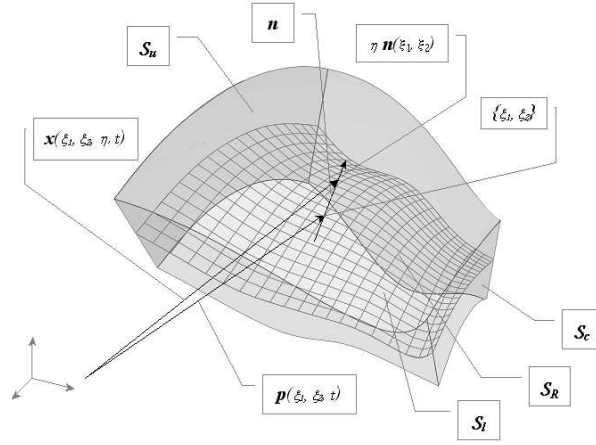
Figure 2.1: Geometry of the shell in the deformed configuration.

contributions from $S_U \bigcup S_L$ and S_C:

$$\oiint_{\mathcal{S}} (\mathbf{t}_A - \mathbf{t}) \cdot \delta \mathbf{u} \, d\mathcal{S} = \iint_{S_U \bigcup S_L} (\mathbf{t}_A - \mathbf{t}) \cdot \delta \mathbf{u} \, d\mathcal{S} + \iint_{S_C} (\mathbf{t}_A - \mathbf{t}) \cdot \delta \mathbf{u} \, d\mathcal{S} \qquad (2.51)$$

2.3.1   Virtual displacement

In this work the formulation for the shell is obtained from the only assumption that the virtual displacement is of the form (see Eqs. (2.16) and (2.18))

$$\delta \mathbf{u} = \delta \mathbf{p} + \eta \; \delta \mathbf{g}_3 \qquad (2.52)$$

Note that initially one should not assume $\delta \mathbf{g}_3$ to be such that $\mathbf{g}_3$ remains normal to the midsurface $\mathcal{S}_M$. Thus, the present formulation implies only that the material lines along the normal remain straight; however they do not remain normal, nor does the thickness remain constant.

It is convenient to express $\delta \mathbf{u}$ as

$$\delta \mathbf{u} = \delta v_\alpha \; \mathbf{a}^\alpha + \delta w \; \mathbf{n} + \eta \; (\delta \theta_\alpha \; \mathbf{a}^\alpha + \delta \kappa \; \mathbf{n}) \qquad (2.53)$$

where

$$\delta v_\alpha = \delta \mathbf{p} \cdot \mathbf{a}_\alpha \qquad (2.54)$$

$$\delta w \; = \delta \mathbf{p} \cdot \mathbf{n} \qquad (2.55)$$

$$\delta \theta_\alpha = \delta \mathbf{g}_3 \cdot \mathbf{a}_\alpha \qquad (2.56)$$

$$\delta \kappa \; = \delta \mathbf{g}_3 \cdot \mathbf{n} \qquad (2.57)$$

Note that for $\eta = \pm h$ one has $2\delta h = (\delta\mathbf{u}_h - \delta\mathbf{u}_{-h}) \cdot \mathbf{n} = 2h\delta\kappa$. Hence, one has $\delta\kappa = \delta h/h$ (*i.e.,* $\delta\kappa$ represents the relative virtual variation of the thickness). Furthermore, let us suppose the virtual rotation of a material fiber normal to the middle surface as the sum of the rotation due to the Kirchhoff-Love assumption (the fibers initially normal to the middle surface remain normal after the deformation) and of a rotation due to the Reissner-Mindlin model, that is:

$$\delta\theta_\alpha = \delta\theta_\alpha\big|_{KL} + \delta\theta_\alpha\big|_{RM} \tag{2.58}$$

where

$$\delta\theta_\alpha\big|_{KL} = \delta\mathbf{n} \cdot \mathbf{a}_\alpha = -\mathbf{n} \cdot \frac{\partial\delta\mathbf{p}}{\partial\xi^\alpha} = -b_\alpha^\beta\,\delta u_\beta - \frac{\partial\delta w}{\partial\xi^\alpha} \tag{2.59}$$

$$\delta\theta_\alpha\big|_{RM} = (\delta\mathbf{g}_3 - \delta\mathbf{n}) \cdot \mathbf{a}_\alpha \tag{2.60}$$

Equation (2.53) may be recast as

$$\delta\mathbf{u} = \sum_{k=0}^{1} \eta^k \left(\delta u_{\alpha_{(k)}}\,\mathbf{a}^\alpha + \delta w_{(k)}\,\mathbf{n}\right) = \sum_{k=0}^{1} \eta^k\,\delta\mathbf{u}_{(k)} \tag{2.61}$$

where

$$\delta u_{\alpha_{(0)}} = \delta v_\alpha \qquad\qquad \delta w_{(0)} = \delta w$$
$$\delta u_{\alpha_{(1)}} = \delta\theta_\alpha \qquad\qquad \delta w_{(1)} = \delta\kappa \tag{2.62}$$

Note that a more general theory may be obtained by replacing, in Eq. (2.61), $\sum_{k=0}^{1}$ with $\sum_{k=0}^{N}$.[‡] In the following the formulation is presented with $\sum_{k=0}^{N}$, and then it is reduced to the case $N = 1$, from which the Midlin-Reissner theory (for which there exist five degrees of freedom corresponding to δv_α, δw and $\delta\theta_\alpha$) is obtained as a general case of the Kirchhoff-Love theory (in which $\mathbf{n}$ is assumed to remain normal so that the degrees of freedom are only δv_α and δw) with the retainment of the thickness distension (corresponding to the sixth degree of freedom $\delta\kappa$).

[‡] A very general case is obtained by replacing η^k with $f_n(\eta)$, using for instance Legendre polynomials or zig-zag functions.

2.3.2   Development of the volume term

In this section, the first term in Eq. (2.50) is recast in a more convenient form. Using a convenient expression for the divergence of a second order tensor, given by Eq. (A.41), one obtains

$$
\iiint_{\mathcal{V}} \operatorname{Div} \mathbf{T} \cdot \ \delta \mathbf{u} \ d\mathcal{V} =
$$
$$
= \iiint_{\mathcal{V}_0} \frac{\partial}{\partial \xi^p} \left(\sqrt{g} \ \tau^{pq} \mathbf{g}_q \right) \cdot \ \delta \mathbf{u} \ d\mathcal{V}_0 \tag{2.63}
$$

where $d\mathcal{V}_0 = d\xi^1 \ d\xi^2 \ d\eta$ is the volume element in the image space ξ^1, ξ^2, η.

In view of the fact that the virtual displacement is expressed in terms of surface base vectors, $\mathbf{a}_\alpha$ and $\mathbf{n}$ (see Eq. (2.61)), it is convenient to use Eq. (2.20) to express $\mathbf{g}_k$ in terms of $\mathbf{a}_\alpha$ and $\mathbf{n}$. This yields

$$
\begin{aligned}
\sqrt{g} \ \tau^{pq} \ \mathbf{g}_q &= \ \sqrt{g} \ \tau^{pq} \ \left(\mathcal{T}_q^\beta \ \mathbf{a}_\beta + \mathcal{T}_q^3 \ \mathbf{n} \right) \\
&= \ \sqrt{a} \ \left(\sigma^{p\beta} \ \mathbf{a}_\beta + \sigma^{p3} \ \mathbf{n} \right)
\end{aligned} \tag{2.64}
$$

with

$$
\sigma^{pr} := \sqrt{\frac{g}{a}} \ \tau^{pq} \ \mathcal{T}_q^r \tag{2.65}
$$

where the use of the factor $\sqrt{g/a}$ will be useful in expressing volume integrals in terms of surface integrals.

Thus, one has

$$
\iiint_{\mathcal{V}} \operatorname{Div} \mathbf{T} \ \cdot \ \delta \mathbf{u} \ d\mathcal{V} =
$$
$$
= \iiint_{\mathcal{V}_0} \frac{\partial}{\partial \xi^\alpha} \ \left(\sqrt{a} \ \sigma^{\alpha\beta} \ \mathbf{a}_\beta + \sqrt{a} \ \sigma^{\alpha 3} \ \mathbf{n} \right) \cdot \delta \mathbf{u} \ d\mathcal{V}_0
$$
$$
+ \iiint_{\mathcal{V}_0} \frac{\partial}{\partial \eta} \ \left(\sqrt{a} \ \sigma^{3\beta} \ \mathbf{a}_\beta + \sqrt{a} \ \sigma^{33} \ \mathbf{n} \right) \cdot \delta \mathbf{u} \ d\mathcal{V}_0 \tag{2.66}
$$

Consider the first term on the right hand side of Eq. (2.66)

$$\iiint_{\mathcal{V}_0} \frac{\partial}{\partial \xi^\alpha} \left(\sqrt{a}\, \sigma^{\alpha\beta}\, \mathbf{a}_\beta \right) \cdot \delta \mathbf{u}\; d\mathcal{V}_0$$

$$= \iint_{\mathcal{S}_0} \int_{h_l}^{h_u} \frac{\partial}{\partial \xi^\alpha} \left(\sqrt{a}\, \sigma^{\alpha\beta}\, \mathbf{a}_\beta \right) \cdot \sum_{k=0}^{N} \eta^k\, \delta \mathbf{u}_{(k)}\; d\eta d\mathcal{S}_0$$

$$= \sum_{k=0}^{N} \left[\iint_{\mathcal{S}_0} \frac{\partial}{\partial \xi^\alpha} \left(\sqrt{a}\, \mathbf{a}_\beta \int_{h_l}^{h_u} \sigma^{\alpha\beta}\, \eta^k\, d\eta \right) - \left(h_{/\alpha}\, \sqrt{a}\, \sigma^{\alpha\beta} \eta^k \right)_{h_l}^{h_u} \mathbf{a}_\beta \right] \cdot \delta \mathbf{u}_{(k)} d\mathcal{S}_0$$

$$= \sum_{k=0}^{N} \iint_{\mathcal{S}_M} \left[\left(n_{(k)/\alpha}^{\alpha\beta} \delta u_{\beta_{(k)}} + b_{\alpha\beta} n_{(k)}^{\alpha\beta} \delta w_{(k)} \right) - \left(h_{/\alpha}\, \sigma^{\alpha\beta}\, \eta^k \right)_{h_l}^{h_u} \delta u_{\beta_{(k)}} \right] d\mathcal{S}_M \qquad (2.67)$$

where we have used Eq. ((A.44)) and the following definition for the integral term of stress

$$n_{(k)}^{\alpha\beta} := \int_{h_l}^{h_u} \sigma^{\alpha\beta}\, \eta^k\, d\eta =$$

$$= \int_{h_l}^{h_u} \sqrt{\frac{g}{a}} \left(\tau^{\alpha\gamma}\, \mathcal{T}_\gamma^\beta + \tau^{\alpha3}\, \mathcal{T}_3^\beta \right) \eta^k\, d\eta =$$

$$= \int_{h_l}^{h_u} \sqrt{\frac{g}{a}} \left(\delta_\gamma^\alpha - \eta\, b_\gamma^\alpha \right) \tau^{\gamma\beta}\, \eta^k\, d\eta \qquad (2.68)$$

Similarly, for the second term on the right hand side of Eq. (2.66), one has

$$\iiint_{\mathcal{V}_0} \frac{\partial}{\partial \xi^\alpha} \left(\sqrt{a}\, \sigma^{\alpha3}\, \mathbf{n} \right) \cdot \delta \mathbf{u}\; d\mathcal{V}_0$$

$$= \iint_{\mathcal{S}_0} \int_{h_l}^{h_u} \frac{\partial}{\partial \xi^\alpha} \left(\sqrt{a}\, \sigma^{\alpha3}\, \mathbf{n} \right) \cdot \sum_{k=0}^{N} \eta^k\, \delta \mathbf{u}_{(k)}\; d\eta d\mathcal{S}_0$$

$$= \sum_{k=0}^{N} \iint_{\mathcal{S}_0} \left[\frac{\partial}{\partial \xi^\alpha} \left(\sqrt{a}\, \mathbf{n} \int_{h_l}^{h_u} \sigma^{\alpha3}\, \eta^k\, d\eta \right) - \left(h_{/\alpha}\, \sqrt{a}\, \sigma^{\alpha3} \eta^k \right)_{h_l}^{h_u} \mathbf{n} \right] \cdot \delta \mathbf{u}_{(k)} d\mathcal{S}_0$$

$$= \sum_{k=0}^{N} \iint_{\mathcal{S}_M} \left[\left(q_{(k)/\alpha}^\alpha\, \delta w_{(k)} - b_\alpha^\beta\, q_{(k)}^\alpha\, \delta u_{\beta_{(k)}} \right) - \left(h_{/\alpha}\, \sigma^{\alpha3}\, \eta^k \right)_{h_l}^{h_u} \delta w_{(k)} \right] d\mathcal{S}_M \qquad (2.69)$$

where we have used Eq. ((A.37)) and the following definition

$$q_{(k)}^\alpha := \int_{h_l}^{h_u} \sigma^{\alpha3}\, \eta^k\, d\eta =$$

$$= \int_{h_l}^{h_u} \sqrt{\frac{g}{a}} \left(\tau^{\alpha\beta}\, \mathcal{T}_\beta^3 + \tau^{\alpha3}\, \mathcal{T}_3^3 \right) \eta^k\, d\eta =$$

$$= \int_{h_l}^{h_u} \sqrt{\frac{g}{a}}\, \tau^{\alpha3}\, \eta^k\, d\eta \qquad (2.70)$$

In addition, for the third term on the right hand side of Eq. (2.66), one has

$$
\iiint_{\mathcal{V}_0} \frac{\partial}{\partial \eta} \left(\sqrt{a}\, \sigma^{3\beta}\, \mathbf{a}_\beta \right) \cdot \delta \mathbf{u}\, d\mathcal{V}_0
$$

$$
= \iint_{\mathcal{S}_0} \int_{h_l}^{h_u} \frac{\partial}{\partial \eta} \left(\sqrt{a}\, \sigma^{3\beta}\, \mathbf{a}_\beta \right) \cdot \sum_{k=0}^{N} \eta^k\, \delta \mathbf{u}_{(k)}\, d\eta d\mathcal{S}_0
$$

$$
= \sum_{k=0}^{N} \iint_{\mathcal{S}_0} \sqrt{a} \left[\left(\sigma^{3\beta} \eta^k \right)_{h_l}^{h_u} - n \int_{h_l}^{h_u} \sigma^{3\beta} \eta^{k-1} d\eta \right] \mathbf{a}_\beta \; \cdot \; \delta \mathbf{u}_{(k)} d\mathcal{S}_0
$$

$$
= \sum_{k=0}^{N} \iint_{\mathcal{S}_M} \left[\left(\sigma^{3\beta}\, \eta^k \right)_{h_l}^{h_u} - n\, p_{(n-1)}^{\beta} \right] \delta u_{\beta(k)} d\mathcal{S}_M \tag{2.71}
$$

where $p_{(-1)}^{\beta} = 0$ and

$$
p_{(k)}^{\beta} \;:=\; \int_{h_l}^{h_u} \sigma^{3\beta}\, \eta^k\, d\eta =
$$

$$
= \int_{h_l}^{h_u} \sqrt{\frac{g}{a}} \tau^{3q}\, \mathcal{T}_q^{\beta}\, \eta^k\, d\eta
$$

$$
= \int_{h_l}^{h_u} \sqrt{\frac{g}{a}} \left(\delta_\alpha^\beta - \eta\, b_\alpha^\beta \right) \tau^{3\alpha}\, \eta^k\, d\eta \tag{2.72}
$$

Furthermore, for the last term in Eq. (2.66), one has

$$
\iiint_{\mathcal{V}_0} \frac{\partial}{\partial \eta} \left(\sqrt{a}\, \sigma^{33}\, \mathbf{n} \right) \cdot \delta \mathbf{u}\, d\mathcal{V}_0
$$

$$
= \iint_{\mathcal{S}_0} \int_{h_l}^{h_u} \frac{\partial}{\partial \eta} \left(\sqrt{a}\, \sigma^{33}\, \mathbf{a}_\beta \right) \cdot \sum_{k=0}^{N} \eta^k\, \delta \mathbf{u}_{(k)}\, d\eta
$$

$$
= \sum_{k=0}^{N} \iint_{\mathcal{S}_0} \sqrt{a} \left[\left(\sigma^{33}\, \eta^k \right)_{h_l}^{h_u} - n \int_{h_l}^{h_u} \sigma^{33} \eta^{k-1}\, d\eta \right] \mathbf{n} \; \cdot \; \delta \mathbf{u}_{(k)}\, d\mathcal{S}_0
$$

$$
= \sum_{k=0}^{N} \iint_{\mathcal{S}_M} \left[\left(\sigma^{33}\, \eta^k \right)_{h_l}^{h_u} - n\, r_{(n-1)} \right] \delta w_{(k)}\, d\mathcal{S}_M \tag{2.73}
$$

where $r_{(-1)}^{\beta} = 0$ and

$$
r_{(k)} \;:=\; \int_{h_l}^{h_u} \sigma^{33}\, \eta^k\, d\eta =
$$

$$
= \int_{h_l}^{h_u} \sqrt{\frac{g}{a}} \tau^{3q}\, \mathcal{T}_q^3\, \eta^k\, d\eta
$$

$$
= \int_{h_l}^{h_u} \sqrt{\frac{g}{a}} \tau^{33}\, \eta^k\, d\eta \tag{2.74}
$$

Finally, consider the virtual work by the volume force $\mathbf{f}$. Using Eq. (2.61), the virtual work by the force $\mathbf{f}$ may be expressed as

$$
\iiint_{\mathcal{V}} \mathbf{f} \cdot \delta\mathbf{u}\,d\mathcal{V} = \iiint_{\mathcal{V}_0} \mathbf{f} \cdot \sum_{k=0}^{N} \eta^k \left(\delta u_{\alpha_{(k)}}\, \mathbf{a}^\alpha + \delta w_{(k)}\, \mathbf{n} \right) \sqrt{g}\,d\mathcal{V}_0
$$

$$
= \sum_{k=0}^{N} \iint_{\mathcal{S}_M} \left(\hat{f}_{(k)}^{\ \alpha}\, \delta u_{\alpha_{(k)}} + \hat{f}_{(k)}^{\ 3}\, \delta w_{(k)} \right) d\mathcal{S}_M \tag{2.75}
$$

where

$$
\hat{f}_{(k)}^{\ k} = \int_{h_l}^{h_u} \sqrt{\frac{g}{a}}\ \eta^k\ f^k d\eta \tag{2.76}
$$

with $f^\alpha = \mathbf{f} \cdot \mathbf{a}^\alpha$ and $f^3 = \mathbf{f} \cdot \mathbf{n}$.

Combining Eqs. (2.66), (2.67), (2.69), (2.71), (2.73) and (2.75) one obtains

$$
\iiint_{\mathcal{V}} (\text{Div }\mathbf{T} + \mathbf{f}) \cdot \delta\mathbf{u}\ d\mathcal{V} =
$$

$$
\sum_{k=0}^{N} \iint_{\mathcal{S}_M} \left\{ n_{(k)/\alpha}^{\alpha\beta} - b_\alpha^\beta\, q_{(k)}^\alpha - n\, p_{(n-1)}^\beta + \hat{f}_{(k)}^{\ \alpha} - \left[\left(h_{/\alpha}\sigma^{\alpha\beta} - \sigma^{3\beta} \right)\eta^k \right]_{h_l}^{h_u} \right\} \delta u_{\beta_{(k)}} d\mathcal{S}_M +
$$

$$
\sum_{k=0}^{N} \iint_{\mathcal{S}_M} \left\{ q_{(k)/\alpha}^\alpha + b_{\alpha\beta}\, n_{(k)}^{\alpha\beta} - n\, r_{(n-1)} + \hat{f}_{(k)}^{\ 3} - \left[\left(h_{/\alpha}\sigma^{\alpha 3} - \sigma^{33} \right)\eta^k \right]_{h_l}^{h_u} \right\} \delta w_{(k)} d\mathcal{S}_M \tag{2.77}
$$

2.3.3   Virtual work from $\mathcal{S}_u \bigcup \mathcal{S}_l$

Consider the virtual work by $\mathbf{t}$ on $\mathcal{S}_u \bigcup \mathcal{S}_l$ (see Eq. (2.51)). Using Eqs. (2.38), (2.40), (2.61) and (2.64), one has

$$
\iint_{\mathcal{S}_u \bigcup \mathcal{S}_l} \mathbf{t} \cdot \delta\mathbf{u}\ d\mathcal{S} = \iint_{\mathcal{S}_u \bigcup \mathcal{S}_l} \mathbf{T}\,\mathbf{n}_{\mathcal{S}} \cdot \delta\mathbf{u}\ d\mathcal{S}
$$

$$
= \iint_{\mathcal{S}_u} \mathbf{T}\,\mathbf{n}^{(u)} d\mathcal{S}_u + \iint_{\mathcal{S}_l} \mathbf{T}\,\mathbf{n}^{(l)} d\mathcal{S}_l
$$

$$
= \iint_{\mathcal{S}_0} \left[\sqrt{\frac{g}{a^{(u)}}}\mathbf{T}\ \left(\mathbf{g}^3 - h_{/\alpha}\,\mathbf{g}^\alpha \right) \cdot \sum_{k=0}^{N} \eta^k\, \delta\mathbf{u}_{(k)}\sqrt{a^{(u)}} \right]_{h_u} d\xi^1 d\xi^2
$$

$$
- \iint_{\mathcal{S}_0} \left[\sqrt{\frac{g}{a^{(l)}}}\mathbf{T}\ \left(\mathbf{g}^3 - h_{/\alpha}\,\mathbf{g}^\alpha \right) \cdot \sum_{k=0}^{N} \eta^k\, \delta\mathbf{u}_{(k)}\sqrt{a^{(l)}} \right]_{h_l} d\xi^1 d\xi^2
$$

$$
= \iint_{\mathcal{S}_M} \left\{ \left[\left(-h_{/\alpha}\,\sigma^{\alpha\beta} + \sigma^{3\beta} \right)\eta^k \right]_{h_l}^{h_u} \delta u_{\beta_{(k)}} + \left[\left(-h_{/\alpha}\,\sigma^{\alpha 3} + \sigma^{33} \right)\eta^k \right]_{h_l}^{h_u} \delta w_{(k)} \right\} d\mathcal{S}_M \tag{2.78}
$$

On the other hand one has

$$\iint_{S_U \bigcup S_L} \mathbf{t}_A \cdot \delta \mathbf{u} \, d\mathcal{S} =$$

$$= \iint_{S_U \bigcup S_L} \mathbf{t}_A \cdot \sum_{k=0}^{N} \eta^k \left(\delta u_{\alpha_{(k)}} \mathbf{a}^\alpha + \delta w_{(k)} \mathbf{n} \right) \sqrt{a_S} \, d\xi^1 d\xi^2$$

$$= \sum_{k=0}^{N} \iint_{S_M} \left[\eta^{k+1} \left(t_A^\alpha \delta u_{\alpha_{(k)}} + t_A^3 \delta w_{(k)} \right) \sqrt{\frac{a_S}{a}} \right]_{\eta=-1}^{\eta=1} d\mathcal{S}_M$$

$$= \sum_{k=0}^{N} \iint_{S_M} \left(\check{f}_{(k)}^{\ \alpha} \delta u_{\alpha_{(k)}} + \check{f}_{(k)}^{\ 3} \delta w_{(k)} \right) d\mathcal{S}_M \qquad (2.79)$$

where

$$\check{f}_{(k)}^{\ k} = \sqrt{\frac{a_U}{a}} \, t_U^k + \sqrt{\frac{a_L}{a}} \, t_L^k \qquad\qquad n = even \qquad (2.80)$$

$$\check{f}_{(k)}^{\ k} = \sqrt{\frac{a_U}{a}} \, t_U^k - \sqrt{\frac{a_L}{a}} \, t_L^k \qquad\qquad n = odd \qquad (2.81)$$

Finally, considering Eqs. (2.77), (2.78) and (2.79) yields (note that the boundary terms in Eq. (A.37) cancel out with the similar ones of Eq. (2.78))

$$\iiint_{\mathcal{V}} (\text{Div } \mathbf{T} + \mathbf{f}) \, \cdot \, \delta \mathbf{u} \, d\mathcal{V} + \iint_{S_U \bigcup S_L} (\mathbf{t}_A - \mathbf{t}) \cdot \delta \mathbf{u} \, d\mathcal{S} =$$

$$\sum_{k=0}^{N} \iint_{\mathcal{S}_M} \left[\left(n_{(k)/\alpha}^{\alpha\beta} - q_{(k)}^\alpha \, b_\alpha^\beta - n p_{(n-1)}^\beta + f_{(k)}^{\ \beta} \right) \, \delta u_{\beta_{(k)}} \right.$$

$$\left. + \left(q_{(k)/\alpha}^\alpha + b_{\alpha\beta} n_{(k)}^{\alpha\beta} - n r_{(n-1)} + f_{(k)}^3 \right) \delta w_{(k)} \right] d\mathcal{S}_M$$

where

$$f_{(k)}^{\ k} = \check{f}_{(k)}^{\ k} + \hat{f}_{(k)}^{\ k} \qquad (2.82)$$

2.3.4 Virtual work from $\mathcal{S}_C$

Consider the virtual work by $\mathbf{t}$ on S_C (see Eq. (2.51)). Using the expression for the normal to S_C, $\mathbf{n}_C$ in Eq. (2.45), the virtual work can be written

$$
\iint_{\mathcal{S}_C} \mathbf{n}_C \cdot \mathbf{T} \, \delta\mathbf{u} \, d\mathcal{S} = \iint_{\mathcal{S}_C} \mathbf{n}_C \cdot \mathbf{g}_i \tau^{ij} \, \delta u_j d\mathcal{S}
$$

$$
= \iint_{\mathcal{S}_C} \sqrt{\frac{g}{a}} \, \mathbf{n}_C \cdot \mathbf{g}_\alpha \left(\sigma^{\alpha\beta} \, \delta u_\beta + \sigma^{\alpha 3} \, \delta w \right) \sqrt{a_C} \, d\eta d\gamma
$$

$$
= \iint_{\mathcal{S}_C} \nu_\alpha \left(\sigma^{\alpha\beta} \, \delta u_\beta + \sigma^{\alpha 3} \, \delta w \right) \, d\eta d\gamma
$$

$$
= \sum_{k=0}^{N} \oint \nu_\alpha \left(\int_{h_l}^{h_u} \eta^k \, \sigma^{\alpha\beta} \, d\eta \, \delta u_{\beta(k)} + \int_{h_l}^{h_u} \eta^k \, \sigma^{\alpha 3} \, d\eta \, \delta w_{(k)} \right) \, d\gamma
$$

$$
= \sum_{k=0}^{N} \oint \nu_\alpha \left(n_{(k)}^{\alpha\beta} \, \delta u_\beta^{(k)} + q_{(k)}^{\alpha} \, \delta w_{(k)} \right) \, d\gamma \tag{2.83}
$$

since $\mathbf{n}_C \cdot \mathbf{g}_3 = \mathbf{n}_C \cdot \mathbf{n} \, h = 0$.

Next, consider the virtual work by $\mathbf{t}_A$ on $\mathcal{S}_C$ (see Eq. (2.51)),

$$
\iint_{\mathcal{S}_C} \mathbf{t}_A \cdot \delta\mathbf{u} \, d\mathcal{S} = \oint \int_{h_l}^{h_u} \mathbf{t}_A \cdot \sum_{k=0}^{N} \eta^k \left(\delta u_{\alpha(k)} \mathbf{a}^\alpha + \delta w_{(k)} \mathbf{n} \right) \sqrt{a_C} \, d\eta d\gamma
$$

$$
= \sum_{k=0}^{N} \oint \left(\int_{h_l}^{h_u} \sqrt{a_C} \eta^k \, t_A^\alpha \, d\eta \, \delta u_{\alpha(k)} + \int_{h_l}^{h_u} \sqrt{a_C} \eta^k \, t_A^3 \, d\eta \, \delta w_{(k)} \right) \, d\gamma
$$

$$
= \sum_{k=0}^{N} \oint \left(S_{(k)}^\alpha \, \delta u_{\alpha(k)} + S_{(k)}^3 \, \delta w_{(k)} \right) \, d\gamma \tag{2.84}
$$

where

$$
S_{(k)}^k := \int_{h_l}^{h_u} \sqrt{a_C} \, \eta^k \, t_A^k \, d\eta \tag{2.85}
$$

Combining Eqs. (2.51),(2.83), and (2.84) yields

$$
\iint_{\mathcal{S}_C} (\mathbf{t}_A - \mathbf{t}) \cdot \delta\mathbf{u} \, d\mathcal{S} = \sum_{k=0}^{N} \oint \left[\left(S_{(k)}^\beta - \nu_\alpha \, n_{(k)}^{\alpha\beta} \right) \delta u_{\beta(k)} + \left(S_{(k)}^3 - \nu_\alpha \, q_{(k)}^\alpha \right) \delta w_{(k)} \right] d\gamma \tag{2.86}
$$

2.3.5   Equilibrium equations for the Reissner-Mindlin model

Let us introduce the hypotheses of the Reissner-Mindlin kinematical model for a shell, that is, express the virtual displacement $\delta u_\alpha^{(1)}$ in the form of Eq.((2.58)). Thus, the virtual work can be written

$$
\begin{aligned}
\delta \mathcal{W} = \iint_{\mathcal{S}_M} & \left\{ \left[n_{(0)/\alpha}^{\alpha\beta} - b_\alpha^\beta \, q_{(0)}^\alpha + f_{(0)}^\beta - b_\gamma^\beta \left(n_{(1)/\delta}^{\delta\gamma} - b_\delta^\gamma \, q_{(1)}^\delta - p_{(0)}^\gamma + f_{(1)}^\gamma \right) \right] \delta u_\beta + \right. \\
& \left[q_{(0)/\alpha}^\alpha + b_{\alpha\beta} \, n_{(0)}^{\alpha\beta} + f_{(0)}^3 + \left(n_{(1)/\delta}^{\delta\gamma} - b_\delta^\gamma \, q_{(1)}^\delta - p_{(0)}^\gamma + f_{(1)}^\gamma \right)_{/\gamma} \right] \delta w + \\
& \left[n_{(1)/\alpha}^{\alpha\beta} - b_\alpha^\beta \, q_{(1)}^\alpha - p_{(0)}^\beta + f_{(1)}^\beta \right] \delta\theta_\beta \big|_{RM} + \\
& \left. \left[q_{(1)/\alpha}^\alpha + b_{\alpha\beta} \, n_{(1)}^{\alpha\beta} + q_{(1)/\alpha}^\alpha - r_{(0)} + f_{(1)}^3 \right] \delta\kappa \right\} d\mathcal{S}_M + \\
\oint & \left\{ \left[S_{(0)}^\beta - \nu_\alpha \, n_{(0)}^{\alpha\beta} \right] \delta u_\beta + \left[S_{(0)}^3 - \nu_\gamma \, q_{(0)}^\gamma - \nu_\gamma \left(n_{(1)/\gamma}^{\alpha\gamma} - b_\alpha^\gamma \, q_{(1)}^\alpha - p_{(0)}^\gamma + f_{(1)}^3 \right) \right] \delta w + \right. \\
& \left. \left[S_{(1)}^\beta - \nu_\alpha \, n_{(1)}^{\alpha\beta} \right] \delta\theta_\beta + \left[S_{(1)}^3 - \nu_\alpha \, q_{(1)}^\alpha \right] \delta\kappa \right\} d\gamma
\end{aligned}
\tag{2.87}
$$

where the following relation has been used

$$
c^\alpha \frac{\partial \delta w}{\partial \xi^\alpha} = \mathrm{div} \left(c^\alpha \, \mathbf{a}_\alpha \, \delta w \right) - c^\gamma{}_{/\gamma} \, \delta w
\tag{2.88}
$$

and the Green-Gauss theorem in order to obtain an integral on the boundary.

It is worth noting that the integral terms related to the shear are not independent, indeed, the following relation states:

$$
q_{(0)}^\alpha = b_\gamma^\alpha \, q_{(1)}^\gamma + p_{(0)}^\alpha
\tag{2.89}
$$

Thus, the application of the Principle of Virtual Work (*i.e.*, the virtual work must be zero for every virtual displacement) leads to following system of equilibrium equations

$$
n_{(0)/\alpha}^{\alpha\beta} - b_\gamma^\beta \, n_{(1)/\alpha}^{\alpha\gamma} + f_{(0)}^\beta - b_\gamma^\beta \, f_{(1)}^\gamma = 0
\tag{2.90}
$$

$$
n_{(1)/\alpha\beta}^{\alpha\beta} + b_{\alpha\beta} n_{(0)}^{\alpha\beta} + f_{(0)}^3 + f_{(1)/\beta}^\beta = 0
\tag{2.91}
$$

$$
n_{(1)/\alpha}^{\alpha\beta} - b_\alpha^\beta \, q_{(1)}^\alpha + + p_{(0)}^\beta + f_{(1)}^\beta = 0
\tag{2.92}
$$

$$
q_{(1)/\alpha}^\alpha + b_{\alpha\beta} n_{(1)}^{\alpha\beta} - r_{(0)} + f_{(1)}^3 = 0
\tag{2.93}
$$

and boundary conditions

$$S^{\beta}_{(0)} - \nu_\alpha \, n^{\alpha\beta}_{(0)} = 0 \qquad or \qquad \delta u_\beta = 0 \tag{2.94}$$

$$S^{3}_{(0)} - \nu_\gamma \left(n^{\alpha\gamma}_{(1)/\gamma} + f^{3}_{(1)} \right) = 0 \qquad or \qquad \delta w = 0 \tag{2.95}$$

$$S^{\beta}_{(1)} - \nu_\alpha \, n^{\alpha\beta}_{(1)} = 0 \qquad or \qquad \delta\theta = 0 \tag{2.96}$$

$$S^{3}_{(1)} - \nu_\alpha \, q^{\alpha}_{(1)} = 0 \qquad or \qquad \delta\kappa = 0 \tag{2.97}$$

Note that Eqs. ((2.90)) and ((2.91)) are the equilibrium equations for the Kirchhoff-Love model, Eq. ((2.92)) is relative to Reissner-Mindlin model being related to the shear of a generic section, and Eq. ((2.93)) is relative to the equilibrium in the thickness direction due to the hypotheses of fiber elongation assumed throughout in this work.

Chapter 3

Preliminaries

In this chapter the formal description of the mathematical structure underlying the definition of a micro-structured continuum is established. First a definition of micro-structure is reported and its physical implication discussed, then, the mathematics needed to deal with this definition is introduced, both from the point of view of the tensors analysis on manifolds (or modern continuum mechanics) and from the point of view of classical mechanics (based on the definition of material coordinates). In particular, in the following, vector and tensor fields, defined on domain of the three-dimensional Euclidean point space $\mathscr{E}$, will be used, so a rigorous definition of $\mathscr{E}$, of the manifolds immersed in it, which concur to the definition of the micro-structure of the continuum, and of the related tangent spaces, is reported. Although, the theory is initially developed in its complete generality, being applicable both to shell and rod-like bodies, then, for the sake of simplicity, the analysis is confined to the study of shells.

3.1 Micro-structure: a definition

In this section, following Refs. [43, 97, 102, 33], the basic kinematic assumptions underlying the definition of a micro-structured continuum are illustrated. First, let us introduce the definition of micro-structured continuum quoting from Ref. [43]: "In the classical description, a continuum is a continuous distribution of *particles*, each of them being represented *geometrically* by a point M and characterized *kinematically* by a velocity U_i. In a theory which takes microstructure into account, from the macroscopic point of view (which is the point of view of a continuum theory), each particle is still represented by a point M, but its kinematical properties are defined in a more refined way. In order to discover how to define the kinematical properties of a particle, one has to look at it from a microscopic point view. At this level of observation, a particle appears itself as a continuum $P(M)$ of small extent. Let us call M its center of mass, M' a point of $P(M)$, U_i the velocity of M, x_i' the co-ordinates of M' in a Cartesian frame parallel to the given frame x_i with M as the origin, U_i' the velocity of M' with respect to the given frame, and x_i the coordinates of M in the given frame.

If one assumes for the moment that the x_i are given, *i.e.*, if one looks at a given particle, the field U_i' appears as a function of the x_i' defined on $P(M)$. As $P(M)$ is of small extent, it is natural to look at the Taylor expansion of U_i' with respect to the x_j' and also, as a first approximation, to stop this expansion with the terms of degree 1. Then, with this assumption, one can write

$$U_i' = U_i + \chi_{ij}\, x_j \tag{3.1}$$

The physical significance of this assumption is clear: one postulates that one can get a sufficient description of the relative motion of the various points of the particle if one assumes that the relative motion is a homogeneous deformation."

The given definition of a micro-structured continuum body is quite general, being applicable to any type of body for which an equation like Eq. (3.1) is true. On the other hand, another definition of micro-structured continuum bodies can be given referring to the geometry of the body immersed in the three-dimensional Euclidean space. This point of view is that used in Refs. [97, 102, 33], where both theories of shells, plates and rods are developed regarding them as continua with a special body structure and a special kinematics consistent with that structure. A central role in this definition is played by the two complementary concepts of support and fiber spaces.

Let $\mathscr{E}$ be a 3-dimensional Euclidean space let $\mathscr{V}$ be the vector space associated with $\mathscr{E}$ and denote with $\mathcal{U} := \{\mathbf{v} \in \mathscr{V} \,|\, \|\mathbf{v}\| = 1\}$ the sphere of all vectors having unit length. One may think of $\mathscr{E}$ as equipped with a Cartesian frame $\{\mathcal{O}; \mathbf{e}_1, \mathbf{e}_2, \mathbf{e}_3\}$ with orthogonal basis vectors $\mathbf{e}_i \in \mathcal{U}$ (i= 1, 2, 3); the Cartesian components of a vector $\mathbf{v} \in \mathscr{V}$ are then $v_i := \mathbf{v} \cdot \mathbf{e}_i$ and, in particular, the triplet $(p_1, p_2, p_3) \in \Re^3$, $p_i := \mathbf{p}(p) \cdot \mathbf{c}_i$, of components of the position vector are the Cartesian coordinates of a point $p \in \mathscr{E}$.

Now a vector field $\mathbf{w}$ on a domain $\mathscr{W} \in \mathscr{V}$ can be defined as a map

$$\mathbf{w} : \mathscr{W} \mapsto \mathscr{V} \tag{3.2}$$

meaning that in every point $p \in \mathscr{E}$ there exists a rule (*i.e.*, a map) which associates to p a vector $\mathbf{w} \in \mathscr{V}$ (examples of vector fields that will be considered later are the displacement field, the velocity field, the acceleration field, *etc*).

At this point one may say a continuum micro-structured if there exists a (differentiable) manifold $\mathcal{S}$ (the "support-space") and another (differentiable manifold) $\mathcal{F}$ (the "fiber-space"), such that the body (differentiable) manifold $\mathcal{B}$ can be written

$$\mathcal{B} = \mathcal{S} \oplus \mathcal{F} \tag{3.3}$$

It is also quite worth noting that at this stage (by means of the previous abstractization) one may deal with any type of structure and configuration, for instance, note that if $\mathcal{S}$ is a 2-D differentiable manifold and $\mathcal{F}$ a 1-D differentiable manifold one is dealing with a shell-like structure (whereas if $\mathcal{S}$

is a 1-D differentiable manifold and $\mathcal{F}$ a 2-D differentiable manifold one is dealing with a rod-like structure) where no restriction* is placed on the geometry of the main surface (line) and on the geometry of main fiber (plane).[†] A helpful visualisation of our reasoning is reported in the following table.

Table 3.1: Possible micro-structured continuum models

Model - Space	Fiber	Support
Rods	$\zeta^1, \zeta^2 \Longrightarrow a = 2$	$\xi^1 \Longrightarrow \alpha = 1$
Shells	$\zeta^1 \Longrightarrow a = 1$	$\xi^1, \xi^2 \Longrightarrow \alpha = 2$

To state precisely the basic kinematic assumptions, underlying the definition of the two subset $\mathcal{S}$ and $\mathcal{F}$ di $\mathcal{B}$, let us define the configuration space $\mathscr{C}$ (a differentiable manifold) of a micro-structured (*one-director Cosserat*) continuum as

$$\mathscr{C} \quad := \quad \left\{ (\mathbf{p}, \mathbf{q}_a) : \mathscr{A} \subset \Re^n \mapsto \Re^3 \times \mathscr{V}^{3-n} \right\} \tag{3.4}$$

where n ($n < 3$) is the dimension of the support-space, $3 - n$ is the dimension of the fiber-space,[‡] whereas $\mathscr{A} \subset \Re^n$ is an open set with smooth boundary $\partial\mathscr{A}$, compact closure $\bar{\mathscr{A}}$, and points $\{\xi^\alpha\}$.[‖] Accordingly, one may define $\mathcal{S}$ and $\mathcal{F}$ to be

$$\mathcal{S} \quad := \quad \left\{ \mathbf{x} \in \Re^3 \| \ \mathbf{x} = \mathbf{p} \ \ with \ \ \mathbf{p} : \mathscr{A} \subset \Re^n \mapsto \Re^3 \right\} \tag{3.5}$$

and

$$\mathcal{F} \quad := \quad \left\{ \mathbf{x} \in \Re^3 \| \ \mathbf{x} = \zeta^a \ \mathbf{q}_a \ \ with \ \ \mathbf{q}_a : \mathscr{A} \subset \Re^n \mapsto \Re^3 \ \ and \ \ \{\zeta^a\} \in \mathscr{B} \subset \Re^{3-n} \right\} \tag{3.6}$$

where $\mathscr{B} \subset \Re^{3-n}$ is an open set with points $\zeta^a \in \mathscr{B}$, defining the domain of existence of the fiber

---

   * Even if this second point of view has not yet been presented in details, it is apparent that while in the first definition of micro-structure a central role is played by the hypothesis of smallness of the *particle*, here this hypothesis has not (until now) been introduced. Nonetheless, it should not been forgot that the two definitions are fully equivalent and this will be delucidated in the following developments where a formal expression of the kinematics is reported. To this aim, note also, that, being the resulting models reduced models with respect to the three-dimensional Cauchy theory, they lie on the assumption that the 3-D motion can be described (*i.e.*, recovered) by the notion of the motion of the support.

   [†] Note that here the term "main" is used to indicate the support and fiber spaces: this should not be confused with their reference configuration which one may consider coincident with the undeformed one. It is also worth noting that frequently, especially, in shell theory (and also here), it is convenient to distinguish between the geometrical middle surface (equidistant to the upper and lower surfaces) and the main one which could be, for instance, the locus of the centers of mass measured along the thickness (or the fiber).

   [‡] Note that for $n = 1$ one has rods, whereas for $n = 2$ one has shells and plates.

   [‖] For the sake of generality (but with the risk to be puzzling) we use here Greek indices ($^\alpha$) to denote quantitites (*i.e.*, points, basis vectors, *etc.*) related to the support, so that α spans from 1 to 2 for shells, whereas α is equal to 1 for rod theories; and we use Latin indices (^{a}) to list quantities related to the fiber space, so that a spans from 1 to 2 for rods, whereas a is equal to 1 for shell theories.

space.[§] Moreover, any configuration of the body is described by a pair (a triplet in the case of rods) of vectors $(\mathbf{p}, \mathbf{q}) \in \mathscr{C}$ $((\mathbf{p}, \mathbf{q}_1, \mathbf{q}_2) \in \mathscr{C}$ for rod-like bodies), where:

(i) The map $\mathbf{p} : \mathscr{A} \mapsto \Re^3$ defines the position vector of each point of the support (*i.e.*, the main surface for shells, and the main line for rods)

(ii) The maps $\mathbf{q}_a : \mathscr{A} \mapsto \mathscr{V}^{3-n}$ define $3 - n$ (*i.e.*, 1 for shell and 2 for rod-like bodies respectively) vector fields at each point of the support, referred to as director (or fiber) fields.

Starting from the previous considerations, one is led to define any configuration of the body $\mathcal{B} \subset \Re^3$ as

$$\mathcal{B} \quad := \quad \left\{ \mathbf{x} \in \Re^3 \| \mathbf{x} = \mathbf{p} + \zeta^a \, \mathbf{q}_a \ \ where \ \ (\mathbf{p}, \mathbf{q}_a) \in \mathscr{C} \ \ and \ \ \{\zeta^a\} \in \mathscr{B} \subset \Re^{3-n} \right\} \quad (3.7)$$

Alternatively to Eq. (3.7), one may state that the actual configuration of the body is represented by the following expression[¶]

$$\mathbf{x} = \hat{\mathbf{x}} \left(\xi^\alpha, \zeta^a \right) = \mathbf{p} \left(\xi^\alpha \right) + \zeta^a \, \mathbf{q}_a \left(\xi^\alpha \right) \qquad for \ \begin{cases} \alpha = 1, 2 \ \ and \ \ a = 1 \ (shells) \\ \alpha = 1 \ \ and \ \ a = 1, 2 \ (rods) \end{cases} \qquad (3.8)$$

where $\mathbf{p} \left(\xi^\alpha \right)$ represent the position vector of the material point $\{\xi^\alpha\}$ in the support space, and $\mathbf{q}_a$ are the directors of order one (or fibers) representing the actual configuration of the fiber space relevant to the support in the point $\{\xi^\alpha\}$ of the support space.

Similarly, the reference configuration, which may be assumed coincident with the undeformed one (or the one assumed by the body at the initial time of observation of the motion), will be given by

$$\mathcal{B}_0 \quad := \quad \left\{ \mathbf{x}_0 \in \Re^3 \| \mathbf{x}_0 = \mathbf{p}_0 + \zeta^a \, \mathbf{q}_{0_a} \ \ where \ \ (\mathbf{p}_0, \mathbf{q}_{0_a}) \in \mathscr{C} \ \ and \ \ \zeta \in \mathscr{B} \subset \Re^{3-n} \right\} \quad (3.9)$$

At this point, before proceeding further, it is important to comment on the physical implications inherent the definition of the configurational space and of the actual configuration of the body given in the previous equations (Eqs. (3.4)-(3.8)). For a better comprehension of our reasoning it would be useful to refer again to the definition of micro-structured continuum given at the beginning of this section. There it was observed that "... as $P(M)$ is of small extent (...) one can get a sufficient description of the relative motion of the various points of the particle if one assumes that this relative motion is a homogeneous deformation". Thus, it is clear that behind the kinematic assumption of Eq. (3.7) there is the request that the relative motion leaves each fiber straight (in the case of

---

[§] $\mathscr{B}$ reduces to an interval of $\mathbf{R}$ for shells.

[¶] Although in Eq. (3.8) clear distinction is placed between the map and its value (the map is endowed with an upper hat $\hat{\ }$) in the following such attention will be released without apparent misleading.

shells) [plane (in the case of rods)] and that it is linear with respect to the co-ordinates ζ^a of the fiber space. Of course, within this model the fiber is permitted to rotate with respect to the fiber space but it cannot curve (or warp in the case of rods). This assumption can be clearly justified with the request of thinness of the fiber with respect to the support (meaning that $\mathrm{diam}[\mathcal{F}] \ll \mathrm{diam}[\mathcal{S}]$) but it would not be necessarily introduced if a higher order director theory (*i.e.*, a theory which, considering a richer kinematics, be capable to describe the curving or warping of the fiber) would be considered.**

3.2   Shells as micro-structured bodies

Henceforth, for the sake simplicity, the theory will be developed renouncing to the generality of Eq. (3.4) and confining the treatment to the case $n = 2$, *i.e.*, to the case of shell-like bodies. In this case Eq. (3.8) reduces to

$$\mathbf{x} \;=\; \hat{\mathbf{x}}\left(\xi^1, \xi^2, \zeta\right) = \mathbf{p}\left(\xi^1, \xi^2\right) + \zeta\, \mathbf{q}\left(\xi^1, \xi^2\right) \qquad for \;\; \zeta \in [-1, 1] \qquad (3.10)$$

To be more specific it has to note that $\mathbf{q}$ can be parametrized with respect to the thickness, thus
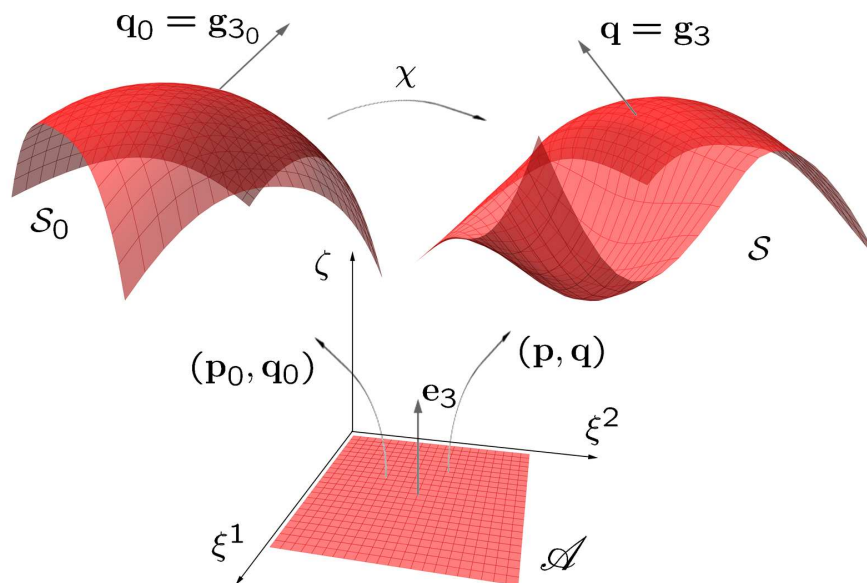
Figure 3.1: Geometry of an extensible one-director Cosserat surface.

** The interested reader could refer to Refs. [79, 80] for a detailed description of these models, or refer to the third part of this thesis where, as an application of the present theory, a swept aircraft wing, starting from a plate-like kinematic assumption, is modeled as a rod-like body including a number of non-classical effects such as the warping, the transverse shear flexibility and the anisotrpy of the material constituents.

emphasizing the extensibility feature of the fiber retained into the model, such that

$$\mathbf{q} \;=\; \hbar\left(\xi^1,\xi^2\right)\; \mathbf{m}\left(\xi^1,\xi^2\right) \tag{3.11}$$

where $\mathbf{m} \in \mathcal{U}$ with $\mathcal{U} := \{\mathbf{v} \in \mathcal{V}|\; \|\mathbf{v}\| = 1\}$ the sphere of all vectors having unit length. Moreover, because in the following it will be made often use of classical concepts of continuum mechanics (such as general co-ordinates, covariant and contra-variant vectors, covariant derivatives, etc) here a short summary of some of these concepts is reported.[††]

At the cost to be repetitive, with respect to the results already presented in Chapter (2),[‡‡] in the following sections the geometry of the main surface, and of the layer, in the actual configuration is presented and discussed. This repetition, limited to the definition of the surface geometry and metrics, is made necessary by the fact that the consideration of a director distinct from the normal in the actual configuration (and, eventually, in the reference configuration) leads to the introduction of new quantities whose meaning can be better understood starting from a reconsideration of the main surface and of the layer geometry. Specifically, one may assume that a general (or convected, or material) curvilinear co-ordinate system[*] $\{\xi^\alpha\}$ is defined on the main surface. Moreover, to take into account the "anormality" of the fiber in the actual configuration, one may decompose the fiber, in each point of co-ordinates $\{\xi^\alpha\}$ on the main surface, in the orthogonal sum of a vector $(h\,\mathbf{n})$ in the direction normal to the tangent plane, and of a vector lying in the tangent plane $(h\,\mathbf{l})$ and so orthogonal to $\mathbf{n}$. Consequently, one should define a second order tensor $(\mathbf{C}$, see later) measuring the variation of the fiber (in length and direction) on the main surface ranging over the surface. This tensor has to be compared with the curvature tensor $(\mathbf{B}$, see later) defined in the classical approach, and measuring the variation of the normal (in direction) on the main surface ranging over the surface.

3.2.1   Main surface geometry

Let the geometry of the main surface $\mathcal{S}$ be described by:

$$\mathcal{S} \;:=\; \left\{\mathbf{x} \in \Re^3\|\; \mathbf{x} = \mathbf{p} \;\; \text{with} \;\; \mathbf{p} : \mathscr{A} \mapsto \Re^3\right\} \tag{3.12}$$

[††] The interested reader is referred to Appendix (A) for a more detailed description of these concepts

[‡‡] Note that those results were relevant to a simple model for shell sharing with the present model a few basic concepts and the stategy for the obtainment of the equilibrium equations.

[*] Classically, theories of shells and rods have been introduced making use of the definition of a general co-ordinate system, often referred also as material or convected co-ordinates. Illustrious examples of this type of approach can be found in Refs.[53, 107, 108, 79, 36] and more recently in Refs. [97, 99, 23]. On the other side, in the modern literature the use of general co-ordinates is often avoided, in favour of the abstraction of the set theory, and manifolds, even if its physical meaning is particular apparent and useful for a immediate comprenhsion of the problem (cfr. Refs [69, 35, 33], and, in particular, Ref. [69] for a presentation and comparison of the two approaches).

or simply (*i.e.*, renouncing to the abstraction of the set theory)

$$\mathbf{x} \;=\; \mathbf{p}\left(\xi^1, \xi^2\right) \tag{3.13}$$

for $\{\xi^\alpha\} \in \mathscr{A} \subset \Re^2$, general curvilinear co-ordinates on $\mathcal{S}$. Note that, leaving ξ^1 (ξ^2) constant and varying ξ^2 (ξ^1), $\mathbf{p}$ describes a curve in $\Re^3$. These curves are referred to as material ξ^2 (ξ^1) lines, being the image in the actual configuration of the straight lines $\xi^1 = const$ $(\xi^2 = const)$ in $\mathscr{A}$.

The covariant base vectors on $\mathcal{S}$ (*i.e.*, the tangent vectors to the material lines on $\mathcal{S}$) are defined by:

$$\mathbf{a}_\alpha := \frac{\partial \mathbf{p}}{\partial \xi^\alpha} \tag{3.14}$$

The contravariant base vectors $\mathbf{a}^\beta$ can be defined by

$$\mathbf{a}_\alpha \cdot \mathbf{a}^\beta = \delta_\alpha^\beta \tag{3.15}$$

and

$$\mathbf{a}^\beta \cdot \mathbf{n} = 0 \tag{3.16}$$

Hence one has

$$\mathbf{a}^1 = \frac{\mathbf{a}_2 \times \mathbf{n}}{\sqrt{a}} \tag{3.17}$$

$$\mathbf{a}^2 = \frac{\mathbf{n} \times \mathbf{a}_1}{\sqrt{a}} \tag{3.18}$$

$$\mathbf{n} = \frac{\mathbf{a}_1 \times \mathbf{a}_2}{\sqrt{a}} \tag{3.19}$$

where

$$\sqrt{a} = \mathbf{a}_1 \times \mathbf{a}_2 \cdot \mathbf{n} = \|\mathbf{a}_1 \times \mathbf{a}_2\| \tag{3.20}$$

Their derivative is given by (first Weingarten and Gauss formula, see [53], p. 37, Eq. 1.13.47.a):

$$\frac{\partial \mathbf{a}_\alpha}{\partial \xi^\beta} = \frac{\partial^2 \mathbf{p}}{\partial \xi^\alpha \partial \xi^\beta} = \Gamma_{\alpha\beta}^\gamma \, \mathbf{a}_\gamma + b_{\alpha\beta} \, \mathbf{n} \tag{3.21}$$

where, by definition, the surface Christoffel symbols $\Gamma_{\alpha\beta}^\gamma$ are given by:

$$\Gamma_{\alpha\beta}^\gamma := \frac{\partial^2 \mathbf{p}}{\partial \xi^\alpha \partial \xi^\beta} \cdot \mathbf{a}^\gamma \tag{3.22}$$

and the covariant components of the second metric tensor:

$$b_{\alpha\beta} := \frac{\partial^2 \mathbf{p}}{\partial \xi^\alpha \partial \xi^\beta} \cdot \mathbf{n} \tag{3.23}$$

Let $\mathbf{n}$ be the surface unit normal. Hence, $\mathbf{n} \cdot \mathbf{a}_\beta = 0, \quad \mathbf{n} \cdot \mathbf{n} = 1$. Differentiating these with respect to ξ^α one obtains

$$\frac{\partial \mathbf{n}}{\partial \xi^\alpha} \cdot \mathbf{a}_\beta = -\mathbf{n} \cdot \frac{\partial \mathbf{a}_\beta}{\partial \xi^\alpha} = -b_{\alpha\beta} \tag{3.24}$$

and

$$\frac{\partial \mathbf{n}}{\partial \xi^\alpha} \cdot \mathbf{n} = 0 \tag{3.25}$$

Hence (second formula of Weingarten and Gauss, [53], p. 37, Eq. 1.13.47.c):

$$\frac{\partial \mathbf{n}}{\partial \xi^\alpha} = -b_{\alpha\beta}\mathbf{a}^\beta = -b_\alpha^\beta \mathbf{a}_\beta \tag{3.26}$$

Alternatively, using a direct (absolute) notation one can state

$$\mathbf{B} \quad := \quad - \operatorname{Grad} \mathbf{n} = -\mathbf{a}^\alpha \otimes \frac{\partial \mathbf{n}}{\partial \xi^\alpha} = -b_{\alpha\beta} \, \mathbf{a}^\alpha \otimes \mathbf{a}^\beta = -b_\alpha^\beta \, \mathbf{a}^\alpha \otimes \mathbf{a}_\beta \tag{3.27}$$

which represents the curvature tensor on $\mathcal{S}$.

3.2.2   Layer geometry

Recalling Eq. (3.10) the layer base vectors are defined by

$$\mathbf{g}_\alpha := \frac{\partial \hat{\mathbf{x}}}{\partial \xi^\alpha} = \frac{\partial \mathbf{p}}{\partial \xi^\alpha} + \zeta \, \frac{\partial (\hbar \, \mathbf{m})}{\partial \xi^\alpha} \tag{3.28}$$

Also,

$$\mathbf{g}_3 := \frac{\partial \hat{\mathbf{x}}}{\partial \zeta} = \hbar \, \mathbf{m} \tag{3.29}$$

In order to compare the present model with the classical one presented in Chapter (2), the following decomposition for $\mathbf{g}_3$ is here introduced

$$\mathbf{g}_3 = \hbar \, \mathbf{m} = h \, (\mathbf{n} + \mathbf{l}) \tag{3.30}$$

where h ($h := \hbar\, \mathbf{m} \cdot \mathbf{n}$) is the semi-thickness of the shell in $\{\xi^\alpha\}$ (measured, by definition, along the normal in $\{\xi^\alpha\}$), whereas $\hbar$ is the semi-length of the fiber (*i.e.*, a sort of thickness measured along the fiber). Finally, $\mathbf{l}$ ($\mathbf{l} = l^\gamma\, \mathbf{a}_\gamma = \mathbf{l} \cdot \mathbf{a}^\gamma\, \mathbf{a}_\gamma$) is a vector lying in the tangent plane to $\mathcal{S}$ in $\{\xi^\alpha\}$, that measures the inclination of the fiber with respect to the normal. Note that, being $\mathbf{m} \in \mathcal{U}$ (*i.e.*, a unit vector), the following relation for the length of $\mathbf{l}$ holds

$$\mathbf{m} \cdot \mathbf{m} = 1 = \frac{h^2}{\hbar^2}\left(1 + l^2\right) \qquad \Longrightarrow \qquad l := \|\mathbf{l}\| = \sqrt{1 - \frac{h^2}{\hbar^2}} \tag{3.31}$$

For further utilization, it is important to consider the expressions of the layer base vectors on the main surface[†]

$$\overset{\circ}{\mathbf{g}}_k \;\; := \;\; \mathbf{g}_k|_{\zeta=0} \tag{3.32}$$

or

$$\overset{\circ}{\mathbf{g}}_\alpha \;\; := \;\; \mathbf{a}_k \qquad and \qquad \overset{\circ}{\mathbf{g}}_3 = \mathbf{g}_3 \tag{3.33}$$

This triad of vectors play a central role in our subsequent developments and define a particular frame: the so-called *Surface convected frame*.[‡] Also recall that the contravariant base vectors are defined by

$$\mathbf{g}_h \cdot \mathbf{g}^k = \delta_h^k \tag{3.34}$$

i.e.,

$$\mathbf{g}^1 = \frac{\mathbf{g}_2 \times \mathbf{g}_3}{\sqrt{g}} \tag{3.35}$$

$$\mathbf{g}^2 = \frac{\mathbf{g}_3 \times \mathbf{g}_1}{\sqrt{g}} \tag{3.36}$$

$$\mathbf{g}^3 = \frac{\mathbf{g}_1 \times \mathbf{g}_2}{\sqrt{g}} \tag{3.37}$$

with

$$\sqrt{g} = \mathbf{g}_1 \times \mathbf{g}_2 \cdot \mathbf{g}_3 \tag{3.38}$$

[†] The upper upper o ($\circ$) over the present kinematical descriptors serves to differentiate them from those defined on the volume base and the surface natural frame, which are marked by an upper bar ($^-$). Similar distinction will be taken into account also in the following developments to differentiate the work-conjugate dynamical descriptors.

[‡] Note that this concept has already been introduced in Ref. [97], where in addition to the fixed inertial frame, two different reference frames on the mid-surface have been introduced: exactly the *Surface convected frame* , and the *Director orthogonal frame* (here not considered).

Similarly, the contravariant volume basis vectors ($\overset{\circ}{\mathbf{g}}{}^{k} = \mathbf{g}^{k}|_{\zeta=0}$) are

$$
\begin{cases}
\overset{\circ}{\mathbf{g}}{}^{1} := \dfrac{\overset{\circ}{\mathbf{g}}_{2} \times \overset{\circ}{\mathbf{g}}_{3}}{\sqrt{\overset{\circ}{g}}} = \mathbf{a}^{1} - l^{1}\,\mathbf{n} \\[4ex]
\overset{\circ}{\mathbf{g}}{}^{2} := \dfrac{\overset{\circ}{\mathbf{g}}_{3} \times \overset{\circ}{\mathbf{g}}_{1}}{\sqrt{\overset{\circ}{g}}} = \mathbf{a}^{2} - l^{2}\,\mathbf{n}
\end{cases}
\qquad\Longrightarrow\qquad \overset{\circ}{\mathbf{g}}{}^{\alpha} = \mathbf{a}^{\alpha} - l^{\alpha}\,\mathbf{n}
\tag{3.39}
$$

whereas for $\overset{\circ}{\mathbf{g}}{}^{3}$ one has

$$
\overset{\circ}{\mathbf{g}}{}^{3} = \frac{\mathbf{n}}{h}
\tag{3.40}
$$

where it has been considered that, using Eq. (3.30), one has

$$
\sqrt{\overset{\circ}{g}} = \overset{\circ}{\mathbf{g}}_{1} \times \overset{\circ}{\mathbf{g}}_{2} \cdot \overset{\circ}{\mathbf{g}}_{3} = h\,\sqrt{a}
\tag{3.41}
$$

It is worth noting that the contravariant vectors $\overset{\circ}{\mathbf{g}}{}^{1}$ and $\overset{\circ}{\mathbf{g}}{}^{2}$ lie in a plane inclined with respect to the tangent plane of $(-\mathbf{l} \cdot \mathbf{a}_{\beta})\,\mathbf{l}$. In other words, they identify the plane normal to the fiber in $\{\xi^{\alpha}\}$. The previous observation is particularly important being the basis of the following developments.

Before proceeding further, let us note that Eq. (3.28) may be conveniently expressed in terms of the surface base vectors using Eqs. (3.30) and (3.23). Indeed, one has

$$
\mathbf{g}_{\alpha} := \left\{ \delta_{\alpha}^{\beta} - \zeta\,\left[h\,b_{\alpha}^{\beta} - \left(h\,l^{\beta} \right)_{/\alpha} \right] \right\}\,\mathbf{a}_{\beta} + \zeta\,\left(h_{/\alpha} + h\,b_{\alpha\gamma}\,l^{\gamma} \right)\,\mathbf{n}
\tag{3.42}
$$

Equation (3.42) may be recast appealing to the definition of shifters. In particular, one can define the shifters between the volume and surface covariant vectors, and the surface and volume contravariant vectors in the following way

$$
\begin{cases}
\mathbf{g}_{h} = \mathscr{T}_{h}^{k}\,\mathbf{a}_{k} \\[1ex]
\mathbf{a}^{k} = \mathscr{T}_{h}^{k}\,\mathbf{g}^{h}
\end{cases}
\qquad\Longrightarrow\qquad \mathscr{T}_{h}^{k} := \mathbf{g}_{h} \cdot \mathbf{a}^{k}
\tag{3.43}
$$

thus

$$
\mathbf{g}_{k} = \mathscr{T}_{k}^{\beta}\,\mathbf{a}_{\beta} + \mathscr{T}_{k}^{3}\,\mathbf{n}
\tag{3.44}
$$

where, using Eqs. (3.28) and (3.29), one has:

$$\mathscr{T}^{\beta}_{\alpha} := \mathbf{g}_{\alpha} \cdot \mathbf{a}^{\beta} = \delta^{\beta}_{\alpha} - \zeta \left[h \, b^{\beta}_{\alpha} - \left(h \, l^{\beta} \right)_{/\alpha} \right] \tag{3.45}$$

$$\mathscr{T}^{3}_{\alpha} := \mathbf{g}_{\alpha} \cdot \mathbf{n} = \zeta \left(h_{/\alpha} + b_{\alpha\beta} \, h \, l^{\beta} \right) \tag{3.46}$$

$$\mathscr{T}^{\alpha}_{3} := \mathbf{g}_{3} \cdot \mathbf{a}^{\beta} = h \, l^{\beta} \tag{3.47}$$

$$\mathscr{T}^{3}_{3} := \mathbf{g}_{3} \cdot \mathbf{n} = h \tag{3.48}$$

Similarly, using Eq. (3.30) one may express the volume base vectors in terms of their components on the volume base vectors at the middle surface, *i.e.*,

$$\mathbf{g}_{\alpha} := \left[\delta^{\beta}_{\alpha} - \zeta \, h \left(b^{\beta}_{\alpha} - l^{\beta}_{/\alpha} + b_{\alpha\gamma} \, l^{\gamma} \, l^{\beta} \right) \right] \overset{\circ}{\mathbf{g}}_{\beta} + \zeta \left(\frac{h_{/\alpha}}{h} + b_{\alpha\gamma} \, l^{\gamma} \right) \overset{\circ}{\mathbf{g}}_{3} \tag{3.49}$$

Again, introducing the definition of shifters between the volume base vectors and the surface convected frame as

$$\begin{cases} \mathbf{g}_{h} = \overset{\circ}{\mathscr{T}}{}^{k}_{h} \, \overset{\circ}{\mathbf{g}}_{k} \\ \overset{\circ}{\mathbf{g}}{}^{k} = \overset{\circ}{\mathscr{T}}{}^{k}_{h} \, \mathbf{g}^{h} \end{cases} \implies \overset{\circ}{\mathscr{T}}{}^{k}_{h} := \mathbf{g}_{h} \cdot \overset{\circ}{\mathbf{g}}{}^{k} \tag{3.50}$$

one has

$$\mathbf{g}_{k} = \overset{\circ}{\mathscr{T}}{}^{\beta}_{k} \, \overset{\circ}{\mathbf{g}}_{\beta} + \overset{\circ}{\mathscr{T}}{}^{3}_{k} \, \overset{\circ}{\mathbf{g}}_{3} \tag{3.51}$$

where, using Eqs. (3.49) and (3.40), one has:

$$\overset{\circ}{\mathscr{T}}{}^{\beta}_{\alpha} := \mathbf{g}_{\alpha} \cdot \overset{\circ}{\mathbf{g}}{}^{\beta} = \delta^{\beta}_{\alpha} - \zeta \, h \left(b^{\beta}_{\alpha} - l^{\beta}_{/\alpha} + b_{\alpha\gamma} \, l^{\gamma} \, l^{\beta} \right) \tag{3.52}$$

$$\overset{\circ}{\mathscr{T}}{}^{3}_{\alpha} := \mathbf{g}_{\alpha} \cdot \overset{\circ}{\mathbf{g}}{}^{3} = \zeta \left(\frac{h_{/\alpha}}{h} + b_{\alpha\beta} l^{\beta} \right) \tag{3.53}$$

$$\overset{\circ}{\mathscr{T}}{}^{\alpha}_{3} := \mathbf{g}_{3} \cdot \overset{\circ}{\mathbf{g}}{}^{\beta} = 0 \tag{3.54}$$

$$\overset{\circ}{\mathscr{T}}{}^{3}_{3} := \mathbf{g}_{3} \cdot \overset{\circ}{\mathbf{g}}{}^{3} = 1 \tag{3.55}$$

3.2.3 Derivatives of the base vectors

In the following section the derivatives of the layer base vectors, of the vectors of the surface natural frame and of the surface convected frame, and their reciprocals (*i.e.*, the contravariant vectors), are reported. Their importance will appear clearly in the following sections because they enter into the definition of the Gradient (both 3-D and 2-D) of a vector and tensor field, thus, they will be instrumental for obtaining of the equilibrium equations for micro-structured continua starting from the Principle of Virtual Work.

The layer base vectors

$$\frac{\partial \mathbf{a}_\alpha}{\partial \xi^\beta} = \frac{\partial^2 \mathbf{p}}{\partial \xi^\alpha \partial \xi^\beta} = \Gamma^\gamma_{\alpha\beta} \, \mathbf{a}_\gamma + b_{\alpha\beta} \, \mathbf{n} \tag{3.56}$$

where, by definition, the surface Christoffel symbols $\Gamma^\gamma_{\alpha\beta}$ are given by:

$$\Gamma^\gamma_{\alpha\beta} := \frac{\partial^2 \mathbf{p}}{\partial \xi^\alpha \partial \xi^\beta} \cdot \mathbf{a}^\gamma \tag{3.57}$$

and the covariant components of the second metric tensor:

$$b_{\alpha\beta} := \frac{\partial^2 \mathbf{p}}{\partial \xi^\alpha \partial \xi^\beta} \cdot \mathbf{n} \tag{3.58}$$

Let $\mathbf{n}$ be the surface unit normal. Hence, $\mathbf{n} \cdot \mathbf{a}_\beta = 0, \quad \mathbf{n} \cdot \mathbf{n} = 1$. Differentiating these with respect to ξ^α one obtains

$$\frac{\partial \mathbf{n}}{\partial \xi^\alpha} \cdot \mathbf{a}_\beta = -\mathbf{n} \cdot \frac{\partial \mathbf{a}_\beta}{\partial \xi^\alpha} = -b_{\alpha\beta} \tag{3.59}$$

and

$$\frac{\partial \mathbf{n}}{\partial \xi^\alpha} \cdot \mathbf{n} = 0 \tag{3.60}$$

Hence (second formula of Weingarten and Gauss, [53], p. 37, Eq. 1.13.47.c):

$$\frac{\partial \mathbf{n}}{\partial \xi^\alpha} = -b_{\alpha\beta}\mathbf{a}^\beta = -b^\beta_\alpha\mathbf{a}_\beta \tag{3.61}$$

The surface natural frame

Recall the derivatives of the surface base vectors introduced in Eqs. (3.21)–(3.26). In particular, the curvature tensor is such that

$$\frac{\partial \mathbf{a}_\alpha}{\partial \xi^\beta} = \Gamma^\beta_{\gamma\alpha}\mathbf{a}_\gamma + b_{\alpha\beta} \, \mathbf{n} \tag{3.62}$$

$$\frac{\partial \mathbf{a}^\alpha}{\partial \xi^\beta} = -\Gamma^\beta_{\gamma\alpha}\mathbf{a}^\gamma + b^\alpha_\beta \, \mathbf{n} \tag{3.63}$$

and

$$\frac{\partial \mathbf{n}}{\partial \xi^\beta} = -b_{\alpha\beta} \, \mathbf{n} = -b^\alpha_\beta \, \mathbf{n} \tag{3.64}$$

where the Christoffel symbols of the second kind, the equality $\mathbf{a}_3 = \mathbf{a}^3 = \mathbf{n}$, and the following equation have been used

$$\Gamma^\gamma_{\alpha\beta} := \frac{\partial \mathbf{a}_\alpha}{\partial \xi^\beta} \cdot \mathbf{a}^\gamma = -\mathbf{a}_\alpha \cdot \frac{\partial \mathbf{a}^\gamma}{\partial \xi^\beta} \tag{3.65}$$

Moreover, note that

$$\Gamma^\alpha_{\alpha\gamma} = \frac{1}{\sqrt{a}} \frac{\partial \sqrt{a}}{\partial \xi^\gamma} \tag{3.66}$$

Indeed

$$
\begin{aligned}
\frac{\partial \sqrt{a}}{\partial \xi^\gamma} &= \frac{\partial}{\partial \xi^\gamma} (\mathbf{a}_1 \times \mathbf{a}_2 \cdot \mathbf{n}) = \\
&= \frac{\partial \mathbf{a}_1}{\partial \xi^\gamma} \cdot \mathbf{a}_2 \times \mathbf{n} + \frac{\partial \mathbf{a}_2}{\partial \xi^\gamma} \cdot \mathbf{n} \times \mathbf{a}_1 + \frac{\partial \mathbf{n}}{\partial \xi^\gamma} \cdot \mathbf{a}_1 \times \mathbf{a}_2 \\
&= \sqrt{a} \, \Gamma^\beta_{1\gamma} \, \mathbf{a}_\beta \cdot \mathbf{a}^1 + \sqrt{a} \, \Gamma^\beta_{2\gamma} \, \mathbf{a}_\beta \cdot \mathbf{a}^2 = \sqrt{a} \, \Gamma^\alpha_{\alpha\gamma}
\end{aligned} \tag{3.67}
$$

The surface convected frame

Finally, consider the derivative of the base vectors of the surface convected frame. In general, one has

$$\frac{\partial \overset{\circ}{\mathbf{g}}_k}{\partial \xi^p} = \overset{\circ}{\Gamma}{}^h_{kp} \overset{\circ}{\mathbf{g}}_h \tag{3.68}$$

where

$$\overset{\circ}{\Gamma}{}^h_{kp} := \frac{\partial \overset{\circ}{\mathbf{g}}_k}{\partial \xi^p} \cdot \overset{\circ}{\mathbf{g}}{}^h \tag{3.69}$$

In particular

$$\frac{\partial \overset{\circ}{\mathbf{g}}_\alpha}{\partial \xi^\beta} = \overset{\circ}{\Gamma}{}^\gamma_{\alpha\beta} \overset{\circ}{\mathbf{g}}_\gamma + \overset{\circ}{\Gamma}{}^3_{\alpha\beta} \overset{\circ}{\mathbf{g}}_3 = \overset{\circ}{\Gamma}{}^\gamma_{\alpha\beta} \overset{\circ}{\mathbf{g}}_\gamma + c_{\alpha\beta} \overset{\circ}{\mathbf{g}}_3 = \Gamma^\gamma_{\alpha\beta} \mathbf{a}_\gamma + b_{\alpha\beta} \mathbf{n} \tag{3.70}$$

thus dotting by $\mathbf{a}^\gamma$ and $\mathbf{n}$ one obtains

$$\Gamma^\gamma_{\alpha\beta} = \overset{\circ}{\Gamma}{}^\gamma_{\alpha\beta} + c_{\alpha\beta} \, h \, l^\gamma \tag{3.71}$$

$$b_{\alpha\beta} = c_{\alpha\beta} \, h \tag{3.72}$$

where $c_{\alpha\beta}$ are the components of an equivalent curvature tensor (indeed, they are related to the components of the curvature tensor through Eq. (3.72)) whose definition is necessary as soon as a

projection on the surface convected frame is considered. In particular one has,

$$c_{\alpha\beta} := \overset{\circ}{\Gamma}{}^{3}_{\alpha\beta} := \frac{\partial \overset{\circ}{\mathbf{g}}_\alpha}{\partial \xi^\beta} \cdot \overset{\circ}{\mathbf{g}}{}^{3} = -\frac{\partial \overset{\circ}{\mathbf{g}}{}^{3}}{\partial \xi^\beta} \cdot \overset{\circ}{\mathbf{g}}_\alpha \tag{3.73}$$

Similarly, for the derivative of $\overset{\circ}{\mathbf{g}}_3$, one has

$$\frac{\partial \overset{\circ}{\mathbf{g}}_3}{\partial \xi^\alpha} = \overset{\circ}{\Gamma}{}^{\beta}_{3\alpha} \, \overset{\circ}{\mathbf{g}}_\beta + \overset{\circ}{\Gamma}{}^{3}_{3\alpha} \, \overset{\circ}{\mathbf{g}}_3 = - \, c^\beta_\alpha \, \overset{\circ}{\mathbf{g}}_\beta + d_\alpha \, \overset{\circ}{\mathbf{g}}_3 \tag{3.74}$$

where

$$- c^\beta_\alpha := \overset{\circ}{\Gamma}{}^{\beta}_{3\alpha} := \frac{\partial \overset{\circ}{\mathbf{g}}_3}{\partial \xi^\alpha} \cdot \overset{\circ}{\mathbf{g}}{}^{\beta} = -h \left(b^\beta_\alpha - l^\beta_{/\alpha} + b_{\alpha\gamma} \, l^\gamma \, l^\beta \right) \tag{3.75}$$

$$d_\alpha := \overset{\circ}{\Gamma}{}^{3}_{3\alpha} := \frac{\partial \overset{\circ}{\mathbf{g}}_3}{\partial \xi^\alpha} \cdot \overset{\circ}{\mathbf{g}}{}^{3} = \frac{h_{/\alpha}}{h} + b_{\alpha\beta} \, l^\beta \tag{3.76}$$

Indeed,

$$\begin{aligned}
\frac{\partial \mathbf{g}_3}{\partial \xi^\alpha} &= \frac{\partial}{\partial \xi^\alpha} \left[h \, (\mathbf{n} + \mathbf{l}) \right] = h_{/\alpha} \, (\mathbf{n} + \mathbf{l}) - h \left(b^\beta_\alpha - l^\beta_{/\alpha} \right) \mathbf{a}_\beta + h \, b_{\alpha\beta} \, l^\beta \, \mathbf{n} \\
&= -h \left(b^\beta_\alpha - l^\beta_{/\alpha} + b_{\alpha\gamma} \, l^\gamma \, l^\beta \right) \overset{\circ}{\mathbf{g}}_\beta + \left(\frac{h_{/\alpha}}{h} + b_{\alpha\beta} \, l^\beta \right) \overset{\circ}{\mathbf{g}}_3
\end{aligned} \tag{3.77}$$

Note that Eqs. (3.70)-(3.76) may be regarded as a generalization of Gauss' Weingarten's formulae, and the tensor $\mathbf{C}$ a generalization of the curvature tensor. Accordingly, one can define $\mathbf{C}$ in the following way (cfr. Eq. (3.27))

$$\mathbf{C} := c_{\alpha\beta} \, \overset{\circ}{\mathbf{g}}{}^{\alpha} \otimes \overset{\circ}{\mathbf{g}}{}^{\beta} = c^\beta_\alpha \, \overset{\circ}{\mathbf{g}}{}^{\alpha} \otimes \overset{\circ}{\mathbf{g}}_\beta \tag{3.78}$$

Finally, for later reference let us consider that

$$\overset{\circ}{\Gamma}{}^{k}_{\alpha k} = \frac{1}{\sqrt{\overset{\circ}{g}}} \frac{\partial \sqrt{\overset{\circ}{g}}}{\partial \xi^\gamma} \tag{3.79}$$

Indeed

$$\begin{aligned}
\frac{\partial \sqrt{\overset{\circ}{g}}}{\partial \xi^\gamma} &= \frac{\partial}{\partial \xi^\gamma} \left(\overset{\circ}{\mathbf{g}}_1 \times \overset{\circ}{\mathbf{g}}_2 \cdot \overset{\circ}{\mathbf{g}}_3 \right) = \\
&= \frac{\partial \overset{\circ}{\mathbf{g}}_1}{\partial \xi^\gamma} \cdot \overset{\circ}{\mathbf{g}}_2 \times \overset{\circ}{\mathbf{g}}_3 + \frac{\partial \overset{\circ}{\mathbf{g}}_2}{\partial \xi^\gamma} \cdot \overset{\circ}{\mathbf{g}}_3 \times \overset{\circ}{\mathbf{g}}_1 + \frac{\partial \overset{\circ}{\mathbf{g}}_3}{\partial \xi^\gamma} \cdot \overset{\circ}{\mathbf{g}}_1 \times \overset{\circ}{\mathbf{g}}_2 \\
&= \sqrt{\overset{\circ}{g}} \, \overset{\circ}{\Gamma}{}^{k}_{1\gamma} \, \overset{\circ}{\mathbf{g}}_k \cdot \overset{\circ}{\mathbf{g}}{}^{1} + \sqrt{\overset{\circ}{g}} \, \overset{\circ}{\Gamma}{}^{k}_{2\gamma} \, \overset{\circ}{\mathbf{g}}_k \cdot \overset{\circ}{\mathbf{g}}{}^{2} + \sqrt{\overset{\circ}{g}} \, \overset{\circ}{\Gamma}{}^{k}_{3\gamma} \, \overset{\circ}{\mathbf{g}}_k \cdot \overset{\circ}{\mathbf{g}}{}^{3} = \sqrt{\overset{\circ}{g}} \, \overset{\circ}{\Gamma}{}^{k}_{k\gamma}
\end{aligned} \tag{3.80}$$

3.3   Covariant derivatives

3.3.1   The surface natural frame

Recalling the definitions for the shifters between the volume and surface covariant vectors, and their reciprocal (see Eq. (3.43)), one can express a generic vector field $\mathbf{v}$ in terms of its components on the surface or volume base vectors as

$$
\begin{aligned}
\mathbf{v} &= \bar{v}^\alpha \, \mathbf{g}_\alpha + \bar{v}^3 \, \mathbf{g}_3 & \mathbf{v} &= v_\alpha \mathbf{a}^\alpha + v_3 \mathbf{n} \\
&= \left(\bar{v}^\alpha \, \mathscr{T}_\alpha^\beta + \bar{v}^3 \, \mathscr{T}_3^\beta \right) \mathbf{a}_\beta & &= \left(v_\alpha \, \mathscr{T}_\alpha^\beta + v_3 \, \mathscr{T}_3^\beta \right) \mathbf{g}^\beta \\
&\quad + \left(\bar{v}^\alpha \, \mathscr{T}_\alpha^3 + \bar{v}^3 \, \mathscr{T}_3^3 \right) \mathbf{n} & &\quad + \left(v_\alpha \, \mathscr{T}_\alpha^3 + v_3 \, \mathscr{T}_3^3 \right) \mathbf{g}^3
\end{aligned}
\tag{3.81}
$$

where with an upper bar $(\bar{})$ it has been denoted the components of the vector field referred to the volume base vectors. Comparing Eqs. (3.81) one can obtain the following results which explain the role of the shifters in terms of the components of a generic vector field

$$
\bar{v}^k = \mathscr{T}_h^k \, v^h \qquad v_h = \mathscr{T}_h^k \, \bar{v}_{(k)}
\tag{3.82}
$$

Contravariant Components

The covariant derivative of a generic vector field in a 3-D Riemannian manifold (*i.e.*, using the volume metric defined in the space) is given by

$$
\frac{\partial \mathbf{v}}{\partial \xi^\alpha} = \bar{v}^h_{\|\alpha} \, \mathbf{g}_h = \bar{v}^h_{\|\alpha} \, \mathscr{T}_h^\gamma \, \mathbf{a}_\gamma + \bar{v}^h_{\|\alpha} \, \mathscr{T}_h^3 \, \mathbf{n}
\tag{3.83}
$$

$$
\frac{\partial \mathbf{v}}{\partial \zeta} = \bar{v}^h_{\|3} \, \mathbf{g}_h = \bar{v}^h_{\|3} \, \mathscr{T}_h^\gamma \, \mathbf{a}_\gamma + \bar{v}^h_{\|3} \, \mathscr{T}_h^3 \, \mathbf{n}
\tag{3.84}
$$

where with the double vertical dash $(_\|)$ it has been denoted the covariant derivative with respect to the volume metrics.

Similarly, using the surface metrics one has

$$
\frac{\partial \mathbf{v}}{\partial \xi^\alpha} = \left(v^\beta_{/\alpha} - b^\beta_\alpha \, v^3 \right) \mathbf{a}_\beta + \left(b_{\alpha\beta} \, v^\beta + v^3_{,\alpha} \right) \mathbf{n}
\tag{3.85}
$$

$$
\frac{\partial \mathbf{v}}{\partial \zeta} = v^\beta_{,3} \, \mathbf{a}_\beta + v^3_{,3} \, \mathbf{n}
\tag{3.86}
$$

where the slash $(_/)$ denotes covariant derivative with respect to the surface metrics and the comma $(_,)$ partial derivative with respect to the co-ordinate ζ. In particular, recall that the covariant derivative of a vector with respect to the surface natural frame can be defined

$$
v^\beta_{/\alpha} := v^\beta_{,\alpha} + v^\gamma \, \Gamma^\beta_{\gamma\alpha}
\tag{3.87}
$$

From the comparison of Eqs. (3.83)–(3.86) one has

$$\bar{v}^h_{\|\alpha} \; \mathscr{T}^\gamma_h \;\; = \;\; v^\beta_{/\alpha} - b^\beta_\alpha \, v^3 \tag{3.88}$$

$$\bar{v}^h_{\|\alpha} \; \mathscr{T}^3_h \;\; = \;\; b_{\alpha\beta} \, v^\beta + v^3_{,\alpha} \tag{3.89}$$

$$\bar{v}^h_{\|3} \; \mathscr{T}^\gamma_h \;\; = \;\; v^\gamma_{,3} \tag{3.90}$$

$$\bar{v}^h_{\|3} \; \mathscr{T}^3_h \;\; = \;\; v^3_{,3} \tag{3.91}$$

Covariant Components

The covariant derivative of a generic vector field in a 3-D Riemannian manifold using its covariant components is given by

$$\frac{\partial \mathbf{v}}{\partial \xi^\alpha} \;\; = \;\; \bar{v}_{h\|\alpha} \, \mathbf{g}^h = \bar{v}_{\gamma\|\alpha} \, \mathbf{g}^\gamma + \bar{v}_{3\|\alpha} \, \mathbf{g}^3 \tag{3.92}$$

$$\frac{\partial \mathbf{v}}{\partial \zeta} \;\; = \;\; \bar{v}_{h\|3} \, \mathbf{g}_h = \bar{v}_{\gamma\|3} \, \mathbf{g}^\gamma + \bar{v}_{3\|3} \, \mathbf{g}^3 \tag{3.93}$$

Similarly, using the surface metrics one has

$$
\begin{aligned}
\frac{\partial \mathbf{v}}{\partial \xi^\alpha} \;\; &= \;\; \left(v_{\beta/\alpha} - b_{\alpha\beta} \, v_3 \right) \mathbf{a}^\beta + \left(b^\beta_\alpha \, v_\beta + v_{3,\alpha} \right) \mathbf{n} \\
&= \;\; \left[\left(v_{\beta/\alpha} - b_{\alpha\beta} \, v_3 \right) \mathscr{T}^\beta_\gamma \; + \left(b^\beta_\alpha \, v_\beta + v_{3,\alpha} \right) \mathscr{T}^3_\gamma \, \right] \mathbf{g}^\gamma \\
&\;\; + \;\; \left[\left(v_{\beta/\alpha} - b_{\alpha\beta} \, v_3 \right) \mathscr{T}^\beta_3 \; + \left(b^\beta_\alpha \, v_\beta + v_{3,\alpha} \right) \mathscr{T}^3_3 \, \right] \mathbf{g}^3
\end{aligned}
\tag{3.94}
$$

$$
\begin{aligned}
\frac{\partial \mathbf{v}}{\partial \zeta} \;\; &= \;\; v_{\beta,3} \, \mathbf{a}_\beta + v_{3,3} \, \mathbf{n} \\
&= \;\; \left(v_{\beta,3} \, \mathscr{T}^\beta_\gamma \; + v_{3,3} \, \mathscr{T}^3_\gamma \, \right) \mathbf{g}^\gamma + \left(v_{\beta,3} \, \mathscr{T}^\beta_3 \; + v_{3,3} \, \mathscr{T}^3_3 \, \right) \mathbf{g}^3
\end{aligned}
\tag{3.95}
$$

From the comparison of Eqs. (3.92)–(3.95) one has

$$\bar{v}_{\gamma\|\alpha} \;\; = \;\; \left(v_{\beta/\alpha} - b_{\alpha\beta} \, v_3 \right) \mathscr{T}^\beta_\gamma \; + \left(b^\beta_\alpha \, v_\beta + v_{3,\alpha} \right) \mathscr{T}^3_\gamma \tag{3.96}$$

$$\bar{v}_{3\|\alpha} \;\; = \;\; \left(v_{\beta/\alpha} - b_{\alpha\beta} \, v_3 \right) \mathscr{T}^\beta_3 \; + \left(b^\beta_\alpha \, v_\beta + v_{3,\alpha} \right) \mathscr{T}^3_3 \tag{3.97}$$

$$\bar{v}_{\gamma\|3} \;\; = \;\; v_{\beta,3} \, \mathscr{T}^\beta_\gamma \; + v_{3,3} \, \mathscr{T}^3_\gamma \tag{3.98}$$

$$\bar{v}_{3\|3} \;\; = \;\; v_{\beta,3} \, \mathscr{T}^\beta_3 \; + v_{3,3} \, \mathscr{T}^3_3 \tag{3.99}$$

Finally, some relations, that will be useful for the subsequent developments, are here reported

$$\frac{\partial}{\partial \xi^\alpha} \left(\sqrt{a} \, \kappa^{\alpha\beta} \, \mathbf{a}_\beta \right) = \sqrt{a} \, \kappa^{\alpha\beta}_{/\alpha} \, \mathbf{a}_\beta + \sqrt{a} \, b_{\alpha\gamma} \, \kappa^{\alpha\gamma} \, \mathbf{n} \tag{3.100}$$

$$\frac{\partial}{\partial \xi^\alpha} \left(\sqrt{a} \, \kappa^{\alpha 3} \, \mathbf{n} \right) = -\sqrt{a} \, \kappa^{\alpha 3} \, b^\beta_\alpha \, \mathbf{a}_\beta + \sqrt{a} \, \kappa^{\alpha 3}_{/\alpha} \, \mathbf{n} \tag{3.101}$$

3.3.2   The surface convected frame

Recalling the definitions for the shifters between the volume and vectors of the surface convected frame, and their reciprocal (see Eq. (3.50)), one can express a generic vector field $\mathbf{v}$ in terms of its components on the surface convected frame or volume base vectors as

$$
\begin{aligned}
\mathbf{v} &= \bar{v}^\alpha\,\mathbf{g}_\alpha + \bar{v}^3\,\mathbf{g}_3 & \mathbf{v} &= \mathring{v}_\alpha\mathring{\mathbf{g}}^\alpha + \mathring{v}_3\mathring{\mathbf{g}}^3 \\
&= \left(\bar{v}^\alpha\,\mathring{\mathscr{T}}_\alpha^{\ \beta} + \bar{v}^3\,\mathring{\mathscr{T}}_3^{\ \beta}\right)\mathring{\mathbf{g}}_\beta & &= \left(\mathring{v}_\alpha\,\mathring{\mathscr{T}}_\alpha^{\ \beta} + \mathring{v}_3\,\mathring{\mathscr{T}}_3^{\ \beta}\right)\mathbf{g}^\beta \\
&+ \left(\bar{v}^\alpha\,\mathring{\mathscr{T}}_\alpha^{\ 3} + \bar{v}^3\,\mathring{\mathscr{T}}_3^{\ 3}\right)\mathring{\mathbf{g}}_3 & &+ \left(\mathring{v}_\alpha\,\mathring{\mathscr{T}}_\alpha^{\ 3} + \mathring{v}_3\,\mathring{\mathscr{T}}_3^{\ 3}\right)\mathbf{g}^3
\end{aligned} \tag{3.102}
$$

where an upper bar (¯) serves to indicate that the components of the vector field are referred to the volume base vectors and with a upper o (∘) those referred to the surface convected frame vectors. Comparing Eqs. (3.102) one can obtain the following results which explain the role of the shifters in terms of the components of a generic vector field

$$
\bar{v}^k = \mathring{\mathscr{T}}_h^{\ k}\,\mathring{v}^h \qquad \mathring{v}_h = \mathring{\mathscr{T}}_h^{\ k}\,\bar{v}_{(k)} \tag{3.103}
$$

Contravariant Components

The covariant derivative of a generic vector field in a 3-D Riemannian manifold (*i.e.*, using the volume metric defined in the space) is given by

$$
\frac{\partial \mathbf{v}}{\partial \xi^\alpha} = \bar{v}^h_{\|\alpha}\,\mathbf{g}_h = \bar{v}^h_{\|\alpha}\,\mathring{\mathscr{T}}_h^{\ \gamma}\,\mathring{\mathbf{g}}_\gamma + \bar{v}^h_{\|\alpha}\,\mathring{\mathscr{T}}_h^{\ 3}\,\mathring{\mathbf{g}}_3 \tag{3.104}
$$

$$
\frac{\partial \mathbf{v}}{\partial \zeta} = \bar{v}^h_{\|3}\,\mathbf{g}_h = \bar{v}^h_{\|3}\,\mathring{\mathscr{T}}_h^{\ \gamma}\,\mathring{\mathbf{g}}_\gamma + \bar{v}^h_{\|3}\,\mathring{\mathscr{T}}_h^{\ 3}\,\mathring{\mathbf{g}}_3 \tag{3.105}
$$

where the double vertical dash ($_\|$) denotes the covariant derivative with respect to the volume metrics.

Similarly, using the metrics associated to the surface convected frame one has

$$
\frac{\partial \mathbf{v}}{\partial \xi^\alpha} = \left(\mathring{v}^\beta_{\angle\alpha} - c^\beta_\alpha\,\mathring{v}^3\right)\mathring{\mathbf{g}}_\beta + \left(c_{\alpha\beta}\,\mathring{v}^\beta + \mathring{v}^3_{,\alpha} - d_\alpha\,\mathring{v}^3\right)\mathring{\mathbf{g}}_3 \tag{3.106}
$$

$$
\frac{\partial \mathbf{v}}{\partial \zeta} = \mathring{v}^\beta_{,3}\,\mathring{\mathbf{g}}_\beta + \mathring{v}^3_{,3}\,\mathring{\mathbf{g}}_3 \tag{3.107}
$$

where the angle ($\angle$) denotes covariant derivative with respect to the surface convected frame metrics and the comma ($,$) partial derivative with respect to the co-ordinate ζ. In particular, recall that the covariant derivative of a vector with respect to the surface convected frame can be defined

$$
\mathring{v}^\beta_{\angle\alpha} := \mathring{v}^\beta_{,\alpha} + \mathring{v}^\gamma\,\mathring{\Gamma}^\beta_{\gamma\alpha} \tag{3.108}
$$

From the comparison of Eqs. (3.104)–(3.107) one has

$$\bar{v}^h_{\|\alpha} \,\overset{\circ}{\mathscr{T}}{}^{\gamma}_{h} = \overset{\circ}{v}{}^{\beta}_{\angle\alpha} - c^{\beta}_{\alpha}\,\overset{\circ}{v}{}^{3} \tag{3.109}$$

$$\bar{v}^h_{\|\alpha} \,\overset{\circ}{\mathscr{T}}{}^{3}_{h} = c_{\alpha\beta}\,\overset{\circ}{v}{}^{\beta} + \overset{\circ}{v}{}^{3}_{,\alpha} - d_{\alpha}\,\overset{\circ}{v}{}^{3} \tag{3.110}$$

$$\bar{v}^h_{\|3} \,\overset{\circ}{\mathscr{T}}{}^{\gamma}_{h} = \overset{\circ}{v}{}^{\beta}_{,3} \tag{3.111}$$

$$\bar{v}^h_{\|3} \,\overset{\circ}{\mathscr{T}}{}^{3}_{h} = \overset{\circ}{v}{}^{3}_{,3} \tag{3.112}$$

Covariant Components

The covariant derivative of a generic vector field in a 3-D Riemannian manifold using its covariant components is given by

$$\frac{\partial \mathbf{v}}{\partial \xi^{\alpha}} = \bar{v}_{h\|\alpha}\,\mathbf{g}^{h} = \bar{v}_{\gamma\|\alpha}\,\mathbf{g}^{\gamma} + \bar{v}_{3\|\alpha}\,\mathbf{g}^{3} \tag{3.113}$$

$$\frac{\partial \mathbf{v}}{\partial \zeta} = \bar{v}_{h\|3}\,\mathbf{g}_{h} = \bar{v}_{\gamma\|3}\,\mathbf{g}^{\gamma} + \bar{v}_{3\|3}\,\mathbf{g}^{3} \tag{3.114}$$

Similarly, using the metrics of the surface convected frame one has

$$\begin{aligned}
\frac{\partial \mathbf{v}}{\partial \xi^{\alpha}} &= \left(\overset{\circ}{v}_{\beta\angle\alpha} - c_{\alpha\beta}\,\overset{\circ}{v}_{3}\right)\overset{\circ}{\mathbf{g}}{}^{\beta} + \left(c^{\beta}_{\alpha}\,\overset{\circ}{v}_{\beta} + \overset{\circ}{v}_{3,\alpha} - d_{\beta}\,\overset{\circ}{v}_{3}\right)\overset{\circ}{\mathbf{g}}{}^{3} \\
&= \left[\left(\overset{\circ}{v}_{\beta\angle\alpha} - c_{\alpha\beta}\,\overset{\circ}{v}_{3}\right)\overset{\circ}{\mathscr{T}}{}^{\beta}_{\gamma} + \left(c^{\beta}_{\alpha}\,\overset{\circ}{v}_{\beta} + \overset{\circ}{v}_{3,\alpha} - d_{\beta}\,\overset{\circ}{v}_{3}\right)\overset{\circ}{\mathscr{T}}{}^{3}_{\gamma}\right]\mathbf{g}^{\gamma} \\
&+ \left[\left(\overset{\circ}{v}_{\beta\angle\alpha} - c_{\alpha\beta}\,\overset{\circ}{v}_{3}\right)\overset{\circ}{\mathscr{T}}{}^{\beta}_{3} + \left(c^{\beta}_{\alpha}\,\overset{\circ}{v}_{\beta} + \overset{\circ}{v}_{3,\alpha} - d_{\beta}\,\overset{\circ}{v}_{3}\right)\overset{\circ}{\mathscr{T}}{}^{3}_{3}\right]\mathbf{g}^{3}
\end{aligned} \tag{3.115}$$

$$\begin{aligned}
\frac{\partial \mathbf{v}}{\partial \zeta} &= \overset{\circ}{v}_{\beta,3}\,\overset{\circ}{\mathbf{g}}{}^{\beta} + \overset{\circ}{v}_{3,3}\,\overset{\circ}{\mathbf{g}}{}^{3} \\
&= \left(\overset{\circ}{v}_{\beta,3}\,\overset{\circ}{\mathscr{T}}{}^{\beta}_{\gamma} + \overset{\circ}{v}_{3,3}\,\overset{\circ}{\mathscr{T}}{}^{3}_{\gamma}\right)\mathbf{g}^{\gamma} + \left(\overset{\circ}{v}_{\beta,3}\,\overset{\circ}{\mathscr{T}}{}^{\beta}_{3} + \overset{\circ}{v}_{3,3}\,\overset{\circ}{\mathscr{T}}{}^{3}_{3}\right)\mathbf{g}^{3}
\end{aligned} \tag{3.116}$$

From the comparison of Eqs. (3.113)–(3.116) one has

$$\bar{v}_{\gamma\|\alpha} = \left(\overset{\circ}{v}_{\beta\angle\alpha} - c_{\alpha\beta}\,\overset{\circ}{v}_{3}\right)\overset{\circ}{\mathscr{T}}{}^{\beta}_{\gamma} + \left(c^{\beta}_{\alpha}\,\overset{\circ}{v}_{\beta} + \overset{\circ}{v}_{3,\alpha} - d_{\beta}\,\overset{\circ}{v}_{3}\right)\overset{\circ}{\mathscr{T}}{}^{3}_{\gamma} \tag{3.117}$$

$$\bar{v}_{3\|\alpha} = \left(\overset{\circ}{v}_{\beta\angle\alpha} - c_{\alpha\beta}\,\overset{\circ}{v}_{3}\right)\overset{\circ}{\mathscr{T}}{}^{\beta}_{3} + \left(c^{\beta}_{\alpha}\,\overset{\circ}{v}_{\beta} + \overset{\circ}{v}_{3,\alpha} - d_{\beta}\,\overset{\circ}{v}_{3}\right)\overset{\circ}{\mathscr{T}}{}^{3}_{3} \tag{3.118}$$

$$\bar{v}_{\gamma\|3} = \overset{\circ}{v}_{\beta,3}\,\overset{\circ}{\mathscr{T}}{}^{\beta}_{\gamma} + \overset{\circ}{v}_{3,3}\,\overset{\circ}{\mathscr{T}}{}^{3}_{\gamma} \tag{3.119}$$

$$\bar{v}_{3\|3} = \overset{\circ}{v}_{\beta,3}\,\overset{\circ}{\mathscr{T}}{}^{\beta}_{3} + \overset{\circ}{v}_{3,3}\,\overset{\circ}{\mathscr{T}}{}^{3}_{3} \tag{3.120}$$

Finally, some relations, that will be useful for the subsequent developments, are here reported

$$\frac{\partial}{\partial \xi^\alpha} \left(\sqrt{\overset{\circ}{g}} \, \kappa^{\alpha\beta} \, \overset{\circ}{\mathbf{g}}_\beta \right) = \sqrt{a} \left[\left(\kappa^{\alpha\beta}_{/\alpha} - b_{\alpha\gamma} \, \kappa^{\alpha\gamma} \, l^\beta \right) \overset{\circ}{\mathbf{g}}_\beta + \frac{b_{\alpha\gamma} \, \kappa^{\alpha\gamma}}{h} \, \overset{\circ}{\mathbf{g}}_3 \right] \tag{3.121}$$

$$\frac{\partial}{\partial \xi^\alpha} \left(\sqrt{\overset{\circ}{g}} \, \kappa^{\alpha 3} \, \overset{\circ}{\mathbf{g}}_3 \right) = \sqrt{a} \left[\kappa^{\alpha 3} \, \overset{\circ}{\Gamma}^\beta_{3\alpha} \overset{\circ}{\mathbf{g}}_\beta + \left(\kappa^{\alpha 3}_{/\alpha} + \kappa^{\alpha 3} \, \overset{\circ}{\Gamma}^3_{3\alpha} \right) \overset{\circ}{\mathbf{g}}_3 \right] \tag{3.122}$$

3.4 The Displacement Gradient

3.4.1 First Approach: The Surface Natural Frame

The three-dimensional gradient of a generic vector field, as any 3-D tensor field, admits a unique decomposition into tangential and normal components with respect to the reference surface

$$\operatorname{Grad} \mathbf{v} = \Pi \operatorname{Grad} \mathbf{v} + (\mathbf{n} \otimes \mathbf{n}) \operatorname{Grad} \mathbf{v} = \Pi \operatorname{Grad} \mathbf{v} + \mathbf{n} \otimes (\operatorname{Grad} \mathbf{v})^T \mathbf{n} \tag{3.123}$$

where Π denotes the projection tensor operator over the tangent plane to the reference surface, whereas $\mathbf{n} \otimes \mathbf{n}$ represents the projection tensor operator over the normal vector $\mathbf{n}$.[†] Then, recall the decomposition of the displacement vector field in tangential and normal components ($\mathbf{v} = \mathbf{u} + w\,\mathbf{n}$), thus Eq. (3.123) becomes[‡]

$$
\begin{aligned}
\operatorname{Grad} \mathbf{v} &= \Pi \operatorname{Grad} \mathbf{u} + \mathbf{n} \otimes \mathbf{n} \left(\operatorname{Grad} \mathbf{u} \right) \\
&+ \Pi \left(\operatorname{grad} w \otimes \mathbf{n} + w \operatorname{Grad} \mathbf{n} \right) + \mathbf{n} \otimes \mathbf{n} \left(\operatorname{grad} w \otimes \mathbf{n} + w \operatorname{Grad} \mathbf{n} \right) \\
&= \nabla \otimes \mathbf{u} + \mathbf{n} \otimes \mathbf{u}' + \mathbf{B}^T \mathbf{u} \otimes \mathbf{n} - w\mathbf{B} + \nabla w \otimes \mathbf{n} + \mathbf{n} \otimes \mathbf{n} \, w'
\end{aligned} \tag{3.125}
$$

where a prime $'$ has been used to denote partial derivative with respect to ζ, and the following identities have been used

$$\left(\operatorname{Grad} \mathbf{u} \right)^T \mathbf{n} = - \left(\operatorname{Grad} \mathbf{n} \right)^T \mathbf{u} \tag{3.126}$$

$$\operatorname{Grad} \mathbf{n} = \Pi \operatorname{Grad} \mathbf{n} = - \mathbf{B} \tag{3.127}$$

$$\Pi \left(\operatorname{grad} w \otimes \mathbf{n} \right) = 0 \tag{3.128}$$

$$\Pi \operatorname{Grad} \mathbf{u} = \nabla \otimes \mathbf{u} + \mathbf{n} \otimes \mathbf{u}' \tag{3.129}$$

$$\operatorname{grad} w = \nabla w + w' \, \mathbf{n} \tag{3.130}$$

[†] In Eq. (3.123) the following tensorial relation, which explains the juxtaposition operation between tensors (see Ref. [94]), has been used

$$\left(\mathbf{a} \otimes \mathbf{b} \right) \mathbf{C} = \mathbf{a} \otimes \mathbf{C}^T \mathbf{b} \tag{3.124}$$

where $\mathbf{a}$, $\mathbf{b}$ are any two vectors, and $\mathbf{C}$ is a generic tensor.

[‡] In the following the nabla operator (∇) has been employed to indicate the operation of gradient and divergence in the two-dimensional manifold represented by the reference surface. In particular refer to Appendix (A) for a definition of these operators, their use and derivation.

and the following definition for the two-dimensional gradient, based on the metrics associated to the surface natural frame, has been used

$$\nabla \otimes \mathbf{u} \quad := \quad \left(\frac{\partial \mathbf{u}}{\partial \xi^\alpha} \cdot \mathbf{a}_\beta \right) \mathbf{a}^\alpha \otimes \mathbf{a}^\beta \qquad \forall \mathbf{u} : \ \mathbf{u} \cdot \mathbf{n} = 0 \tag{3.131}$$

Collect now from Eq. (3.125) all the terms that live in the support space ($\boxed{1}$), those associated to the fiber space ($\boxed{2}$), and the transverse terms which can be grouped into two groups: one representing in-plane the out-of-plane variation of some quantity ($\boxed{3}$) and the other associated to the in-plane variation of some other quantity out-of-plane ($\boxed{4}$). Thus, the 3-D gradient can be recast in following way

$$\begin{aligned} \mathrm{Grad}\,\mathbf{v} \quad &= \quad \boxed{1} + \boxed{2} + \boxed{3} + \boxed{4} = \boxed{(\nabla \otimes \mathbf{u} - w\mathbf{B})} + \boxed{\mathbf{n} \otimes \mathbf{n}\, w'} \\ &+ \quad \boxed{\mathbf{n} \otimes \mathbf{u}'} + \boxed{(\nabla w + \mathbf{B}\mathbf{u}) \otimes \mathbf{n}} \end{aligned} \tag{3.132}$$

Invoking the one-to-one correspondence between the space of three-dimensional second-order tensors and the space of 3×3 matrices (or linear transformations), and using Eq. (3.132), one can represent the gradient of the displacement field $\mathbf{v}$ in the following matrix form

$$\mathrm{Grad}\,\mathbf{v}^T \quad = \quad \left[\begin{array}{c|c} \boxed{1} & \boxed{3} \\ \hline \boxed{4} & \boxed{2} \end{array} \right] = \left[\begin{array}{c|c} \nabla \otimes \mathbf{u} - w\mathbf{B} & \mathbf{u}' \\ \hline \nabla w + \mathbf{B}\mathbf{u} & w' \end{array} \right] \tag{3.133}$$

It is worth noting that, in this equation, the structure and the inherent symmetry of this operator (which are a reflection of the inner structure of the continuum or, if one prefers, of the structure of the base manifold) is particularly apparent. Indeed, the first two columns are obtained by the application of the 2-D gradient on the in-plane and out-of-plane components of the displacement respectively, plus a coupling term which is due to the non-flatness of the support space, the third column represents, instead, the out-of-plane (or "along the fiber") variation of the in-plane and out-of-plane components of the displacement.

3.4.2 Second Approach: The Surface Mixed Frame

It is also interesting, for the future developments, to report the expression of the displacement gradient when only the out-of-plane displacement takes into account the "anormality" of the material fiber. To this aim recall that $\mathbf{g}_3 = h\,(\mathbf{n} + \mathbf{l})$, thus, one has

$$u_3 \quad = \quad \mathbf{v} \cdot \mathbf{g}_3 = h\,(\mathbf{l} \cdot \mathbf{u} + w) \tag{3.134}$$

Substituting Eq. (3.134) in Eq. (3.132) one has

$$
\begin{aligned}
\operatorname{Grad} \mathbf{v} \;=\; & \boxed{\left(\nabla \otimes \mathbf{u} - \frac{u_3}{h}\,\mathbf{B} + \mathbf{l} \cdot \mathbf{u}\,\mathbf{B}\right)} + \boxed{\mathbf{n} \otimes \mathbf{n}\left(\frac{u_3'}{h} - \mathbf{l} \cdot \mathbf{u}'\right)} \\
& + \boxed{\mathbf{u}' \otimes \mathbf{n}} + \boxed{\mathbf{n} \otimes \left[\nabla\left(\frac{u_3}{h}\right) - \nabla\left(\mathbf{l} \cdot \mathbf{u}\right) + \mathbf{B}\mathbf{u}\right]}
\end{aligned}
\tag{3.135}
$$

In the previous equation it is apparent that, if the surface basis vectors are chosen to represent the in-plane displacement together with Eq. (3.134),[†] then the gradient has a structure dissimilar to that of Eq. (3.145), with the explicit dependence on the vector $\mathbf{l}$ which measures the inclination of the fiber with respect to the normal.

3.4.3   Third Approach: The Surface Convected Frame

If one considered the tangent plane and the director as principal directions for the projection of the virtual displacement (instead of the tangent plane and its normal), what would be the expression of the gradient? In order to answer to this question, in this section some considerations are reported, together with the final expression of the gradient which will be useful in the subsequent developments. In particular, it will be shown that, when a revised version of the Kirchhoff-Love constraint is retained into the model, it is natural to adopt as reference direction for the out-of-plane displacement that of the material fiber or director and to refer to the surface convected frame the components of the stress tensor and related fields.

First, recall that the displacement field can be written

$$
\mathbf{v} \;=\; \mathbf{u} + w\,\mathbf{n} = \overset{\circ}{\mathbf{u}} + \overset{\circ}{u}_3\,\overset{\circ}{\mathbf{g}}{}^3
\tag{3.136}
$$

where u_3 measures the displacement along the fiber whereas $\overset{\circ}{\mathbf{u}}$ is the displacement in the plane normal to the fiber, and so it is distinct from $\mathbf{u}$, and it is given by[*]

$$
\overset{\circ}{\mathbf{u}} \;=\; \overset{\circ}{u}_\alpha\,\overset{\circ}{\mathbf{g}}{}^\alpha
\tag{3.137}
$$

where

$$
\overset{\circ}{u}_\alpha \;=\; \overset{\circ}{\mathbf{u}} \cdot \overset{\circ}{\mathbf{g}}_\alpha = \mathbf{v} \cdot \mathbf{a}_\alpha = u_\alpha
\tag{3.138}
$$

Recalling the expression of the contravariant volume basis vectors (Eq. (3.39)), one can relates the

---

[†] This approach is equivalent to consider a non-orthogonal basis vector in an Euclidean vector space.

[*] The upper o on the vector $\overset{\circ}{\mathbf{u}}$ serves to indicate that its components are evaluated on the contravariant volume basis vectors for $\zeta = 0$. A similar notation will be adopted later to indicate the stress resultant in those directions.

displacement $\overset{\circ}{\mathbf{u}}$ to the in-plane displacement $\mathbf{u}$ in the following way

$$\overset{\circ}{\mathbf{u}} \;=\; u_\alpha \left(\mathbf{a}^\alpha - l^\alpha \mathbf{n} \right) = \mathbf{u} - \left(\mathbf{l} \cdot \mathbf{u} \right) \mathbf{n} \tag{3.139}$$

Note that, because $\mathbf{l} \cdot \mathbf{n} = 0$, also the inverse relation holds

$$\mathbf{u} \;=\; \overset{\circ}{\mathbf{u}} + \left(\mathbf{l} \cdot \overset{\circ}{\mathbf{u}} \right) \mathbf{n} \tag{3.140}$$

Recall, finally, the relation between the displacement field along the fiber and that along the normal, Eq. (3.134), thus, from Eqs. (3.139) and (3.134) it is apparent that what is subtracted from the in-plane displacement in the normal direction when considering the projection along the fiber is gained by the displacement field in the fiber direction.[†]

Let us now express the displacement gradient in terms of the displacement along the fiber simply. To this aim, recall the expression of the covariant derivatives of the displacement field given in Section 3.3.2. Thus, starting from the definition of gradient one has

$$
\begin{aligned}
\mathrm{Grad}\, \mathbf{v} \;:=\; & \overset{\circ}{\mathbf{g}}{}^{k} \otimes \frac{\partial \mathbf{v}}{\partial \xi^k} = \overset{\circ}{\mathbf{g}}{}^{\beta} \otimes \left(\frac{\partial \overset{\circ}{\mathbf{u}}}{\partial \xi^\beta} + \frac{\partial \overset{\circ}{u}_3 \overset{\circ}{\mathbf{g}}{}^{3}}{\partial \xi^\beta} \right) + \overset{\circ}{\mathbf{g}}{}^{3} \otimes \left(\frac{\partial \overset{\circ}{\mathbf{u}}}{\partial \zeta} + \frac{\partial \overset{\circ}{u}_3 \overset{\circ}{\mathbf{g}}{}^{3}}{\partial \zeta} \right) \\
\;=\; & \overset{\circ}{\nabla} \otimes \mathbf{u} + \mathbf{C}^T \overset{\circ}{\mathbf{u}} \otimes \overset{\circ}{\mathbf{g}}{}^{3} + \overset{\circ}{\mathbf{g}}{}^{3} \otimes \overset{\circ}{\mathbf{u}}{}' + \left(\overset{\circ}{\nabla} \overset{\circ}{u}_3 - \mathbf{d}\, \overset{\circ}{u}_3 \right) \otimes \overset{\circ}{\mathbf{g}}{}^{3} \\
& - \overset{\circ}{u}_3\, \mathbf{C}^T + \overset{\circ}{u}_3{}'\, \overset{\circ}{\mathbf{g}}{}^{3} \otimes \overset{\circ}{\mathbf{g}}{}^{3}
\end{aligned}
\tag{3.141}
$$

where the following definitions have been used

$$\overset{\circ}{\nabla} \otimes \overset{\circ}{\mathbf{u}} \;:=\; \overset{\circ}{\mathbf{g}}{}^{\beta} \otimes \left(\frac{\partial \overset{\circ}{\mathbf{u}}}{\partial \xi^\beta} \cdot \overset{\circ}{\mathbf{g}}_\alpha \right) \overset{\circ}{\mathbf{g}}{}^{\alpha} = \overset{\circ}{u}_{\alpha \angle \beta}\, \overset{\circ}{\mathbf{g}}{}^{\beta} \otimes \overset{\circ}{\mathbf{g}}{}^{\alpha} \qquad \forall \overset{\circ}{\mathbf{u}} : \ \overset{\circ}{\mathbf{u}} \cdot \overset{\circ}{\mathbf{g}}_3 = 0 \tag{3.142}$$

$$\mathbf{C} \;=\; c_{\alpha\beta}\, \overset{\circ}{\mathbf{g}}{}^{\alpha} \otimes \overset{\circ}{\mathbf{g}}{}^{\beta} = c^\alpha_\beta\, \overset{\circ}{\mathbf{g}}_\alpha \otimes \overset{\circ}{\mathbf{g}}{}^{\beta} \tag{3.143}$$

$$\mathbf{d} \;:=\; \left(\frac{\partial \overset{\circ}{\mathbf{g}}_3}{\partial \xi^\beta} \cdot \overset{\circ}{\mathbf{g}}{}^{3} \right) \overset{\circ}{\mathbf{g}}{}^{\beta} = d_\beta\, \overset{\circ}{\mathbf{g}}{}^{\beta} \tag{3.144}$$

Eq. (3.141) may be recast as

$$
\begin{aligned}
\mathrm{Grad}\, \mathbf{v} \;=\; & \boxed{1} + \boxed{2} + \boxed{3} + \boxed{4} = \boxed{\left(\overset{\circ}{\nabla} \otimes \overset{\circ}{\mathbf{u}} - \overset{\circ}{u}_3\, \mathbf{C}^T \right)} + \boxed{\overset{\circ}{\mathbf{g}}{}^{3} \otimes \overset{\circ}{\mathbf{g}}{}^{3}\, \overset{\circ}{u}_3{}'} \\
& + \boxed{\mathbf{g}^3 \otimes \overset{\circ}{\mathbf{u}}{}'} + \boxed{\left(\overset{\circ}{\nabla} \overset{\circ}{u}_3 + \mathbf{C}^T \overset{\circ}{\mathbf{u}} - \mathbf{d}\, \overset{\circ}{u}_3 \right) \otimes \mathbf{g}^3}
\end{aligned}
\tag{3.145}
$$

[†] Indeed, recall that $\mathbf{g}^3 = \mathbf{n}/h$, so the thickness which explicitly appears in Eq. (3.134) is balanced by the thickness of $\mathbf{g}^3$.

It is worth noting that the expression of the displacement gradient maintains the same structure already encountered in Eq. (3.132) also when considering the displacement projected along the surface convected frame. The differences, a part from the name of the operators ($\overset{\circ}{\nabla}$ instead of ∇, $\mathbf{C}$ instead of $\mathbf{B}$, and the presence of the inedited $\mathbf{d}$ which measure the variation of the fiber ranging over the main surface in the normal direction) is included in the definition of the covariant differentiation on the surface convected frame.

Chapter 4

Virtual work

In this chapter the mechanical virtual work and its reduction for the case of a microstructured continuum body are studied. Following the considerations of the previous Chapter, in an attempt to utmost simplify the resulting equilibrium equations, the analyses will be presented with respect to three different frames: (i) the Surface Natural Frame; (ii) the Surface Mixed Frame; (iii) the Surface Convected Frame. For each case the inner virtual work is derived and then, applying the Virtual Work Principle (*i.e.*, equating them), the final equilibrium equations are obtained together with the related boundary conditions.

4.1   Preliminaries: inner virtual work for a 3-D body

In this Section the inner virtual work exerted by a 3-D Cauchy body, that will be useful for the forthcoming developments, is derived.

The inner virtual work exerted by a 3-D Cauchy body in the deformed configuration due to the application of a virtual displacement field may be written

$$\mathcal{W}_i \quad := \quad \int_{\mathcal{B}} \mathbf{T} \cdot \operatorname{Grad} \mathbf{v} \tag{4.1}$$

where $\mathbf{T}$ is the three-dimensional Cauchy stress tensor (*i.e.*, the stress tensor evaluated on the actual configuration of the body), $\operatorname{Grad} \mathbf{v}$ is the three-dimensional gradient of the assumed virtual displacement field $\mathbf{v}$, and $\mathcal{B}$ denotes the domain of integration (*i.e.*, the space occupied by the body in the actual - deformed - configuration). Recalling the definition of the 3-D gradient

$$\operatorname{Grad} \mathbf{v} \quad := \quad \mathbf{g}^k \otimes \frac{\partial \mathbf{v}}{\partial \xi^k} = \bar{v}_{p\|k} \ \mathbf{g}^k \otimes \mathbf{g}^p \tag{4.2}$$

one can expand the summation over indices k and p and isolate the following four groups

$$\operatorname{Grad} \mathbf{v} \quad := \quad \bar{v}_{\gamma\|\beta} \ \mathbf{g}^\beta \otimes \mathbf{g}^\gamma + \bar{v}_{\gamma\|3} \ \mathbf{g}^3 \otimes \mathbf{g}^\gamma + \bar{v}_{3\|\beta} \ \mathbf{g}^\beta \otimes \mathbf{g}^3 + \bar{v}_{3\|3} \ \mathbf{g}^3 \otimes \mathbf{g}^3 \tag{4.3}$$

Similarly, one can decompose the stress tensor (dual of the deformation tensor with respect to the inner work) in the following way[*]

$$\mathbf{T} \quad := \quad \tau^{\beta\gamma}\, \mathbf{g}_\beta \otimes \mathbf{g}_\gamma + \tau^{3\gamma}\, \mathbf{g}_3 \otimes \mathbf{g}_\gamma + \tau^{\beta 3}\, \mathbf{g}_\beta \otimes \mathbf{g}_3 + \tau^{33}\, \mathbf{g}_3 \otimes \mathbf{g}_3 \qquad (4.4)$$

whereby, the inner virtual work exerted by the body per unit of volume can be written

$$\mathbf{T} \cdot \mathrm{Grad}\, \mathbf{v} \quad = \quad \tau^{\beta\gamma}\, \bar{v}_{\gamma\|\beta} + \tau^{3\gamma}\, \bar{v}_{\gamma\|3} + \tau^{\beta 3}\, \bar{v}_{3\|\beta} + \tau^{33}\, \bar{v}_{3\|3} \qquad (4.5)$$

4.2 First Approach: The Surface Natural Frame

4.2.1 Inner Virtual Work

Applying Eqs. (3.94)-(3.99), which represent the volume-metrics covariant derivatives in terms of the surface metrics, to Eq. (4.5) yields

$$
\begin{aligned}
\mathbf{T} \quad \cdot \quad \mathrm{Grad}\, \mathbf{v} = {} & \tau^{\alpha\gamma}\, \mathscr{T}_\gamma^\beta\, \left(v_{\beta/\alpha} - b_{\alpha\beta}u_3\right) + \tau^{\alpha\gamma}\, \mathscr{T}_\gamma^3\, \left(v_{3,\alpha} + b_\alpha^\beta u_\beta\right) + \tau^{3\gamma}\, \mathscr{T}_\gamma^\beta\, v_{\beta,3} + \tau^{3\gamma}\, \mathscr{T}_\gamma^3\, v_{3,3} \\
+ {} & \tau^{\alpha 3}\, \mathscr{T}_3^\beta\, \left(v_{\beta/\alpha} - b_{\beta\alpha}u_3\right) + \tau^{\alpha 3}\, \mathscr{T}_3^3\, \left(v_{3,\alpha} + b_\alpha^\beta u_\beta\right) + \tau^{33}\, \mathscr{T}_3^\beta\, v_{\beta,3} + \tau^{33}\, \mathscr{T}_3^3\, v_{3,3} \qquad (4.6)
\end{aligned}
$$

The previous equation may be recast in the following way

$$\mathbf{T} \cdot \mathrm{Grad}\, \mathbf{v} \quad = \quad \sqrt{\frac{a}{g}}\, \left[\sigma^{\alpha\beta}\, \left(v_{\beta/\alpha} - b_{\alpha\beta}u_3\right) + \sigma^{\alpha 3}\, \left(v_{3,\alpha} + b_\alpha^\beta u_\beta\right) + \sigma^{3\beta}\, v_{\beta,3} + \sigma^{33}\, v_{3,3}\right] \quad (4.7)$$

where

$$\sigma^{\alpha\beta} \quad := \quad \sqrt{\frac{g}{a}}\, \left(\tau^{\alpha\gamma}\, \mathscr{T}_\gamma^\beta\, + \tau^{\alpha 3}\, \mathscr{T}_3^\beta\, \right) \qquad (4.8)$$

$$\sigma^{\alpha 3} \quad := \quad \sqrt{\frac{g}{a}}\, \left(\tau^{\alpha\gamma}\, \mathscr{T}_\gamma^3\, + \tau^{3\alpha}\, \mathscr{T}_3^3\, \right) \qquad (4.9)$$

$$\sigma^{3\beta} \quad := \quad \sqrt{\frac{g}{a}}\, \left(\tau^{3\gamma}\, \mathscr{T}_\gamma^\beta\, + \tau^{33}\, \mathscr{T}_3^\beta\, \right) \qquad (4.10)$$

$$\sigma^{33} \quad := \quad \sqrt{\frac{g}{a}}\, \left(\tau^{3\gamma}\, \mathscr{T}_\gamma^3\, + \tau^{33}\, \mathscr{T}_3^3\, \right) \qquad (4.11)$$

---

[*] For a 3-D Cauchy body the stress tensor in a symmetric tensor, thus the current decomposition could appear artful; nonetheless, this decomposition is instrumental for the subsequent decomposition of the stress resultants (or integrals) defined in the development of the shell theory.

Equation (4.7) can also be written in the following compact (direct) form

$$
\begin{aligned}
\mathbf{T} \cdot \mathrm{Grad}\, \mathbf{v} \;=\; & \sqrt{\frac{a}{g}} \left\{ \bar{\mathbf{S}} \cdot (\nabla \otimes \mathbf{u} - w\mathbf{B}) + \bar{\mathbf{Q}} \cdot [\mathbf{n} \otimes (\nabla w + \mathbf{B}\mathbf{u})] \right. \\
& + \left. \bar{\mathbf{P}} \cdot (\mathbf{u}' \otimes \mathbf{n}) + \bar{\mathbf{R}} \cdot (w'\mathbf{n} \otimes \mathbf{n}) \right\}
\end{aligned}
\tag{4.12}
$$

where with a prime ($'$) it has been denoted differentiation with respect to ζ and the following definitions hold

$\mathbf{v} := \mathbf{u} + w\mathbf{n}$ $\implies$ decomposition of the virtual displacements in in-plane and out-of-plane displacements

$\bar{\mathbf{S}} := \sigma^{\alpha\beta}\, \mathbf{a}_\alpha \otimes \mathbf{a}_\beta$ $\implies$ restriction to the tangent plane of the shell stress tensor

$\bar{\mathbf{Q}} := \sigma^{\alpha 3}\, \mathbf{a}_\alpha \otimes \mathbf{n}$ $\implies$ in-plane transversal stress tensor

$\bar{\mathbf{P}} := \sigma^{3\beta}\, \mathbf{n} \otimes \mathbf{a}_\beta$ $\implies$ out-of-plane transversal stress tensor

$\bar{\mathbf{R}} := \sigma^{33}\, \mathbf{n} \otimes \mathbf{n}$ $\implies$ normal stress tensor

Similarly, for the displacement gradient the following decomposition rules have been used

$\nabla \otimes \mathbf{u} := u_{\beta/\alpha}\, \mathbf{a}^\alpha \otimes \mathbf{a}^\beta$ $\implies$ restriction to the tangent plane of the surface gradient of the tangential displacement vector

$\nabla w := w_{3,\beta}\, \mathbf{a}^\beta$ $\implies$ surface gradient of the out-of-plane displacement vector

$\mathbf{B} := -\nabla \otimes \mathbf{n} = b_{\alpha\beta}\, \mathbf{a}^\alpha \otimes \mathbf{a}^\beta$ $\implies$ curvature tensor

For the forthcoming developments it is useful to consider the following representation of the displacement field

$$
\mathbf{v} \;=\; \sum_{k=0}^{N} \zeta^k \left(\mathbf{u}_{(k)} + w_{(k)}\, \mathbf{n} \right)
\tag{4.13}
$$

where $\mathbf{u}_{(k)}$ is the in-plane displacement of order k, whereas $w_{(k)}$ is the out-of-plane displacement of order k. It is worth noting that if the summation in the previous expression is limited to the first

order[*] this implies that the material line elements through the thickness remains straight after the deformation (consistently with the formal representation of the shell-like structure considered in the current configuration [see Eq. (3.10)]). Actually, the limitation of the summation in the displacement field representation is necessary in order to guarantee that the kinematical model assumed in the previous developments be consistent with the consideration of material co-ordinates, otherwise the material points mapped by the director $\mathbf{g}_3$ would not be the same at each point (or configuration) of the configurational space covered by the body during its motion, unless only a static analysis is considered. Higher order theories within a consistent material modeling (in dynamics) require refined kinematical models (*i.e.*, multi-director theories). Finally, note that $\mathbf{u}_{(0)}$ represent the displacement in the tangent plane of the reference surface, $\mathbf{u}_{(1)}$ the tangential displacement of the material points in the layer, whereas $w_{(0)}$ and $w_{(1)}$ the corresponding out-of-plane displacements. Moreover, it is straightforward to recognize that $w_{(1)}$ is directly a measure of the deformation (variation) of the thickness.

At conclusion of this section, let us note that the previous developments could be obtained also starting from the direct decomposition of the three-dimensional tensor gradient of the three-dimensional displacement vector field. To this goal recall the expression of the displacement gradient obtained of Eq. (3.132). Having in view this decomposition of the gradient operator, it is straightforward to associate to each term appearing in Eq. (3.132) a conjugate stress (dual with respect to the inner work), such as the stress tensor may be written

$$\mathbf{T} \;=\; \sqrt{\frac{a}{g}}\,\left(\bar{\mathbf{S}} + \bar{\mathbf{R}} + \bar{\mathbf{P}} + \bar{\mathbf{Q}}\right) \tag{4.14}$$

or, in matrix form

$$\mathbf{T} \;=\; \sqrt{\frac{a}{g}}\left[\begin{array}{c|c} \bar{\mathbf{S}} & \bar{\mathbf{Q}}^T\mathbf{n} \\ \hline \bar{\mathbf{P}}\mathbf{n} & \bar{\mathbf{R}}\cdot\mathbf{n}\otimes\mathbf{n} \end{array}\right] = \sqrt{\frac{a}{g}}\left[\begin{array}{c|c} \bar{\mathbf{S}} & \bar{\mathbf{q}} \\ \hline \bar{\mathbf{p}} & \bar{r} \end{array}\right] \tag{4.15}$$

where the following definitions have been used

$$\bar{\mathbf{q}} \;:=\; \bar{\mathbf{Q}}^T\mathbf{n} \tag{4.16}$$

$$\bar{\mathbf{p}} \;:=\; \bar{\mathbf{P}}\mathbf{n} \tag{4.17}$$

$$\bar{r} \;:=\; \bar{\mathbf{R}}\cdot\mathbf{n}\otimes\mathbf{n} \tag{4.18}$$

---

[*] At this point, it is important to comment on the relationship between the present formulation, which can be intended *à la* Cosserat, and a standard Galerkin procedure for the approximate solution of the three-dimensional equations. Following Ref. [94] one may state that (see [94, page 127] for further details) most of the already obtained and future developments are consistent with a Galerkin approach which uses the kinematic assumption (3.10) and two weighting functions (1 and ζ [or $f(\zeta)$]).

Thus, the inner virtual work may now be rewritten as (cfr. Eq. (4.12))

$$\mathbf{T} \cdot \operatorname{Grad} \mathbf{v} \;=\; \sqrt{\frac{a}{g}} \left\{ \bar{\mathbf{S}} \cdot (\nabla \otimes \mathbf{u} - w\mathbf{B}) + \bar{\mathbf{q}} \cdot (\nabla w + \mathbf{B}\mathbf{u}) + \bar{\mathbf{p}} \cdot \mathbf{u}' + \bar{r}\, w' \right\} \tag{4.19}$$

4.2.2   Integration along the thickness

Before proceeding further with the development of the inner virtual work, recall that the volume integral can be written

$$\int_{\mathcal{B}} \mathsf{c}\, d\mathcal{V} \;=\; \int_{\mathcal{F}} \int_{\mathcal{S}} \mathsf{c}\, \sqrt{g}\, d\xi^1\, d\xi^2\, d\zeta = \int_{\mathcal{S}_M} \int_{-1}^{1} \bar{c}\, d\zeta\, d\mathcal{S} = \int_{\mathcal{S}_M} c\, d\mathcal{S} \tag{4.20}$$

where

$$\bar{c} \;:=\; \mathsf{c}\, \sqrt{\frac{a}{g}} \tag{4.21}$$

and

$$d\mathcal{S}_M \;:=\; \sqrt{a}\, d\xi^1\, d\xi^2 \tag{4.22}$$

Let us now apply the virtual displacement representation of Eq. (4.13) in Eq. (4.12)

$$\nabla \otimes \mathbf{u} \;=\; \sum_{k=0}^{N} \zeta^k\, \nabla \otimes \mathbf{u}_{(k)} \tag{4.23}$$

$$\nabla w \;=\; \sum_{k=0}^{N} \zeta^k\, \nabla w_{(k)} \tag{4.24}$$

$$\mathbf{u}' \;=\; \sum_{k=0}^{N} k\, \zeta^{k-1}\, \mathbf{u}_{(k)} \tag{4.25}$$

$$w' \;=\; \sum_{k=0}^{N} k\, \zeta^{k-1}\, w_{(k)} \tag{4.26}$$

Introducing the following integral stress definitions

$$\mathbf{N}_{(k)} \;:=\; \int_{\mathcal{F}} \zeta^k\, \bar{\mathbf{S}} \tag{4.27}$$

$$\mathbf{P}_{(k)} \;:=\; \int_{\mathcal{F}} \zeta^k\, \bar{\mathbf{p}} \tag{4.28}$$

$$\mathbf{q}_{(k)} \;:=\; \int_{\mathcal{F}} \zeta^k\, \bar{\mathbf{q}} \tag{4.29}$$

$$r_{(k)} \;:=\; \int_{\mathcal{F}} \zeta^k\, \bar{r} \tag{4.30}$$

Thus, using Eq. (4.12) one has

$$
\begin{aligned}
\delta\mathcal{W}_i \;=\; & \sum_{k=0}^{N}\int_{\mathcal{S}_M}\Big[\mathbf{N}_{(k)}\cdot\big(\nabla\otimes\mathbf{u}_{(k)}-\mathbf{B}\,w_{(k)}\big)+\mathbf{q}_{(k)}\cdot\big(\nabla w_{(k)}+\mathbf{B}\mathbf{u}_{(k)}\big) \\
& +\; k\,\mathbf{p}_{(k-1)}\cdot\mathbf{u}_{(k)}+k\,r_{(k-1)}\,w_{(k)}\Big]\;d\mathcal{S}
\end{aligned}
\tag{4.31}
$$

Recalling the Green-Gauss theorem

$$
\int_{\mathcal{S}}\mathbf{A}\cdot\nabla\otimes\mathbf{b} \;=\; \int_{\partial\mathcal{S}}\mathbf{A}\mathbf{b}\cdot\mathbf{n}_\partial - \int_{\mathcal{S}}\nabla\cdot\mathbf{A}\cdot\mathbf{b}
\tag{4.32}
$$

$$
\int_{\mathcal{S}}\mathbf{a}\cdot\nabla b \;=\; \int_{\partial\mathcal{S}} b\,\mathbf{a}\cdot\mathbf{n}_\partial - \int_{\mathcal{S}} b\,\nabla\cdot\mathbf{a}
\tag{4.33}
$$

and applying it in Eq. (4.31) one has

$$
\begin{aligned}
\delta\mathcal{W}_i \;=\; & \sum_{k=0}^{N}\int_{\mathcal{S}_M}\Big\{\big[-\nabla\cdot\mathbf{N}_{(k)}+\mathbf{B}^T\,\mathbf{q}_{(k)}+k\,\mathbf{p}_{(k-1)}\big]\cdot\mathbf{u}_{(k)} \\
& +\;\big[-\nabla\cdot\mathbf{q}_{(k)}-\mathbf{N}_{(k)}\cdot\mathbf{B}+k\,r_{(k-1)}\big]\,w_{(k)}\Big\}\;d\mathcal{S}+B.T.
\end{aligned}
\tag{4.34}
$$

where with $B.T.$ it has been denoted the boundary terms, descending from the application of the Green-Gauss theorem (Eqs. (4.32)-(4.33)),

$$
B.T. \;=\; \int_{\partial\mathcal{S}}\big[\mathbf{N}_{(k)}^T\mathbf{n}_\partial\cdot\mathbf{u}_{(k)}+\mathbf{q}_{(k)}\cdot\mathbf{n}_\partial\,w_{(k)}\big]
\tag{4.35}
$$

Applying the Virtual Work Principle (*i.e.*, the virtual work is zero for any virtual displacement) one gets the following six equilibrium equations (in the absence of external applied loads)

$$
-\nabla\cdot\mathbf{N}_{(k)}+\mathbf{B}^T\,\mathbf{q}_{(k)}+k\,\mathbf{p}_{(k-1)}=0
\tag{4.36}
$$

$$
-\nabla\cdot\mathbf{q}_{(k)}-\mathbf{B}\cdot\mathbf{N}_{(k)}+k\,r_{(k-1)}=0
\tag{4.37}
$$

where the following definitions have been employed for the integral stress resultants in the transverse and normal directions

$$
\mathbf{q}_{(k)} \;:=\; \mathbf{Q}_{(k)}^T\mathbf{n}
\tag{4.38}
$$

$$
\mathbf{p}_{(k)} \;:=\; \mathbf{P}_{(k)}\mathbf{n}
\tag{4.39}
$$

$$
r_{(k)} \;:=\; \mathbf{R}_{(k)}\cdot\mathbf{n}\otimes\mathbf{n}
\tag{4.40}
$$

4.3   Second Approach: The Surface Mixed Frame

In this section another formulation will be developed starting from the geometrical assumptions on the shell-like body. In particular, with reference to the Cosserat formulation for directed bodies a formulation retaining the presence of an intrinsic principal direction not coincident with the thickness is provided. This approach fully developed in [90] using a tensorial co-ordinate representation is here reported using a direct, coordinate-free (or absolute), approach.

Recalling the relation between the displacement field in the material fiber and the one in the thickness direction one has

$$u_3 := \mathbf{v} \cdot \mathbf{g}_3 = \sum_{k=0}^{N} \zeta^k \left(\mathbf{u}_{(k)} + w_{(k)} \, \mathbf{n} \right) \cdot h \, (\mathbf{n} + \mathbf{l}) = \sum_{k=0}^{N} \zeta^k h \left(\mathbf{l} \cdot \mathbf{u}_{(k)} + w_{(k)} \right) =: \sum_{k=0}^{N} \zeta^k \, u_{3_{(k)}} \tag{4.41}$$

Thus the two-dimensional gradient and the derivative with respect to ζ of the out-plane displacement (cfr. Eqs. (4.24) and (4.26)) become

$$\nabla w_{(k)} \;=\; \nabla \left(\frac{u_{3_{(k)}}}{h} \right) - (\nabla \otimes \mathbf{l})^T \, \mathbf{u} - (\nabla \otimes \mathbf{u})^T \, \mathbf{l} \tag{4.42}$$

$$w' \;=\; \sum_{k=0}^{N} k \, \zeta^{k-1} \left(\frac{u_{3_{(k)}}}{h} - \mathbf{l} \cdot \mathbf{u}_{(k)} \right) \tag{4.43}$$

Equation (4.12) can now be rewritten

$$
\begin{aligned}
\mathbf{T} \cdot \mathrm{Grad}\,\mathbf{v} \;=\; & \sqrt{\frac{a}{g}} \left\{ \bar{\mathbf{S}} \cdot \left[\nabla \otimes \mathbf{u} - \frac{u_3}{h} \, \mathbf{B} + (\mathbf{l} \cdot \mathbf{u}) \, \mathbf{B} \right] \right. \\
& + \; \bar{\mathbf{Q}} \cdot \mathbf{n} \otimes \left[\nabla \left(\frac{u_3}{h} \right) - (\nabla \otimes \mathbf{l})^T \, \mathbf{u} - (\nabla \otimes \mathbf{u})^T \, \mathbf{l} + \mathbf{B} \mathbf{u} \right] \\
& + \left. \bar{\mathbf{P}} \cdot (\mathbf{u}' \otimes \mathbf{n}) + \bar{\mathbf{R}} \cdot (\mathbf{n} \otimes \mathbf{n}) \left(\frac{u_3'}{h} - \mathbf{l} \cdot \mathbf{u}' \right) \right\}
\end{aligned}
\tag{4.44}
$$

Let us introduce the following definitions for the integral stress terms, representing the dynamical descriptors dual of the kinematical ones when the out-plane displacement is directed in the material fiber direction,[†]

$$\hat{\mathbf{S}} \;:=\; \bar{\mathbf{S}} - \mathbf{l} \otimes \bar{\mathbf{q}} \tag{4.45}$$

$$\hat{\mathbf{q}} \;:=\; \frac{\bar{\mathbf{q}}}{h} \tag{4.46}$$

$$\hat{\mathbf{p}} \;:=\; \bar{\mathbf{p}} - \bar{r} \, \mathbf{l} \tag{4.47}$$

$$\hat{r} \;:=\; \frac{\bar{r}}{h} \tag{4.48}$$

[†] The upper hat (^) over the present dynamical descriptors serves to differentiate them from those defined on the surface basis vectors and the normal, which are marked by an upper bar (‾), and from another class of terms, which will be introduced later, relevant to the director orthogonal frame, which are identified by an upper o (∘).

29th May 2005

thus, Eq. (4.44) becomes

$$
\begin{aligned}
\mathbf{T} \cdot \operatorname{Grad} \mathbf{v} \;=\;& \sqrt{\frac{a}{g}} \Big\{ \hat{\mathbf{S}} \cdot \nabla \otimes \mathbf{u} + \Big[\big(\hat{\mathbf{S}} \cdot \mathbf{B} \big) \; \mathbf{l} + h \, (\mathbf{B} - \nabla \otimes \mathbf{l}) \; \hat{\mathbf{q}} + h \, \mathbf{B} \cdot (\mathbf{l} \otimes \hat{\mathbf{q}}) \; \mathbf{l} \Big] \cdot \mathbf{u} \\[2mm]
& + \; \hat{\mathbf{p}} \cdot \mathbf{u}' - \Big[\big(\hat{\mathbf{S}} + \mathbf{l} \otimes \hat{\mathbf{q}} \big) \cdot \mathbf{B} + \frac{\hat{\mathbf{q}}}{h} \cdot \nabla h \Big] \; u_3 + \hat{r} \; u_3' + \hat{\mathbf{q}} \cdot \nabla u_3 \Big\}
\end{aligned}
\tag{4.49}
$$

4.3.1 Integration along the thickness

Introducing for the displacement field the representation of Eq. (4.13) with the subsequent transformation of Eqs. (4.41)–(4.43) one has

$$
\begin{aligned}
\delta \mathcal{W}_i \;=\;& \sum_{k=0}^{N} \int_{\mathcal{S}_M} \Big\{ \hat{\mathbf{N}}_{(k)} \cdot \nabla \otimes \mathbf{u}_{(k)} + \Big[\hat{\mathbf{N}}_{(k)} \cdot \mathbf{B} \, \mathbf{l} + h \, (\mathbf{B} - \mathbf{D}) \; \hat{\mathbf{q}}_{(k)} + h \, \mathbf{l} \otimes \hat{\mathbf{q}}_{(k)} \cdot \mathbf{B} \, \mathbf{l} + k \; \hat{\mathbf{p}}_{(k-1)} \Big] \cdot \mathbf{u}_{(k)} \\[2mm]
& + \; \hat{\mathbf{q}}_{(k)} \cdot \nabla u_{3_{(k)}} - \Big[\hat{\mathbf{N}}_{(k)} \cdot \mathbf{B} + \mathbf{l} \otimes \hat{\mathbf{q}}_{(k)} \cdot \mathbf{B} + \frac{\hat{\mathbf{q}}_{(k)}}{h} \cdot \nabla h - k \; \hat{r}_{(k-1)} \Big] \; u_{3_{(k)}} \Big\}
\end{aligned}
\tag{4.50}
$$

where $\mathbf{D}$ is a measure of the correction to the curvature when the material fiber is not directed through the thickness and it is given by[*]

$$
\mathbf{D} \;=\; \nabla \otimes \mathbf{l}
\tag{4.51}
$$

It is worth noting that the presence of the tensor $\mathbf{D}$ assures a coupling between the in-plane and out-of-plane equilibrium equations also when a flat geometry for the reference surface is considered. Indeed, in that case $\mathbf{B} = -\nabla \otimes \mathbf{n} = 0$ whereas $\mathbf{D}$ may be different from zero if the material fiber is assumed not uniformly distributed on the reference plane. Thus, the application of a virtual stretch in the plane will produce shear terms in the fibers direction because the fibers have different directions moving in the plane.

Let us applying the Green-Gauss theorem in the form of Eqs. (4.32) and (4.33), thus

$$
\begin{aligned}
\delta \mathcal{W}_i \;=\;& \sum_{k=0}^{N} \int_{\mathcal{S}_M} \Big\{ \Big[-\nabla \cdot \hat{\mathbf{N}}_{(k)} + \hat{\mathbf{N}}_{(k)} \cdot \mathbf{B} \, \mathbf{l} + h \, (\mathbf{B} - \mathbf{D}) \, \hat{\mathbf{q}}_{(k)} + h \, \mathbf{l} \otimes \hat{\mathbf{q}}_{(k)} \cdot \mathbf{B} \, \mathbf{l} + k \; \hat{\mathbf{p}}_{(k)} \Big] \cdot \mathbf{u}_{(k)} \\[2mm]
& - \; \Big[-\nabla \cdot \hat{\mathbf{q}}_{(k)} + \hat{\mathbf{N}}_{(k)} \cdot \mathbf{B} + \mathbf{l} \otimes \hat{\mathbf{q}}_{(k)} \cdot \mathbf{B} + \frac{\hat{\mathbf{q}}_{(k)}}{h} \cdot \nabla h - k \; \hat{r}_{(k-1)} \Big] \; u_{3_{(k)}} \Big\} + B.T.
\end{aligned}
\tag{4.52}
$$

where the boundary terms $(B.T.)$ appear due to the application of the Green-Gauss theorem, and

---

[*] Another way to understand the role of the tensor $\mathbf{D}$ is considering the gradient of the material fiber in the bi-dimensional manifold represented by the reference surface. Indeed, recall that $\mathbf{g}_3 = h \, (\mathbf{n} + \mathbf{l})$ thus $\nabla \otimes \mathbf{g}_3 / h = -\mathbf{B} + \nabla \otimes \mathbf{l}$.

are given by

$$B.T. \;=\; \int_{\partial \mathcal{S}} \left[\hat{\mathbf{N}}^T_{(k)} \mathbf{n}_\partial \cdot \mathbf{u}_{(k)} + \hat{\mathbf{q}}_{(k)} \cdot \mathbf{n}_\partial \; u_{3_{(k)}} \right] \tag{4.53}$$

Applying the Virtual Work Principle one gets the following system of equilibrium equations (in the absence of external applied loads)

$$-\nabla \cdot \hat{\mathbf{N}}_{(k)} + \hat{\mathbf{N}}_{(k)} \cdot \mathbf{B}\,\mathbf{l} + h \left(\mathbf{B} - \mathbf{D} \right) \hat{\mathbf{q}}_{(k)} + h\,\mathbf{l} \otimes \hat{\mathbf{q}}_{(k)} \cdot \mathbf{B}\,\mathbf{l} + k\;\hat{\mathbf{p}}_{(k-1)} = 0 \tag{4.54}$$

$$-\frac{1}{h}\nabla \cdot \frac{\hat{\mathbf{q}}_{(k)}}{h} + \hat{\mathbf{N}}_{(k)} \cdot \mathbf{B} + \hat{\mathbf{q}}_{(k)} \otimes \mathbf{l} \cdot \mathbf{B} - k\;\hat{r}_{(k-1)} = 0 \tag{4.55}$$

The previous system of equilibrium equations has to be compared with that of Eqs. (4.36)-(4.37) obtained considering virtual displacements of order zero and one in the tangent plane and in the normal direction to the reference surface. In particular it can be observed that Eqs. (4.54) and (4.55) reduce to Eqs. (4.36)-(4.37) when the material fiber is not inclined with respect to the normal (*i.e.,* $\mathbf{l} = 0$). Moreover, while Eqs. (4.36)-(4.37) are composed of four terms, the divergence, the coupling term through the curvature tensor, the out-of-plane transversal and normal stress resultants (only for the first order equations), and the external loads (in a D'Alambert sense), in Eqs. (4.54) and (4.55) there exist additional terms. These are related to the inclination of the material fiber along which the virtual displacements and consequently the virtual work have been evaluated. Consistently with the redefinition of the virtual displacement, and so of virtual deformations within the body, a redefinition of the integral stress terms have been mandatory. These new quantities measure the stress in the tangent plane and in the material fiber (both tangentially and normally to it). In this sense it can be better understood the sign in front of the tensor $\mathbf{D}$ in Eq. (4.54). This term tends to compensate the coupling of the in-plane tangential equation due to the presence of a positive curvature.

4.4   Third Approach: The Surface Convected Frame

As a matter of fact let us re-obtain the equilibrium equations with a consistent choice of virtual displacements. As it was observed at conclusion of the section on the displacement gradient, when the in-plane displacement is assumed equal to that of Eq. (3.139), the displacement gradient can be written as in Eq. (3.145); consistently, the stress tensor may be decomposed in the following way

$$\mathbf{T} \;=\; \sqrt{\frac{\overset{\circ}{g}}{g}} \left(\overset{\circ}{\sigma}{}^{\alpha\beta} \; \overset{\circ}{\mathbf{g}}_\alpha \otimes \overset{\circ}{\mathbf{g}}_\beta + \overset{\circ}{\sigma}{}^{33} \; \overset{\circ}{\mathbf{g}}_3 \otimes \overset{\circ}{\mathbf{g}}_3 + \overset{\circ}{\sigma}{}^{\alpha 3} \; \overset{\circ}{\mathbf{g}}_\alpha \otimes \overset{\circ}{\mathbf{g}}_3 + \overset{\circ}{\sigma}{}^{3\beta} \; \overset{\circ}{\mathbf{g}}_3 \otimes \overset{\circ}{\mathbf{g}}_\beta \right)$$

$$=\; \sqrt{\frac{\overset{\circ}{g}}{g}} \left(\overset{\circ}{\mathbf{S}} + \overset{\circ}{\mathbf{R}} + \overset{\circ}{\mathbf{P}} + \overset{\circ}{\mathbf{Q}} \right) = \sqrt{\frac{\overset{\circ}{g}}{g}} \left(\overset{\circ}{\mathbf{S}} + \overset{\circ}{r} \; \overset{\circ}{\mathbf{g}}_3 \otimes \overset{\circ}{\mathbf{g}}_3 + \overset{\circ}{\mathbf{p}} \otimes \overset{\circ}{\mathbf{g}}_3 + \mathbf{g}_3 \otimes \overset{\circ}{\mathbf{q}} \right) \tag{4.56}$$

where the $\overset{\circ}{\mathbf{S}}$, $\overset{\circ}{\mathbf{R}}$, $\overset{\circ}{\mathbf{P}}$, and $\overset{\circ}{\mathbf{Q}}$ are the conjugate pair of the displacement gradient in Eq. (3.145). Accordingly, the inner virtual work can be written

$$
\begin{aligned}
\mathbf{T} \cdot \operatorname{Grad} \mathbf{v} \;=\; & \sqrt{\frac{\overset{\circ}{g}}{g}} \left\{ \overset{\circ}{\mathbf{S}} \cdot \left(\overset{\circ}{\nabla} \otimes \overset{\circ}{\mathbf{u}} - \overset{\circ}{u}_3 \mathbf{C} \right) + \overset{\circ}{r}\, \overset{\circ}{u}_3' + \overset{\circ}{\mathbf{p}} \cdot \overset{\circ}{\mathbf{u}}' \right. \\
& + \; \overset{\circ}{\mathbf{q}} \cdot \left. \left[\overset{\circ}{\nabla} \overset{\circ}{u}_3 - \mathbf{d}\, \overset{\circ}{u}_3 + \mathbf{C}^T \overset{\circ}{\mathbf{u}} \right] \right\}
\end{aligned}
\tag{4.57}
$$

where the new set of dynamical descriptors ($\overset{\circ}{\sigma}{}^{hk}$) are given by the following relations

$$
\overset{\circ}{\mathbf{S}} \cdot \overset{\circ}{\mathbf{g}}{}^{\alpha} \otimes \overset{\circ}{\mathbf{g}}{}^{\beta} \;=\; \overset{\circ}{\sigma}{}^{\alpha\beta} \;=\; \sqrt{\frac{g}{\overset{\circ}{g}}} \left(\tau^{\alpha\gamma} \overset{\circ}{\mathscr{T}}{}^{\beta}_{\gamma} + \tau^{\alpha3} \overset{\circ}{\mathscr{T}}{}^{\beta}_{3} \right)
\tag{4.58}
$$

$$
\overset{\circ}{\mathbf{p}} \cdot \overset{\circ}{\mathbf{g}}{}^{\beta} \;=\; \overset{\circ}{\sigma}{}^{3\beta} \;=\; \sqrt{\frac{g}{\overset{\circ}{g}}} \left(\tau^{3\gamma} \overset{\circ}{\mathscr{T}}{}^{\beta}_{\gamma} + \tau^{33} \overset{\circ}{\mathscr{T}}{}^{\beta}_{3} \right)
\tag{4.59}
$$

$$
\overset{\circ}{\mathbf{q}} \cdot \overset{\circ}{\mathbf{g}}{}^{\alpha} \;=\; \overset{\circ}{\sigma}{}^{\alpha3} \;=\; \sqrt{\frac{g}{\overset{\circ}{g}}} \left(\tau^{\alpha\gamma} \overset{\circ}{\mathscr{T}}{}^{3}_{\gamma} + \tau^{\alpha3} \overset{\circ}{\mathscr{T}}{}^{3}_{3} \right)
\tag{4.60}
$$

$$
\overset{\circ}{r} \;=\; \overset{\circ}{\sigma}{}^{33} \;=\; \sqrt{\frac{g}{\overset{\circ}{g}}} \left(\tau^{3\gamma} \overset{\circ}{\mathscr{T}}{}^{3}_{\gamma} + \tau^{33} \overset{\circ}{\mathscr{T}}{}^{3}_{3} \right)
\tag{4.61}
$$

where $\overset{\circ}{\mathscr{T}}{}^{k}_{h}$ are the shifters between the volume reference frame and the surface convected frame, whose expression is given in Eqs. (3.52)-(3.55). Note that $\mathbf{g}_3$ is coincident with $\overset{\circ}{\mathbf{g}}_3$ in a single-director model and so the shifters $\overset{\circ}{\mathscr{T}}{}^{\beta}_{3}$ are zero, whereas $\overset{\circ}{\mathscr{T}}{}^{3}_{3}$ is equal to one.

4.4.1   Integration along the thickness

On the base of Eq. (3.136), one may use for the displacement field representation the following relation instead of Eq. (4.13)

$$
\mathbf{v} \;=\; \sum_{k=0}^{N} \zeta^k \left(\overset{\circ}{\mathbf{u}}_{(k)} + \overset{\circ}{u}_{3(k)}\, \mathbf{g}^3 \right)
\tag{4.62}
$$

or

$$
\overset{\circ}{\mathbf{u}} \;=\; \sum_{k=0}^{N} \zeta^k \, \overset{\circ}{\mathbf{u}}_{(k)}
\tag{4.63}
$$

$$
\overset{\circ}{u}_3 \;=\; \sum_{k=0}^{N} \zeta^k \, \overset{\circ}{u}_{3(k)}
\tag{4.64}
$$

Accordingly, the displacement gradient and the derivatives with respect to ζ of the displacement field may be written

$$\overset{\circ}{\nabla} \otimes \overset{\circ}{\mathbf{u}} = \sum_{k=0}^{N} \zeta^k \, \overset{\circ}{\nabla} \otimes \overset{\circ}{\mathbf{u}}_{(k)} \tag{4.65}$$

$$\overset{\circ}{\nabla}\overset{\circ}{u}_{3_{(k)}} = \sum_{k=0}^{N} \zeta^k \, \overset{\circ}{\nabla}\overset{\circ}{u}_{3_{(k)}} \tag{4.66}$$

$$\overset{\circ}{\mathbf{u}}{}' = \sum_{k=0}^{N} k \, \zeta^{k-1} \, \overset{\circ}{\mathbf{u}}_{(k)} \tag{4.67}$$

$$\overset{\circ}{u}{}'_{3_{(k)}} = \sum_{k=0}^{N} k \, \zeta^{k-1} \, \overset{\circ}{u}_{3_{(k)}} \tag{4.68}$$

Thus, the inner virtual work, when the director orthogonal frame is chosen as reference frame to compute the virtual displacements, becomes

$$\begin{aligned}
\delta\mathcal{W}_i = \sum_{k=0}^{N} \int_{\mathcal{S}_M} & \left\{ \overset{\circ}{\mathbf{N}}_{(k)} \cdot \left(\overset{\circ}{\nabla} \otimes \overset{\circ}{\mathbf{u}}_{(k)} - \overset{\circ}{u}_{3_{(k)}} \mathbf{C} \right) + k \, \overset{\circ}{r}_{(k-1)} \, \overset{\circ}{u}_{3_{(k)}} \right. \\
& \left. + \; k \, \overset{\circ}{\mathbf{p}}_{(k-1)} \cdot \overset{\circ}{\mathbf{u}}_{(k)} + \overset{\circ}{\mathbf{q}}_{(k)} \cdot \left[\overset{\circ}{\nabla}\overset{\circ}{u}_{3_{(k)}} - \mathbf{d} \, \overset{\circ}{u}_{3_{(k)}} + \mathbf{C}^T \overset{\circ}{\mathbf{u}}_{(k)} \right] \right\}
\end{aligned} \tag{4.69}$$

where integral stress resultants $\overset{\circ}{\mathbf{N}}_{(k)}$, $\overset{\circ}{\mathbf{q}}_{(k)}$, $\overset{\circ}{\mathbf{r}}_{(k)}$, and $\overset{\circ}{r}_{(k)}$ are given by

$$\overset{\circ}{\mathbf{N}}_{(k)} := \int_{\mathcal{F}} \zeta^k \, \overset{\circ}{\mathbf{S}} \tag{4.70}$$

$$\overset{\circ}{\mathbf{P}}_{(k)} := \int_{\mathcal{F}} \zeta^k \, \overset{\circ}{\mathbf{p}} \tag{4.71}$$

$$\overset{\circ}{\mathbf{q}}_{(k)} := \int_{\mathcal{F}} \zeta^k \, \overset{\circ}{\mathbf{q}} \tag{4.72}$$

$$\overset{\circ}{r}_{(k)} := \int_{\mathcal{F}} \zeta^k \, \overset{\circ}{r} \tag{4.73}$$

Let us applying the Green-Gauss theorem in the form of Eqs. (4.32) and (4.33), thus

$$\begin{aligned}
\delta\mathcal{W}_i = \sum_{k=0}^{N} \int_{\mathcal{S}_M} & \left[\left(-\overset{\circ}{\nabla} \cdot \overset{\circ}{\mathbf{N}}_{(k)} \right) \cdot \overset{\circ}{\mathbf{u}}_{(k)} - \left(\overset{\circ}{\mathbf{N}}_{(k)} \cdot \mathbf{C} \right) \overset{\circ}{u}_{3_{(k)}} \right. \\
& + \left(-\overset{\circ}{\nabla} \cdot \overset{\circ}{\mathbf{q}}_{(k)} \right) \overset{\circ}{u}_{3_{(k)}} - \overset{\circ}{\mathbf{q}}_{(k)} \cdot \mathbf{d} \, \overset{\circ}{u}_{3_{(k)}} + \mathbf{C}\overset{\circ}{\mathbf{q}}_{(k)} \cdot \overset{\circ}{\mathbf{u}}_{(k)} \\
& \left. + \; k \, \overset{\circ}{\mathbf{p}}_{(k-1)} \cdot \overset{\circ}{\mathbf{u}}_{(k)} + k \, \overset{\circ}{r}_{(k-1)} \, \overset{\circ}{u}_{3_{(k)}} \right] \, d\mathcal{S} + B.T.
\end{aligned} \tag{4.74}$$

29th May 2005

where again with $B.T.$ are denoted the boundary terms descending from the application of the Green-Gauss theorem (Eqs. (4.32)-(4.33))

$$B.T. \ = \ \int_{\partial \mathcal{S}} \left[\overset{\circ}{\mathbf{N}}{}_{(k)}^{T} \mathbf{n}_\partial \cdot \overset{\circ}{\mathbf{u}}_{(k)} + \overset{\circ}{\mathbf{q}}_{(k)} \cdot \mathbf{n}_\partial \; \overset{\circ}{u}_{3_{(k)}} \right] \tag{4.75}$$

The application of the Virtual Work Principle limitedly to the inner work leads to the following system of equilibrium equations

$$-\overset{\circ}{\nabla} \cdot \overset{\circ}{\mathbf{N}}_{(k)} + \mathbf{C}^{T} \, \overset{\circ}{\mathbf{q}}_{(k)} + k \, \overset{\circ}{\mathbf{p}}_{(k-1)} = 0 \tag{4.76}$$

$$-\overset{\circ}{\nabla} \cdot \overset{\circ}{\mathbf{q}}_{(k)} - \mathbf{C} \cdot \overset{\circ}{\mathbf{N}}_{(k)} - \overset{\circ}{\mathbf{q}}_{(k)} \cdot \mathbf{d} + k \, \overset{\circ}{r}_{(k-1)} = 0 \tag{4.77}$$

It is worth noting that these equations have the same formal structure of those obtained considering the surface natural frame as frame for representing the virtual displacements (Eqs. (4.36)-(4.37)). Nonetheless, it is also worthy to recall that the definition of the dynamical descriptors appearing here is different from that there, being the latter relevant to a different choice of displacements that keep knowledge of the inclination of the fiber in the actual configuration of the body, whereas the former affects only the actual configuration of the mid-surface.

Chapter 5

Kirchhoff–Love revised

5.1 Introduction

The issue of kinematical constraints has been extensively addressed in the current literature, but it has also been criticized to an extent that, thus far, no complete agreement exist within the researchers in this field, and at least two main approaches can be identified. In particular, in Ref. [96] it has been argued that a correct approach in the modeling of simplifying shells (and rods) theories should depart from constitutive consideration nor kinematical ones in order to avoid unacceptable physical conclusions. In particular, the author suggests that, the limitation on the motion of the material points within the body, have to be deduced as a consequence of the limitation of the possible stresses arising in the body in any admissible motion. The author, in other words, has moved the point of view from the kinematics to the dynamics, introducing between the lines, the concept of active stress which perform work in the admissible motion. A different (and more conscious) point of view has been taken by Gurtin and Podio-Guidugli in their paper on constrained elasticity. In particular in Refs. [54, 89, 87] these authors have treated in a unified manner the definition of a material constraint (as *a limitation on the possible motion of a material point* within the body) and its consequences on the thermodynamics, and, consequently, constitutive relations, of the model. This approach, following Ref. [112], start with an *a priori* additive decomposition of the stress into reactive and active components with the reactive component assumed to be powerless in all motions that satisfy the constraints and the active component given by a constitutive equation. The same approach to the problem have also guided Davì in his formulation of anisotropic and piezoelectric rod-like bodies (see Refs. [28, 29, 30]). In these works the internal constraints have been treated as an exact mathematical restriction on the admissible motion and then consequences on the form of the constitutive equations (deduced from the three-dimensional theory) have been addressed. This same approach have also inspired Podio-Guidugli in Ref. [65] (and more recently in Ref. [33]) in his derivation of a plate and shell theory from the three-dimensional linear elasticity. Nonetheless, an important contribution to this issue has been given by Simo who, in the formulation of rod-like

69

and shell-like models (see Refs. [97, 98, 100, 101, 99, 102]), has recovered the original treatment of material constraints proposed by Kirchhoff and then elaborated by Love (cfr. [68]) which consists in developing the theory from just a few hypotheses on the geometry and the kinematics of the body (thus assigning the configurational space of the continuum) and then deducing the equilibrium equations from the application of the virtual work (with an appropriate definition of the stress resultants and couples). Interestingly enough, for his own admission, *the model described above falls within the class of constrained Cosserat models in which the directors are constrained to be the orthonormal basis vectors.* In this sense, it does not surprise that similar considerations and treatments can be found in [94]. Note, finally, that in a recent paper (Ref. [21]) this issue has been discussed again and the authors arrived to the conclusion that a geometrically-based approach has to be preferred in the treatments of internal constraints.

At this point it is important to remark that, whilst the cited authors have developed theories of constrained materials in contrast to the general theory of unconstrained materials, here, instead, the concept of constraint is introduced in an instrumental way. Specifically, in a constrained theory of the Kirchhoff-Love type one assumes that the motion of the body is carefully describable by the motion of its main (or mid-) surface (if the thickness of the shell is small compared to the other dimensions) and in this sense the displacement field of the layer is expressed in terms of the displacement field of the main surface. Once the motion of the main surface is known (from the solution of the associated equations and constitutive relations), the cited authors, such as, for instance, Podio-Guidugli (cfr. Refs. [87, 33]), suggest to recover information of the relative motion from the determination of the reactive stresses due to the constraints and, eventually, to determine the consequent deformation of the micro-structure (or fiber) assuming a constrain backdown in the final configuration of the Kirchhoff-Love type motion. Instead, the point of view developed here consists in retaining information of the constrain backdown directly in the equilibrium equations of the Kirchhoff-Love motion. This is done exploiting in full the potentiality of the Principle of Virtual Work and then decomposing the displacement field in the sum of the displacement due to a pure a Kirchhoff-Love type motion plus a relative displacement that takes into account the constrain backdown. It is worthy, at this point, to recall the essence of the Virtual Work Principle. It states that, at the equilibrium, the inner virtual work exerted by the continuum under the effect of a field of realizable (see ref. [33]) velocities (or virtual displacements) must equal the work exerted by the field of external forces acting on the continuum at the equilibrium under the same field of realizable velocities. This implies that, if one selects, among the set of realizable velocities, those permitted by a constraint he can recover the tensional state provided by the constrained motion. Subsequently, selecting as virtual displacement that of an unconstrained motion one can determine the tensional state due to this relative motion and then identify the exact deformation of the body. It is worth noting that this decomposition is not done *a posteriori* and so the displacement field of the main surface will take into account the real, unconstrained, motion of the shell, whereas in the other approach the solution in terms of the in-plane unknwons remains the solution of the constrained

model. In other words, here a coupled problem will be solved, where the coupling is between the motion of the main surface and the relative motion of the layer, whereas the former approach see the relative motion as a by-product (one-way coupling) of the motion of the main surface. Furthermore, observe that in practical applications the difference between the RM and the KL formulations is small. Thus, it is convenient to recast the RM equations into a format that emphasizes this feature. This is important not only from a conceptual point of view (to show how the RM equations reduce in the limit to the KL equations), but also from a computational point of view, because the resulting equations isolate the "big contribution" (KL) from the "small contribution" (MR equations, *i.e.*, those for $k = 1$).

   This goal is achieved in this chapter, as said before, by exploiting in full the potentialities of the virtual work approach, specifically, the arbitrariness of the virtual displacement from the deformed configuration of the shell. Indeed, the virtual displacements $\delta\mathbf{u}_{(1)}$, representing the tangential displacement on the upper and lower surfaces, even in the context of the Reissner-Mindlin hypotheses, can be expressed as the sum of the displacement due to the Kirchhoff-Love assumption and of an arbitrary additional displacement.

$$\delta\mathbf{u}_{(1)} = \delta\mathbf{u}_{(1)}\big|_{KL} + \delta\mathbf{u}_{(1)}\big|_{RM} \tag{5.1}$$

where $\delta\mathbf{u}_{(1)}\big|_{KL}$ is specified imposing the KL constraints to the motion of the director. Classically (see for instance Ref. [106]) the KL constraints are identified by the two following conditions:

(i) Points [..] lying initially on a normal-to-the-middle plane [..] remain on the normal-to-the-middle surface after bending.

(ii) The normal stresses in the direction transverse to the plate can be disregarded.

Instead, in this thesis, in order to derive a simpler formulation for piezoelectric shells having piezoelectric fibers through the thickness inclined with respect to the normal, a revised version of the previous constraints will be introduced. Specifically, one may assume that:

(i) The fiber cannot stretch.

(ii) No shear is permitted along a fiber;

5.2   Material Constraints

The first constraint that has to be imposed is the unextensibility of the fiber, $\mathbf{g}_3 \cdot \mathbf{g}_3 = constant$, yields

$$\delta\mathbf{g}_3 \cdot \mathbf{g}_3 = 0 \tag{5.2}$$

Recalling that $\mathbf{g}_3 = h\,(\mathbf{n} + \mathbf{l})$, one obtains $\delta\mathbf{g}_3 \cdot \mathbf{n} + \delta\mathbf{g}_3 \cdot \mathbf{l}$, or[*]

$$\delta w_{(1)} = -\,\mathbf{l}\cdot\delta\mathbf{u}_{(1)} \tag{5.3}$$

alternatively, using Eq. (4.41), one has

$$\delta u_{3_{(1)}} \;=\; 0 \tag{5.4}$$

which means that the material fibers cannot stretch, but must retain their length in any admissible motion (when the constraint is applied).

The second constraint to be imposed is the conservation of the covariant component of the director during the deformation (see, for instance Ref. [94]), $\mathbf{g}_3 \cdot \mathbf{a}_\alpha = constant$, yields $\delta\mathbf{g}_3 \cdot \mathbf{a}_\alpha = -\,\mathbf{g}_3 \cdot \partial\delta\mathbf{p}/\partial\xi^\alpha$, or

$$
\begin{aligned}
\delta\mathbf{g}_3 \cdot \mathbf{a}_\alpha = \left(\mathbf{u}_{(1)} + w_{(1)}\,\mathbf{n}\right)\cdot\mathbf{a}_\alpha = \mathbf{u}_{(1)}\cdot\mathbf{a}_\alpha \;&=\; -\,\mathbf{g}_3 \cdot \left[\mathrm{Grad}\,\left(\mathbf{u}_{(0)} + w_{(0)}\,\mathbf{n}\right)\right]\mathbf{a}_\alpha \\
&=\; -\,\left[\mathrm{Grad}\,\left(\mathbf{u}_{(0)} + w_{(0)}\,\mathbf{n}\right)\right]\cdot\left(\mathbf{g}_3 \otimes \mathbf{a}_\alpha\right) \\
&=\; -\,\left\{\left[\mathrm{Grad}\,\left(\mathbf{u}_{(0)} + w_{(0)}\,\mathbf{n}\right)\right]^T \mathbf{g}_3\right\}\cdot\mathbf{a}_\alpha \tag{5.5}
\end{aligned}
$$

It is worth noting that Eq. (5.5) does not mean that the angle between the tangent plane and the director remains. To the contrary, when the base surface is deformed, a rotation of the fiber is permitted in such a way that, if the tangent plane is stretched, then the angle between the director and the plane is increased.

Using Eq. (3.132) and noting that $(\mathbf{n}\otimes\mathbf{n}\,w',\mathbf{u}'\otimes\mathbf{n})\;\mathbf{a}_\alpha = 0$ one has

$$\mathbf{u}_{(1)} \;=\; -\left[\left(\nabla\otimes\mathbf{u}_{(0)} - w_{(0)}\mathbf{B}\right) + \mathbf{n}\otimes\left(\nabla w_{(0)} + \mathbf{B}\mathbf{u}_{(0)}\right)\right]^T \mathbf{g}_3 \tag{5.6}$$

Thus, using Eq. (5.3), one obtains

$$
\begin{aligned}
w_{(1)} \;&=\; \mathbf{l}\cdot\left[\left(\nabla\otimes\mathbf{u}_{(0)} - w_{(0)}\mathbf{B}\right) + \mathbf{n}\otimes\left(\nabla w_{(0)} + \mathbf{B}\mathbf{u}_{(0)}\right)\right]^T \mathbf{g}_3 \\
&=\; \left[\left(\nabla\otimes\mathbf{u}_{(0)} - w_{(0)}\mathbf{B}\right) + \mathbf{n}\otimes\left(\nabla w_{(0)} + \mathbf{B}\mathbf{u}_{(0)}\right)\right]\cdot\left(\mathbf{g}_3 \otimes \mathbf{l}\right) \tag{5.7}
\end{aligned}
$$

Note that if the material fiber is assumed initially normal, then the application of the K-L material constraint during the motion yields $\mathbf{g}_3 = h\,\mathbf{n}$ and from Eq. (5.6) one has

$$\mathbf{u}_{(1)} \;=\; -\,h\left(\nabla w_{(0)} + \mathbf{B}\mathbf{u}_{(0)}\right) \tag{5.8}$$

---

[*] Recall that a virtual variation of $\mathbf{p}$ is equal to a virtual displacement of the reference surface ($\mathbf{v}_{(0)}$ or $\delta\mathbf{v}_{(0)}$), whereas a virtual variation of the director $\mathbf{g}_3$ coincides with a virtual displacement of the fiber ($\mathbf{v}_{(1)}$ or $\delta\mathbf{v}_{(1)}$).

5.3   An illustrative example

In order to prove the validity of the considerations exposed in the Introduction of the thesis and of this Chapter, the case of an unextensible beam, immersed in a 2-D space, with transverse shear effect included (classically denoted as Timoshenko's beam theory),[†] where to apply some of the concepts developed thus far, and to introduce some subsequent enhancements, is considered. In particular, the equilibrium equations for the beam model will be written from the application of the Virtual Work Principle both using the traditional Reissner-Mindlin kinematical hypothesis, and the innovative KL+RM decomposition. In particular, it will be shown that, solving numerically the two subsequent formulations, in one case, the one corresponding to the KL+RM decomposition and in which the solution is sought in terms of transversal displacement and difference between the RM and the KL rotation of the fiber, the numerical solution reproduce exactly the analytical solution, found using a Laplace transform approach, whereas in the other case, the one corresponding to the RM model in which the solution is sought in terms of transversal displacement and fiber rotation, the numerical solution is affected by some errors. The main reason for the presence of these errors is due to the smallness of the transverse shear for this particular problem. Therefore, in the case in which the transverse shear is treated independently (RM+KL) one obtains good results, whereas in the case when the transverse shear has to be obtained as the difference of the derivative of the transverse displacement and of the fiber rotation the numerical solution brings errors due to the closeness of the present model to the KL kinematical hypotheses. It is worth noting that in both the numerical cases, it has been adopted a finite difference scheme with five points, and the same level of discretization in the domain of integration so that the results are potentially equivalent.

This section is structured in the following way: first, the equilibrium equations for the beam model will be derived using the Virtual Work Principle, then, the KL+RM decomposition will be introduced to see how the equilibrium equations reduce in this limit, finally, a discussion of the numerical and analytical results will follow after a brief presentation of the solution methodology employed.

At conclusion of this section, it is worth noting that, recently, a paper has been published (see Ref. [95]) focusing on the consideration of the unconstrained solution as a deviation from the constrained one. Nonetheless, the analysis is there limited to the consideration of plane circular arches, whereas, in the present thesis, is formulated in terms of arbitrary microstructured shells. Moreover, in Ref. [95], the proposed model is not derived from a three-dimensional continuum as done in the present activity. Finally, let us observe that, in the same reference, the equilibrium

---

[†] The interested reader will find further improvements relevant to beam models in Chapter 7, where an aero-thermo-elastic application is presented, with particular emphasis on the effect of the transverse shear flexibility, warping restraint and aero-thermo-elastic interaction. Furthermore, let us observe, that, while here the goal is directed towards the evaluation of the KL+RM decomposition of the displacement field, there, the analysis does not retain this decomposition: however, the Kirchhoff-Love (or more correctly the Euler-Bernoulli's beam model) represents an ideal landfall to which one arrives from the Reissner-Mindlin (or Timoshenko's model) using material considerations.

equations are derived from a formal power series expansion of the exact measures of deformation, whereas here the decomposition is treated in a more complete fashion on the basis of physical considerations and exploiting the potentialities of the Virtual Work Principle.

5.3.1   Equilibrium equations

In this Section the equilibrium equations for an unextensible beam, of constant thickness, and rectilinear axis, immersed in a 2-D space are derived in a way similar, but much more simplified, to what has been done in the previous Chapters with reference to shell-like continuum bodies.

By virtue of the previous modeling hypotheses, the field of admissible displacements can be written as

$$\mathbf{v}\left(x, z\right) \;\; = \;\; z \; u_1\left(x\right) \mathbf{e}_1 + w_0\left(x\right) \mathbf{e}_3 \tag{5.9}$$

where, as usual, the axis co-ordinate has been denoted with x and the corresponding unit vector with $\mathbf{e}_1$, whereas the co-ordinate in the fiber direction (assumed normal to the reference axis) with z and the corresponding unit vector (normal to the reference axis) with $\mathbf{e}_3$. Furthermore, in Eq. (5.9), l represents the spanwise length of the beam, and $\mathcal{A}$ its cross section (or fiber). The inner virtual work can now be written as

$$
\begin{aligned}
\delta\mathcal{W}_i \;\; &= \;\; \int_0^l \int_{\mathcal{A}} \left(\sigma^{11}\,\delta\varepsilon_{11} + 2\,\sigma^{13}\,\delta\varepsilon_{13} + \sigma^{33}\,\delta\varepsilon_{33}\right)\; dA\; dx \\
&= \;\; \int_0^l \left[M\,u_1' + Q\,\left(u_1 + w_0'\right)\right]\; dx
\end{aligned}
\tag{5.10}
$$

where M and Q are, respectively, the flexural moment and shear resultant, defined by the following relations

$$M \;\; := \;\; \int_{\mathcal{A}} \sigma^{11}\; z\; dA \tag{5.11}$$

$$Q \;\; := \;\; \int_{\mathcal{A}} \sigma^{13}\; dA \tag{5.12}$$

Let us, now apply the integration by parts theorem in Eq. (5.10):

$$\delta\mathcal{W}_i \;\; = \;\; \left[M\,u_1 + Q\,w_0\right]_0^l - \int_0^l \left[(M' - Q)\,u_1 + Q'\,w_0\right]\; dx \tag{5.13}$$

At this point let us introduce the KL+RM decomposition of the virtual displacements

$$u_1 \;\; = \;\; u_1|_{KL} + u_1|_{RM} \tag{5.14}$$

where the Kirchhoff-Love part of the displacement is given imposing the KL kinematical constraint

of no shear deformation among the fibers. The KL constraint in this case is

$$\varepsilon_{13}|_{KL} = 0 \qquad \Longrightarrow \qquad u_1|_{KL} + w_0' = 0 \tag{5.15}$$

whereas the Reissner-Mindlin part is the difference between the solution of the original problem and the solution obtainable considering the material constraint in the motion, and, for this reason, it will be denoted henceforth as Δu_1. Using Eq. (5.14) in Eq. (5.13) one has

$$\delta \mathcal{W}_i = [M \; \Delta u_1 - M \; w_0' + Q \; w_0]_0^l - \int_0^l [(M' - Q) \Delta u_1 - (M' - Q) w_0' + Q' \; w_0] \; dx \tag{5.16}$$

Applying the an integration by parts in the preceding equation, one has

$$\delta \mathcal{W}_i = [M \; \Delta u_1 - M \; w_0' + M' \; w_0]_0^l - \int_0^l [(M' - Q) \Delta u_1 - M'' \; w_0] \; dx \tag{5.17}$$

Similarly, for the external virtual work, considering both the work in the domain and the work on the boundaries, one has

$$\begin{aligned}
\delta \mathcal{W}_e &= \int_0^l \int_{\mathcal{A}} \left(\hat{f}_1 \; z \; u_1 + \hat{f}_3 \; w_0 \right) \; dA \; dx + [\bar{m} \; u_1 + \bar{q} \; w_0]_0^l \\
&= \int_0^l (g_1 \; u_1 + f_3 \; w_0) \; dA \; dx + [\bar{m} \; u_1 + \bar{q} \; w_0]_0^l
\end{aligned} \tag{5.18}$$

where g_1 and f_3 represent the resultant external loads acting on the beam, defined by the following relations

$$g_1 := \int_{\mathcal{A}} \hat{f}_1 \; z \; dA \tag{5.19}$$

$$f_3 := \int_{\mathcal{A}} \hat{f}_3 \; dA \tag{5.20}$$

Introducing also in this case the KL+RM decomposition of the displacement field one has

$$\begin{aligned}
\delta \mathcal{W}_e &= \int_0^l (g_1 \; \Delta u_1 - g_1 \; w_0' + f_3 \; w_0) \; dA \; dx + [\bar{m} \; u_1 + \bar{q} \; w_0]_0^l \\
&= \int_0^l [g_1 \; \Delta u_1 + (g_1' + f_3) \, w_0] \; dA \; dx + [\bar{m} \; u_1 + (\bar{q} - g_1) \; w_0]_0^l
\end{aligned} \tag{5.21}$$

Before proceeding further, assume that the material is homogeneous and isotropic; consequently, the constitutive relations may be written

$$\sigma^{11} = E \; \varepsilon_{11} = E \; z \; u_1' \tag{5.22}$$

$$\sigma^{13} = 2 \; G \; \varepsilon_{13} = G \, (u_1 + w_0') \tag{5.23}$$

Invoking again the KL+RM decomposition, the previous system of constitutive relations becomes

$$\sigma^{11} = E\,z\left(\Delta u_1' - w_0''\right) \tag{5.24}$$

$$\sigma^{13} = G\,\Delta u_1 \tag{5.25}$$

Using now the Virtual Work Principle one can write two systems of equilibrium equations and boundary conditions for the original Reissner-Mindlin (or Timoshenko) problem and for the KL+RM (or Bernoulli-Euler + Timoshenko) problem respectively.

Reissner-Mindlin formulation

In this case equating the inner virtual work in Eq. (5.13) to the external virtual work in Eq. (5.18), one obtains the following system of equilibrium equations

$$w_0 \quad : \qquad Q' + f_3 = 0 \tag{5.26}$$

$$u_1 \quad : \qquad M' - Q + g_1 = 0 \tag{5.27}$$

Similarly, the related boundary conditions, assuming a clamped-free condition, are

$$w_0 = 0 \qquad \text{and} \qquad u_1 = 0 \qquad \text{for } x = 0 \tag{5.28}$$

$$Q = \hat{q} \qquad \text{and} \qquad M = \hat{m} \qquad \text{for } x = l \tag{5.29}$$

Using the constitutive relations in Eqs. (5.22)-(5.23) in the integral relations of Eqs. (5.11)-(5.12), substituting them in Eqs. (5.26)-(5.29), and introducing a redefinition of the displacement variables (*i.e.*, $y_1 := EIw_0$, $y_2 := EIu_1$), the equilibrium equations become

$$y_1 : \qquad -k\left(y_1'' + y_2'\right) = f_3 \tag{5.30}$$

$$y_2 : \qquad -y_2'' + k\,y_1' + k\,y_2 = g_1 \tag{5.31}$$

where $k = GA/EI$ is the ratio of the transverse shear stiffness to the flexural stiffness. Similarly, in terms of these new variables the boundary conditions become

$$y_1 = 0 \qquad \text{and} \qquad y_2 = 0 \qquad \text{for } x = 0 \tag{5.32}$$

$$k\left(y_1' + y_2\right) = \hat{q} \qquad \text{and} \qquad y_2' = \hat{m} \qquad \text{for } x = l \tag{5.33}$$

RM+KL formulation

In this other case, to obtain the equilibrium equations from the application of the Virtual Work Principle, one should equate the inner virtual work in Eq. (5.17) to the external virtual work in Eq.

(5.21). In this way, one obtains the following system of equilibrium equations

$$w_0 \quad : \qquad M'' + g_1' + f_3 = 0 \tag{5.34}$$

$$\Delta u_1 \quad : \qquad M' - Q + g_1 = 0 \tag{5.35}$$

Similarly, the related boundary conditions, assuming a clamped-free condition, are

$$w_0 \;=\; 0 \qquad \text{and} \qquad \Delta u_1 - w_0' = 0 \qquad \text{for } x = 0 \tag{5.36}$$

$$M' \;=\; \hat{q} - g_1 \qquad \text{and} \qquad M = \hat{m} \qquad \text{for } x = l \tag{5.37}$$

Using the constitutive relations in Eqs. (5.24)-(5.25) in the integral relations of Eqs. (5.11)-(5.12), substituting them in Eqs. (5.34)-(5.37), and introducing the same new displacement variables already defined (*i.e.*, $y_1 := EI w_0$, $\Delta y_2 := EI \Delta u_1$), the equilibrium equations become[‖]

$$y_1 : \qquad y_1^{(IV)} - \Delta y_2''' = g_1' + f_3 \tag{5.39}$$

$$\Delta y_2 : \qquad y_1''' - \Delta y_2'' + k \; \Delta y_2 = g_1 \tag{5.40}$$

Similarly, the boundary conditions become

$$y_1 \;=\; 0 \qquad \text{and} \qquad \Delta y_2 - y_1' = 0 \qquad \text{for } x = 0 \tag{5.41}$$

$$\Delta y_2'' - y_1''' \;=\; \hat{q} - g_1 \qquad \text{and} \qquad \Delta y_2' - y_1'' = \hat{m} \qquad \text{for } x = l \tag{5.42}$$

As a matter of fact, in order to emphasize the simplification potentialities of the proposed approach, the equilibrium equations should be recast in a different format. In particular, it may be observed that the decomposition of the displacement field in a part related to the KL model plus a difference between the KL and the RM model, which characterizes the obtainment of the equilibrium equations in terms of the stress resultants (Eqs. (5.34)-(5.35)), may not be necessarily retained also in the evaluation of the kinematical relations and, consequently, of the constitutive relations (Eqs. (5.24)-(5.25)). Indeed, substituting Eqs. (5.22)-(5.23) in Eqs. (5.34)-(5.35), one obtains the following system of equilibrium equations

$$y_2 \quad : \quad y_2''' = -g_1' + f_3 \tag{5.43}$$

$$\Delta y_2 \quad : \quad y_1' = g_1 - y_2 + \frac{1}{k} \; y_2'' \tag{5.44}$$

[‖] As a matter of fact let us observe that the structural operator $\mathbf{L}$ appearing in Eqs. (5.39)-(5.40) and defined as

$$\mathbf{L} \quad := \quad \begin{bmatrix} d/dx^4 & -d/dx^3 \\ d/dx^3 & k - d/dx^2 \end{bmatrix} \tag{5.38}$$

is self-adjoint, and that, consequently, the previous system of equilibrium equations could be derived also as the minimum of a functional.

In this case, it is apparent that, although the structural operator is no more self-adjoint, the equilibrium equations haqve been reduced to a system of two independent equations.[†] Indeed, the first equation (Eq. (5.43)) is an equation containing only y_2 and it may be solved independently; once the solution in terms of y_2 is known, one may use it to solve the second equation (Eq. (5.44)), that is an equation of the first order in y_1.[‡]

5.3.2 Solution methodology and numerical results

The two systems of equilibrium equations previously presented, are, obviously, equivalent, therefore, from the point of view of the analytical solution one should expect to find the same results, either solving the former or the latter. On the other hand, solving numerically the two problems one will find different solutions and in particular will observe that the numerical solution of the KL+RM formulation is closer to the analytical solution than the RM one.

Analytical solution

Here the RM problem is solved using a Laplace transform approach.[**] In particular, let us observe that one may rewrite Eqs. (5.30)-(5.31) in the following compact form

$$- \mathsf{L} y'' + \mathsf{K} y' + \mathsf{H} y = \mathsf{f} \tag{5.45}$$

where $\mathsf{y} = \{y_1, y_2\}^T$, and the matrices L, K and H are given by

$$\mathsf{L} := \begin{bmatrix} k & 0 \\ 0 & 1 \end{bmatrix} \quad , \quad \mathsf{K} := \begin{bmatrix} 0 & -k \\ k & 0 \end{bmatrix} \quad , \quad \mathsf{H} := \begin{bmatrix} 0 & 0 \\ 0 & k \end{bmatrix} \tag{5.46}$$

Similarly the boundary conditions can be written as

$$\mathsf{y}' + \mathsf{M} \mathsf{y} = \mathsf{m} \tag{5.47}$$

[†] To facilitate the comprehension of our reasoning the reader should refer to the definition of triangular matrices, and to the intrinsic advantages contained in the solution of algebraic problems characterized by such linear operators. In this case, in fact, one can solve in cascade all the equations starting from the last and moving forward in the substitutions.

[‡] It is worth noting that the order of the previous system of equations is the fourth, equal to the number of boundary conditions. Nonetheless, this fact should not lead to the conclusion that the system of Eqs. (5.39)-(5.40) is not well-posed; indeed, in that case the order of the system is only fictitiously the seventh, as it may be proved evaluating the order of the associated characteristic equation (*i.e.*, the fourth).

[**] The interested reader is referred to Chapter 7 for an extensive presentation of the Laplace transform methodology for the solution of structural problems.

where $\mathsf{m} = \{\hat{q}, \hat{m}\}^T$, and the matrix M is given by

$$\mathsf{M} := \begin{bmatrix} 0 & 1 \\ 0 & 0 \end{bmatrix} \tag{5.48}$$

Thus, the analytical solution can be written as

$$\mathsf{y}(x) = \mathsf{g}(x) - \mathsf{A}(x) \left[\mathsf{A}'(l) + \mathsf{MA}(l)\right]^{-1} \left[\mathsf{g}'(l) + \mathsf{Mg}(l) + \mathsf{m}\right] \tag{5.49}$$

where the matrix A is defined as

$$\mathsf{A}(x) := \mathcal{L}_p^{-1} \left\{ \left[-p^2 \, \mathsf{L} + p \, \mathsf{K} + \mathsf{H}\right]^{-1} \right\} \tag{5.50}$$

and g is given by

$$\mathsf{g}(x) := \mathcal{L}_p^{-1} \left\{ \left[-p^2 \, \mathsf{L} + p \, \mathsf{K} + \mathsf{H}\right]^{-1} \mathcal{L}_x \{\mathsf{f}\} \right\} \tag{5.51}$$

Implementing the previous relations the following results in terms of the displacements y_1, y_2 and $\Delta y_2 \; (= y_2 + y_1')$ have been found, having assumed the geometrical, material and loading data reported in Tab. 5.1. In particular, Figs. 5.1 show the vertical displacement of the beam axis and

length l (m)	1.00
thickness t (m)	0.001
Poisson' coefficient ν	0.2
$k = 3/(2t^2(1+\nu))$	$1.25 \; 10^6$
$\hat{m}$	0
$\hat{q}$	0
g_1	0
f_3	$2 \; 10^7 \; t \; \sin[\pi x/l]$

Table 5.1: Piezoelectric material moduli.

the rotation of the fiber, whereas Fig. 5.2 shows the difference between the fiber rotation found within the KL model and the exact solution due to the RM hypothesis.

Numerical solution

Here the KL+RM and the RM problem are solved numerically using a finite difference scheme.[††] As it was observed earlier, the highest degree of the derivatives for the KL+RM formulation is the fourth; thus, one may use five-points finite differences and obtain a Δx-accuracy expression. Using

---

[††] The interested reader is referred to Chapter 6 for a presentation of the finite differences scheme employed for the solution of structural problems.

29th May 2005

(a) Transversal

(b) Rotation
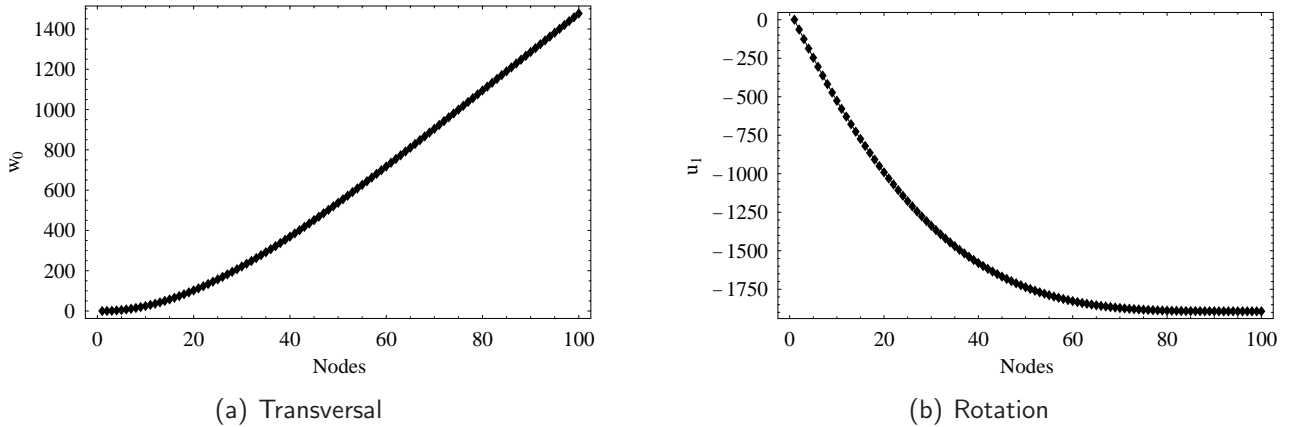
Figure 5.1: Analytical approach: displacement components of the beam.
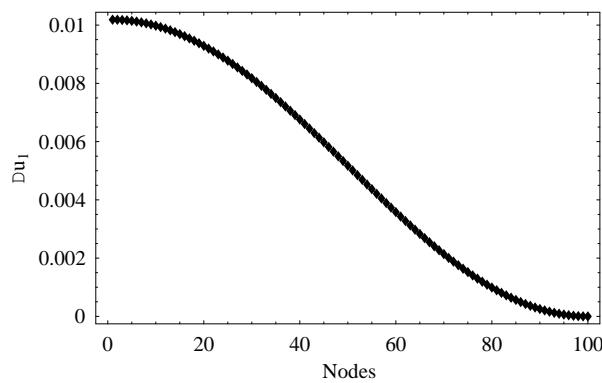
Figure 5.2: Analytical approach: difference of the solutions of the KL and RM models.

the same level of accuracy, the algebraic problem resulting from the numerical discretization of the equilibrium equations and boundary conditions for both the RM (see Eqs.(5.45) and (5.47)) and KL+RM (see Eqs. (5.39)-(5.42)) formulations has been solved. Finally, using the same material and geometrical parameters already introduced in the previous Section, the following results in terms of displacements have been found. In particular, Figs. 5.3 show the vertical displacement of the

(a) Transversal
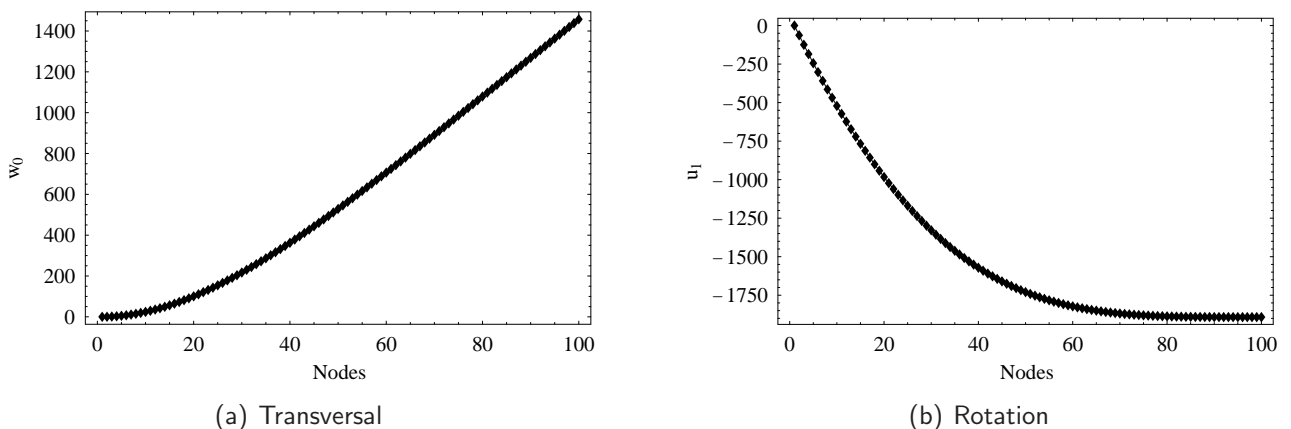
(b) Rotation

Figure 5.3: Numerical approach: KL+RM formulation. Displacement components of the beam.

beam axis and the rotation of the fiber using the KL+RM formulation, whereas Fig. 5.4 shows the
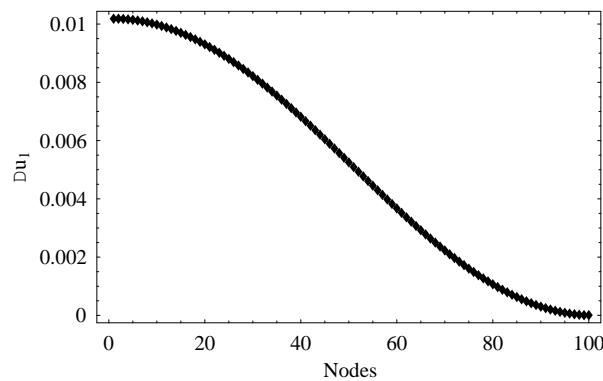
Figure 5.4: Numerical approach: KL+RM formulation. Difference of the solutions of the KL and RM models.

difference between the fiber rotation due to the KL model and the one due to the RM hypothesis using the same mixed formulation.

Similarly, Figs. 5.5 show the vertical displacement of the beam axis and the rotation of the fiber,

(a) Transversal
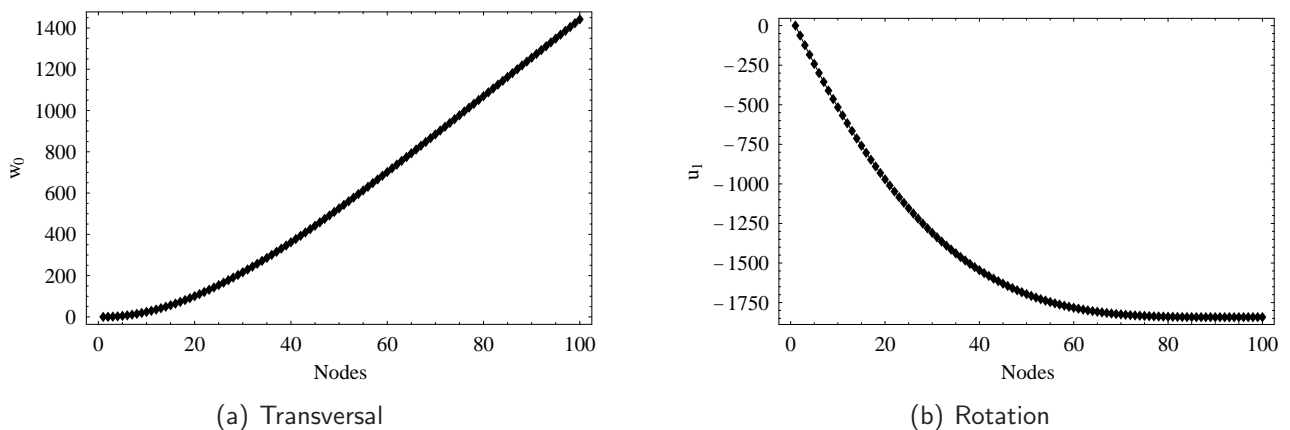
(b) Rotation

Figure 5.5: Numerical approach: RM formulation. Displacement components of the beam.

whereas Fig. 5.6 shows the difference between the fiber rotation due to the KL model and the one due to the RM hypothesis.

It is apparent, that, whilst the numerical discretization scheme based on the mixed KL+RM approach reproduces accurately the results of the analytical approach, the numerical results available with the RM formulation are affected by some errors in the Δu_1 displacement field (cfr. Figs. 5.6 and 5.4). These errors, as it has been already anticipated, are due to the fact that, for the problem under exam (*i.e.*, for the assumed transverse to bending stiffness ratio k), the KL kinematical hypothesis is particularly accurate and thus the fiber rotation is almost given by the derivative of the transversal displacement. In other words, the difference between the derivative of the transversal displacement and the fiber rotation is small and should be trated in a separate manner: this is what has been done in the KL+RM approach. Finally, it is worth noting that the numerical errors encountered in
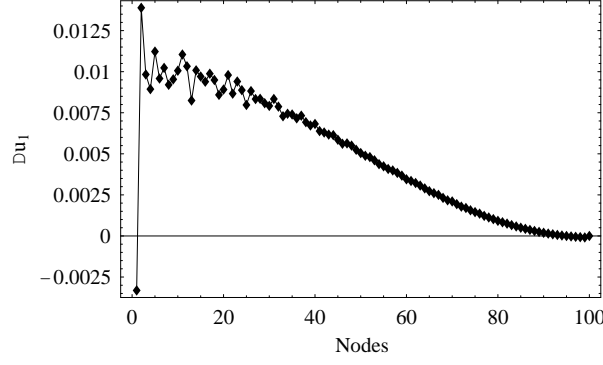
Figure 5.6: Numerical approach: RM formulation. Difference of the solutions of the KL and RM models.

the solution of the RM problem would decrease decreasing the transverse to bending stiffness ratio (*i.e.*, increasing, for this particular problem, the thicknees of the beam).

5.4   Constrained Inner Work

5.4.1   First Approach: The Surface Natural Frame

Let us now apply the previous constraints (Eqs. (5.6)-(5.7)) in the expression of the virtual work. Refer for the moment to Eq. (4.31), that, for convenience, is here reported in a form valid for $N = 1$, *i.e.*, for a single-director theory

$$\delta \mathcal{W}_i \;=\; \int_{\mathcal{S}_M} \Big[\mathbf{N}_{(0)} \cdot \big(\nabla \otimes \mathbf{u}_{(0)} - \mathbf{B}\, w_{(0)} \big) + \mathbf{q}_{(0)} \cdot \big(\nabla w_{(0)} + \mathbf{B}\mathbf{u}_{(0)} \big) + \mathbf{N}_{(1)} \cdot \big(\nabla \otimes \mathbf{u}_{(1)} - \mathbf{B}\, w_{(1)} \big) +$$
$$+ \;\; \mathbf{q}_{(1)} \cdot \big(\nabla w_{(1)} + \mathbf{B}\mathbf{u}_{(1)} \big) + \; \mathbf{p}_{(0)} \cdot \mathbf{u}_{(1)} + r_{(0)}\, w_{(1)} \Big] \, d\mathcal{S} \tag{5.52}$$

Using the Green-Gauss theorem with respect to the first-oder terms in the previous equation, one has (cfr Eq. (4.34))

$$\delta \mathcal{W}_i = \int_{\mathcal{S}_M} \Big\{ \big[\mathbf{N}_{(0)} \cdot \big(\nabla \otimes \mathbf{u}_{(0)} - \mathbf{B}\, w_{(0)} \big) + \mathbf{q}_{(0)} \cdot \big(\nabla w_{(0)} + \mathbf{B}\mathbf{u}_{(0)} \big) \big]$$
$$+ \big[-\nabla \cdot \mathbf{N}_{(1)} + \mathbf{B}\, \mathbf{q}_{(1)} + \mathbf{p}_{(0)} \big] \cdot \mathbf{u}_{(1)}$$
$$+ \big[-\nabla \cdot \mathbf{q}_{(1)} - \mathbf{N}_{(1)} \cdot \mathbf{B} + r_{(0)} \big] w_{(1)} \Big\} \; d\mathcal{S} + BT_{(1)} \tag{5.53}$$

then, introducing the constraints (Eqs. (5.6)-(5.7)) in the previous equation, one has

$$
\begin{aligned}
\delta\mathcal{W}_i \;=\; \int_{\mathcal{S}_M} \Big\{ & \big[\mathbf{N}_{(0)} \cdot \big(\nabla \otimes \mathbf{u}_{(0)} - \mathbf{B}\, w_{(0)} \big) + \mathbf{q}_{(0)} \cdot \big(\nabla w_{(0)} + \mathbf{B}\mathbf{u}_{(0)} \big) \big] \\
- \;& \big[-\nabla \cdot \mathbf{N}_{(1)} + \mathbf{B}\, \mathbf{q}_{(1)} + \mathbf{p}_{(0)} \big] \cdot \big[\big(\nabla \otimes \mathbf{u}_{(0)} - w_{(0)}\mathbf{B} \big) + \mathbf{n} \otimes \big(\nabla w_{(0)} + \mathbf{B}\mathbf{u}_{(0)} \big) \big]^T \mathbf{g}_3 \\
+ \;& \big[-\nabla \cdot \mathbf{q}_{(1)} - \mathbf{N}_{(1)} \cdot \mathbf{B} + r_{(0)} \big] \ \mathbf{l} \cdot \big[\big(\nabla \otimes \mathbf{u}_{(0)} - w_{(0)}\mathbf{B} \big) \\
+ \;& \mathbf{n} \otimes \big(\nabla w_{(0)} + \mathbf{B}\mathbf{u}_{(0)} \big) \big]^T \mathbf{g}_3 \Big\} \ d\mathcal{S} + BT_{(1)}
\end{aligned}
\tag{5.54}
$$

where $BT_{(1)}$ are the boundary terms due to the application of the divergence theorem with respect to the first-order terms, and are given by

$$
BT_{(1)} \;=\; \int_{\partial \mathcal{S}} \big(\mathbf{N}_{(1)}\mathbf{u}_{(1)} \cdot \mathbf{n}_\partial + w_{(1)}\mathbf{q}_{(1)} \cdot \mathbf{n}_\partial \big)
\tag{5.55}
$$

Recalling that $\mathbf{n} \cdot \mathbf{g}_3 = h$ and that $\mathbf{a} \cdot \mathbf{B}^T \mathbf{c} = \mathbf{c} \otimes \mathbf{a} \cdot \mathbf{B}$ for any vector $\mathbf{a}$, $\mathbf{c}$, and any tensor $\mathbf{B}$, eq. (5.54) may be recast as

$$
\begin{aligned}
\delta\mathcal{W}_i \;=\; \int_{\mathcal{S}_M} & \Big\{ \mathbf{N}_{(0)} - \mathbf{g}_3 \otimes \big[\big(-\nabla \cdot \mathbf{N}_{(1)} + \mathbf{B}\, \mathbf{q}_{(1)} + \mathbf{p}_{(0)} \big) - \big(-\nabla \cdot \mathbf{q}_{(1)} - \mathbf{N}_{(1)} \cdot \mathbf{B} + r_{(0)} \big) \ \mathbf{l} \big] \Big\} \\
& \cdot \ \big(\nabla \otimes \mathbf{u}_{(0)} - w_{(0)}\mathbf{B} \big) \ d\mathcal{S} \\
+\; \int_{\mathcal{S}_M} & \Big\{ \mathbf{q}_{(0)} - h \big[\big(-\nabla \cdot \mathbf{N}_{(1)} + \mathbf{B}\, \mathbf{q}_{(1)} + \mathbf{p}_{(0)} \big) - \big(-\nabla \cdot \mathbf{q}_{(1)} - \mathbf{N}_{(1)} \cdot \mathbf{B} + r_{(0)} \big) \ \mathbf{l} \big] \Big\} \\
& \cdot \ \big(\nabla w_{(0)} + \mathbf{B}\mathbf{u}_{(0)} \big) \ d\mathcal{S} + BT_{(1)}
\end{aligned}
\tag{5.56}
$$

Finally, noting that $(\mathbf{g}_3 \otimes \mathbf{a}) \cdot \mathbf{D} = (h\, \mathbf{l} \otimes \mathbf{a}) \cdot \mathbf{D}$ for any $\mathbf{a} \in \mathscr{V}_\mathcal{S}$ and for any $\mathbf{D} \in \mathscr{T}_\mathcal{S}$,* one has

$$
\begin{aligned}
\delta\mathcal{W}_i \;=\; \int_{\mathcal{S}_M} & \Big\{ \mathbf{N}_{(0)} - \mathbf{l} \otimes h \big[\big(-\nabla \cdot \mathbf{N}_{(1)} + \mathbf{B}\, \mathbf{q}_{(1)} + \mathbf{p}_{(0)} \big) - \big(-\nabla \cdot \mathbf{q}_{(1)} - \mathbf{N}_{(1)} \cdot \mathbf{B} + r_{(0)} \big) \ \mathbf{l} \big] \Big\} \\
& \cdot \ \big(\nabla \otimes \mathbf{u}_{(0)} - w_{(0)}\mathbf{B} \big) \ d\mathcal{S} \\
+\; \int_{\mathcal{S}_M} & \Big\{ \mathbf{q}_{(0)} - h \big[\big(-\nabla \cdot \mathbf{N}_{(1)} + \mathbf{B}\, \mathbf{q}_{(1)} + \mathbf{p}_{(0)} \big) - \big(-\nabla \cdot \mathbf{q}_{(1)} - \mathbf{N}_{(1)} \cdot \mathbf{B} + r_{(0)} \big) \ \mathbf{l} \big] \Big\} \\
& \cdot \ \big(\nabla w_{(0)} + \mathbf{B}\mathbf{u}_{(0)} \big) \ d\mathcal{S} + BT_{(1)}
\end{aligned}
\tag{5.57}
$$

For the sake of simplicity let us rewrite the previous equation in a more compact form

$$
\begin{aligned}
\delta\mathcal{W}_i \;=\; \int_{\mathcal{S}_M} \Big\{ & \big[\mathbf{N}_{(0)} - \mathbf{l} \otimes h \big(\mathbf{a}_{(1)} - b_{(1)}\mathbf{l} \big) \big] \cdot \big(\nabla \otimes \mathbf{u}_{(0)} - w_{(0)}\mathbf{B} \big) \\
+ \;& \big[\mathbf{q}_{(0)} - h \big(\mathbf{a}_{(1)} - b_{(1)} \ \mathbf{l} \big) \big] \cdot \big(\nabla w_{(0)} + \mathbf{B}\mathbf{u}_{(0)} \big) \Big\} \ d\mathcal{S} + BT_{(1)}
\end{aligned}
\tag{5.58}
$$

---

* Recall that with $\mathscr{V}_\mathcal{S}$ and $\mathscr{T}_\mathcal{S}$, the vector and tensor spaces associated to the reference surface (or support space) of the body have been denoted respecetively.

where $\mathbf{a}_{(1)}{}^{\dagger}$ and $b_{(1)}$ are the vector and scalar quantities in parenthesis which multiply the displacement terms in Eq. (5.57). Thus, performing the Green-Gauss theorem on Eq. (5.58) one has

$$
\begin{aligned}
\delta \mathcal{W}_i \;=\; & \int_{\mathcal{S}_M} \Big\{ - \big[\nabla \cdot \big(\mathbf{N}_{(0)} - \mathbf{l} \otimes h \left(\mathbf{a}_{(1)} - b_{(1)} \mathbf{l} \right) \big) - \mathbf{B}^T \big(\mathbf{q}_{(0)} - h \left(\mathbf{a}_{(1)} - b_{(1)} \, \mathbf{l} \right) \big) \big] \, \mathbf{u}_{(0)} \\
& - \big[\nabla \cdot \big(\mathbf{q}_{(0)} - h \left(\mathbf{a}_{(1)} - b_{(1)} \, \mathbf{l} \right) \big) + \mathbf{B} \cdot \big(\mathbf{N}_{(0)} - \mathbf{l} \otimes h \left(\mathbf{a}_{(1)} - b_{(1)} \mathbf{l} \right) \big) \big] \; w_{(0)} \Big\} \; d\mathcal{S} \\
& + \; BT_{(0)} + BT_{(1)}
\end{aligned}
\tag{5.59}
$$

where $BT_{(0)}$ represent the boundary terms resulting from the application of the divergence theorem, given by

$$
\begin{aligned}
BT_{(0)} \;=\; & \int_{\partial \mathcal{S}} \big[\big(\mathbf{N}_{(0)} - \mathbf{l} \otimes h \left(\mathbf{a}_{(1)} - b_{(1)} \mathbf{l} \right) \big) \, \mathbf{u}_{(0)} \cdot \mathbf{n}_{\partial} \\
& + \; w_{(0)} \left(\mathbf{q}_{(0)} - h \left(\mathbf{a}_{(1)} - b_{(1)} \, \mathbf{l} \right) \right) \cdot \mathbf{n}_{\partial} \big]
\end{aligned}
\tag{5.60}
$$

Using Eqs. (4.45)-(4.48) it can be proved that the following relation hold

$$
\begin{aligned}
- h \, \mathbf{a}_{(1)} + h \, b_{(1)} \, \mathbf{l} \;=\; & -h \left(-\nabla \cdot \mathbf{N}_{(1)} + \mathbf{B} \, \mathbf{q}_{(1)} + \mathbf{p}_{(0)} \right) + h \, \left(-\nabla \cdot \mathbf{q}_{(1)} - \mathbf{N}_{(1)} \cdot \mathbf{B} + r_{(0)} \right) \, \mathbf{l} \\
\;=\; & -\nabla \cdot \left(h \, \hat{\mathbf{N}}_{(1)} \right) + \mathbf{q}_{(0)}
\end{aligned}
\tag{5.61}
$$

Being the previous relation particular important for the following developments, its proof is here reported. Note that the complexity of the passages needed to perform this proof motivates the abandon of the direct notation in favour of the more mechanical component-based formulation (see Ref. [37] for a discussion on the differences between the two approaches). Thus, let us write the expression of the integral stress resultants in terms of the Cauchy stress resultants

$$
\begin{aligned}
n_{(k)}^{\alpha\beta} \;=\; & y_{(k)}^{\alpha\beta} - h \, b_{\gamma}^{\beta} \, y_{(k+1)}^{\alpha\gamma} + \left(h \, l^{\beta} \right)_{/\gamma} y_{(k+1)}^{\alpha\gamma} + h \, l^{\beta} \, y_{(k)}^{\alpha 3}
\end{aligned}
\tag{5.62}
$$

$$
\begin{aligned}
q_{(k)}^{\alpha} \;=\; & h \, y_{(k)}^{\alpha 3} + \left(h_{/\beta} + h \, b_{\gamma\beta} \, l^{\gamma} \right) y_{(k+1)}^{\alpha\beta}
\end{aligned}
\tag{5.63}
$$

$$
\begin{aligned}
p_{(k)}^{\gamma} \;=\; & y_{(k)}^{\gamma 3} - h \, b_{\beta}^{\gamma} \, y_{(k+1)}^{\beta 3} + \left(h \, l^{\gamma} \right)_{/\beta} y_{(k+1)}^{\beta 3} + h \, l^{\gamma} \, y_{(k)}^{33}
\end{aligned}
\tag{5.64}
$$

$$
\begin{aligned}
r_{(k)} \;=\; & h \, y_{(k)}^{33} + \left(h_{/\beta} + h \, b_{\gamma\beta} \, l^{\gamma} \right) y_{(k+1)}^{\beta 3}
\end{aligned}
\tag{5.65}
$$

where

$$
y_{(k)}^{pq} \;:=\; \int_{-1}^{+1} \sqrt{\frac{g}{a}} \, \tau^{pq} \, \zeta^k \, d\zeta
\tag{5.66}
$$

$\dagger$ The reader will note that, with a slight abuse of notation, the combination of resultant stress terms in paratheses in Eq. (5.57) has been denoted with a symbol only slightly different from that used to represent the covariant surface basis vector $\mathbf{a}_1$ (indeed, the footnote 1 is here in parantheses), clearly, they should not be confused.

Thus, Eq. (5.61) may be written in covariant components

$$
\begin{aligned}
- \; a^{\gamma}_{(1)} + l^{\gamma} \, b_{(1)} \;=&\; \left(n^{\alpha\gamma}_{(1)/\alpha} - l^{\gamma} \, q^{\alpha}_{(1)/\alpha} \right) - \left(b^{\gamma}_{\alpha} \, q^{\alpha}_{(1)} + l^{\gamma} \, b_{\alpha\sigma} \, n^{\alpha\sigma}_{(1)} \right) \\
&\; - \left(p^{\gamma}_{(0)} - l^{\gamma} \, r_{(0)} \right) = \boxed{1} - \boxed{2} - \boxed{3}
\end{aligned}
\tag{5.67}
$$

where

$$
\begin{aligned}
\boxed{1} \;:=&\; n^{\alpha\gamma}_{(1)/\alpha} - l^{\gamma} \, q^{\alpha}_{(1)/\alpha} = y^{\alpha\gamma}_{(1)/\alpha} - \left[h \, \left(b^{\gamma}_{\beta} - l^{\gamma}_{/\beta} + b_{\beta\sigma} \, l^{\sigma} \, l^{\gamma} \right) y^{\alpha\beta}_{(2)} \right]_{/\alpha} \\
&\; + \; l^{\gamma}_{/\alpha} \, h_{/\beta} \, y^{\alpha\beta}_{(2)} + l^{\gamma}_{/\alpha} \, h \, b_{\beta\sigma} \, l^{\sigma} \, y^{\alpha\beta}_{(2)} + l^{\gamma}_{/\alpha} \, h \, y^{\alpha 3}_{(1)}
\end{aligned}
\tag{5.68}
$$

$$
\begin{aligned}
\boxed{2} \;:=&\; b^{\gamma}_{\alpha} \, q^{\alpha}_{(1)} + l^{\gamma} \, b_{\alpha\sigma} \, n^{\alpha\sigma}_{(1)} = b^{\gamma}_{\alpha} \, \left(h_{/\beta} \, y^{\alpha\beta}_{(2)} + h \, y^{\alpha 3}_{(1)} \right) \\
&\; + \; b_{\alpha\sigma} \, l^{\gamma} \, \left[y^{\alpha\sigma}_{(1)} + (h \, l^{\sigma})_{/\beta} \, y^{\alpha\beta}_{(2)} + h \, l^{\sigma} \, y^{\alpha 3}_{(1)} \right]
\end{aligned}
\tag{5.69}
$$

$$
\boxed{3} \;:=\; p^{\gamma}_{(0)} - l^{\gamma} \, r_{(0)} = y^{\gamma 3}_{(0)} - h \, \left(b^{\gamma}_{\alpha} - l^{\gamma}_{/\alpha} + b_{\alpha\beta} \, l^{\beta} \, l^{\gamma} \right) \, y^{\alpha 3}_{(1)}
\tag{5.70}
$$

thus, recalling the definition of the dynamical descriptors given in Eq. (4.45) (and correspondigly for the stress resultants) when the inclination of the fiber is retained into the model, one has

$$
- \; h \, \left(a^{\gamma}_{(1)} - l^{\gamma} \, b_{(1)} \right) = \left(h \, \hat{n}^{\alpha\gamma}_{(1)} \right)_{/\alpha} - n^{\gamma 3}_{(0)}
\tag{5.71}
$$

or, in direct notation

$$
- \; h \, \left(\mathbf{a}_{(1)} - \mathbf{l} \, b_{(1)} \right) = \nabla \cdot \left(h \, \hat{\mathbf{N}}_{(1)} \right) - \mathbf{q}_{(0)}
\tag{5.72}
$$

With the use of Eq. (5.61) the inner virtual (Eq. (5.59)) work may now be written

$$
\begin{aligned}
\delta \mathcal{W}_i \;=&\; \int_{\mathcal{S}_M} - \left\{ \nabla \cdot \mathbf{N}_{(0)} + \nabla \cdot \left[\mathbf{l} \otimes \left(\nabla \cdot \left(h\hat{\mathbf{N}}_{(1)} \right) - \mathbf{q}_{(0)} \right) \right] - \mathbf{B} \left[\mathbf{q}_{(0)} + \nabla \cdot \left(h\hat{\mathbf{N}}_{(1)} \right) - \mathbf{q}_{(0)} \right] \right\} \cdot \mathbf{u}_{(0)} \\
&\; - \left\{ \nabla \cdot \left[\mathbf{q}_{(0)} + \nabla \cdot \left(h\hat{\mathbf{N}}_{(1)} \right) - \mathbf{q}_{(0)} \right] + \mathbf{B} \cdot \left[\mathbf{N}_{(0)} + \mathbf{l} \otimes \left(\nabla \cdot \left(h\hat{\mathbf{N}}_{(1)} \right) - \mathbf{q}_{(0)} \right) \right] \right\} w_{(0)} \; d\mathcal{S}_M \\
=&\; \int_{\mathcal{S}_M} - \left\{ \left[\nabla \cdot \hat{\mathbf{N}}_{(0)} - (\mathbf{B} - \mathbf{D}) \, \nabla \cdot \left(h\hat{\mathbf{N}}_{(1)} \right) + \mathbf{l} \, \nabla^2 \left(h\hat{\mathbf{N}}_{(1)} \right) \right] \cdot \mathbf{u}_{(0)} \right. \\
&\; + \left. \left[\nabla^2 \left(h\hat{\mathbf{N}}_{(1)} \right) + \mathbf{B} \cdot \hat{\mathbf{N}}_{(0)} + \mathbf{B}^T \mathbf{l} \cdot \nabla \cdot \left(h\hat{\mathbf{N}}_{(1)} \right) \right] w_{(0)} \right\}
\end{aligned}
\tag{5.73}
$$

Applying the Principle of Virtual Work to the previous equation one gets the following system of equilibrium equations valid for a constrained material (*à la* Kirchhoff-Love) in absence of external

loads[*]

$$\nabla \cdot \hat{\mathbf{N}}_{(0)} - (\mathbf{B} - \mathbf{D}) \, \nabla \cdot \left(h \hat{\mathbf{N}}_{(1)} \right) + \mathbf{l} \, \nabla^2 \left(h \hat{\mathbf{N}}_{(1)} \right) = 0 \tag{5.74}$$

$$\nabla^2 \left(h \hat{\mathbf{N}}_{(1)} \right) + \mathbf{B} \cdot \hat{\mathbf{N}}_{(0)} + \mathbf{B}^T \mathbf{l} \cdot \nabla \cdot \left(h \hat{\mathbf{N}}_{(1)} \right) = 0 \tag{5.75}$$

From Eq. (5.75) it is apparent that one can express the Laplacian operator in terms of the remaining terms and substitute it in Eq. (5.74). Performing this substitution one has

$$\nabla \cdot \hat{\mathbf{N}}_{(0)} - \left(\mathbf{B} - \mathbf{D} + \mathbf{l} \otimes \mathbf{B}^T \mathbf{l} \right) \nabla \cdot \left(h \hat{\mathbf{N}}_{(1)} \right) - \mathbf{l} \, \mathbf{B} \cdot \hat{\mathbf{N}}_{(0)} = 0 \tag{5.76}$$

Before proceeding further, it is worth noting that Eqs. (5.75)-(5.76) represent the equilibrium equations in terms of stress resultants when a constrained material is considered, or, if the formal decomposition of the virtual displacement in Eq. (5.1) is carried out, they represent the contributions to the equilibrium state provided by the K-L part of the motion. In this sense the remaining equilibrium equations (those for $k = 1$ in Eqs. (4.54)-(4.55)) provide the contribuion to the equilibrium of the R-M (or shearable) model, and for this reason they can be considered as a pertubation from the K-L equilibrium due to the consideration of shear effects.

It is also worth noting that the substitution that has leaded to Eq. (5.76) is equivalent to express the virtual displacement in the normal direction in terms of the virtual displacement in the fiber direction plus the in-plane contribution as stated in Eq. (4.41).

5.4.2   Second Approach: The Surface Mixed Frame

As it was observed at the end of the preceding section the equilibrium equations relevant to the K-L model in their final form could be obtained more directly considering a mixed approach in the evaluation of the virtual displacements and work. In particular, using Eq. (4.41) (*i.e.*, using the so-called surface convected frame to project the displacement field), the constraint equation (Eq. (5.6)) becomes

$$
\begin{aligned}
\mathbf{u}_{(1)} \;=\; & -\left\{ \left(\nabla \otimes \mathbf{u}_{(0)} - \frac{u_{3_{(0)}}}{h} \, \mathbf{B} + \mathbf{l} \cdot \mathbf{u}_{(0)} \, \mathbf{B} \right) \right. \\
& + \left. \mathbf{n} \otimes \left[\nabla \left(\frac{u_{3_{(0)}}}{h} \right) - \nabla \left(\mathbf{l} \cdot \mathbf{u}_{(0)} \right) + \mathbf{B} \mathbf{u}_{(0)} \right] \right\}^T \mathbf{g}_3
\end{aligned}
\tag{5.77}
$$

Let us rewrite Eq. (4.52) in the following compact form

$$\delta \mathcal{W}_i \;=\; \int_{\mathcal{S}_M} \left(\mathbf{a}_{(0)} \cdot \mathbf{u}_{(0)} + \mathbf{a}_{(1)} \cdot \mathbf{u}_{(1)} - b_{(0)} \, u_{3_{(0)}} - b_{(1)} \, u_{3_{(1)}} \right) \, d\mathcal{S} \tag{5.78}$$

---

[*] Although the present results are limited to the considertaion of only the inner virtual work, consideration of the outer work produced by the external loads does not yield substantial modifications except for the presence of some forcing terms in the equilibrium equations. The consideration of the outer mechanical work and of the other work terms will be carried out later.

Recalling he first material constraint of Eq. (5.4), and introducing Eq. (5.77) in the previous relation one has

$$
\begin{aligned}
\delta \mathcal{W}_i &= \int_{\mathcal{S}_M} \left\{ \mathbf{a}_{(0)} \cdot \mathbf{u}_{(0)} - b_{(0)}\, u_{3_{(0)}} - \mathbf{a}_{(1)} \left[\left(\nabla \otimes \mathbf{u}_{(0)} - \frac{u_{3_{(0)}}}{h}\, \mathbf{B} + \mathbf{l} \cdot \mathbf{u}_{(0)}\, \mathbf{B} \right) \right. \right. \\
&\quad \left. \left. + \mathbf{n} \otimes \left(\nabla \left(\frac{u_{3_{(0)}}}{h} \right) - \nabla \left(\mathbf{l} \cdot \mathbf{u}_{(0)} \right) + \mathbf{B}\mathbf{u}_{(0)} \right) \right]^T \mathbf{g}_3 \right\}\, d\mathcal{S} \\
&= \int_{\mathcal{S}_M} \left\{ \left[\mathbf{a}_{(0)} - h\, \mathbf{B}\, \mathbf{a}_{(1)} - \left(\mathbf{B}\, \mathbf{a}_{(1)} \cdot \mathbf{g}_3 \right) \mathbf{l} + h\, \mathbf{D}\, \mathbf{a}_{(1)} \right] \cdot \mathbf{u}_{(0)} - \left[\mathbf{g}_3 \otimes \mathbf{a}_{(1)} - h\, \mathbf{l} \otimes \mathbf{a}_{(1)} \right] \right. \\
&\quad \left. \cdot \nabla \otimes \mathbf{u}_{(0)} - \left[b_{(0)} - \frac{1}{h}\mathbf{B} \cdot \mathbf{g}_3 \otimes \mathbf{a}_{(1)} - \frac{1}{h}\nabla h \cdot \mathbf{a}_{(1)} \right] u_{3_{(0)}} - \mathbf{a}_{(1)} \cdot \nabla u_{3_{(0)}} \right\}\, d\mathcal{S} \quad (5.79)
\end{aligned}
$$

where some tensorial identities, reported in the appendix and not displayed here, the following relation have been used in Eq. (5.79)

$$
\left[\mathbf{g}_3 \otimes \mathbf{a}_{(1)} - h\, \mathbf{l} \otimes \mathbf{a}_{(1)} \right] \cdot \nabla \otimes \mathbf{u}_{(0)} = \left[h\, \mathbf{n} \otimes \mathbf{a}_{(1)} \right] \cdot \nabla \otimes \mathbf{u}_{(0)} = 0 \qquad \forall \mathbf{u}_{(0)} \in \mathscr{V}_{\mathcal{S}} \,(5.80)
$$

Let us applying once again the Green-Gauss theorem on Eq. (5.79)

$$
\begin{aligned}
\delta \mathcal{W}_i &= \int_{\mathcal{S}_M} \left\{ \left[\mathbf{a}_{(0)} - h\, \mathbf{B}\, \mathbf{a}_{(1)} + h\nabla \otimes \mathbf{l}\, \mathbf{a}_{(1)} - \left(\mathbf{B}\, \mathbf{a}_{(1)} \cdot \mathbf{g}_3 \right) \mathbf{l} \right] \cdot \mathbf{u}_{(0)} \right. \\
&\quad \left. - \left[b_{(0)} - \frac{1}{h}\mathbf{B} \cdot \nabla \mathbf{g}_3 \otimes \mathbf{a}_{(1)} - \frac{1}{h}\nabla h \cdot \mathbf{a}_{(1)} - \nabla \cdot \mathbf{a}_{(1)} \right] u_{3_{(0)}} \right\}\, d\mathcal{S} + BT \quad (5.81)
\end{aligned}
$$

Noting that

$$
h\, \mathbf{a}_{(1)} = -\nabla \cdot \left(h\, \hat{\mathbf{N}}_{(1)} \right) + h\, \hat{\mathbf{q}}_{(0)} \tag{5.82}
$$

and substituting to $\mathbf{a}_{(0)}$ and $b_{(0)}$ their expression in terms of stress resultants, Eq. (5.81) reduces to

$$
\begin{aligned}
\delta \mathcal{W}_i &= \int_{\mathcal{S}_M} \left\{ \left[-\nabla \cdot \hat{\mathbf{N}}_{(0)} + (\mathbf{B} - \mathbf{D}) \nabla \cdot \left(h\, \hat{\mathbf{N}}_{(1)} \right) + \left(\hat{\mathbf{N}}_{(0)} \cdot \mathbf{B} \right) \mathbf{l} \right] \cdot \mathbf{u}_{(0)} \right. \\
&\quad \left. - \left[\nabla^2 \left(h\, \hat{\mathbf{N}}_{(1)} \right) + \mathbf{B}\mathbf{l} \cdot \nabla \left(h\, \hat{\mathbf{N}}_{(1)} \right) + h\, \hat{\mathbf{N}}_{(0)} \cdot \mathbf{B} \right] u_{3_{(0)}} \right\}\, d\mathcal{S} + BT \quad (5.83)
\end{aligned}
$$

The application of the Virtual Work Principle to Eq. (5.83) leads to a system of equilibrium equations identical to that obtained at the end of the previous section after having expressed the former stress resultants (defined on the surface natural frame) in terms of the latter ones (associated to the surface convected frame).

5.4.3 Third Approach: The Surface Convected Frame

Finally, let us adopt the director orthogonal frame for representing the in-plane displacement field (see Eq. (3.138)), in this case the second K-L constraint becomes

$$\mathring{\mathbf{u}}_{(1)} = -\left(\mathring{\nabla}\mathring{u}_{3_{(0)}} - \mathbf{d}\,\mathring{u}_{3_{(0)}} + \mathbf{C}^T\mathbf{u}_{(0)}\right) \tag{5.84}$$

indeed, recall that

$$
\begin{aligned}
\delta\mathring{\mathbf{g}}_\beta &= \frac{\partial\delta\mathbf{p}}{\partial\xi^\beta} = \frac{\partial}{\partial\xi^\beta}\left(\mathring{\mathbf{u}}_{(0)} + \mathring{u}_{3_{(0)}}\,\mathring{\mathbf{g}}^3\right) \\
&= \mathring{u}_{\alpha_{(0)}\angle\beta}\,\mathring{\mathbf{g}}^\alpha + c_\beta^\alpha\,\mathring{u}_{\alpha_{(0)}}\,\mathring{\mathbf{g}}^3 + \left(\mathring{u}_{3_{(0)},\beta} - d_\beta\,\mathring{u}_{3_{(0)}}\right)\mathring{\mathbf{g}}^3 - c_{\alpha\beta}\,\mathring{u}_{3_{(0)}}\mathring{\mathbf{g}}^\alpha \\
&= \left(\mathring{u}_{\alpha_{(0)}\angle\beta} - c_{\alpha\beta}\,\mathring{u}_{3_{(0)}}\right)\mathring{\mathbf{g}}^\alpha + \left(\mathring{u}_{3_{(0)},\beta} - d_\beta\,\mathring{u}_{3_{(0)}} + c_\beta^\alpha\,\mathring{u}_{\alpha_{(0)}}\right)\mathring{\mathbf{g}}^3
\end{aligned} \tag{5.85}
$$

thus, form Eq. (5.5) one has

$$\delta\mathring{\mathbf{g}}_3 \cdot \mathring{\mathbf{g}}_\beta = \mathring{\mathbf{u}}_{(1)} \cdot \mathring{\mathbf{g}}_\beta = -\mathring{\mathbf{g}}_3 \cdot \delta\mathring{\mathbf{g}}_\beta = -\left(\mathring{u}_{3_{(0)},\beta} - d_\beta\,\mathring{u}_{3_{(0)}} + c_\beta^\alpha\,\mathring{u}_{\alpha_{(0)}}\right) \tag{5.86}$$

From Eqs. (4.69) and (4.74), introducing the two constraint equations (Eq. (5.6)) and (Eq. (5.84)), one has

$$
\begin{aligned}
\delta\mathcal{W}_i &= \int_{\mathcal{S}_M}\Bigg[\left(-\mathring{\nabla}\cdot\mathring{\mathbf{N}}_{(0)} + \mathbf{C}\,\mathring{\mathbf{q}}_{(0)}\right)\cdot\mathring{\mathbf{u}}_{(0)} + \left(-\mathring{\nabla}\cdot\mathring{\mathbf{q}}_{(0)} - \mathring{\mathbf{N}}_{(0)}\cdot\mathbf{C} - \mathring{\mathbf{q}}_{(0)}\cdot\mathbf{d}\right)\mathring{u}_{3_{(0)}} \\
&\quad + \left(-\mathring{\nabla}\cdot\mathring{\mathbf{N}}_{(1)} + \mathbf{C}\,\mathring{\mathbf{q}}_{(1)} + \mathring{\mathbf{p}}_{(0)}\right)\cdot\left(-\mathring{\nabla}\mathring{u}_{3_{(0)}} + \mathbf{d}\,\mathring{u}_{3_{(0)}} - \mathbf{C}^T\mathring{\mathbf{u}}_{(0)}\right)\Bigg]\,d\mathcal{S}_M + B.T. \tag{5.87}
\end{aligned}
$$

where with $B.T.$ still denotes the boundary terms descending from the application of the Green-Gauss theorem (see Eq. (4.75)). Before proceeding further, let us note that the previous equation is almost identical to Eq. (2.87) relevant to the case of a shell whose normal fiber remains normal after the deformation and whose thickness remains unchanged. In that occasion it was easily shown the existence of an algebraic relation between the shear resultants via the curvature tensor, similarly, it will be shown that also in this case an algebraic relation exist between the shear resultants (via the tensor $\mathbf{C}$) and the tensor of first order in-plane stress resultants. Indeed, recall that

$$
\begin{aligned}
\mathring{n}_{(1)}^{\alpha\beta} &= \int_{-1}^{+1}\zeta\,\mathring{\sigma}^{\alpha\beta}\,d\zeta = \int_{-1}^{+1}\sqrt{\frac{g}{\mathring{g}}}\,\zeta\left(\tau^{\alpha\gamma}\,\mathring{\mathscr{T}}_\gamma^\beta + \tau^{\alpha3}\,\mathring{\mathscr{T}}_3^\beta\right)d\zeta \\
&= \int_{-1}^{+1}\sqrt{\frac{g}{\mathring{g}}}\,\zeta\,\tau^{\alpha\gamma}\left(\delta_\gamma^\beta - \zeta\,c_\gamma^\beta\right)d\zeta = y_{(1)}^{\alpha\beta} - c_\gamma^\beta\,y_{(2)}^{\alpha\gamma} \tag{5.88}
\end{aligned}
$$

similarly for the shear stress resultants one has

$$
\begin{aligned}
\overset{\circ}{q}{}^{\alpha}_{(k)} &= \int_{-1}^{+1} \zeta^k \, \overset{\circ}{\sigma}{}^{\alpha 3} \, d\zeta = \int_{-1}^{+1} \sqrt{\frac{g}{\overset{\circ}{g}}} \, \zeta^k \left(\tau^{\alpha\gamma} \, \overset{\circ}{\mathscr{T}}{}^{\,3}_{\gamma} + \tau^{\alpha 3} \, \overset{\circ}{\mathscr{T}}{}^{\,3}_{3} \right) d\zeta \\
&= \int_{-1}^{+1} \sqrt{\frac{g}{\overset{\circ}{g}}} \, \zeta^k \left(\tau^{\alpha\gamma} \, \zeta \, \overset{\circ}{\Gamma}{}^{\,3}_{\gamma 3} + \tau^{\alpha 3} \right) d\zeta = y^{\alpha\gamma}_{(k+1)} \, d_{\gamma} + y^{\alpha 3}_{(k)}
\end{aligned}
\tag{5.89}
$$

and

$$
\begin{aligned}
\overset{\circ}{p}{}^{\beta}_{(0)} &= \int_{-1}^{+1} \overset{\circ}{\sigma}{}^{3\beta} \, d\zeta = \int_{-1}^{+1} \sqrt{\frac{g}{\overset{\circ}{g}}} \left(\tau^{3\gamma} \, \overset{\circ}{\mathscr{T}}{}^{\,\beta}_{\gamma} + \tau^{33} \, \overset{\circ}{\mathscr{T}}{}^{\,\beta}_{3} \right) d\zeta \\
&= \int_{-1}^{+1} \sqrt{\frac{g}{\overset{\circ}{g}}} \, \tau^{3\gamma} \left(\delta^{\beta}_{\gamma} - \zeta \, c^{\beta}_{\gamma} \right) d\zeta = y^{3\beta}_{(0)} - c^{\beta}_{\gamma} \, y^{3\beta}_{(1)}
\end{aligned}
\tag{5.90}
$$

where the $y^{pq}_{(k)}$ are defined as the stress resultants on the Cauchy stress tensor, *i.e.*,

$$
y^{pq}_{(k)} := \int_{-1}^{+1} \sqrt{\frac{g}{\overset{\circ}{g}}} \, \zeta^k \, \tau^{pq}
\tag{5.91}
$$

Combining eqs. (5.88)-(5.90) one obtains the following relation

$$
\overset{\circ}{q}{}^{\alpha}_{(0)} - \overset{\circ}{n}{}^{\alpha\beta}_{(1)} \, d_{\beta} = c^{\alpha}_{\beta} \, \overset{\circ}{q}{}^{\beta}_{(1)} + \overset{\circ}{p}{}^{\beta}_{(0)}
\tag{5.92}
$$

or, using a direct notation

$$
\overset{\circ}{\mathbf{q}}_{(0)} - \overset{\circ}{\mathbf{N}}_{(1)} \, \mathbf{d} = \mathbf{C} \, \overset{\circ}{\mathbf{q}}_{(1)} + \overset{\circ}{\mathbf{p}}_{(0)}
\tag{5.93}
$$

Indeed, using Eqs. (5.88)– (5.90) in Eq. (5.92), one has for the right hand side of the equations

$$
LHS = y^{\alpha\beta}_{(1)} \, d_{\beta} + y^{\alpha 3}_{(0)} - \left(y^{\alpha\beta}_{(1)} - y^{\alpha\gamma}_{(2)} \, c^{\beta}_{\gamma} \right) d_{\beta} = y^{\alpha 3}_{(0)} + y^{\alpha\gamma}_{(2)} \, c^{\beta}_{\gamma} \, d_{\beta}
\tag{5.94}
$$

whereas the left hand side becomes

$$
RHS = c^{\alpha}_{\beta} \left(y^{\beta\gamma}_{(2)} \, d_{\gamma} + y^{\beta 3}_{(1)} \right) + y^{3\beta}_{(0)} - y^{3\gamma}_{(1)} \, c^{\beta}_{\gamma} = y^{3\beta}_{(0)} + y^{\beta\gamma}_{(2)} \, c^{\alpha}_{\beta} \, d_{\gamma}
\tag{5.95}
$$

Finally, due to the symmetry of the Cauchy stress tensor, it is proved that Eq. (5.92) holds. Using Eq. (5.92) in Eq. (5.87) one has

$$
\begin{aligned}
\delta \mathcal{W}_i \;=\; & \int_{\mathcal{S}_M} \left\{ \left[-\overset{\circ}{\nabla} \cdot \overset{\circ}{\mathbf{N}}_{(0)} + \mathbf{C}\overset{\circ}{\nabla} \cdot \overset{\circ}{\mathbf{N}}_{(1)} + \mathbf{C}\overset{\circ}{\mathbf{N}}_{(0)}\mathbf{d} \right] \cdot \overset{\circ}{\mathbf{u}}_{(0)} \right. \\
& + \left[-\overset{\circ}{\mathbf{N}}_{(0)} \cdot \mathbf{C} - \overset{\circ}{\nabla} \cdot \left(\overset{\circ}{\nabla} \cdot \overset{\circ}{\mathbf{N}}_{(1)} \right) - \overset{\circ}{\nabla} \cdot \left(\overset{\circ}{\mathbf{N}}_{(0)} \; \mathbf{d} \right) \right. \\
& \left. \left. - \left(\overset{\circ}{\nabla} \cdot \overset{\circ}{\mathbf{N}}_{(1)} \right) \cdot \mathbf{d} - \left(\overset{\circ}{\mathbf{N}}_{(0)}\mathbf{d} \right) \cdot \mathbf{d} \right] \overset{\circ}{u}_{3_{(0)}} \right\} d\mathcal{S} + B.T. + B.T.|_{KL} \quad (5.96)
\end{aligned}
$$

where with $B.T.|_{KL}$ denotes the boundary terms descending from the application of the Green-Gauss theorem due to the KL hypotheses[†]

$$
B.T.|_{KL} \;=\; \int_{\partial \mathcal{S}} - \left[-\overset{\circ}{\nabla} \cdot \overset{\circ}{\mathbf{N}}_{(1)}^{\;T} + \mathbf{C}\overset{\circ}{\mathbf{q}}_{(1)} + \overset{\circ}{\mathbf{p}} \right] \overset{\circ}{u}_{3_{(0)}} \cdot \mathbf{n}_{\partial} \qquad (5.97)
$$

Let us now apply the Principle of Virtual Work in Eq. (5.96), then, the equilibrium equations relative to the Kirchhoff-Love part of the motion (see the introduction for a discussion of this issue), in the absence of external loads are

$$
-\overset{\circ}{\nabla} \cdot \overset{\circ}{\mathbf{N}}_{(0)} + \mathbf{C}\overset{\circ}{\nabla} \cdot \mathbf{N}_{(1)} + \mathbf{C} \left(\overset{\circ}{\mathbf{N}}_{(0)}\mathbf{d} \right) = 0 \qquad (5.98)
$$

$$
-\overset{\circ}{\nabla} \cdot \left(\overset{\circ}{\nabla} \cdot \overset{\circ}{\mathbf{N}}_{(1)} \right) - \overset{\circ}{\nabla} \cdot \left(\overset{\circ}{\mathbf{N}}_{(1)}\mathbf{d} \right) - \left(\overset{\circ}{\nabla} \cdot \overset{\circ}{\mathbf{N}}_{(1)} \right) \cdot \mathbf{d} - \overset{\circ}{\mathbf{N}}_{(0)}\mathbf{d} \cdot \mathbf{d} - \overset{\circ}{\mathbf{N}}_{(0)} \cdot \mathbf{C} = 0 \quad (5.99)
$$

[†] The interested reader may refer to Appendix B for a presentation of these results starting from two different strategies.

Part II

Applications

Chapter 6

A simple micro-structured piezo-electric shell

6.1 Introduction

This section is dedicated to the implementation of the theoretical model for micro-structured continuum bodies developed and discussed in the first part of the thesis, with special reference to the case of a shell having fibers made of piezo-electric materials and inclined with respect to the normal. Moreover, in order to simplify the mathematical treatment of the problem, it is assumed that the shell be infinitely long in a direction, and that experiences only small deformations. The numerical results and the equilibrium equations are limited to statics, furthermore, it is assumed that the shell is loaded by means of an external electric field imposed across the boundaries. Moreover, the electric field is assumed constant across the thickness (so that the electric potential is linear in ζ). As a consequence of this hypothesis, the first Maxwell's equation that governs the electrical unknowns of the problem, is considered to be independent of (but influencing) the displacement field. This is true as well for the constitutive equations that relate the electrical displacement field with the deformations and the electric potential. Consequently, it will be obtained an equivalent beam model capable of describing shear effects and thickness change. Finally, let us remark that the results are intended to demonstrate the potentiality of the model and so a special fiber distribution is assumed throughout the main surface.

6.2 Geometry and kinematical hypotheses

As it was already stated in the Introduction, here it is studied the deformation of a shell that, in the undeformed configuration, is a flat plate with constant thickness h_0. Moreover, in order to eliminate a dimension, and thus to utmost simplify the formulation and the consequent analysis, it is assumed that the shell have a symmetric distribution of loads and it be infinitely long in a direction. Thus,

in the reference configuration one has

$$\mathbf{x}_0\left(\xi^\alpha,\zeta\right) \;=\; \mathbf{p}_0\left(\xi^\alpha\right) + \zeta\,\mathbf{q}_0\left(\xi^\alpha\right) \tag{6.1}$$

where $\mathbf{p}_0$ represents the mid-surface in the reference configuration and it is given by

$$\mathbf{p}_0\left(\xi^\alpha\right) \;=\; \xi^1\,\mathbf{e}_1 + \xi^2\,\mathbf{e}_2 \tag{6.2}$$

whereas, $\mathbf{q}_0$ represents the fiber distribution in the reference configuration and it is given by

$$\mathbf{q}_0\left(\xi^\alpha\right) \;=\; \hbar\left(\xi^\alpha\right)\,\mathbf{m}\left(\xi^\alpha\right) = h_0\left[\mathbf{e}_3 + f\left(\xi^1\right)\,\mathbf{e}_1\right] \tag{6.3}$$

where $f\left(\xi^1\right)$ is a measure of the inclination of the fiber with respect to the normal in the reference configuration,[†] and $\{\mathbf{e}_1,\mathbf{e}_2,\mathbf{e}_3\}$ are the Cartesian base vectors chosen in the Euclidean space to describe the geometry of the shell, with $\mathbf{e}_1$ and $\mathbf{e}_2$ lying in the reference mid-surface and $\mathbf{e}_3$ normal to it. Moreover, it is assumed $\mathbf{e}_2$ to be the direction in which the shell is infinitely long.

Consistently, in the deformed configuration one may assume the shell given by the following map

$$\begin{aligned}
\mathbf{x}\left(\xi^\alpha,\zeta\right) \;&=\; \mathbf{x}_0\left(\xi^\alpha,\zeta\right) + \mathbf{v}\left(\xi^\alpha,\zeta\right) = \mathbf{p}\left(\xi^\alpha\right) + \zeta\,\mathbf{q}\left(\xi^\alpha\right)\\
&=\; \mathbf{p}_0\left(\xi^\alpha\right) + \mathbf{v}_0\left(\xi^\alpha\right) + \zeta\left[\mathbf{q}_0\left(\xi^\alpha\right) + \mathbf{v}_1\left(\xi^\alpha\right)\right]
\end{aligned} \tag{6.4}$$

where $\mathbf{v}$ denotes the displacement field from the reference configuration. For the sake of notation simplicity one may denote the Cartesian component of the displacement field in the following way

$$u_k \;:=\; \mathbf{v}_k \cdot \mathbf{e}_1 \qquad for\ k = 0,1 \tag{6.5}$$

$$w_k \;:=\; \mathbf{v}_k \cdot \mathbf{e}_3 \qquad for\ k = 0,1 \tag{6.6}$$

where it has been assumed the displacements in the $\mathbf{e}_2$ direction identically zero because of the hypotheses of symmetry in that direction introduced before. Furthermore, one may denote the ξ^1 co-ordinate simply with ξ, and the derivatives with respect to ξ with a prime ($'$).

Using the previous considerations and equations, the surface base vectors in the deformed configuration may be written

$$\mathbf{a}_1 \;=\; \overset{\circ}{\mathbf{g}}_1 = \frac{\partial\mathbf{p}}{\partial\xi} = \left(1 + u_0'\right)\mathbf{e}_1 + w_0'\,\mathbf{e}_3 \tag{6.7}$$

$$\mathbf{a}_2 \;=\; \overset{\circ}{\mathbf{g}}_2 = \frac{\partial\mathbf{p}}{\partial\xi^2} = \mathbf{e}_2 \tag{6.8}$$

[†] Note that, respect to the First Part of this thesis, where it has been chosen to indicate the fiber inclination with $\mathfrak{l}$, here it has been preferred to use a scalar quantity and to denote it as f. Nonetheless, it should be noted that its meaning and role in the formulation remains unchanged.

Accordingly, the determinant of the metric surface tensor in the deformed configuration will be

$$a\left(\xi^{\alpha}\right) \quad := \quad \|\mathbf{a}_1 \times \mathbf{a}_2\| = \sqrt{\left(1 + u_0'\right)^2 + \left(w_0'\right)^2} \tag{6.9}$$

whereas the normal is given by

$$\mathbf{n}\left(\xi^{\alpha}\right) \quad = \quad \frac{\mathbf{a}_1 \times \mathbf{a}_2}{\sqrt{a}} = \frac{\left(1 + u_0'\right) \mathbf{e}_3 - \left(w_0'\right) \mathbf{e}_1}{\sqrt{\left(1 + u_0'\right)^2 + \left(w_0'\right)^2}} \tag{6.10}$$

Similarly, for the volume base vectors one has

$$\mathbf{g}_1 \quad = \quad \frac{\partial \mathbf{x}}{\partial \xi^1} = \left[\left(1 + u_0'\right) + \zeta\left(h_0 \ f' + u_1'\right)\right] \mathbf{e}_1 + \left(w_0' + \zeta \ w_1'\right) \mathbf{e}_3 \tag{6.11}$$

$$\mathbf{g}_2 \quad = \quad \frac{\partial \mathbf{x}}{\partial \xi^2} = \mathbf{e}_2 \tag{6.12}$$

Finally, for the director (or material fiber vector) one has

$$\mathbf{g}_3 \quad := \quad \mathbf{q}\left(\xi\right) = \left(h_0 \ f + u_1\right) \mathbf{e}_1 + \left(h_0 + w_1\right) \mathbf{e}_3 \tag{6.13}$$

From Eqs. (6.11)-(6.13), setting $\{u_0, w_0, u_1, w_1\} = 0$, one obtains also the expression of the volume base vectors in the reference configuration,[‡] whereas the contravariant base vectors (associated to the volume and surface covariant ones) are determined directly using Eqs. (3.17)-(3.18), (3.35)-(3.37), and (3.39)-(3.40). Accordingly, one obtains, using the previous relations, all the information needed to represent the deformed configuration of the shell once the displacement field is known. In particular, the deformation tensor is given by

$$\mathbf{E} \quad = \quad \frac{1}{2}\left(\mathbf{C} - \mathbf{C}_0\right) = \frac{1}{2}\left(g_{kh} - g_{kh_0}\right) \mathbf{g}_0^k \otimes \mathbf{g}_0^h \tag{6.14}$$

where $\mathbf{E}$ is the Cauchy-Green deformation tensor, $\mathbf{C} = \mathbf{F}^T \mathbf{F}$ is the right Cauchy-Green tensor (with $\mathbf{F} = \mathbf{g}^k \otimes \mathbf{g}_{k_0}$), and $\mathbf{g}_0^k$ are the volume contravariant base vectors in the reference configuration. We will consider in the application only infinitesimal deformations, thus in this case the components of the deformation tensor may be written

$$\epsilon_{hk} \quad = \quad \frac{1}{2}\left(\mathbf{g}_{h_0} \cdot \frac{\partial \mathbf{v}}{\partial \xi^k} + \frac{\partial \mathbf{v}}{\partial \xi^h} \cdot \mathbf{g}_{k_0}\right) \tag{6.15}$$

With the use of the previous relations for the particular problem under consideration the components

---

[‡] Note that, because it has been assumed that the material fiber are inclined with respect to the normal in the reference configuration, $\mathbf{g}_{3_0}$ is different from $\mathbf{e}_3$.

29th May 2005

different from zero of the linear part of the deformation tensor may be written as

$$\epsilon_{11} = (1 + \zeta\ h_0\ f')\,(u'_0 + \zeta\ u'_1) \tag{6.16}$$

$$\epsilon_{33} = h_0\,(w_1 + f\ u_1) \tag{6.17}$$

$$\epsilon_{13} = \frac{1}{2}\,[(1 + \eta\ h_0\ f')\,u_1 + h_0\,(w'_0 + \zeta\ w'_1) + h_0\ f\,(u'_0 + \zeta\ u'_1)] \tag{6.18}$$

Before proceeding further, it is worth noting that the previous relations represent the components of the deformation tensor with respect to the volume base vectors in the undeformed configuration. On the other hand, in the following the constitutive relations will be expressed in the deformed configuration using a special frame which, according to the definition given in Ref. [97], may be denoted "Convected Orthogonal Frame", and is characterized by the fact that one of the base vectors is along the fiber. This will be denoted by $\mathbf{m}$, the other two by $\mathbf{m}_1$ and $\mathbf{m}_2$. The reason for introducing this second frame will appear clear later. For the moment, let us only observe that in our case $\mathbf{m}_2$ coincides with $\mathbf{e}_2$ and thus that $\mathbf{m}_1$ is equal to the unit vector parallel to $\overset{\mathrm{o}}{\mathbf{g}}{}^{1}$. In terms of the $\mathbf{m}_k$ base vectors the deformation tensor can be written

$$\mathbf{E} = \epsilon_{hk}\ \mathbf{g}_0^h \otimes \mathbf{g}_0^k = \bar{\epsilon}_{hk}\ \mathbf{m}_h \otimes \mathbf{m}_k \tag{6.19}$$

where

$$\bar{\epsilon}_{hk} := \epsilon_{pq}\,(\mathbf{g}_0^p \otimes \mathbf{g}_0^q) \cdot (\mathbf{m}_h \otimes \mathbf{m}_k) = \epsilon_{pq}\,(\mathbf{g}_0^p \cdot \mathbf{m}_h)\,(\mathbf{g}_0^q \cdot \mathbf{m}_k) \tag{6.20}$$

Using an array representation one arrives to the following relations which express the kinematical relations (*i.e.*, the relations between deformation and displacement components)

$$\mathsf{z} = \mathsf{D}\,(\xi, \zeta)\,\mathsf{x}' + \mathsf{E}\,(\xi, \zeta)\,\mathsf{x} \tag{6.21}$$

where $\mathsf{z}\,(= \{\bar{\epsilon}_{11}, \bar{\epsilon}_{33}, \bar{\epsilon}_{13}\}^T)$ is a column matrix whose elements are the ordered non-zero components of the deformation tensor in the $\mathbf{m}_k$ basis, whereas $\mathsf{x}\,(= \{u_0, w_0, u_1, w_1\}^T)$ is a column matrix whose elements are the ordered non-zero components of the displacement vector field in the $\mathbf{e}_k$ basis.

6.3   Electro-elastic constitutive equations

The main hypothesis underlying the present application and the mathematical model from which it is derived, is the existence of a privileged direction in the material (denoted with $\mathbf{q}$ or $\mathbf{g}_3$). In particular, one can assume that

(i) the polarization direction, for piezo-electric part of the constitutive relations, coincides with the direction of transversal isotropy for elasticity tensor;

(ii) $\mathbf{g}_3$ identifies such a direction.

Therefore, denotes with $\mathbf{m}$ the unit vector associated to $\mathbf{g}_3$, and let us call (as it was anticipated at the end of the previous Section) $\mathbf{m}_1$ and $\mathbf{m}_2$ two mutually orthogonal directions to $\mathbf{m}$. The triad $\{\mathbf{m}_1, \mathbf{m}_2, \mathbf{m}\}$ constitutes the triad of orthonormal vectors, with respect to one can express the constitutive relations. In particular, using the piezo-elastic constitutive relations given in Refs. [83, 88], one has

$$\mathbf{T} = \mathbb{C}\mathbf{E} - \mathbb{H}\mathfrak{e} \tag{6.22}$$
$$\mathfrak{d} = \mathbb{H}^T\mathbf{E} + \mathbf{K}\mathfrak{e} \tag{6.23}$$

where $\mathbf{T}$ and $\mathbf{E}$ are the Cauchy stress tensor and the Cauchy-Green deformation tensor respectively, $\mathfrak{d}$ and $\mathfrak{e}$ are the electric displacement and the electric field respectively, $\mathbb{C}$ is the 4-th order elasticity tensor, $\mathbb{H}$ is the 3-rd piezo-electric coupling tensor, whereas $\mathbf{K}$ is the 2-nd order dielectric tensor.

Equations (6.22)-(6.23) can be simplified introducing a strong and restrictive hypothesis, already mentioned in the Introduction, that the piezo-electric coupling be of one-directional type, in the sense that one may assume that the electric field be completely defined by the electric boundary conditions. In other words, one may assume that the electric field can affect the stresses but that the stresses (or the mechanical deformations) cannot affect the electric field.[‡] Thus, as it will appear clearly later, the electric field results in an external load for the mechanical equilibrium[§] of the shell. Furthermore, one may assume that each fiber is electrically isolated from the others, and that, consistently, the electric field is constant and directed only in the fiber direction. Finally, assuming that the edges of each fiber can be accessed independently, one can assume that the electric field be given by

$$\mathfrak{e} = e\left(\xi\right)\mathbf{m}\left(\xi\right) = -\frac{\Delta\phi\left(\xi\right)}{2\hbar\left(\xi\right)}\mathbf{m}\left(\xi\right) \tag{6.24}$$

where $\Delta\phi\left(\xi\right)\left(= \phi_{upper}\left(\xi\right) - \phi_{lower}\left(\xi\right)\right)$ is the electric voltage difference applied at the edges of each fiber.

[‡] In a certain sense, the present approach may be intended as a "return to the past". Indeed, although the current literature is directed towards the implementation of coupled formulations for piezo-electricity (see, for instance, Ref. [92]), here the coupling is neglected, because the interest is placed mostly in the definition of the kinematical hypotheses needed to correctly model the mechanical, rather than electrical, unknowns.

[§] As it was anticipated in the Overview of this thesis, the previous hypothesis are unusual in the current literature of piezoelectricity even if an actuator mode for the piezoelectric material is invoked. On the other hand, the negligence of the effect of the current deformation on the temperature field, is a hypothesis traditionally assumed in the current literature of thermoelasticity (see for instance Ref.[17]). This fact permits to trace a clear link between the present application, involving the analysis of piezoelectric bodies, with the following application that regards the analysis of a thermoelastic problem in which a one-way coupling thermo-elastic model is considered. Finally, it is worth noting that the role played by the electric voltage here will be played by the temperature field there, and, for this reason, a similar solution methodology is used in the two cases.

Using the previous equations the non-zero components of the stress tensor in the $\mathbf{m}_k$ base vectors can be written

$$\bar{\tau}^{11} \;=\; \left(\lambda + 2\mu\right)\bar{\epsilon}_{11} + \tau_2\,\bar{\epsilon}_{33} + \delta_1\,\frac{\Delta\phi\left(\xi\right)}{2\hbar\left(\xi\right)} \tag{6.25}$$

$$\bar{\tau}^{33} \;=\; \tau_2\,\bar{\epsilon}_{11} + \tau_1\,\bar{\epsilon}_{33} + \delta_3\,\frac{\Delta\phi\left(\xi\right)}{2\hbar\left(\xi\right)} \tag{6.26}$$

$$\bar{\tau}^{13} \;=\; 2\eta\,\bar{\epsilon}_{33} \tag{6.27}$$

where λ, μ, τ_1, τ_2 and η are the elastic material moduli of a transversely isotropic material, whereas δ_1 and δ_3 are the piezo-electric coupling coefficients (see Refs. [83, 88]).[¶]

Before proceeding further, it should be observed that Eqs. (6.25)-(6.27), are the components of the stress tensor in the $\mathbf{m}_k$ base vectors; on the other hand, the integral relations, that define the stress resultants in terms of which the equilibrium equations for the shell model have been written, refer to the components of the stress tensor in the $\mathbf{g}_k$ base vectors. Hence, one may write

$$\mathbf{T} \;=\; \tau^{hk}\mathbf{g}_h \otimes \mathbf{g}_k = \bar{\tau}^{hk}\mathbf{m}_h \otimes \mathbf{m}_k \tag{6.28}$$

thus one has

$$\tau^{hk} \;:=\; \bar{\tau}^{pq}\left(\mathbf{m}_p \otimes \mathbf{m}_q\right)\cdot\left(\mathbf{g}^h \otimes \mathbf{g}^k\right) = \bar{\tau}^{pq}\left(\mathbf{m}_p \cdot \mathbf{g}^h\right)\left(\mathbf{m}_q \cdot \mathbf{g}^k\right) \tag{6.29}$$

Similarly to the conclusion of the previous Section, one can arrive, using an array representation for the non-zero components of the stress and deformation tensors, to the following relation

$$\mathsf{w} \;=\; \mathsf{G}\left(\xi,\zeta\right)\mathsf{z} + \mathsf{h}\left(\xi,\zeta\right)\,\Delta\phi \tag{6.30}$$

where w $\left(= \{\bar{\tau}^{11}, \bar{\tau}^{33}, \bar{\tau}^{13}\}\right)$ is a column matrix whose components are the non-zero components of the stress tensor in the $\mathbf{g}_k$ basis, G is a matrix representing the elastic stiffness matrix, and h is the piezo-elastic coupling vector.

6.4   Equilibrium equations

The equilibrium equations are given in terms of the stress resultants in Eqs. (5.98)-(5.99) for the part of equilibrium due to the Kirchhoff-Love type motion, whereas the equations due to the difference between the Reissner-Mindlin type motion (or effective motion) and the previous are obtained from

---

[¶] In an attempt to create links between the different Chapters of this thesis, the interested reader should notice that also in the following Chapter the case of a transversely isotropic material is considered. In particular, in that case special attention will be placed in the evaluation of the effect of the transverse shear on the aerothermoelastic response and stability of the model.

Eqs. ([4.76](#))-([4.77](#)) for $k = 1$. In particular, in this case, one has

$$-\overset{\circ}{n}{}^{11}_{(0)\angle 1} + c^1_1 \, \overset{\circ}{n}{}^{11}_{(1)\angle 1} + c^1_1 \, \overset{\circ}{n}{}^{11}_{(0)} \, d_1 = 0 \tag{6.31}$$

$$\overset{\circ}{n}{}^{11}_{(1)\angle 11} + \left(\overset{\circ}{n}{}^{11}_{(0)} d_1 \right)_{\angle 1} + \overset{\circ}{n}{}^{11}_{(1)\angle 1} \, d_1 + \overset{\circ}{n}{}^{11}_{(0)} \, d_1 \, d_1 + \overset{\circ}{n}{}^{11}_{(0)} \, c_{11} = 0 \tag{6.32}$$

$$-\overset{\circ}{n}{}^{11}_{(1)\angle 1} + \overset{\circ}{q}{}^{1}_{(0)} - \overset{\circ}{n}{}^{11}_{(1)} \, d_1 = 0 \tag{6.33}$$

$$\overset{\circ}{q}{}^{1}_{(1)\angle 1} + c_{11} \, \overset{\circ}{n}{}^{11}_{(1)} + \overset{\circ}{q}{}^{1}_{(1)} \, d_1 - \overset{\circ}{r}_{(0)} = 0 \tag{6.34}$$

Introducing an array representation, one can rewrite the previous system of equilibrium equations in the following compact form

$$\mathsf{A}\left(\xi \right) \mathsf{y}'' + \mathsf{B}\left(\xi \right) \mathsf{y}' + \mathsf{C}\left(\xi \right) \mathsf{y} = 0 \tag{6.35}$$

where $\mathsf{y} \left(= \left[\overset{\circ}{n}{}^{11}_{(0)}, \overset{\circ}{n}{}^{11}_{(1)}, \overset{\circ}{q}{}^{1}_{(0)}, \overset{\circ}{q}{}^{1}_{(1)}, \overset{\circ}{r}_{(0)} \right] \right)$ is column matrix whose elements are the non-zero unknowns stress resultants, whereas A, B and C are the matrices of coefficients that multiply the derivatives of the stress resultants in the equilibrium equations[‖]

Now, recall the relations between the stress resultants and the components of the Cauchy stress tensor (see Eqs. ([4.58](#))-([4.61](#))), using again an array representation, one can express those relations in the following form

$$\mathsf{y} \;=\; \int_{-1}^{+1} \mathsf{L}\left(\xi, \zeta \right) \mathsf{w} \; d\zeta \tag{6.36}$$

where w has been already defined and represents the array of the non-zero components of the Cauchy stress tensor, whereas L is a matrix whose coefficients are given by the shifters between the volume and the surface metrics.

6.5 Boundary conditions

Similarly to the previous Section, also the boundary conditions can be easily obtained from the discussion of the First Part. In particular, it will be assumed that the shell be clamped at one side, and unloaded on the other. Therefore, the boundary conditions on the clamped edge will be written

$$\mathbf{x} \;=\; 0 \qquad \text{for } \xi = 0 \tag{6.37}$$

[‖] The reader may have noticed that in Eqs. ([6.31](#))-([6.34](#)) the stress resultants are derived by means of covariant derivatives, therefore, in matrices B and C will be the components of the curvature tensor and the Christoffel symbols that where employed for the definitions of the covariant derivatives in the convected surface frame.

whereas, using Eqs. (4.75) and (5.97), on the free edge one will have

$$\mathsf{T}y' + \mathsf{U}y = 0 \qquad \text{for } \xi = l \tag{6.38}$$

where T and U are two matrices whose elements are the coefficients of the stress resultants in the boundary equations.

6.6   Kirchhoff-Love + Reissner-Mindlin decomposition

It is worth noting that till now the KL + RM decomposition has been employed only in the determination of the equilibrium equations from the Virtual Work Principle. We have been entitled to do that for the fact that the virtual displacements are an arbitrary set of displacements, and in this sense one would not be constrained to solve the present problem in terms of the variables employed to obtain the equilibrium. Nonetheless, the consideration of that decomposition also in the definition of the real displacements would bring several advantages in the formulation, some of which have been already enlightened in the First part of the thesis; in particular, one may observe that the resulting structural operator is self-adjoint.

In particular, with reference to the problem under discussion, the First revised KL constraint, under the hypothesis of small deformations, yields

$$\mathbf{g}_3 \cdot \mathbf{g}_3 \;=\; \text{const} \qquad \longrightarrow \qquad \mathbf{v}_1\|_{KL} \cdot \mathbf{q}_0 = 0 \tag{6.39}$$

thus, using Eq. (6.3) one has

$$w_1\|_{KL} \;=\; -f \; u_1\|_{KL} \tag{6.40}$$

Similarly, for the second constraint one has

$$\mathbf{g}_3 \cdot \overset{\circ}{\mathbf{g}}_1 \;=\; const \qquad \longrightarrow \qquad \mathbf{v}_1\|_{KL} \cdot \frac{\partial \mathbf{p}_0}{\partial \xi} = -\mathbf{q}_0 \cdot \frac{\partial \mathbf{v}_0}{\partial \xi} \tag{6.41}$$

thus, using Eq. (6.2) and Eq. (6.3) one has

$$u_1\|_{KL} \;=\; -h_0 \; w_0' - h_0 \; f \; u_0' \tag{6.42}$$

At this point setting that the displacement $\mathbf{v}_1$ is given by the sum of the displacement due to the KL-type motion $(\mathbf{v}_1\|_{KL})$, plus a corrective displacement that measures the distance between the KL solution and the real (RM) solution.

Introducing the new set of displacement unknowns $\hat{\mathsf{x}}$ $(= \{\hat{u}_0, \hat{w}_0, \hat{u}_1, \hat{w}_1\})$, and using the previous

relations one has

$$x = \hat{A}(\xi)\hat{x}' + \hat{x} \tag{6.43}$$

where the matrix $\hat{A}$ is obtained applying the transformation rule identified by the KL constraints and KL+RM decomposition.

6.7   Solution procedure

Equations (6.21), (6.30), (6.35), and (6.36) constitute a system of 15 non-linear equations in 15 unknowns (w, x, y and z). They could be solved together, or, one can substitute them in order to arrive to a smaller system of equilibrium equations in only four unknowns (the displacements x) with a higher order of derivation. In the application presented it has been chosen to follow this second way. In particular, substituting Eq. (6.21) in Eq. (6.30), yields

$$w = G(\xi,\zeta)\,D(\xi,\zeta)\,x' + G(\xi,\zeta)\,E(\xi,\zeta)\,x + h(\xi,\zeta)\,\Delta\phi \tag{6.44}$$

Substituting, Eq. (6.44) in Eq. (6.36) yields

$$y = M(\xi)\,x' + N(\xi)\,x + g(\xi)\,\Delta\phi \tag{6.45}$$

where

$$M(\xi) := \int_{-1}^{+1} L(\xi,\zeta)\,G(\xi,\zeta)\,D(\xi,\zeta)\ d\zeta \tag{6.46}$$

$$N(\xi) := \int_{-1}^{+1} L(\xi,\zeta)\,G(\xi,\zeta)\,E(\xi,\zeta)\ d\zeta \tag{6.47}$$

$$g(\xi) := \int_{-1}^{+1} L(\xi,\zeta)\,h(\xi,\zeta)\ d\zeta \tag{6.48}$$

Similarly, substituting Eq. (6.45) in Eq. (6.35), yields

$$P(\xi)\,x''' + Q(\xi)\,x'' + R(\xi)\,x' + S(\xi)\,x = f(\xi) \tag{6.49}$$

where

$$P\left(\xi\right) \quad := \quad A\left(\xi\right)M\left(\xi\right) \tag{6.50}$$

$$Q\left(\xi\right) \quad := \quad A\left(\xi\right)\left[2M'\left(\xi\right)+N\left(\xi\right)\right]+B\left(\xi\right)M\left(\xi\right) \tag{6.51}$$

$$R\left(\xi\right) \quad := \quad A\left(\xi\right)\left[M''\left(\xi\right)+2N'\left(\xi\right)\right]+B\left(\xi\right)\left[M'\left(\xi\right)+N\left(\xi\right)\right]+C\left(\xi\right)M\left(\xi\right) \tag{6.52}$$

$$R\left(\xi\right) \quad := \quad A\left(\xi\right)N''\left(\xi\right)+B\left(\xi\right)N'\left(\xi\right)+C\left(\xi\right)N\left(\xi\right) \tag{6.53}$$

$$f\left(\xi\right) \quad := \quad -\left\{A\left(\xi\right)\left[g\left(\xi\right)\Delta\phi\right]''+B\left(\xi\right)\left[g\left(\xi\right)\Delta\phi\right]'+C\left(\xi\right)\left[g\left(\xi\right)\Delta\phi\right]\right\} \tag{6.54}$$

Again, introducing Eq. (6.45) in the boundary conditions (Eq. (6.38)), one has

$$Vx''+Wx'+Yx = L \qquad for\ \xi = l \tag{6.55}$$

where

$$V \quad = \quad TM\left(l\right) \tag{6.56}$$

$$W \quad = \quad TM'\left(l\right)+TN\left(l\right)+UM\left(l\right) \tag{6.57}$$

$$Y \quad = \quad TN'\left(l\right)+UN\left(l\right) \tag{6.58}$$

$$L \quad = \quad -T\left(g\Delta\phi\right)'-Ug\Delta\phi \tag{6.59}$$

At this point one may introduce the KL+RM decomposition, which, by virtue of the considerations of the previous Section, is equivalent to a change of variables defined by Eq. (6.43). Therefore, substituting Eq. (6.43) in Eq. (6.49) one has

$$\hat{B}\left(\xi\right)\hat{x}^{IV}+\hat{C}\left(\xi\right)\hat{x}'''+\hat{D}\left(\xi\right)\hat{x}''+\hat{E}\left(\xi\right)\hat{x}'+S\left(\xi\right)\hat{x} = f \tag{6.60}$$

where

$$\hat{B} \quad = \quad P\hat{A} \tag{6.61}$$

$$\hat{C} \quad = \quad P\left(3\ \hat{A}'+I\right)+Q\hat{A} \tag{6.62}$$

$$\hat{D} \quad = \quad P\ 3\ \hat{A}''+Q\left(2\ \hat{A}'+I\right)+R\hat{A} \tag{6.63}$$

$$\hat{E} \quad = \quad P\hat{A}'''+Q\hat{A}''+R\left(\hat{A}'+I\right)+S\hat{A} \tag{6.64}$$

Similarly, for the boundary conditions at the clamped edge, one has

$$\hat{A}\left(0\right)\hat{x}'+\hat{x} = 0 \qquad for\ \xi = 0 \tag{6.65}$$

whereas, at the free edge, substituting Eq. (6.43) in Eq. (6.55) one has

$$\hat{\mathsf{F}}\hat{\mathsf{x}}''' + \hat{\mathsf{G}}\hat{\mathsf{x}}'' + \hat{\mathsf{H}}\hat{\mathsf{x}}' + \mathsf{Y}\hat{\mathsf{x}} = \mathsf{L} \qquad for \; \xi = l \tag{6.66}$$

where

$$\hat{\mathsf{F}} = \mathsf{V}\hat{\mathsf{A}} \tag{6.67}$$

$$\hat{\mathsf{G}} = \mathsf{V}\left(2\,\hat{\mathsf{A}} + \mathsf{I}\right) + \mathsf{W}\hat{\mathsf{A}} \tag{6.68}$$

$$\hat{\mathsf{H}} = \mathsf{V}\hat{\mathsf{A}}'' + \mathsf{W}\left(\hat{\mathsf{A}}' + \mathsf{I}\right) + \mathsf{Y}\hat{\mathsf{A}} \tag{6.69}$$

By means of the preceding relations, the system of 15 equations, whose maximum order of derivative is the second, in 15 unknowns has been reduced to a system of only 4 equations, whose maximum order of derivative is the fourth, in 4 unknowns (the KL + RM displacement components).

Before proceeding further, it is worth noting that the matrices comparing in the equilibrium equations may be functions not only of the co-ordinate ξ but also of the present displacement being the original equilibrium equations written in the deformed (or present) configuration, and being the Christoffel symbols, among the others, function of the displacement field. Therefore, in order to obtain the exact solution of the problem one should consider an iterative approach, that, starting from an initial solution, determine the matrices comparing in the equilibrium equations ($\hat{\mathsf{B}}$, $\hat{\mathsf{C}}$, $\hat{\mathsf{D}}$, etc.) from the data available at the previous step, and then solve for each step the linear part of the system of equations. This is what has been done in this application, although only one step of iteration has been considered for simplicity.

6.8   Numerical results

The numerical results here presented have been obtained using a finite difference numerical scheme. The principal milestones of this numerical solution procedure are reported briefly in the following.

Because the maximum order of derivatives of the equilibrium equations is the fourth, one is forced to use finite differences with five points to discretize the derivatives. Thus, introducing a discretization of the domain with $N + 1$ nodes, and denoting with X the array of displacements $\hat{\mathsf{x}}$ evaluated in each node of the domain (*i.e.*, $\mathsf{X} = \{\hat{\mathsf{x}}\left(\xi_0\right), ..., \hat{\mathsf{x}}\left(\xi_k\right), ..., \hat{\mathsf{x}}\left(\xi_N\right)\}^T$), one may denote the central finite difference of a derivative of order p as

$$\mathsf{X}^{(p)} = \mathsf{D}_4^C\mathsf{X} \tag{6.70}$$

where D_4^C is the matrix of the central finite difference with five points. Similarly, for a finite forward or backward difference one can substitute the upper C with an Fx or a Bx, where x is a number denoting the number of nodes considered forward or backward to write the finite difference

approximation.

To solve numerically the problem one has to build at every step (i) of the iteration the following matrix based on the central difference approximation of the derivatives comparing in the equilibrium equations

$$
\begin{aligned}
A^C_{(i)} &= \begin{bmatrix} \ddots & & \\ & \hat{B}_{(i-1)}(\xi_k) & \\ & & \ddots \end{bmatrix} D^C_4 + \begin{bmatrix} \ddots & & \\ & \hat{C}_{(i-1)}(\xi_k) & \\ & & \ddots \end{bmatrix} D^C_3 + \begin{bmatrix} \ddots & & \\ & \hat{D}_{(i-1)}(\xi_k) & \\ & & \ddots \end{bmatrix} D^C_2 \\
&+ \begin{bmatrix} \ddots & & \\ & \hat{E}_{(i-1)}(\xi_k) & \\ & & \ddots \end{bmatrix} D^C_1 + \begin{bmatrix} \ddots & & \\ & \hat{S}_{(i-1)}(\xi_k) & \\ & & \ddots \end{bmatrix}
\end{aligned}
\tag{6.71}
$$

Similarly, to take into account the nodes close to the boundaries one needs to define at each step two other matrices $A^{B1}_{(i)}$ and $A^{F1}_{(i)}$ that are obtained using respectively one point forward and backward finite difference approximations of the derivatives.

Furthermore, at the boundaries one has to impose the boundary conditions (Eqs. (6.65)-(6.66)). To do that define, at every step, the two following matrices for the clamped edge

$$
B^{F2} = \begin{bmatrix} \ddots & & \\ & \hat{A}_{(i-1)}(\xi_k) & \\ & & \ddots \end{bmatrix} D^{F2}_1 + \begin{bmatrix} \ddots & & \\ & I & \\ & & \ddots \end{bmatrix}
\tag{6.72}
$$

and for the free edge

$$
\begin{aligned}
B^{B2} &= \begin{bmatrix} \ddots & & \\ & \hat{F}_{(i-1)}(\xi_k) & \\ & & \ddots \end{bmatrix} D^{B2}_3 + \begin{bmatrix} \ddots & & \\ & \hat{G}_{(i-1)}(\xi_k) & \\ & & \ddots \end{bmatrix} D^{B2}_2 + \begin{bmatrix} \ddots & & \\ & \hat{H}_{(i-1)}(\xi_k) & \\ & & \ddots \end{bmatrix} D^{B2}_1 \\
&+ \begin{bmatrix} \ddots & & \\ & \hat{Y}_{(i-1)}(\xi_k) & \\ & & \ddots \end{bmatrix}
\end{aligned}
\tag{6.73}
$$

Similarly, for the load vector one has

$$
b_{(i)} = \{0, f(\xi_1), ..., (\xi_k), ..., (\xi_{N-1}), L\}^T
\tag{6.74}
$$

At this point, the solution of the problem can be obtained at every step inverting the matrix $A_{(i)}$ constructed with the first two rows (in a vectorial sense) of $B^{F2}_{(i)}$, the third and the fourth rows of $A^{F1}_{(i)}$, the rows from the fifth to the $(N-1)$-th of $A^C_{(i)}$, the N-th row of $A^{B1}_{(i)}$ and the $(N+1)$-th

row of $B^{B2}_{(i)}$. Once this assembly has been performed at every step, the solution of the problem is thus reduced to the solution of the following algebraic problem

$$A_{(i)}X_{(i)} \;\; = \;\; b_{(i)} \tag{6.75}$$

The previous solution procedure has been conducted starting from a zero displacement condition for the system for several value of initial inclination of the fiber and the corresponding results are reported in the subsequent figures.
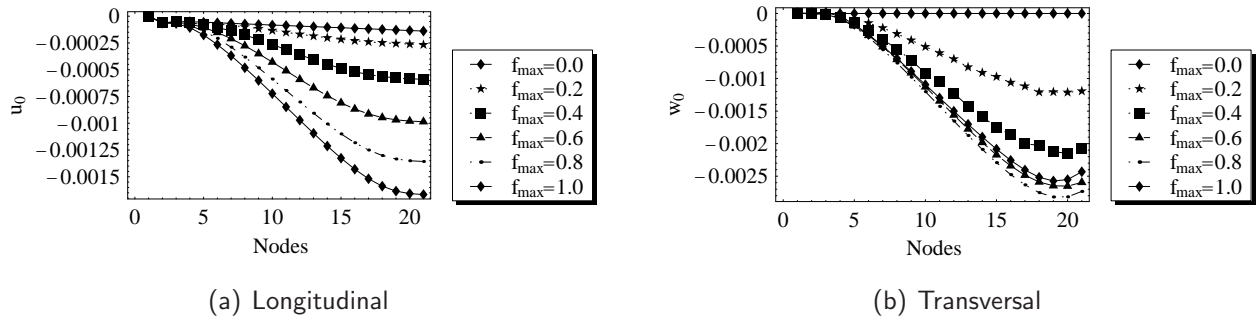

(a) Longitudinal

(b) Transversal

Figure 6.1: Displacements of the main surface: a comparison in terms of inclination.

(a) Longitudinal

(b) Transversal
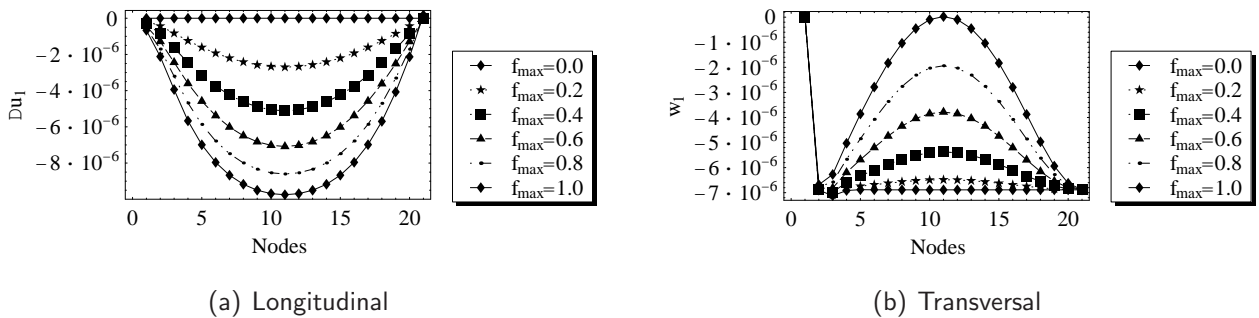
Figure 6.2: Displacements of the fiber: a comparison in terms of inclination.

(a) $f(\xi) = \sin(\pi\xi/l)$

(b) $f(\xi) = \sin(2\pi\xi/l)$
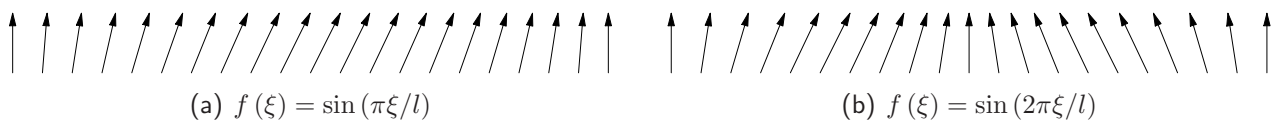
Figure 6.3: Microstructure of the shell: a visual representation of the fiber distribution in the undeformed configuration.

In particular, the same material properties for the piezoelectric material that compose the fibers of the shell reported in Refs. [83, 88] have been considered. For convenience, these material parameters are reported in the following table (Tab. 6.1). Geometrically, it has been assumed that the shell has a span of 1 meter and an initial thickness of only 2 mm. The numerical results are relevant to a 20 nodes finite difference scheme and to a condition of constant electric voltage difference at

μ (GPa)	24.95
λ (GPa)	82.30
τ_1 (GPa)	120.00
τ_2 (GPa)	83.70
η (GPa)	29.50
δ_1 (C/m^2)	11.80
δ_3 (C/m^2)	16.70

Table 6.1: Piezoelectric material moduli.

the edges of the fibers ($\Delta\phi = 10 \ kV$). Moreover, in order to evaluate the influence of the fiber distribution on the displacement field, Figs. 6.4-6.5, show the static response, in terms of axis and fiber displacements, for the two different fiber distributions schematically showed in Figs. 6.3.

(a) Longitudinal   (b) Transversal
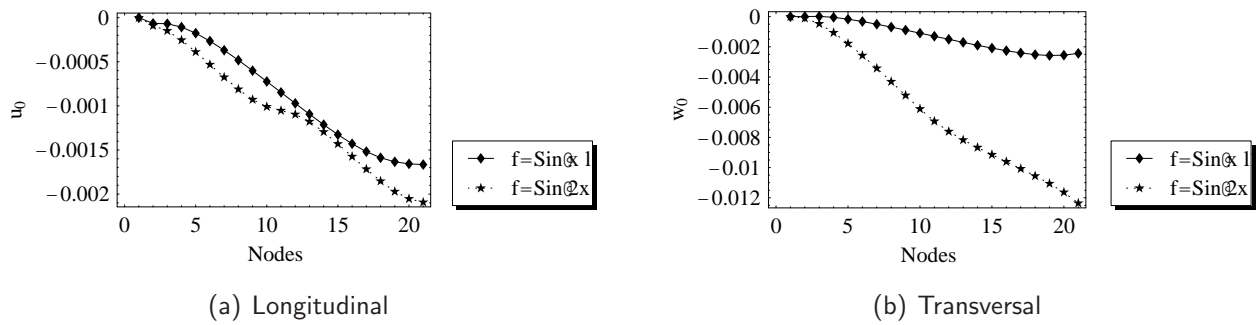
Figure 6.4: Displacements of the main surface: a comparison in terms of fiber distribution.

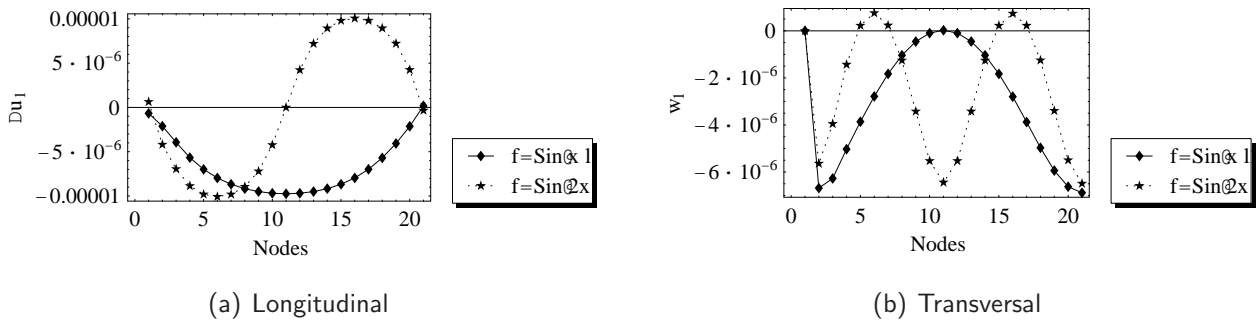(a) Longitudinal   (b) Transversal

Figure 6.5: Displacements of the fiber: a comparison in terms of fiber distribution.

Before concluding this Section, it is worth noting that the presented results have to be considered only as preliminary ones, either because the problem, intrinsically nonlinear, has been solved only in a first step of iteration, either because of the several modeling simplifications assumed in the previous Sections. Finally, observe that the novelty of the proposed problem does not permit an immediate validation of the results that should be verified either with refined numerical model, either with experimental tests.

6.9 Concluding remarks

In this Chapter, the model and the numerical solution of a infinitely long shell made of piezoelectric fibers inclined with respect to the normal has been presented. Two aspects have to be underlined in order to comment this application: first, that this problem has a natural setting in the formulation discussed and developed in the First Part of this thesis, because of the importance that has been placed on the inclination of the material fibers in the continuum, second, that this type of problems opens a variety of interesting practical applications in the aerospace field (*e.g.*, the design of morphing wings), exploiting the potentiality of the piezoelectric materials and of the micro-structured continua. Indeed, in our opinion this model can be viewed as a benchmark model for the definition of future possible adaptive structures.

Finally, observe that, as it is apparent from the results presented, the actuation capabilities of the structure are highly dependent on the fiber distribution. This fact places an interesting optimization problem, that should be solved in order to obtain the best actuation performances and that will be put under our consideration in the future developments.

Chapter 7

Aircraft swept wing impacted by a laser beam

7.1 Introduction

In this Chapter, a closed form solution for the aeroelastic response of an aircraft swept wing made of advanced composite materials, whose upper surface is impacted by a laser beam is presented. The expression of the thermal field acting on the system as an external input, has been obtained using the Green's function method performed for the case under consideration. For the aircraft wing, an advanced structural model is developed by converting the equations of the 3-D elasticity theory to the 1-D ones, and by including the effects of transverse shear, warping restraint, and thermoelastic anisotropy of the constituent materials. It is supposed that the wing is immersed in a subsonic incompressible flow whose speed is lower than the flutter critical speed of the system. In order to generate the aero-thermo-elastic governing equations, a generalization of a previously developed structural model for advanced aircraft swept wings[58, 59, 60, 45] made up of monoclinic multi-layered composites is carried out. For computational purposes, and towards highlighting the effects of a number of physical and geometrical parameters, the case of a rectangular single-layered swept wing composed of a transversely isotropic material is considered. Having in view its exceptional features in the thermal protection of aerospace structures[38, 84], the pyrolytic graphite that features thermo-mechanical transversely isotropic properties is considered. Due to the time-dependence of the thermal field, the unsteady aerodynamic theory of lifting surfaces has been considered in the time-domain. Then, the problem is solved analytically in a double Laplace transform space domain, where both the space and time co-ordinates are converted to their Laplace variable space counterparts. Within this approach, the problem is reduced to the solution of an algebraic problem in the transformed kinematical unknowns, and the solution in the physical space and time domain was obtained via an inverse double Laplace transform. Although this analysis is confined to the study of the dynamic aeroelastic response in the subcritical speed range, important information regarding the

conditions of occurrence of the flutter instability can be obtained. In the presentation and discussion of results, special emphasis has been placed on the effects of transverse shear flexibility, sweep angle, laser power time dependence, and flight speed on aeroelastic response.

7.2   Geometry and kinematical hypotheses

The wing will be considered as plate-like body with appropriate internal constraints. This means, for instance, that the geometry of the wing is represented by the following map

$$\mathbf{x}\left(x_\alpha, x_3, t\right) = \mathbf{p}\left(x_\alpha, t\right) + x_3 \ \mathbf{n}\left(x_\alpha, t\right) \qquad [x_3 \in (h_l, h_u)] \tag{7.1}$$

where $\mathbf{p}\left(x_\alpha, t\right)$ represents the geometry of the midsurface at a generic instant of time t, whereas $\mathbf{n}\left(x_\alpha, t\right)$ is the actual normal to the mid-surface and h_l, h_u are, respectively, the distances (with sign) of the lower and upper surfaces from the reference surface. In the framework of linearized kinematical model and small displacements with respect to a reference configuration one may always assume the following representation for the displacement field

$$\mathbf{u}\left(x_\alpha, x_3, t\right) := \mathbf{x}\left(x_\alpha, x_3, t\right) - \mathbf{x}\left(x_\alpha, x_3, 0\right) = \mathbf{v}\left(x_\alpha, t\right) + x_3 \ \mathbf{w}\left(x_\alpha, t\right) \tag{7.2}$$

where it has been assumed as reference configuration the geometry of the wing at the initial time. Thus, introducing an ortho-normal Cartesian reference system as reported in Fig. 7.1, one has
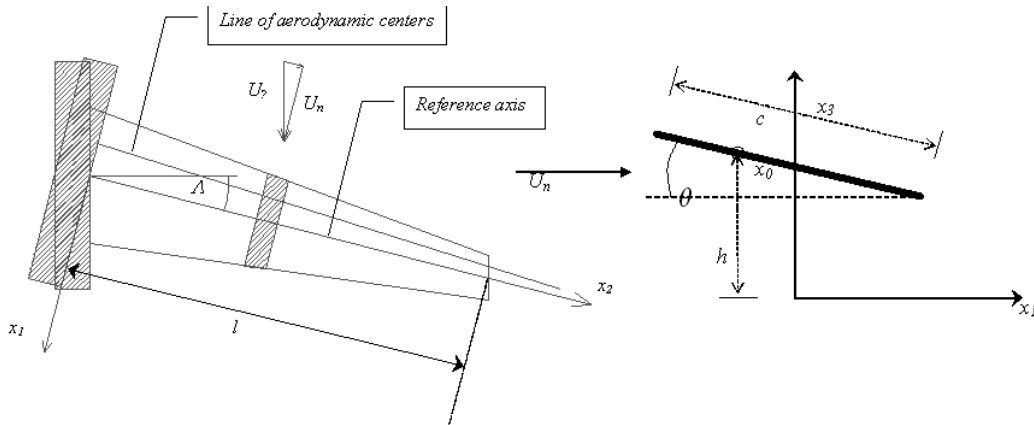

Figure 7.1: Geometry of the swept wing.

$$u_\alpha\left(x_\alpha, x_3, t\right) = v_\alpha\left(x_\alpha, t\right) + x_3 \ w_\alpha\left(x_\alpha, t\right) \tag{7.3}$$

$$u_3\left(x_\alpha, x_3, t\right) = v_3\left(x_\alpha, t\right) \tag{7.4}$$

From Eq. 7.4 it is apparent that with it one introduces the first kinematical constraint into the model, that is, no thickness distension is allowed. Moreover, Equation 7.3 is equivalent to say that

the plate-like structure is composed of inextensible needles attached in the middle to the base surface of the plate. At this initial stage they are free to rotate with respect to an arbitrary axis in the reference plane.

In order to achieve a 1-D model of the wing structure one needs to impose other internal constraints to the displacement field (*i.e.*, to the material structure). Particularly, it will be assumed that the rotation around the x_2 axis is unaffected by the x_1 coordinates, that means that all the fibers laying on a chord (or chord-wise) will rotate rigidly

$$v_1\left(x_\alpha, t\right) = 0 \tag{7.5}$$

$$w_1\left(x_\alpha, t\right) = \theta\left(x_2, t\right) \tag{7.6}$$

where $\theta\left(x_2, t\right)$ represents the rotation of the fiber with respect to the span-wise direction.

Furthermore, it will be assumed that warping (*i.e.*, flexible rotation around x_2) is permitted and so one should consider

$$w_2\left(x_\alpha, t\right) = \beta\left(x_2, t\right) + x_1\ g\left(x_2, t\right) \tag{7.7}$$

where $\beta\left(x_2, t\right)$ represents the rotation of the fiber on the reference coordinate axis x_1, and $g\left(x_2, t\right)$ is the rotation gradient in the x_1 direction. Finally, one may postulate for the displacement in the normal direction the following map

$$v_3\left(x_\alpha, t\right) = h\left(x_2, t\right) - \left(x_1 - x_0\left(x_2\right)\right)\ \theta\left(x_2, t\right) \tag{7.8}$$

where $x_0\left(x_2\right)$ is the position of the elastic axis along the chord.

Based on Eqs. 7.3-7.8, within the linear theory of elasticity (*i.e.*, linear deformation tensor), the engineering strain-tensor components ε_i are

$$\varepsilon_1 := \varepsilon_{11}\left(x_k, t\right) = \frac{\partial u_1}{\partial x_1} = 0 \tag{7.9}$$

$$\varepsilon_2 := \varepsilon_{22}\left(x_k, t\right) = \frac{\partial u_2}{\partial x_2} = u_{2,2} + x_3\ \left(\beta_{,2} + x_1\ g_{,2}\right) \tag{7.10}$$

$$\varepsilon_3 := \varepsilon_{33}\left(x_k, t\right) = \frac{\partial u_3}{\partial x_3} = 0 \tag{7.11}$$

$$\varepsilon_4 := \gamma_{23}\left(x_k, t\right) = \frac{\partial u_2}{\partial x_3} + \frac{\partial u_3}{\partial x_2} = \beta + x_1\ g + h_{,2} - x_1\ \theta_{,2} + \left(x_0\ \theta\right)_{,2} \tag{7.12}$$

$$\varepsilon_5 := \gamma_{13}\left(x_k, t\right) = \frac{\partial u_1}{\partial x_3} + \frac{\partial u_3}{\partial x_1} = 0 \tag{7.13}$$

$$\varepsilon_6 := \gamma_{12}\left(x_k, t\right) = \frac{\partial u_1}{\partial x_2} + \frac{\partial u_2}{\partial x_1} = x_3\ \theta_{,2} + x_3\ g \tag{7.14}$$

where Eq. 7.9 states that no deformation is considered in the chord-wise direction, similarly, Eq. 7.11 states that no thickness distension is permitted, and, eq. 7.13 that a chord section is rigid with respect to the $x_2 = const$ plane and no shear is allowed between x_1 and x_3 axes. On the other hand, Eqs. 7.12 and 7.14 state that shear between the x_2 and x_3, and x_1 and x_2 axes is allowed. In view of Eqs. 7.9-7.14, it is apparent that a refined Euler-Bernoulli model (some times called Timoshenko beam model) has been set up, in which shear is allowed.

7.2.1   Euler-Bernoulli model

For future reference, in this section the relationships, that should be considered among the displacement unknowns in order to deal with the Euler-Bernoulli model, are presented and discussed. From Eqs. 7.12, it is apparent that the following relations yield to the introduction of a unshearable constraint of the chord section (*i.e.*, a discard of the warping effect)

$$\beta = -h_{,2} - (x_0\,\theta)_{,2} \tag{7.15}$$

$$g = \theta_{,2} \tag{7.16}$$

Substituting these relations in Eqs. 7.10-7.14 yields

$$\varepsilon_2 = x_3\left[-h_{,22} - (x_0\,\theta)_{,22} + x_1\,\theta_{,22}\right] \tag{7.17}$$

$$\varepsilon_6 = 2\,x_3\,\theta_{,2} \tag{7.18}$$

Similarly, for the displacement filed one has

$$u_1 = x_3\,\theta \tag{7.19}$$

$$u_2 = u_2 + x_3\left[-h_{,2} - (x_0\,\theta)_{,2} + x_1\,\theta_{,2}\right] \tag{7.20}$$

$$u_3 = h - (x_1 - x_0)\,\theta \tag{7.21}$$

7.3   The equations of motion and the boundary conditions

In order to obtain the equilibrium equations and the related boundary conditions, introduce the following functional:

$$J = \int_{t_0}^{t_1} \left(\mathcal{U} - \mathcal{K} + \mathcal{A}\right) dt \tag{7.22}$$

where $\mathcal{U}$ is the strain energy, $\mathcal{K}$ the kinetic energy and $\mathcal{A}$ the external work. From the Hamilton's principle for non-conservative phenomena, one may easily obtain

$$\delta J = \int_{t_0}^{t_1} \left\{ -\int_{\mathcal{B}} \Sigma \cdot \operatorname{Grad} \delta \mathbf{u} + \int_{\mathcal{B}} \rho \left(\mathbf{H} - \ddot{\mathbf{u}} \right) \cdot \delta \mathbf{u} + \int_{\partial \mathcal{B}} \mathbf{t}^A \cdot \delta \mathbf{u} \right\} dt \qquad (7.23)$$

where Σ is the Piola-Kirchhoff stress tensor, $\mathbf{H}$ are the applied body forces, and $\mathbf{t}^A$ are the applied surface forces.

The first integral in Eq. (7.23) can be recast in the following way

$$\begin{aligned}
\int_{\mathcal{B}} \Sigma \cdot \operatorname{Grad} \delta \mathbf{u} &= \int_0^l \int_{\mathcal{A}(x_2)} \left\{ \sigma_{22} \left(\delta u_{2,2} + x_3 \, \delta \beta_{,2} + x_3 \, x_1 \, \delta g_{,2} \right) \right. \\
&+ \sigma_{23} \left[\delta \beta + x_1 \, \delta g + \delta h_{,2} - x_1 \, \delta \theta_{,2} + \left(x_0 \, \delta \theta \right)_{,2} \right] \\
&+ \left. \sigma_{12} \left(x_3 \, \delta \theta_{,2} + x_3 \, \delta g \right) \right\} d\mathcal{A} \, dx_2
\end{aligned} \qquad (7.24)$$

where $\mathcal{A}(x_2)$ is the cross section area and it is assumed function of the span-wise location. Let us now introduce the following definition

$$T_{ij}^{(m,n)} := \int_{\mathcal{A}(x_2)} \sigma_{ij} \, x_1^m \, x_3^n \, d\mathcal{A} \qquad (7.25)$$

then, one has

$$\begin{aligned}
\int_{\mathcal{B}} \Sigma \cdot \operatorname{Grad} \delta \mathbf{u} &= \int_0^l \left[T_{22}^{(0,0)} \, \delta u_{2,2} + T_{22}^{(0,1)} \, \delta \beta_{,2} + \left(T_{23}^{(1,0)} + T_{12}^{(0,1)} \right) \delta g \right. \\
&+ T_{22}^{(1,1)} \, \delta g_{,2} + T_{23}^{(0,0)} \, \delta \beta + \left(T_{12}^{(0,1)} - T_{23}^{(1,0)} + T_{23}^{(0,0)} \, x_0 \right) \, \delta \theta_{,2} \\
&+ \left. T_{23}^{(0,0)} \, x_{0,2} \, \delta \theta + T_{23}^{(0,0)} \, \delta h_{,2} \right] \, dx_2
\end{aligned} \qquad (7.26)$$

Performing the integration by parts, *i.e.*,

$$\int_0^l F \, \delta b_{,2} \, dx_2 = \left[F \, \delta b \right]_0^l - \int_0^l F_{,2} \, \delta b \, dx_2 \qquad (7.27)$$

one has

$$\begin{aligned}
\int_{\mathcal{B}} \Sigma \cdot \operatorname{Grad} \delta \mathbf{u} &= \int_0^l \left\{ T_{23}^{(0,0)} \, x_{0,2} \, \delta \theta - T_{22,2}^{(0,0)} \, \delta u_2 - \left(T_{22,2}^{(0,1)} - T_{23}^{(0,0)} \right) \delta \beta \right. \\
&- \left(T_{22,2}^{(1,1)} - T_{23}^{(1,0)} - T_{12}^{(0,1)} \right) \, \delta g - \left(T_{12,2}^{(0,1)} - T_{23,2}^{(1,0)} + T_{23,2}^{(0,0)} \, x_0 \right) \, d\theta \\
&- \left. T_{23,2}^{(0,0)} \, \delta h \right\} \, dx_2 + \left[T_{22}^{(0,0)} \, \delta u_2 + T_{22}^{(0,1)} \, \delta \beta + T_{22}^{(1,1)} \, \delta g \right. \\
&+ \left. \left(T_{12}^{(0,1)} - T_{23}^{(1,0)} + T_{23}^{(0,0)} \, x_0 \right) \, \delta \theta + T_{23}^{(0,0)} \, \delta h \right]_0^l
\end{aligned} \qquad (7.28)$$

Let us now express explicitly the acceleration components in terms of the basic unknowns

$$\ddot{u}_1 = x_3 \, \ddot{\theta} \tag{7.29}$$

$$\ddot{u}_2 = \ddot{u}_2 + x_3 \, \ddot{\beta} + x_1 \, x_3 \, \ddot{g} \tag{7.30}$$

$$\ddot{u}_3 = \ddot{h} - (x_1 - x_0) \, \ddot{\theta} \tag{7.31}$$

Introducing the following definitions for the external body forces and the inertial properties of the body

$$F_i^{(m,n)} := \int_{\mathcal{A}(x_2)} \rho \, H_i \, x_1^m \, x_3^n d\mathcal{A} \tag{7.32}$$

$$I^{(m,n)} := \int_{\mathcal{A}(x_2)} \rho \, x_1^m \, x_3^n d\mathcal{A} \tag{7.33}$$

one has

$$
\begin{aligned}
\int_{\mathcal{B}} \rho \, (\mathbf{H} - \ddot{\mathbf{u}}) \cdot \delta \mathbf{u} = & \int_0^l \left\{ \left[F_2^{(0,0)} - \left(I^{(0,0)} \, \ddot{u}_2 + I^{(0,1)} \, \ddot{\beta} + I^{(1,1)} \, \ddot{g} \right) \right] \, \delta u_2 \right. \\
& + \left[F_2^{(0,1)} - \left(I^{(0,1)} \, \ddot{u}_2 + I^{(0,2)} \, \ddot{\beta} + I^{(1,2)} \, \ddot{g} \right) \right] \, \delta \beta \\
& + \left[F_2^{(1,1)} - \left(I^{(1,1)} \, \ddot{u}_2 + I^{(1,2)} \ddot{\beta} + I^{(2,2)} \ddot{g} \right) \right] \, \delta g \\
& + \left[F_1^{(0,1)} - F_3^{(1,0)} + F_3^{(0,0)} \, x_0 - \left(\left(I^{(0,2)} + I^{(2,0)} - 2 \, I^{(1,0)} \, x_0 \right. \right. \right. \\
& + \left. I^{(0,0)} \, x_0^2 \right) \, \ddot{\theta} + \left(I^{(0,0)} \, x_0 - I^{(1,0)} \right) \, \ddot{h} \Big) \Big] \, \delta \theta + \\
& + \left. \left[F_3^{(0,0)} - \left(I^{(0,0)} \, \ddot{h} - I^{(1,0)} \, \ddot{\theta} + I^{(0,0)} \, x_0 \, \ddot{\theta} \right) \right] \, \delta h \right\} dx_2 \tag{7.34}
\end{aligned}
$$

Before substituting the obtained results in Eq. (7.23), one should evaluate the virtual work exerted by the surface tractions (or applied external surface forces) on the boundary. At this aim, let us note that the boundary can be divided into three parts, specifically

$$\partial \mathcal{B} = \mathcal{S}_u \cup \mathcal{S}_l \cup \mathcal{S}_r \tag{7.35}$$

where $\mathcal{S}_u$, $\mathcal{S}_l$ are the upper and lower surfaces of the wing, while $\mathcal{S}_r$ is the right side. Furthermore, assume that the external loads acting on the upper and lower surfaces can be separated into two parts, specifically, the aerodynamic load and a generic mechanical load (*e.g.*, a blast)

$$\mathbf{t}^A = \mathbf{t}_{aero}^A + \mathbf{t}_{mech}^A \tag{7.36}$$

Moreover, for the aerodynamic load assume

$$\left(t^A_{aero}\right)_\alpha = 0 \quad \left(t^A_{aero}\right)_3 = p^+ \quad on \ \mathcal{S}_u \tag{7.37}$$

$$\left(t^A_{aero}\right)_\alpha = 0 \quad \left(t^A_{aero}\right)_3 = p^- \quad on \ \mathcal{S}_l \tag{7.38}$$

which means that no viscous shear is considered in the model. Thus the integral of virtual work of the surface tractions can be written

$$\int_{\partial\mathcal{B}} \mathbf{t}^A \cdot \delta\mathbf{u} = \int_{\mathcal{S}_u \cup \mathcal{S}_l} \mathbf{t}^A_{aero} \cdot \delta\mathbf{u} + \int_{\mathcal{S}_u \cup \mathcal{S}_l} \mathbf{t}^A_{mech} \cdot \delta\mathbf{u} + \int_{\mathcal{S}_r} \mathbf{t}^A \cdot \delta\mathbf{u} \tag{7.39}$$

where the first integral reads

$$\int_{\mathcal{S}_u \cup \mathcal{S}_l} \mathbf{t}^A_{aero} \cdot \delta\mathbf{u} = \int_0^l \left(\mathcal{L} \ \delta h - \mathcal{M} \ \delta\theta + \mathcal{L} \ x_0 \ \delta\theta\right) dx_2 \tag{7.40}$$

where

$$\mathcal{L} := \int_{LE(x_2)}^{TE(x_2)} \Delta p\left(x_1, x_2\right) \ dx_1 \tag{7.41}$$

$$\mathcal{M} := \int_{LE(x_2)}^{TE(x_2)} \Delta p\left(x_1, x_2\right) \ x_1 \ dx_1 \tag{7.42}$$

Similarly, for the second integral in Eq. (7.212), one has

$$\begin{aligned}
\int_{\mathcal{S}_u \cup \mathcal{S}_l} \mathbf{t}^A_{mech} \cdot \delta\mathbf{u} = & \int_0^l \left[\phi_2^{(0,0)} \ \delta u_2 + \left(\phi_1^{(1,0)} + \phi_{2,2}^{(1,0)} \ x_0 - \phi_2^{(1,1)} - \phi_3^{(0,1)} + \phi_3^{(0,0)} \ x_0\right) \delta\theta \right. \\
& \left. + \ \left(\phi_{2,2}^{(1,0)} + \phi_3^{(0,0)}\right) \ \delta h\right] dx_2 - \left[\phi_2^{(1,0)} \ \delta h + \left(\phi_2^{(1,0)} \ x_0 - \phi_2^{(1,1)}\right) \ \delta\theta\right]_0^l
\end{aligned} \tag{7.43}$$

where by definition

$$\phi_i^{(m,n)} := \int_{TE(x_2)}^{LE(x_2)} \left[\left(t_i^A \ x_3^n\right)_{x_3=t_u} + \left(t_i^A \ x_3^n\right)_{x_3=t_l}\right] x_1^m \ dx_1 \tag{7.44}$$

Finally, for the third integral in Eq. (7.212), one has

$$\int_{\mathcal{S}_r} \mathbf{t}^A \cdot \delta\mathbf{u} = \psi_2^{(0,0)} \ \delta u_2 + \psi_2^{(0,1)} \ \delta\beta + \psi_2^{(1,1)} \ \delta g + \left(\psi_1^{(0,1)} - \psi_3^{(1,0)} + \psi_3^{(0,0)} \ x_0\left(l\right)\right) \delta \tag{7.45}$$

where by definition

$$\psi_i^{(m,n)} := \int_{\mathcal{A}(l)} t_i^A \ x_1^m \ x_3^n \ dx_1 \ dx_2 \tag{7.46}$$

29th May 2005

Collecting all the terms and substituting them in Eq. (7.23), one finally obtains five equilibrium equations relevant to arbitrary variations of the five degrees of freedom, associated to the displacement field by means of the internal kinematical constraints

$$T_{22,2}^{(0,0)} + F_2^{(0,0)} - I^{(0,0)}\ \ddot{u}_2 - I^{(0,1)}\ \ddot{\beta} - I^{(1,1)}\ \ddot{g} = 0 \tag{7.47}$$

$$T_{22,2}^{(0,1)} - T_{23}^{(0,0)} + F_2^{(0,1)} - I^{(0,1)}\ \ddot{u}_2 - I^{(0,2)}\ \ddot{\beta} - I^{(1,2)}\ \ddot{g} = 0 \tag{7.48}$$

$$T_{22,2}^{(1,1)} - T_{23}^{(1,0)} - T_{12}^{(0,1)} + F_2^{(1,1)} - I^{(1,1)}\ \ddot{u}_2 - I^{(1,2)}\ \ddot{\beta} - I^{(2,2)}\ \ddot{g} = 0 \tag{7.49}$$

$$T_{12,2}^{(0,1)} - T_{23,2}^{(1,0)} + T_{23,2}^{(0,0)}\ x_0 + F_1^{(0,1)} - F_3^{(1,0)} + F_3^{(0,0)}\ x_0 - $$
$$\left(I^{(0,2)} + I^{(2,0)} - 2\ I^{(1,0)}\ x_0 + I^{(0,0)}\ x_0^2\right)\ \ddot{\theta} - $$
$$\left(I^{(1,0)} - I^{(0,0)}\ x_0\right)\ \ddot{h} - \mathcal{M} + \mathcal{L}\ x_0 = 0 \tag{7.50}$$

$$T_{23,2}^{(0,0)} + F_3^{(0,0)} - I^{(0,0)}\ \ddot{h} + \left(I^{(1,0)} - I^{(0,0)}\ x_0\right)\ \ddot{\theta} + \mathcal{L} = 0 \tag{7.51}$$

The associated boundary conditions are

$$T_{22}^{(0,0)} = \psi_2^{(0,0)} \tag{7.52}$$
$$T_{22}^{(0,1)} = \psi_2^{(0,1)} \tag{7.53}$$
$$T_{22}^{(1,1)} = \psi_2^{(1,1)} \tag{7.54}$$
$$T_{12}^{(0,1)} - T_{23}^{(1,0)} + T_{23}^{(0,0)}\ x_0 = \psi_1^{(0,1)} - \psi_3^{(1,0)} + \psi_3^{(0,0)}\ x_0 \tag{7.55}$$
$$T_{23}^{(0,0)} = \psi_3^{(0,0)} \tag{7.56}$$

Equations (7.47)-(7.51) constitute a system of five differential equations of the second order whose natural boundary conditions are represented by Eqs. (7.52) -(7.56) in the following five unknowns

$$u_2 \quad \beta \quad g \quad \theta \quad h \tag{7.57}$$

7.3.1   Euler-Bernoulli equilibrium equations

In this section the equlibrium equations with respect to the Euler-Bernoulli model are reported. Substituting Eqs. (7.15) -(7.16) in Eq. (7.24), one has

$$\int_{\mathcal{B}} \Sigma \cdot \mathrm{Grad}\ \delta \mathbf{u} = \int_0^l \int_{\mathcal{A}(x_2)} \left\{ \sigma_{22} \left[\delta u_{2,2} + x_3 \left(-\delta h_{,22} - (x_0\ \delta\theta)_{,22} \right) \right. \right.$$
$$+ \left. \left. x_3\ x_1\ \delta\theta_{,22} \right] + \sigma_{12}\ 2\ x_3\ \delta\theta_{,2} \right\} d\mathcal{A}\ dx_2 \tag{7.58}$$

Using the definitions in Eq. (7.25) and performing a double integration by parts one has

$$
\begin{aligned}
\int_{\mathcal{B}} \Sigma \cdot \operatorname{Grad} \delta \mathbf{u} \;=\;& \int_0^l \left\{ -T_{22,2}^{(0,0)} \, \delta u_2 - \left(-T_{22,22}^{(1,1)} + x_0 \, T_{22,22}^{(0,1)} + 2 \, T_{12,2}^{(0,1)} \right) \, \delta\theta \right. \\
& \left. - \; T_{22,22}^{(0,1)} \, \delta h \right\} dx_2 + \left[T_{22}^{(0,0)} \, \delta u_2 - T_{22}^{(0,1)} \, \delta h_{,2} - T_{22}^{(0,1)} \, x_{0,2} \, \delta\theta - T_{22}^{(0,1)} \, x_0 \, \delta\theta_{,2} \right. \\
& \left. + \; T_{22,2}^{(0,1)} \, (\delta h + x_0 \, \delta\theta) + T_{22}^{(1,1)} \, \delta\theta_{,2} - T_{22,2}^{(1,1)} \, \delta\theta + 2 \, T_{12}^{(0,1)} \, \delta\theta \right]_0^l \qquad (7.59)
\end{aligned}
$$

Similarly, for the work done by the external body forces, substituting Eqs. (7.15) -(7.16) in Eq. (7.34) and using Eq. (7.32), yields

$$
\begin{aligned}
\int_{\mathcal{B}} \rho \, \mathbf{H} \cdot \delta \mathbf{u} \;=\;& \int_0^l \left\{ F_2^{(0,0)} \, \delta u_2 + \left(F_1^{(0,1)} + F_{2,2}^{(0,1)} \, x_0 - F_{2,2}^{(1,1)} - F_3^{(1,0)} + x_0 \, F_3^{(0,0)} \right) \, \delta\theta \right. \\
& \left. + \; \left(F_3^{(0,0)} + F_{2,2}^{(0,1)} \right) \, \delta h \right\} dx_2 - \left[F_2^{(0,1)} \, \delta h + \left(F_2^{(0,1)} \, x_0 - F_2^{(1,1)} \right) \, \delta\theta \right]_0^l (7.60)
\end{aligned}
$$

For the kinetic energy virtual variation one has to modify the acceleration components in Eqs. (7.29)-(7.63) according to Eqs. (7.19) - (7.21)

$$
\ddot{u}_1 = x_3 \, \ddot{\theta} \tag{7.61}
$$

$$
\ddot{u}_2 = \ddot{u}_2 + x_3 \, \left(-\ddot{h} - x_0 \, \ddot{\theta} \right)_{,2} + x_1 \, x_3 \, \ddot{\theta}_{,2} \tag{7.62}
$$

$$
\ddot{u}_3 = \ddot{h} - (x_1 - x_0) \, \ddot{\theta} \tag{7.63}
$$

substituting these equations in Eq. (7.34) yields

$$
\begin{aligned}
\int_{\mathcal{B}} \rho \, \ddot{\mathbf{u}} \cdot \delta \mathbf{u} \;=\;& \int_0^l \left\{ \left[I^{(0,0)} \, \ddot{u}_2 - I^{(0,1)} \, \ddot{h}_{,2} - I^{(0,1)} \left(x_0 \, \ddot{\theta} \right)_{,2} + I^{(1,1)} \ddot{\theta}_{,2} \right] \delta u_2 \right. \\
& + \; \left[I^{(0,2)} \, \ddot{\theta} + \left(I^{(0,1)} \, \ddot{u}_2 \right)_{,2} x_0 - \left(I^{(1,1)} \, \ddot{u}_2 \right)_{,2} - \left(I^{(0,2)} \, \ddot{h}_{,2} \right)_{,2} x_0 \right. \\
& + \; \left(I^{(1,2)} \, \ddot{h}_{,2} \right)_{,2} - \left(I^{(0,2)} \left(x_0 \, \ddot{\theta} \right)_{,2} \right)_{,2} x_0 + \left(I^{(1,2)} \left(x_0 \, \ddot{\theta} \right)_{,2} \right)_{,2} \\
& + \; \left(I^{(1,2)} \, \ddot{\theta}_{,2} \right)_{,2} x_0 - \left(I^{(2,2)} \, \ddot{\theta}_{,2} \right)_{,2} - I^{(1,0)} \, \ddot{h} + I^{(0,0)} \, x_0 \, \ddot{h} \\
& + \; I^{(2,0)} \, \ddot{\theta} - 2 \, I^{(1,0)} \, x_0 \, \ddot{\theta} + I^{(0,0)} \, x_0^2 \right] \delta\theta
\end{aligned}
$$

$$+ \left[\left(I^{(0,1)}\ \ddot{u}_2 \right)_{,2} - \left(I^{(0,2)}\ \ddot{h}_{,2} \right)_{,2} - \left(I^{(0,2)}\ \left(x_0\ \ddot{\theta} \right)_{,2} \right)_{,2} + \right.$$

$$+ \ \left(I^{(1,2)}\ \ddot{\theta}_{,2} \right)_{,2} + I^{(0,0)}\ \ddot{h} - I^{(1,0)}\ \ddot{\theta} + I^{(0,0)}\ x_0\ \ddot{\theta} \Big]\ \delta h$$

$$+ \ \left[-I^{(0,1)}\ \ddot{u}_2\ (\delta h + x_0\ \delta\theta) + I^{(1,1)}\ \ddot{u}_2\ \delta\theta + I^{(0,2)}\ \ddot{h}_{,2}\ (\delta h + x_0\ \delta\theta) - I^{(1,2)}\ \ddot{h}_{,2}\ \delta\theta \right.$$

$$+ \ I^{(0,2)}\ \left(x_0\ \ddot{\theta} \right)_{,2}\ (\delta h + x_0\ \delta\theta) - I^{(1,2)}\ \left(x_0\ \ddot{\theta} \right)_{,2}\ \delta\theta$$

$$- \ I^{(1,2)}\ \ddot{\theta}_{,2}\ (\delta h + x_0\ \delta\theta) + I^{(2,2)}\ddot{\theta}_{,2}\ \delta\theta \Big]_0^l \tag{7.64}$$

Finally, considering the work done by the surface tractions, Eq. (7.212), it can be noted that the two first integrals, using Eq. (7.44), can be recast as

$$\int_{\mathcal{S}_u \cup \mathcal{S}_l} \mathbf{t}^A \cdot \delta\mathbf{u} \ = \ \int_0^l \left(\mathcal{L}\ \delta h - \mathcal{M}\ \delta\theta + \mathcal{L}\ x_0\ \delta\theta \right) dx_2$$

$$+ \ \int_0^l \left[\phi_2^{(0,0)}\ \delta u_2 + \left(\phi_1^{(0,1)} + \phi_{2,2}^{(0,1)}\ x_0 - \phi_2^{(1,1)} - \phi_3^{(1,0)} + \phi_3^{(0,0)}\ x_0 \right) \delta\theta \right.$$

$$+ \ \left(\phi_{2,2}^{(0,1)} + \phi_3^{(0,0)} \right)\ \delta h \Big]\ dx_2 - \left[\phi_2^{(0,1)}\ \delta h + \left(\phi_2^{(0,1)}\ x_0 - \phi_2^{(1,1)} \right)\ \delta\theta \right]_0^l \tag{7.65}$$

Similarly for the third integral one has

$$\int_{\mathcal{S}_r} \mathbf{t}^A \cdot \delta\mathbf{u} \ = \ \psi_2^{(0,0)}\ \delta u_2 + \left(\psi_1^{(0,1)} - \psi_3^{(1,0)} + \psi_3^{(0,0)}\ x_0 \right) \delta\theta$$

$$+ \ \psi_3^{(0,0)}\ \delta h - \psi_2^{(0,1)}\ \delta h_{,2} - \psi_2^{(0,1)}\ (x_0\ \delta\theta)_{,2} + \psi_2^{(1,1)}\ \delta\theta_{,2} \tag{7.66}$$

Collecting all the terms one obtains a system of three differential equations

$$\delta v_2: \quad T_{22,2}^{(0,0)} + F_2^{(0,0)} - \left[I^{(0,0)}\ \ddot{u}_2 - I^{(0,1)}\ \ddot{h}_{,2} - I^{(0,1)}\ \left(x_0\ \ddot{\theta} \right)_{,2} + I^{(1,1)}\ddot{\theta}_{,2} \right] + \phi_2^{(0,0)} = 0 \tag{7.67}$$

$$\delta\theta: \quad \left(-T_{22,22}^{(1,1)} + x_0\ T_{22,22}^{(0,1)} + 2\ T_{12,2}^{(0,1)} \right) + F_1^{(0,1)} - F_{2,2}^{(0,1)}\ x_0 - F_{2,2}^{(1,1)} + F_3^{(1,0)} + x_0\ F_3^{(0,0)}$$

$$- \left[I^{(0,2)}\ \ddot{\theta} + \left(I^{(0,1)}\ \ddot{u}_2 \right)_{,2}\ x_0 - \left(I^{(1,1)}\ \ddot{u}_2 \right)_{,2} - \left(I^{(0,2)}\ \ddot{h}_{,2} \right)_{,2}\ x_0 \right.$$

$$+ \left(I^{(1,2)}\ \ddot{h}_{,2} \right)_{,2} - \left(I^{(0,2)}\ \left(x_0\ \ddot{\theta} \right)_{,2} \right)_{,2}\ x_0 + \left(I^{(1,2)}\ \left(x_0\ \ddot{\theta} \right)_{,2} \right)_{,2}$$

$$+ \left(I^{(1,2)}\ \ddot{\theta}_{,2} \right)_{,2}\ x_0 - \left(I^{(2,2)}\ \ddot{\theta}_{,2} \right)_{,2} - I^{(1,0)}\ \ddot{h} + I^{(0,0)}\ x_0\ \ddot{h}$$

$$+ I^{(2,0)}\ \ddot{\theta} - 2\ I^{(1,0)}\ x_0\ \ddot{\theta} + I^{(0,0)}\ x_0^2 \Big]$$

$$+ \phi_1^{(0,1)} + \phi_{2,2}^{(0,1)}\ x_0 - \phi_2^{(1,1)} - \phi_3^{(1,0)} + \phi_3^{(0,0)}\ x_0 - \mathcal{M} + \mathcal{L}\ x_0 = 0 \tag{7.68}$$

$$\delta h : \quad T_{22,22}^{(0,1)} + F_3^{(0,0)} + F_{2,2}^{(0,1)} - \left[\left(I^{(0,1)} \, \ddot{u}_2 \right)_{,2} - \left(I^{(0,2)} \, \ddot{h}_{,2} \right)_{,2} - \left(I^{(0,2)} \, \left(x_0 \, \ddot{\theta} \right)_{,2} \right)_{,2} + \right.$$

$$\left. + \left(I^{(1,2)} \, \ddot{\theta}_{,2} \right)_{,2} + I^{(0,0)} \, \ddot{h} - I^{(1,0)} \, \ddot{\theta} + I^{(0,0)} \, x_0 \, \ddot{\theta} \right] + \phi_{2,2}^{(0,1)} + \phi_3^{(0,0)} = 0 \qquad (7.69)$$

7.4   Thermo-elastic constitutive equations

As it is apparent from the definition of the Hamiltonian functional in Eq. (7.22), we are not dealing with a coupled thermo-elastic problem, but we are admitting that the temperature distribution is not affected by the actual deformation of the structure. For this reason the temperature will enter into the problem by means of the constitutive relations. In particular, in the frame-work of linear thermo-elasticity one may refer to the Hooke-Duhamhel constitutive equation. Using a tensorial notation this relation reads

$$\mathbf{E} = \mathbb{F} \, \Sigma + \mathbf{A} \, T \qquad (7.70)$$

where $\mathbb{F}$ is the material flexibility tensor, whereas $\mathbf{A}$ is the tensor of thermal expansion coefficients. An inverted expression of Eq. (7.70) is

$$\Sigma = \mathbb{C} \, \mathbf{E} - \mathbf{B} \, T \qquad (7.71)$$

where $\mathbb{C}$ is the material compliance (or stiffness) tensor and $\mathbf{B}$ is related to $\mathbf{A}$ by means of the following relation

$$\mathbf{B} = \mathbb{C} \, \mathbf{A} \qquad (7.72)$$

Restricting ourselves to the case of monoclinic material and using a compact notation, Eq. (7.71) can be written

$$\left\{ \begin{array}{c} \sigma_1 \\ \sigma_2 \\ \sigma_3 \\ \sigma_4 \\ \sigma_5 \\ \sigma_6 \end{array} \right\} = \left[\begin{array}{cccccc} C_{11} & C_{12} & C_{13} & 0 & 0 & C_{16} \\ C_{12} & C_{22} & C_{23} & 0 & 0 & C_{26} \\ C_{13} & C_{23} & C_{33} & 0 & 0 & C_{36} \\ 0 & 0 & 0 & C_{44} & C_{45} & 0 \\ 0 & 0 & 0 & C_{45} & C_{55} & 0 \\ C_{16} & C_{26} & C_{36} & 0 & 0 & C_{66} \end{array} \right] \left\{ \begin{array}{c} \varepsilon_1 \\ \varepsilon_2 \\ \varepsilon_3 \\ \varepsilon_4 \\ \varepsilon_5 \\ \varepsilon_6 \end{array} \right\} - \left\{ \begin{array}{c} \beta_1 \\ \beta_2 \\ \beta_3 \\ 0 \\ 0 \\ \beta_6 \end{array} \right\} T \qquad (7.73)$$

where use has been made of the material symmetry hypothesis with respect to the plane $x_3 = 0$ in order to conclude that

$$\alpha_4 = \alpha_5 = 0 \qquad \text{and} \qquad C_{\alpha 4} = C_{\alpha 5} = C_{64} = C_{65} = 0 \qquad (7.74)$$

It is worth noting that in the compact notation here used, the shear strain components $(\varepsilon_4, \varepsilon_5, \varepsilon_6)$ and the coefficient of thermal expansion (α_6) are equal to two times their tensorial counterpart, *i.e.,*

$$\varepsilon_4 = 2\varepsilon_{23} = \gamma_{23} \tag{7.75}$$

$$\varepsilon_5 = 2\varepsilon_{13} = \gamma_{13} \tag{7.76}$$

$$\varepsilon_6 = 2\varepsilon_{12} = \gamma_{12} \tag{7.77}$$

$$\alpha_6 = 2\alpha_{12} \tag{7.78}$$

For future reference, it is useful to explicit Eq. (7.72) using a compact notation

$$\beta_1 = C_{11}\,\alpha_1 + C_{12}\,\alpha_2 + C_{13}\,\alpha_3 + C_{16}\,\alpha_6 \tag{7.79}$$

$$\beta_2 = C_{21}\,\alpha_1 + C_{22}\,\alpha_2 + C_{23}\,\alpha_3 + C_{26}\,\alpha_6 \tag{7.80}$$

$$\beta_3 = C_{31}\,\alpha_1 + C_{32}\,\alpha_2 + C_{33}\,\alpha_3 + C_{36}\,\alpha_6 \tag{7.81}$$

$$\beta_6 = C_{61}\,\alpha_1 + C_{62}\,\alpha_2 + C_{63}\,\alpha_3 + C_{66}\,\alpha_6 \tag{7.82}$$

Now let us introduce the following hypothesis

$$O\left(\sigma_{33}\right) \ll O\left(\sigma_{ij}\right) \qquad for \;\; i,j \neq 3 \tag{7.83}$$

then, from Eq. (7.71) one has

$$\varepsilon_3 = -\frac{C_{3\alpha}}{C_{33}}\varepsilon_\alpha - \frac{C_{36}}{C_{33}}\varepsilon_6 + \frac{\beta_3}{C_{33}}T \tag{7.84}$$

substituting Eq. (7.84) in Eq. (7.73) yields

$$\begin{Bmatrix} \sigma_1 \\ \sigma_2 \\ \sigma_6 \\ \sigma_4 \\ \sigma_5 \end{Bmatrix} = \begin{bmatrix} Q_{11} & Q_{12} & Q_{16} & 0 & 0 \\ Q_{12} & Q_{22} & Q_{26} & 0 & 0 \\ Q_{16} & Q_{26} & Q_{66} & 0 & 0 \\ 0 & 0 & 0 & Q_{44} & Q_{45} \\ 0 & 0 & 0 & Q_{45} & Q_{55} \end{bmatrix} \begin{Bmatrix} \varepsilon_1 \\ \varepsilon_2 \\ \varepsilon_6 \\ \varepsilon_4 \\ \varepsilon_5 \end{Bmatrix} - \begin{Bmatrix} \gamma_1 \\ \gamma_2 \\ \gamma_6 \\ 0 \\ 0 \end{Bmatrix} T \tag{7.85}$$

where

$$Q_{\alpha\beta} = \frac{C_{\alpha\beta}C_{33} - C_{\alpha3}C_{3\beta}}{C_{33}} \tag{7.86}$$

$$Q_{\alpha6} = \frac{C_{\alpha6}C_{33} - C_{\alpha3}C_{36}}{C_{33}} \tag{7.87}$$

$$Q_{66} = \frac{C_{66}C_{33} - C_{63}C_{36}}{C_{33}} \tag{7.88}$$

$$Q_{44} = Q_{55} = C_{44} \tag{7.89}$$

$$Q_{45} = C_{45} \tag{7.90}$$

$$\gamma_{\alpha} = \frac{\beta_{\alpha}C_{33} - C_{\alpha3}\beta_3}{C_{33}} \tag{7.91}$$

$$\gamma_6 = \frac{\beta_6 C_{33} - C_{63}\beta_3}{C_{33}} \tag{7.92}$$

It is worth noting that, introducing the hypothesis (7.83), yields to a loss of information in terms of the transverse thermal expansion coefficient, that is from Eqs. (7.91) and (7.79) - (7.82) one obtains

$$\gamma_{\alpha} = \beta_{\alpha} - \frac{C_{\alpha3}}{C_{33}}\beta_3 = Q_{\alpha\beta}\ \alpha_\beta + Q_{\alpha6}\ \alpha_6 \tag{7.93}$$

$$\gamma_6 = \beta_6 - \frac{C_{63}}{C_{33}}\beta_3 = Q_{6\beta}\ \alpha_\beta + Q_{66}\ \alpha_6 \tag{7.94}$$

from which it is apparent the independence from the transverse thermal expansion coefficient (α_3).

7.4.1   Composite structure

In this section the problem of composite laminated structure, of which the wing is assumed to be composed, will be addressed. Specifically, we will assume the wing composed of N laminae of monoclinic material each of thickness $t^{(k)}$ so that the thickness of the wing, at a certain location, is

$$t\,(x_1, x_2) = \sum_{k=1}^{N} t^{(k)}\,(x_1, x_2) \tag{7.95}$$

Let us now express the stress resultants defined in eq. (7.25) in terms of the strains using Eqs. (7.85) and (7.95)

$$T_i^{(m,n)} = \int_{LE(x_2)}^{TE(x_2)} x_1^m \left[\sum_{k=1}^{N} \int_{t_l(x_1,x_2)}^{t_u(x_1,x_2)} \left(Q_{ip}^{(k)}\ \varepsilon_p + \gamma_i^{(k)}\ T \right)\ x_3^n\ dx_3 \right] dx_1 \tag{7.96}$$

where use has been made of a compact notation also for the stress resultants. With the help of Eqs. (7.9) - (7.14) one may write

$$\varepsilon_p = a_p\left(x_2\right) + x_1\, b_p\left(x_2\right) + x_3\, c_p\left(x_2\right) + x_1\, x_3\, d_p\left(x_2\right) \tag{7.97}$$

thus

$$\sum_{k=1}^{N} \int_{t_l(x_1,x_2)}^{t_u(x_1,x_2)} \left(Q_{ip}^{(k)}\, \varepsilon_p + \gamma_i^{(k)}\, T\right)\, x_3^n\, dx_3 = A_{ip}^{(n)}\left(x_1,x_2\right)\left(a_p + x_1\, b_p\right)$$
$$+ A_{ip}^{(n+1)}\left(x_1,x_2\right)\left(c_p + x_1\, d_p\right) - \vartheta_i^{(n)}\left(x_1,x_2\right) \tag{7.98}$$

where, by definition,

$$A_{ip}^{(n)}\left(x_1,x_2\right) := \sum_{k=1}^{N} \int_{t_l(x_1,x_2)}^{t_u(x_1,x_2)} Q_{ip}^{(k)}\, x_3^n\, dx_3 \tag{7.99}$$

$$\vartheta_i^{(n)}\left(x_1,x_2\right) := \sum_{k=1}^{N} \int_{t_l(x_1,x_2)}^{t_u(x_1,x_2)} \gamma_i^{(k)}\, T\left(x_1,x_2,x_3,t\right)\, x_3^n\, dx_3 \tag{7.100}$$

Integrating over x_1, one has

$$T_i^{(m,n)} = B_{ip}^{(m,n)}\, a_p + B_{ip}^{(m+1,n)}\, b_p + B_{ip}^{(m,n+1)}\, c_p + B_{ip}^{(m+1,n+1)}\, d_p - \Theta_i^{(m,n)} \tag{7.101}$$

where, by definition,

$$B_{ip}^{(m,n)}\left(x_2\right) := \int_{LE(x_2)}^{TE(x_2)} x_1^m\, A_{ip}^{(n)}\, dx_1 \tag{7.102}$$

$$\Theta_i^{(m,n)}\left(x_2\right) := \int_{LE(x_2)}^{TE(x_2)} x_1^m\, \vartheta_i^{(n)}\, dx_1 \tag{7.103}$$

Let us now specialize these results to the present model. Using Eqs. (7.9) - (7.14) one has

$$
\begin{array}{ll}
a_1 = 0 & b_1 = 0 \\
a_2 = u_{2,2} & b_2 = 0 \\
a_6 = 0 & b_6 = 0 \\
a_4 = \beta + h_{,2} + \left(x_0\, \theta\right)_{,2} & b_4 = g - \theta_{,2} \\
a_5 = 0 & b_5 = 0
\end{array}
$$

$$
\begin{aligned}
c_1 &= 0 & d_1 &= 0 \\
c_2 &= \beta_{,2} & d_2 &= g_{,2} \\
c_6 &= g + \theta_{,2} & d_6 &= 0 \\
c_4 &= 0 & d_4 &= 0 \\
c_5 &= 0 & d_5 &= 0
\end{aligned}
\tag{7.104}
$$

With the help of the previous Equations, one may explicitly express the integral stress resultants which appear in the equilibrium equations

$$
T_2^{(0,0)} = B_{22}^{(0,0)}\, u_{2,2} + B_{22}^{(0,1)}\, \beta_{,2} + B_{26}^{(0,1)}\, (g + \theta_{,2}) + B_{22}^{(1,1)}\, g_{,2} - \Theta_2^{(0,0)} \tag{7.105}
$$

$$
T_2^{(0,1)} = B_{22}^{(0,1)}\, u_{2,2} + B_{22}^{(0,2)}\, \beta_{,2} + B_{26}^{(0,2)}\, (g + \theta_{,2}) + B_{22}^{(1,2)}\, g_{,2} - \Theta_2^{(0,1)} \tag{7.106}
$$

$$
T_2^{(1,1)} = B_{22}^{(1,1)}\, u_{2,2} + B_{22}^{(1,2)}\, \beta_{,2} + B_{26}^{(1,2)}\, (g + \theta_{,2}) + B_{22}^{(2,2)}\, g_{,2} - \Theta_2^{(1,1)} \tag{7.107}
$$

$$
T_4^{(0,0)} = B_{44}^{(0,0)}\, \left(\beta + h_{,2} + (x_0\,\theta)_{,2}\right) + B_{44}^{(1,0)}\, (g - \theta_{,2}) \tag{7.108}
$$

$$
T_4^{(1,0)} = B_{44}^{(1,0)}\, \left(\beta + h_{,2} + (x_0\,\theta)_{,2}\right) + B_{44}^{(2,0)}\, (g - \theta_{,2}) \tag{7.109}
$$

$$
T_6^{(0,1)} = B_{62}^{(0,1)}\, u_{2,2} + B_{62}^{(0,2)}\, \beta_{,2} + B_{66}^{(0,2)}\, (g + \theta_{,2}) + B_{62}^{(1,2)}\, g_{,2} - \Theta_6^{(0,1)} \tag{7.110}
$$

For convenient reference to the original works on this model ([104, 58, 59, 60, 45, 44, 46, 47]) let us introduce the following relations

$$
\begin{aligned}
B_{22}^{(0,0)} &= \bar{A}_{22} & B_{44}^{(0,0)} &= \bar{A}_{44} & B_{44}^{(1,0)} &= \bar{\bar{A}}_{44} & B_{44}^{(2,0)} &= \bar{\bar{\bar{A}}}_{44} & B_{22}^{(0,1)} &= \bar{B}_{22} \\
B_{22}^{(1,1)} &= \bar{\bar{B}}_{22} & B_{26}^{(0,1)} &= \bar{B}_{26} & B_{22}^{(0,2)} &= \bar{D}_{22} & B_{22}^{(1,2)} &= \bar{\bar{D}}_{22} & B_{22}^{(2,2)} &= \bar{\bar{\bar{D}}}_{22} \\
B_{26}^{(0,2)} &= \bar{D}_{26} & B_{26}^{(1,2)} &= \bar{\bar{D}}_{26} & B_{26}^{(2,2)} &= \bar{\bar{\bar{D}}}_{26} & B_{66}^{(0,2)} &= \bar{D}_{66}
\end{aligned}
\tag{7.111}
$$

Using Eqs. (7.111), the replacement of Eqs. (7.105) - (7.110) in Eqs. (7.47) - (7.51) leads to the following system of equilibrium equations in the basic unknown ((7.57)

$$
\left(\bar{A}_{22}\, u_{2,2}\right)_{,2} + \left(\bar{B}_{22}\, \beta_{,2}\right)_{,2} + \left(\bar{B}_{26}\, g\right)_{,2} + \left(\bar{B}_{26}\, \theta_{,2}\right)_{,2} + \left(\bar{\bar{B}}_{22}\, g_{,2}\right)_{,2}
$$
$$
- \Theta_{2,2}^{(0,0)} + F_2^{(0,0)} - I^{(0,0)}\, \ddot{u}_2 - I^{(0,1)}\, \ddot{f}_2 - I^{(1,1)}\, \ddot{g}_2 = 0 \tag{7.112}
$$

$$
\left(\bar{B}_{22}\, u_{2,2}\right)_{,2} + \left(\bar{D}_{22}\, \beta_{,2}\right)_{,2} + \left(\bar{D}_{26}\, g\right)_{,2} + \left(\bar{D}_{26}\, \theta_{,2}\right)_{,2} + \left(\bar{\bar{D}}_{22}\, g_{,2}\right)_{,2}
$$
$$
- \bar{A}_{44}\, \beta - \bar{A}_{44}\, h_{,2} - \bar{A}_{44}\, (x_0\,\theta)_{,2} - \bar{\bar{A}}_{44}\, g + \bar{\bar{A}}_{44}\, \theta_{,2}
$$
$$
- \Theta_{2,2}^{(0,1)} + F_2^{(0,1)} - I^{(0,1)}\, \ddot{u}_2 - I^{(0,2)}\, \ddot{f}_2 - I^{(1,2)}\, \ddot{g}_2 = 0 \tag{7.113}
$$

$$\left(\bar{\bar{B}}_{22}\, u_{2,2}\right)_{,2} + \left(\bar{\bar{D}}_{22}\, \beta_{,2}\right)_{,2} + \left(\bar{\bar{D}}_{26}\, g\right)_{,2} + \left(\bar{\bar{D}}_{26}\, \theta_{,2}\right)_{,2} + \left(\bar{\bar{\bar{D}}}_{22}\, g_{,2}\right)_{,2}$$

$$-\bar{\bar{A}}_{44}\, \beta - \bar{\bar{A}}_{44}\, h_{,2} - \bar{\bar{A}}_{44}\, (x_0\, \theta)_{,2} - \bar{\bar{\bar{A}}}_{44}\, g + \bar{\bar{\bar{A}}}_{44}\, \theta_{,2}$$

$$-\bar{B}_{26}\, u_{2,2} - \bar{D}_{26}\, \beta_{,2} - \bar{D}_{66}\, g - \bar{D}_{66}\, \theta_{,2} - \bar{\bar{D}}_{26}\, g_{,2}$$

$$-\Theta_{2,2}^{(1,1)} + \Theta_{12}^{(0,1)} + F_2^{(1,1)} - I^{(1,1)}\, \ddot{u}_2 - I^{(1,2)}\, \ddot{f}_2 - I^{(2,2)}\, \ddot{g}_2 = 0 \qquad (7.114)$$

$$\left(\bar{B}_{26}\, u_{2,2}\right)_{,2} + \left(\bar{D}_{26}\, \beta_{,2}\right)_{,2} + \left(\bar{D}_{66}\, g\right)_{,2} + \left(\bar{D}_{66}\, \theta_{,2}\right)_{,2} + \left(\bar{\bar{D}}_{26}\, g_{,2}\right)_{,2}$$

$$-\left(\bar{\bar{A}}_{44}\, \beta\right)_{,2} - \left(\bar{\bar{A}}_{44}\, h_{,2}\right)_{,2} - \left(\bar{\bar{A}}_{44}\, (x_0\, \theta)_{,2}\right)_{,2} - \left(\bar{\bar{\bar{A}}}_{44}\, g\right)_{,2} + \left(\bar{\bar{\bar{A}}}_{44}\, \theta_{,2}\right)_{,2}$$

$$+\left[\left(\bar{A}_{44}\, \beta\right)_{,2} + \left(\bar{A}_{44}\, h_{,2}\right)_{,2} + \left(\bar{A}_{44}\, (x_0\, \theta)_{,2}\right)_{,2} + \left(\bar{\bar{A}}_{44}\, g\right)_{,2} - \left(\bar{\bar{A}}_{44}\, \theta_{,2}\right)_{,2}\right]\, x_0$$

$$-\Theta_6^{(0,1)} + F_1^{(0,1)} - F_3^{(1,0)} + F_3^{(0,0)}\, x_0 - \left(I^{(0,2)} + I^{(2,0)} - 2\, I^{(1,0)}\, x_0 + I^{(0,0)}\, x_0^2\right)\, \ddot{\theta}$$

$$+\left(I^{(1,0)} - I^{(0,0)}\, x_0\right)\, \ddot{h} - \mathcal{M} + \mathcal{L}\, x_0 = 0 \qquad (7.115)$$

$$\left(\bar{A}_{44}\, \beta\right)_{,2} + \left(\bar{A}_{44}\, h_{,2}\right)_{,2} + \left(\bar{A}_{44}\, (x_0\, \theta)_{,2}\right)_{,2} + \left(\bar{\bar{A}}_{44}\, g\right)_{,2} - \left(\bar{\bar{A}}_{44}\, \theta_{,2}\right)_{,2}$$

$$+F_3^{(0,0)} - I^{(0,0)}\, \ddot{h} + \left(I^{(1,0)} - I^{(0,0)}\, x_0\right)\, \ddot{\theta} + \mathcal{L} = 0 \qquad (7.116)$$

Similarly, for the boundary conditions in terms of the basic unknown one has

$$B_{22}^{(0,0)}\, u_{2,2} + B_{22}^{(0,1)}\, \beta_{,2} + B_{26}^{(0,1)}\, (g + \theta_{,2}) + B_{22}^{(1,1)}\, g_{,2} - \Theta_2^{(0,0)} = \psi_2^{(0,0)} \qquad (7.117)$$

$$B_{22}^{(0,1)}\, u_{2,2} + B_{22}^{(0,2)}\, \beta_{,2} + B_{26}^{(0,2)}\, (g + \theta_{,2}) + B_{22}^{(1,2)}\, g_{,2} - \Theta_2^{(0,1)} = \psi_2^{(0,1)} \qquad (7.118)$$

$$B_{22}^{(1,1)}\, u_{2,2} + B_{22}^{(1,2)}\, \beta_{,2} + B_{26}^{(1,2)}\, (g + \theta_{,2}) + B_{22}^{(2,2)}\, g_{,2} - \Theta_2^{(1,1)} = \psi_2^{(1,1)} \qquad (7.119)$$

$$B_{62}^{(0,1)}\, u_{2,2} + B_{62}^{(0,2)}\, \beta_{,2} + B_{66}^{(0,2)}\, (g + \theta_{,2}) + B_{62}^{(1,2)}\, g_{,2} - \Theta_6^{(0,1)}$$

$$-B_{44}^{(1,0)}\, \left(\beta + h_{,2} + (x_0\, \theta)_{,2}\right) - B_{44}^{(2,0)}\, (g - \theta_{,2})$$

$$+\left[B_{44}^{(0,0)}\, \left(\beta + h_{,2} + (x_0\, \theta)_{,2}\right) + B_{44}^{(1,0)}\, (g - \theta_{,2})\right]\, x_0$$

$$= \psi_1^{(0,1)} - \psi_3^{(1,0)} + \psi_3^{(0,0)}\, x_0 \qquad (7.120)$$

$$B_{44}^{(0,0)}\, \left(\beta + h_{,2} + (x_0\, \theta)_{,2}\right) + B_{44}^{(1,0)}\, (g - \theta_{,2}) = \psi_3^{(0,0)} \qquad (7.121)$$

From Eqs. (7.112)-(7.121) it is apparent that in this modeling the thermal effect is treated in the same manner as an external load. Moreover, the temperature enters into the problem both from the equilibrium equations and from the boundary conditions.

7.5   Case study

In this section the previous model will be particularized to the case of a rectangular single-layered and transversely isotropic wing subjected to a laser heating in a incompressible, inviscid flow.

7.5.1   Transverse isotropy

For a transversely isotropic material, in the frame-work of linear thermo-elasticity, the number of material coefficients to be determined experimentally is seven. Nonetheless, by means of the assumption contained in Eq. (7.83) and of the following considerations, one can recognize that the number of thermo-elastic coefficients to assigned are only four, specifically, one has

$$Q_{11} = Q_{22} = \frac{E}{1 - \nu^2} \tag{7.122}$$

$$Q_{12} = \frac{E\,\nu}{1 - \nu^2} \tag{7.123}$$

$$Q_{66} = \frac{E}{2\,(1 + \nu)} \tag{7.124}$$

$$Q_{44} = Q_{55} = G' \tag{7.125}$$

$$\gamma_1 = \gamma_2 = \frac{E}{1 - \nu}\alpha \tag{7.126}$$

where E, ν, α are, respectively, the Young modulus, the Poisson modulus and the coefficient of thermal expansion in the plane of isotropy, whereas G' is the transverse shear modulus. It is remarkable that, as already stated in Eqs. (7.93)-(7.94), any dependence from the transversal coefficient of thermal expansion has been lost introducing the assumption of Eq. (7.83). Nonetheless, it should be noted that in order to recover this material dependence the constraint of inextensibility along the thickness should be relaxed.

7.5.2   Single layered rectangular wing

The introduction of the hypothesis that the wing is composed of a single layer of transverse isotropic material, simplify considerably the model. In particular it is found that

$$t_l \neq t_l\,(x_1, x_2) \qquad t_u \neq t_u\,(x_1, x_2) \tag{7.127}$$

$$LE \neq LE\,(x_2) \qquad TE \neq TE\,(x_2) \tag{7.128}$$

Because we are dealing with a rectangular, single-layered wing it is reasonable to choose the origin of the coordinate axes in the center of the cross section. With this choice and the following definitions

$$t_l = -\bar{h}/2 \qquad t_u = \bar{h}/2 \tag{7.129}$$

$$LE = -c/2 \qquad TE = c/2 \tag{7.130}$$

one has

$$T_2^{(0,0)} = c\,\bar{h}\,Q_{22}\,u_{2,2} - \Theta_2^{(0,0)} \tag{7.131}$$

$$T_2^{(0,1)} = \frac{c\,\bar{h}^3}{12}\,Q_{22}\,\beta_{,2} - \Theta_2^{(0,1)} \tag{7.132}$$

$$T_2^{(1,1)} = \frac{c^3\,\bar{h}^3}{144}\,Q_{22}\,g_{,2} - \Theta_2^{(1,1)} \tag{7.133}$$

$$T_4^{(0,0)} = c\,\bar{h}\,Q_{44}\,(\beta + h_{,2}) \tag{7.134}$$

$$T_4^{(1,0)} = \frac{c^3\,\bar{h}}{12}\,Q_{44}\,(g - \theta_{,2}) \tag{7.135}$$

$$T_6^{(0,1)} = \frac{c\,\bar{h}^3}{12}\,Q_{66}\,(g + \theta_{,2}) \tag{7.136}$$

Similarly, let us express the non-zero inertial terms

$$I^{(0,0)} = \rho\,\bar{h}\,c = m \tag{7.137}$$

$$I^{(0,2)} = \rho\,c\,\frac{\bar{h}^3}{12} = m\frac{\bar{h}^2}{12} \tag{7.138}$$

$$I^{(2,0)} = \rho\,\bar{h}\,\frac{c^3}{12} = m\frac{c^2}{12} \tag{7.139}$$

$$I^{(2,2)} = \rho\,\frac{\bar{h}^3}{12}\frac{c^3}{12} = m\frac{c^2\,\bar{h}^2}{144} \tag{7.140}$$

The equilibrium equations can now be recast in the following way

$$c\,\bar{h}\,Q_{22}\,u_{2,22} - \Theta_{2,2}^{(0,0)} + F_2^{(0,0)} - m\,\ddot{u}_2 = 0 \tag{7.141}$$

$$\frac{c\,\bar{h}^3}{12}\,Q_{22}\,\beta_{,22} - c\,\bar{h}\,Q_{44}\,\beta - c\,\bar{h}\,Q_{44}\,h_{,2} - \Theta_{2,2}^{(0,1)} + F_2^{(0,1)} - m\,\frac{\bar{h}^2}{12}\ddot{f}_2 = 0 \tag{7.142}$$

$$\frac{c^3\,\bar{h}^3}{144}\,Q_{22}\,g_{,22} - \frac{c^3\,\bar{h}}{12}\,Q_{44}\,g + \frac{c^3\,\bar{h}}{12}\,Q_{44}\,\theta_{,2}$$
$$- \frac{c\,\bar{h}^3}{12}\,Q_{66}\,g - \frac{c\,\bar{h}^3}{12}\,Q_{66}\,\theta_{,2} - \Theta_{2,2}^{(1,1)} + F_2^{(1,1)} - m\,\frac{c^2\,\bar{h}^2}{144}\,\ddot{g}_2 = 0 \tag{7.143}$$

$$\frac{c\,\bar{h}^3}{12}\,Q_{66}\,g_{,2} + \frac{c\,\bar{h}^3}{12}\,Q_{66}\,\theta_{,22} - \frac{c^3\,\bar{h}}{12}\,Q_{44}\,g_{,2}$$

$$+\frac{c\,\bar{h}^3}{12}\,Q_{44}\,\theta_{,22} + F_1^{(0,1)} - F_3^{(1,0)} - \mathcal{M} - \frac{m}{12}\,\left(c^2 + \bar{h}^2\right)\,\ddot{\theta}_2 = 0 \qquad (7.144)$$

$$c\,\bar{h}\,Q_{44}\,\beta_{,22} - c\,\bar{h}\,Q_{44}h_{,22} + F_3^{(0,0)} - m\,\ddot{h} + \mathcal{L} = 0 \qquad (7.145)$$

where, because of the hypotheses on the geometry and of the location of the reference axes, one may assume $x_0 = 0$. Similarly, for the boundary conditions one has

$$c\,\bar{h}\,Q_{22}\,u_{2,2} - \Theta_2^{(0,0)} = 0 \qquad (7.146)$$

$$\frac{c\,\bar{h}^3}{12}\,Q_{22}\,\beta_{,2} - \Theta_2^{(0,1)} = 0 \qquad (7.147)$$

$$\frac{c^3\,\bar{h}^3}{144}\,Q_{22}\,g_{,2} - \Theta_2^{(1,1)} = 0 \qquad (7.148)$$

$$\left(\bar{h}^2\,Q_{66} - c^2\,Q_{44}\right)g + \left(\bar{h}^2\,Q_{66} + c^2\,Q_{44}\right)\theta_{,2} = 0 \qquad (7.149)$$

$$\beta + h_{,2} = 0 \qquad (7.150)$$

where a free-end condition at the right side of the wing (i.e., $\psi_i^{(m,n)} = 0$) has been assumed.

It is worth noting that the dynamics of the wing in its plane is independent of the the other dynamics and so one may solve two separated problems involving one (u_2) and four (β, g, θ, h) independent unknowns respectively. Moreover, it is apparent that the thermal loads appear only in the first three equilibrium equations and boundary conditions. These are the equations related to arbitrary variations of the displacement in the span-wise direction and of the warping. Thus, it can be concluded that, as already stated with respect to the thickness inextensibility constraint, the discard of this effect (i.e., the introduction of unshearable constraint) would translate in a loss of information, specifically, of thermo-mechanical coupling.

7.6   Thermal excitation

As it was stated in the Introduction, the case of a laser beam impacting the upper surface of the wing is considered. Mathematically the problem may be stated in terms of the following system of equations[17, 22, 116, 13]

$$\text{Div}\,(\mathbf{K}\nabla T) - \rho c_t \frac{\partial T}{\partial t} = 0 \qquad \text{for } \mathbf{x} \in \mathcal{B},\ t \in \mathcal{T} \qquad (7.151)$$

$$\mathbf{K}\nabla T \cdot \mathbf{n} = \mathbf{q} \cdot \mathbf{n} \qquad \text{for } \mathbf{x} \in \mathcal{S}_U,\ t \in \mathcal{T} \qquad (7.152)$$

$$\nabla T \cdot \mathbf{n} = 0 \qquad \text{for } \mathbf{x} \in \partial\mathcal{B}/\mathcal{S}_U,\ t \in \mathcal{T} \qquad (7.153)$$

$$T = 0 \qquad \text{for } \mathbf{x} \in \partial\mathcal{B},\ t = 0 \qquad (7.154)$$

where $T(\mathbf{x}, t)$ is the temperature field, $\mathbf{K}$ is the thermal conductivity tensor,[20] c_t is the specific heat, $\mathbf{n}$ is the external normal to the surface body and $\mathbf{q}$ is the external heat flux impacting the wing. Because we are dealing with a transversely isotropic thermal conductivity tensor, one has

$$\mathbf{K} := \begin{pmatrix} k_1 & 0 & 0 \\ 0 & k_1 & 0 \\ 0 & 0 & k_3 \end{pmatrix} \tag{7.155}$$

Using the following co-ordinate transformation

$$x := \xi^1 \qquad y := \xi^2 \qquad z := \sqrt{k_1/k_3}\ \xi^3 \tag{7.156}$$

the original problem may be recast in the following form

$$\begin{aligned} k_1 \nabla^2 T - \rho c_t \frac{\partial T}{\partial t} &= 0 & \text{for } \mathbf{x} \in \mathcal{B},\ t \in \mathcal{T} & \tag{7.157} \\ k_1 \nabla T \cdot \mathbf{n} &= \mathbf{q} \cdot \mathbf{n} & \text{for } \mathbf{x} \in \mathcal{S}_U,\ t \in \mathcal{T} & \tag{7.158} \\ \nabla T \cdot \mathbf{n} &= 0 & \text{for } \mathbf{x} \in \partial\mathcal{B}/\mathcal{S}_U,\ t \in \mathcal{T} & \tag{7.159} \\ T &= 0 & \text{for } \mathbf{x} \in \partial\mathcal{B},\ t = 0 & \tag{7.160} \end{aligned}$$

Note that the change of variables defined in Eq. (7.156) is equivalent to a virtual stretch or contraction (depending on the ratio k_1/k_3) of space in the thickness direction (z).

In order to, determine analytically the temperature field within the body, a Green's approach has been performed.[19] Thus, one may associate to the problem in Eqs.(7.157)-(7.160) the following adjoint one

$$\begin{aligned} k_1 \nabla^2 G + \rho c_t \frac{\partial T}{\partial t} &= \delta(\mathbf{x} - \mathbf{x}^*)\delta(t - t^*) & \text{for } \mathbf{x} \in \mathcal{B},\ t \in \mathcal{T} & \tag{7.161} \\ \nabla G \cdot \mathbf{n} &= 0 & \text{for } \mathbf{x} \in \partial\mathcal{B} & \tag{7.162} \\ G &= 0 & \text{for } \mathbf{x} \in \mathcal{B},\ t = \hat{t} & \tag{7.163} \end{aligned}$$

where $G(\mathbf{x}, \mathbf{x}^*, t, t^*)$ is the Green's function for the problem under consideration, assumed zero at the final time $(\hat{t})$.

Multiplying Eq. (7.157) by $T(\mathbf{x}, t)$ and Eq. (7.161) by $G(\mathbf{x}, \mathbf{x}^*, t, t^*)$, one has

$$T(\mathbf{x}^*, t^*) = -\int_0^{\hat{t}} \int_{\mathcal{S}_U} \frac{1}{\rho c_t}\ G(\mathbf{x}, \mathbf{x}^*, t, t^*)\ \mathbf{q}(\mathbf{x}, t) \cdot \mathbf{n}(\mathbf{x}, t)\ dS(\mathbf{x})\ dt \tag{7.164}$$

Assuming for the body a rectangular parallelepiped configuration ,*i.e.*,

$$\mathcal{B} = \{(x, y, z)\,\|\,0 \le x \le \bar{x};\ 0 \le y \le \bar{y};\ 0 \le z \le \bar{z}\} \tag{7.165}$$

one obtains the following expression for the Green's function

$$G\left(\mathbf{x}, \mathbf{x}^*, t, t^*\right) \;=\; -\sum_{l,m,n=0}^{\infty} \phi_{lmn}\left(\mathbf{x}\right)\ \phi_{lmn}\left(\mathbf{x}^*\right)\ H\left(t-t^*\right) e^{-\frac{k_1 \lambda_{lmn}}{\rho c_t}\left(t-t^*\right)} \qquad (7.166)$$

where $H\left(t-t^*\right)$ is the Heaviside's function,

$$\phi_{lmn}\left(\mathbf{x}\right) \;=\; \frac{8}{\bar{x}\bar{y}\bar{z}}\ \cos\frac{l\pi x}{\bar{x}}\ \cos\frac{m\pi y}{\bar{y}}\ \cos\frac{n\pi z}{\bar{z}} \qquad (7.167)$$

are the eigenfunctions of the Laplacian operator for this problem, and λ_{lmn} are the corresponding eigenvalues

$$\lambda_{lmn} \;=\; -\left(\frac{l^2\pi^2}{\bar{x}} + \frac{m^2\pi^2}{\bar{y}} + \frac{n^2\pi^2}{\bar{z}}\right) \qquad (7.168)$$

Note that using the above expressions the temperature field in Eq. (7.164) may be recast as

$$T\left(\mathbf{x}^*, t^*\right) \;=\; \sum_{l,m,n=0}^{\infty} \frac{\phi_{lmn}\left(\mathbf{x}^*\right)}{\rho c_t} \int_0^{\bar{x}} \int_0^{\bar{y}} \phi_{lmn}\left(\mathbf{x}\right) \int_0^{t^*} e^{-\frac{k_1 \lambda_{lmn}}{\rho c_t}\left(t-t^*\right)}\ \mathbf{q}\left(\mathbf{x}, t\right) \cdot \mathbf{n}\left(\mathbf{x}, t\right)\ dt\ dy\ dx$$

Finally, from Eq. (7.169) it is apparent that one can established for the temperature field a relationship with the Lagrangean coordinates chosen for representing the displacement field and thus obtain a closed-loop system between the thermal field and the displacement one. Specifically, chosen a system of material coordinate on the upper surface of the wing, which may be considered coincident with the Cartesian ones in the linear approximation, one has

$$\mathbf{n}\left(\mathbf{x}, t\right) \;:=\; \frac{\mathbf{g}_1 \times \mathbf{g}_2}{\|\mathbf{g}_1 \times \mathbf{g}_2\|} = \frac{\left(\overset{\circ}{\mathbf{g}}_1 + \dfrac{\partial \mathbf{u}}{\partial \xi^1}\right) \times \left(\overset{\circ}{\mathbf{g}}_2 + \dfrac{\partial \mathbf{u}}{\partial \xi^2}\right)}{\|\mathbf{g}_1 \times \mathbf{g}_2\|} \qquad (7.169)$$

where $\mathbf{g}_\alpha := \partial \mathbf{x}/\partial \xi^\alpha$ are the tangent base vectors at the material coordinates on the surface. Choosing a system of Cartesian coordinate coincident with that depicted in Fig. (7.1) and performing a linearization one has

$$\mathbf{n}\left(\mathbf{x}, t\right) \;\cong\; \mathbf{e}_3 - h_{,2}\left(y, t\right) \mathbf{e}_2 + \theta\left(y, t\right) \mathbf{e}_1 \qquad (7.170)$$

Substituting Eq. (7.170) into Eq. (7.169) one may express the temperature field as the sum of three contributions

$$T\left(\mathbf{x}^*, t^*\right) \;=\; T_1\left(\mathbf{x}^*, t^*\right) + T_2\left(\mathbf{x}^*, t^*\right) + T_3\left(\mathbf{x}^*, t^*\right) \qquad (7.171)$$

where

$$T_1\left(\mathbf{x}^*, t^*\right) = \sum_{l,m,n=0}^{\infty} \frac{\phi_{lmn}\left(\mathbf{x}^*\right)}{\rho c_t} \int_0^{\bar{x}} \int_0^{\bar{y}} \phi_{lmn}\left(\mathbf{x}\right) \int_0^{t^*} e^{-\frac{k_1 \lambda_{lmn}}{\rho c_t}(t-t^*)} q_1\left(\mathbf{x}, t\right) \theta\left(y, t\right) \, dt \, dy \, dx$$

$$T_2\left(\mathbf{x}^*, t^*\right) = -\sum_{l,m,n=0}^{\infty} \frac{\phi_{lmn}\left(\mathbf{x}^*\right)}{\rho c_t} \int_0^{\bar{x}} \int_0^{\bar{y}} \phi_{lmn}\left(\mathbf{x}\right) \int_0^{t^*} e^{-\frac{k_1 \lambda_{lmn}}{\rho c_t}(t-t^*)} q_2\left(\mathbf{x}, t\right) h_{,2}\left(y, t\right) \, dt \, dy \, dx$$

$$T_3\left(\mathbf{x}^*, t^*\right) = \sum_{l,m,n=0}^{\infty} \frac{\phi_{lmn}\left(\mathbf{x}^*\right)}{\rho c_t} \int_0^{\bar{x}} \int_0^{\bar{y}} \phi_{lmn}\left(\mathbf{x}\right) \int_0^{t^*} e^{-\frac{k_1 \lambda_{lmn}}{\rho c_t}(t-t^*)} q_3\left(\mathbf{x}, t\right) \, dt \, dy \, dx$$

For a visual illustration of our reasoning in Fig. (7.2) a snapshot of the deformed configuration
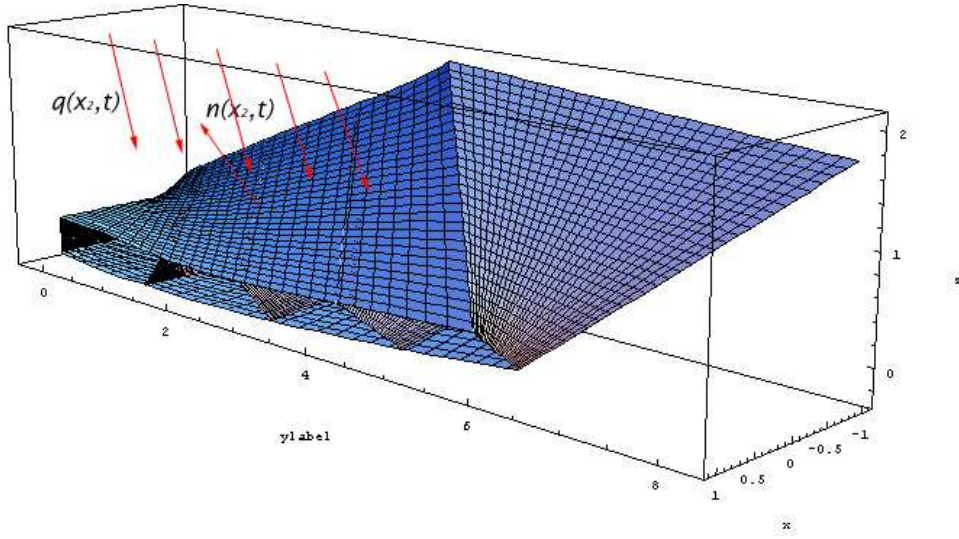
Figure 7.2: Deformed configuration of the wing structure exposed to an external heat flux.

of the wing structure considered in the applications is reported. Here the laser beam is simbolized by a set of arrows $\left(\mathbf{q}\left(\xi^2, t\right)\right)$ whereas the normal is denoted by $\mathbf{n}\left(\xi^2, t\right)$.

It is worth noting that Eqs. (7.172)-(7.172) may be seen as convolutions of the Lagrangean variables θ and h respectively with respect to time, and convolutions and correlations with respect to space. Nonetheless, explicit solutions of these integrals cannot be found, and in order to include the thermoelastic feedback one could solve iteratively the displacement problem due to a thermal input like T_3 which does not depend on $\mathbf{u}$, then obtain T_1 and T_2 by direct integration.

7.7 Aerodynamic loads

In this section the aerodynamic loads generated by the incompressible flow field over the wing, taking into account the effect of the sweep angle, are reported and discussed. The formulation used here is analogous to that employed by Theodorsen [105] and reported in Bisplinghoff et al. [16] but including the effect of the sweep angle as developed in [70]. The first step in the consideration of

an aerodynamic load over a body is to define the boundary condition on its surface. Specifically, it is assumed the surface to be impermeable, that means the relative velocity with which the fluid particle hits the body has normal component to its surface equal to zero, this requirement translates in the following relation

$$\left(\mathbf{v}_{air} - \mathbf{v}_{body} \right) \cdot \mathbf{n} = 0 \tag{7.172}$$

where the air speed is measured in a rigid frame attached to the center of mass of the plane, and thus[†]

$$\mathbf{v}_{air} = U_\infty \mathbf{c}_1 + \nabla \varphi \tag{7.173}$$

whereas the velocity of the body is simply the derivative with respect to time of the displacement field

$$\mathbf{v}_{body} = \frac{\partial \mathbf{u}}{\partial t} \tag{7.174}$$

and the normal to the external surface of the body can be expressed

$$\mathbf{n} = \frac{\mathbf{g}_1 \times \mathbf{g}_2}{\sqrt{g}} = \frac{1}{\sqrt{g}} \left(\overset{\circ}{\mathbf{g}}_1 + \frac{\partial \mathbf{u}}{\partial x_1} \right) \times \left(\overset{\circ}{\mathbf{g}}_2 + \frac{\partial \mathbf{u}}{\partial x_2} \right) \tag{7.175}$$

Substituting Eqs. (7.173)-(7.175) in Eq. (7.172) and retaining only the linear term, one has

$$\frac{\partial \varphi}{\partial n} = \frac{\partial u_3}{\partial t} + U_\infty \frac{\partial u_3}{\partial x_1} \tag{7.176}$$

In order to particularize this equation to the case of a swept wing, the following change of variable is introduced

$$\bar{x}_1 = x_1 \cos \Lambda - x_2 \sin \Lambda \tag{7.177}$$

$$\bar{x}_2 = x_1 \sin \Lambda + x_2 \cos \Lambda \tag{7.178}$$

$$\bar{x}_3 = x_3 \tag{7.179}$$

Recalling that the displacement in the x_3 direction in the rotated frame is

$$u_3 = \bar{u}_3 = h\left(\bar{x}_2, t \right) - \left(\bar{x}_1 - \bar{x}_0 \right)\, \theta\left(\bar{x}_2, t \right) \tag{7.180}$$

[†] Following Podio-Guidugli [87], let $\mathcal{E}$ be a 3-dimensional Euclidean space, let $\mathcal{V}$ be the vector space associated with $\mathcal{E}$ and denote with $\mathcal{U} := \{ \mathbf{v} \in \mathcal{V} | \, \|\mathbf{v}\| = 1 \}$ the sphere of all vectors having unit length. We think of $\mathcal{E}$ as equipped with a Cartesian frame $\{ \mathcal{O}; \mathbf{c}_1, \mathbf{c}_2, \mathbf{c}_3 \}$ with orthogonal basis vectors $\mathbf{c}_i \in \mathcal{U}$ (i= 1, 2, 3); the Cartesian components of a vector $\mathbf{v} \in \mathcal{V}$ are then $v_i := \mathbf{v} \cdot \mathbf{c}_i$ and, in particular, the triplet $(p_1, p_2, p_3) \in \Re^3$, $p_i := \mathbf{p}\left(p \right) \cdot \mathbf{c}_i$, of components of the position vector are the Cartesian coordinates of a point $p \in \mathcal{E}$.

one has

$$\frac{\partial u_3}{\partial t} = \frac{\partial h}{\partial t} - (x - x_0) \frac{\partial \theta}{\partial t} \tag{7.181}$$

$$\frac{\partial u_3}{\partial x} = -\theta \, \cos \Lambda + \frac{\partial h}{\partial y} \, \sin \Lambda - (x - x_0) \frac{\partial \theta}{\partial y} \, \sin \Lambda + \frac{\partial x_0}{\partial y} \, \theta \, \sin \Lambda \tag{7.182}$$

where

$$\bar{x}_1 = x \, , \quad \bar{x}_2 = y \, , \quad \bar{x}_3 = z \tag{7.183}$$

Equation (7.176) can now be written

$$\frac{\partial \varphi}{\partial z} = \dot{h} - (x - x_0) \, \dot{\theta} + U_\infty \cos \Lambda \left[-\theta + (h' - (x - x_0) \, \theta' + x_0' \theta) \tan \Lambda \right] \tag{7.184}$$

The study of thin airfoils oscillating in incompressible flow (developed by Theodorsen [105], and discussed in Bisplinghhoff et al. [16, page 251, sec. 5-6]) yield to the following closed-form solution for the lift and pitching moment due to oscillatory vertical translation and pitching (see [16, page 272, Eqs. (5-311) and (5-312)])

$$\mathcal{L} = \pi \rho b^2 \left[\ddot{h} + U \, \dot{\alpha} - ba \, \ddot{\alpha} \right] + 2\pi \rho U b C \left(k \right) \left[\dot{h} + U\alpha + b \left(\frac{1}{2} - a \right) \dot{\alpha} \right] \tag{7.185}$$

$$\mathcal{M} = \pi \rho b^2 \left[ba\ddot{h} - Ub \left(\frac{1}{2} - a \right) \dot{\alpha} - b^2 \left(\frac{1}{8} + a^2 \right) \ddot{\alpha} \right] +$$

$$+ 2\pi \rho U b^2 \left(a + \frac{1}{2} \right) C \left(k \right) \left[\dot{\alpha} + U\alpha + b \left(\frac{1}{2} - a \right) \dot{\alpha} \right] \tag{7.186}$$

Note that accordingly to Theodorsen's method, the solution is composed of two parts: one, associated with an appropriate distribution of sources and sinks just above and below the line $z = 0$, and represented by the first addenda in Eqs. (7.185) and (7.186), satisfies the boundary condition over the airfoil but produces no circulation and it is so-called the "non-circulatory" part of the lift; the other, produced by a pattern of vortices with countervortices along the wake to infinity is such to fulfill the Kutta's hypothesis without disturbing the boundary condition at the airfoil, and it is associated with the Theodorsen's function ($C \left(k \right)$) in Eqs. (7.185) and (7.186). Moreover, let us note that the terms in brackets which multiply the Theodorsen's function represent the normal velocity of a fluid particle located at three-quartes along the chord (measured from the leading edge), indeed:

$$w_{3/4} = \dot{h} - U_\infty \theta - b \left(\frac{1}{2} - a \right) \dot{\theta} \tag{7.187}$$

where Eq. (7.184) has been employed and $\Lambda = 0$ has been considered. Actually, in Eqs. (7.185) and (7.185) the expressions in brackets are different from Eq. (7.187) because in Bisplinghoff h is positive downward while in Eq. (7.187) and (7.180) another more coherent convention (*i.e.*, positive upward) has been adopted.

Finally, let us note that in Eqs. (7.185) and (7.187), a represents the position of the elastic axis (adimensionalized with respect to the semi-chord) measured from the origin (chosen to be at the middle-chord).

In order to extend the previous model to arbitrary motions of the airfoil, and to include the effect of the sweep angle in a way similar to that adopted by Marzocca et al. [70], let us refer to Bisplinghoff [16, page 282, sec. 5-7] where the loads generated aerodynamically over an airfoil in arbitrary motion is reported. There it is stated that the noncirculatory results are correct regardless the nature of the unsteady motion, so long as it is small. The idea carried on by Wagner in its problem of step change in angle of attack and extended by Kussner for a sharped-edge gust striking the leading edge of the airfoil at $t = 0$, is based on the principle of superposition which is applicable because of the linearity assumed through out the problem. In this sense the circulatory part of the lift per unit span for any Fourier with unit amplitude of $w - 3/4$ is[†]

$$\tilde{\mathcal{L}}_c = -2\pi\rho U b C(k) \tag{7.188}$$

Using the convolution integral in order to express the circulatory part of the lift in the time domain, one has

$$\mathcal{L}_c = -2\pi\rho U b \int_{-\infty}^{t} \phi(t-\tau) \; \frac{\partial w_{3/4}(\tau)}{\partial \tau} \; \tau \tag{7.189}$$

where $\phi(\tau)$ is the Wagner's function given by (see [77, page 195, Eq. (8.85)])

$$\phi(\tau) := \frac{1}{2\pi} \int_{-\infty}^{+\infty} \frac{C(k)}{jk} e^{jk\tau} \; dk \tag{7.190}$$

This function describes the transient of the lift up to its steady value and formally represents the response to the unit step of a system having the Theodorsen's function as transfer function. Equation (7.190) must be specialized for the case of a swept wing substituting Eq. (7.184) in it

$$
\begin{aligned}
\mathcal{L}_c(y,t) \;\; = \;\; & -2\pi\rho U_n b_n \int_{-\infty}^{t} \phi(t-\tau) \left\{ \ddot{h} - b_n \left(\frac{1}{2} - a \right) \ddot{\theta} \right. \\
& + \;\; U_n \left[-\dot{\theta} + \left(\dot{h}' - b_n \left(\frac{1}{2} - a \right) \dot{\theta}' \right) \tan\Lambda \right] \right\} \; d\tau
\end{aligned} \tag{7.191}
$$

[†] These considerations can be alternatively stated using a more systematic point of view and referring to Eq. (7.188) as the transfer function of the lift with respect to $w - 3/4$ as the input.

where it has been assumed the hypothesis $\partial x_0/\partial y = 0$ and also $x = b_n/2$.

Similarly, for the noncirculatory terms, one has (see [16, page 260, Eq. 5-262])

$$
\begin{aligned}
\mathcal{L}_{nc} &= -\int_{-b_n}^{b_n} (p_u - p_l) \ dx \\
&= 2\rho \int_{-b_n}^{b_n} \frac{\partial \varphi_u}{\partial t} \ dx + 2\rho U_n \int_{-b_n}^{b_n} \frac{\partial \varphi_u}{\partial x} \ dx \\
&= 2\rho b_n \frac{\partial}{\partial t} \int_0^\pi \varphi_u \ \sin \beta \ d\beta
\end{aligned}
\tag{7.192}
$$

where

$$
\varphi_u = -\frac{b_n}{\pi} \int_\beta^\pi \int_0^\pi \frac{w \ \sin^2 \gamma \ d\gamma \ d\beta}{\cos \gamma \cos \beta}
\tag{7.193}
$$

Replacing Eq. (7.184) in Eq. (7.193) one has

$$
\varphi_u = b_n \left[-\dot{h} + U_n \left(\theta - h' \tan \Lambda \right) \right] \sin \beta + b_n^2 \left[\dot{\theta} + U_n \tan \Lambda \ \theta' \right] \sin \beta \left(\frac{1}{2} \cos \beta - a \right)
\tag{7.194}
$$

where the following identities have been used

$$
\int_\beta^\pi \int_0^\pi \frac{\sin^2 \gamma \ d\gamma \ d\beta}{\cos \gamma - \cos \beta} = \pi \sin \beta
\tag{7.195}
$$

$$
\int_\beta^\pi \int_0^\pi \frac{(\cos \gamma - a) \sin^2 \gamma \ d\gamma \ d\beta}{\cos \gamma - \cos \beta} = \pi \sin \beta \left(\frac{1}{2} \cos \beta - a \right)
\tag{7.196}
$$

Performing the integral in Eq. (7.192) one has

$$
\mathcal{L}_{nc} = \pi \rho b_n^2 \left[-\ddot{h} + U_n \ \dot{\theta} - b_n a \ \ddot{\theta} - U_n \tan \Lambda \left(\dot{h}' + a b_n \ \dot{\theta}' \right) \right]
\tag{7.197}
$$

Similarly, for the aerodynamic moment one has

$$
\begin{aligned}
\mathcal{M}_{nc} &= \int_{-b_n}^{b_n} (p_u - p_l) \left(x - ba \right) \ dx \\
&= 2\rho b_n U_n \int_0^\pi \varphi_u \ \sin \beta \ d\beta - 2\rho b_n^2 \frac{\partial}{\partial t} \int_0^\pi \varphi_u \ (\cos \beta - a) \sin \beta \ d\beta
\end{aligned}
\tag{7.198}
$$

Performing the integral and the derivation with respect to time one gets

$$
\begin{aligned}
\mathcal{M}_{nc} &= \pi \rho b_n^2 \left[-U_n \dot{h} - b_n a \ddot{h} + U_n^2 \theta - b_n^2 \left(\frac{1}{8} + a^2 \right) \ddot{\theta} \right] \\
&\quad - \pi \rho b_n^2 U_n \left[U_n h' + U_n a b_n \theta' + a b_n \dot{\theta}' + b_n^2 \left(\frac{1}{8} + a^2 \right) \dot{\theta}' \right] \tan \Lambda
\end{aligned}
\tag{7.199}
$$

Note that Eqs. (7.197) and (7.199) reduce to Eqs. (7.185) and (7.186) for $\Lambda = 0$. Note also that to derive Eqs. (7.197) and (7.199) the following results have been considered

$$\int_0^\pi \sin^2 \beta \, d\beta = \frac{\pi}{2} \tag{7.200}$$

$$\int_0^\pi \sin^2 \beta \left(\frac{1}{2} \cos \beta - a \right) d\beta = -a\frac{\pi}{2} \tag{7.201}$$

$$\int_0^\pi \sin^2 \beta \left(\cos \beta - a \right) d\beta = -a\frac{\pi}{2} \tag{7.202}$$

$$\int_0^\pi \sin^2 \beta \left(\frac{1}{2} \cos \beta - a \right) \left(\cos \beta - a \right) d\beta = \frac{\pi}{2} \left(\frac{1}{8} + a^2 \right) \tag{7.203}$$

Grouping the terms of the non-circulatory part of the lift associated with the same order of derivatives and those associated with the sweep angle, one has

$$\mathcal{L}_{nc1} = -\pi\rho b_n^2 \left(\ddot{h} + b_n a \ddot{\theta} \right) \tag{7.204}$$

$$\mathcal{L}_{nc2} = \pi\rho b_n^2 U \dot{\theta} \tag{7.205}$$

$$\mathcal{L}_{nc3} = \pi\rho b_n^2 U \tan \Lambda \left(\dot{h}' + \dot{\theta}' \right) \tag{7.206}$$

similarly, for the aerodynamic moment

$$\mathcal{M}_{nc1} = -\pi\rho b_n^3 \left(a\ddot{h} + b_n \left(\frac{1}{8} + a^2 \right) \ddot{\theta} \right) \tag{7.207}$$

$$\mathcal{M}_{nc2} = -\pi\rho b_n^3 U \dot{h} \tag{7.208}$$

$$\mathcal{M}_{nc3} = \pi\rho b_n^2 U^2 \theta \tag{7.209}$$

$$\mathcal{M}_{nc4} = -\pi\rho b_n^2 U \tan \Lambda \left[U_n h' + U_n a b_n \theta' + a b_n \dot{\theta}' + b_n^2 \left(\frac{1}{8} + a^2 \right) \dot{\theta}' \right] \tag{7.210}$$

In order to include the effect of the finiteness of the wing (*i.e.*, of the three-dimensionality of the flow over it), it is useful to recall that (see, for instance, [11, page 253] and [16, page 250]) there exist some semi-empirical formulas which relate the lift slope for a finite wing to that of its airfoil sections. Specifically, for a finite wing of general planform one has

$$\frac{dC_\mathcal{L}}{d\alpha} := C_{\mathcal{L}_\alpha} \frac{a_0}{1 + (a_0/\pi AR)(1 + \tau)} \tag{7.211}$$

where a_0 is the lift slope of the airfoil, AR is the aspect-ratio of the wing, and τ is a function of the lift distribution over the span. Values of τ typically range between 0.05 and 0.25.

Once that the expression of the lift and of the aerodynamic moment have been obtained as function of the sweep angle and of the aspect ratio, they can be replaced in the equilibrium equations of the flexible wing under consideration. Specifically, recall that the aerodynamic loads in the

Hamilton's equation are

$$\int_{\partial\mathcal{B}} \mathbf{t}^A \cdot \delta\mathbf{u} = \int_{\mathcal{S}_u \cup \mathcal{S}_l} \mathbf{t}^A_{aero} \cdot \delta\mathbf{u} + \int_{\mathcal{S}_u \cup \mathcal{S}_l} \mathbf{t}^A_{mech} \cdot \delta\mathbf{u} + \int_{\mathcal{S}_r} \mathbf{t}^A \cdot \delta\mathbf{u} \tag{7.212}$$

where the first integral is

$$\int_{\mathcal{S}_u \cup \mathcal{S}_l} \mathbf{t}^A_{aero} \cdot \delta\mathbf{u} = \int_0^l (\mathcal{L}\ \delta h + \mathcal{M}\ \delta\theta)\, dx_2 \tag{7.213}$$

and

$$\mathcal{L} := -\int_{LE(x_2)}^{TE(x_2)} \Delta p\,(x_1, x_2, t)\ dx_1 \tag{7.214}$$

$$\mathcal{M} := \int_{LE(x_2)}^{TE(x_2)} \Delta p\,(x_1, x_2, t)\ (x_1 - x_0)\ dx_1 \tag{7.215}$$

where

$$\Delta p\,(x_1, x_2, t) := p_u\,(x_1, x_2, t) - p_l\,(x_1, x_2, t) \tag{7.216}$$

7.8   Solution Procedure

In this Section the solution procedure enabling one to solve the aero-thermo-elastic problem considered in this Chapter, see Eqs. (7.47)–(7.51) is presented. With respect to a rectangular single-layered wing, made of a transversely isotropic material uniformly distributed in the span-wise direction, a number of stiffness quantities (see Eq. (7.102)) vanishes (*i.e.*, $B_{ij}^{(1,n)} = B_{ij}^{(m,1)} = B_{26}^{(m,n)} = 0$). The remaining quantities can be written

$$\begin{array}{lll} B_{22}^{(0,0)} := A\ Q_{22} & B_{22}^{(0,2)} := C_1\ Q_{22} & B_{22}^{(2,2)} := D\ Q_{22} \\ B_{44}^{(0,0)} := A\ Q_{44} & B_{44}^{(2,0)} := C_3\ Q_{44} & B_{66}^{(0,2)} := C_1\ Q_{66} \end{array} \tag{7.217}$$

where A is the area of the cross-section, C_1 and C_3 are the geometric moments of inertia with respect to the chord-wise and thickness direction, and D is the warping rigidity, respectively given by

$$\begin{array}{ll} A := \int_{-b}^{b} \int_{-d/2}^{d/2} d\xi^3\ d\xi^1 & C_1 := \int_{-b}^{b} \int_{-d/2}^{d/2} \xi^{3^2}\ d\xi^3\ d\xi^1 \\[4mm] C_3 := \int_{-b}^{b} \xi^{1^2} \int_{-d/2}^{d/2} d\xi^3\ d\xi^1 & D := \int_{-b}^{b} \xi^{1^2} \int_{-d/2}^{d/2} \xi^{3^2}\ d\xi^3\ d\xi^1 \end{array} \tag{7.218}$$

Moreover, Q_{22}, Q_{44}, and Q_{66} are the nonzero elastic coefficients, which, for a transversely isotropic material, can be written

$$Q_{22} := \frac{E}{1 - \nu^2} \qquad\qquad Q_{44} := G' \qquad\qquad Q_{66} := \frac{E}{2\,(1 + \nu)} \qquad (7.219)$$

Using the previous expressions, the governing equations Eqs. (7.47)–(7.51) are recast in a suitable compact form by using the following set of unknowns

$$y_1 := u_2 \qquad y_2 := \beta \qquad y_3 := g \qquad y_4 := \theta \qquad y_5 := h \qquad (7.220)$$

Substituting Eqs. (7.217)-(7.220) into Eqs. (7.105)-(7.110) and then in the equilibrium equations (Eqs. (7.47)-(7.51)) one has

$$\mathsf{K}\mathsf{y}'' + \mathsf{L}\mathsf{y}' + \mathsf{P}\mathsf{y} + \mathsf{M}\ddot{\mathsf{y}} = \mathsf{f}^A + \mathsf{f}^T + \mathsf{f}^M \qquad (7.221)$$

where K, L, P are the stiffness matrices whose expression is reported in Appendix C, whereas f^A is the vector of aerodynamic loads, f^T is the vector of thermal load and f^M is the vector of mechanical loads resulting from the external time-dependent loads acting on the wing during the operational flight of the flight vehicle (*e.g.*, explosive blast loads). In particular, using Eqs. (7.220) into Eqs. (7.185)-(7.186) one has

$$\mathsf{f}^A\left(\mathsf{y}, \dot{\mathsf{y}}, \ddot{\mathsf{y}}, \mathsf{y}', \dot{\mathsf{y}}', \tau, \xi^2\right) = \begin{Bmatrix} 0 \\ 0 \\ 0 \\ \mathcal{M} \\ \mathcal{L} \end{Bmatrix} = \mathsf{A}\,\ddot{\mathsf{y}} + \mathsf{B}\,\dot{\mathsf{y}} + \mathsf{C}\,\mathsf{y}' + \mathsf{D}\,\dot{\mathsf{y}}' + \mathsf{E}\int_0^\tau \varphi\left(\tau - \hat{\tau}\right)\ddot{\mathsf{y}}\left(\hat{\tau}\right)\,d\hat{\tau}$$

$$+\mathsf{F}\int_0^\tau \varphi\left(\tau - \hat{\tau}\right)\dot{\mathsf{y}}\left(\hat{\tau}\right)\,d\hat{\tau} \quad + \quad \mathsf{G}\int_0^\tau \varphi\left(\tau - \hat{\tau}\right)\dot{\mathsf{y}}'\left(\hat{\tau}\right)\,d\hat{\tau} \qquad (7.222)$$

where the matrices A, B, C, D, E, F, and G, whose expressions are reported in Appendix C, are obtained comparing Eq. (7.222) with Eqs. (7.188)-(7.216). The boundary conditions, associated to Eq. (7.221) and obtained performing the same transformations on Eqs. (7.52)-(7.56), at the root ($\xi^2 = 0$) and the tip ($\xi^2 = l = \xi_{tip}^2$), are

$$\mathsf{y}\left(0, \tau\right) = 0 \qquad\qquad (7.223)$$

$$\mathsf{R}\,\mathsf{y}'\left(\xi_{tip}^2, \tau\right) + \mathsf{S}\,\mathsf{y}\left(\xi_{tip}^2, \tau\right) = \mathsf{c}\left(\tau\right) \qquad\qquad (7.224)$$

Note that in c are contained the thermal moments, which, for the particular temperature distribution considered in the application, enters into the problem just only through the boundary

conditions.[†]

Performing the Laplace transform with respect to time on Eqs. (7.221)-(7.224) and assuming zero initial conditions one has

$$\mathsf{K}\tilde{\mathsf{y}}'' + \tilde{\mathsf{N}}\left(s, U_n\right)\tilde{\mathsf{y}}' + \tilde{\mathsf{Q}}\left(s, U_n\right)\tilde{\mathsf{y}} = -\tilde{\mathsf{f}}^T - \tilde{\mathsf{f}}^M \tag{7.225}$$

where the tilde (̃) denotes Laplace transform with respect to time, s is the time counterpart in the Laplace domain, and

$$\tilde{\mathsf{N}}\left(s, U_n\right) \quad := \quad \mathsf{L} - \mathsf{C} - s\,\mathsf{D} - s\,\tilde{\varphi}\,\mathsf{G} \tag{7.226}$$
$$\tilde{\mathsf{Q}}\left(s, U_n\right) \quad := \quad \mathsf{P} + s^2\left(\mathsf{M} - \mathsf{A} - \tilde{\varphi}\,\mathsf{E}\right) - s\left(\mathsf{B} + \tilde{\varphi}\,\mathsf{F}\right) \tag{7.227}$$

where $\tilde{\varphi}$ is the Laplace transform of the Wagner's function and it is given by

$$\tilde{\varphi} \quad := \quad L_\tau\left[\varphi\left(\tau\right)\right] = \frac{C\left(s\right)}{s} \tag{7.228}$$

Performing the Laplace transform with respect to space, and denoting with the upper bar (̄) the corresponding Laplace transform quantities, and recalling that the wing is considered to be clamped at the root (that is for $y = 0$), one has

$$\bar{\tilde{\mathsf{y}}}\left(p, s\right) = \left[p^2\mathsf{K} + p\tilde{\mathsf{N}}\left(s, U_n\right) + \tilde{\mathsf{Q}}\left(s, U_n\right)\right]^{-1}\left[-\bar{\tilde{\mathsf{f}}}^T\left(p, s\right) - \bar{\tilde{\mathsf{f}}}^M\left(p, s\right) + \mathsf{K}\tilde{\mathsf{y}}'\left(0, s\right)\right] \tag{7.229}$$

where p is the space counterpart in the Laplace domain.

Let us define

$$\bar{\tilde{\mathsf{H}}}\left(p, s, U_n\right) := \left[p^2\mathsf{K} + p\tilde{\mathsf{N}}\left(s, U_n\right) + \tilde{\mathsf{Q}}\left(s, U_n\right)\right]^{-1} \tag{7.230}$$

which can be regarded, a part the boundary conditions, as the aeroelastic operator. Thus Eq. (7.229) may be cast as

$$\bar{\tilde{\mathsf{y}}}\left(p, s\right) = -\bar{\tilde{\mathsf{H}}}\left(p, s, U_n\right)\left[\bar{\tilde{\mathsf{f}}}^T\left(p, s\right) + \bar{\tilde{\mathsf{f}}}^M\left(p, s\right)\right] + \bar{\tilde{\mathsf{H}}}\left(p, s, U_n\right)\mathsf{K}\tilde{\mathsf{y}}'\left(0, s\right) \tag{7.231}$$

Performing the inverse Laplace transform with respect to space one has

$$\tilde{\mathsf{y}}\left(\xi^2, s\right) = -\int_0^{\xi^2}\tilde{\mathsf{H}}\left(\eta, s\right)\tilde{\mathsf{f}}\left(\xi^2 - \eta, s\right)\,d\eta + \tilde{\mathsf{H}}\left(\xi^2, s\right)\mathsf{K}\tilde{\mathsf{y}}'\left(0, s\right) \tag{7.232}$$

[†] Indeed, in the applications the external heat flux has been assumed uniformly distributed on the wing surface depending only on time, whereas the elastic feedback in the temperature expression has not been considered.

Let us introduce the following definition for the convolution integral

$$\tilde{g}\left(\xi^2, s\right) := -\int_0^{\xi^2} \tilde{H}\left(\eta, s\right)\tilde{f}\left(\xi^2 - \eta, s\right)\ d\eta \tag{7.233}$$

Thus

$$\tilde{y}\left(\xi^2, s\right) = \tilde{g}\left(\xi^2, s\right) + \tilde{H}\left(\xi^2, s\right)K\tilde{y}'\left(0, s\right) \tag{7.234}$$

and

$$\tilde{y}'\left(\xi^2, s\right) = \tilde{g}'\left(\xi^2, s\right) + \tilde{H}'\left(\xi^2, s\right)K\tilde{y}'\left(0, s\right) \tag{7.235}$$

The boundary conditions at the tip (Eq. (7.224)) are

$$R\left[\tilde{g}'\left(\xi_{tip}^2, s\right) + \tilde{H}'\left(\xi_{tip}^2, s\right)K\tilde{y}'\left(0, s\right)\right] + S\left[\tilde{g}\left(\xi_{tip}^2, s\right) + \tilde{H}\left(\xi_{tip}^2, s\right)K\tilde{y}'\left(0, s\right)\right] = \tilde{c} \tag{7.236}$$

thus

$$\tilde{y}'\left(0, s\right) = \left[R\ \tilde{H}'\left(\xi_{tip}^2, s\right)K + S\tilde{H}\left(\xi_{tip}^2, s\right)K\right]^{-1}\left[\tilde{c} - \left(R\tilde{g}'\left(\xi_{tip}^2, s\right) + S\tilde{g}\left(\xi_{tip}^2, s\right)\right)\right] \tag{7.237}$$

Finally, the solution vector, in the Laplace domain (with respect to time), may be written

$$
\begin{aligned}
\tilde{y}\left(\xi^2, s\right) \ = \ & -\int_0^{\xi^2}\tilde{H}\left(\eta, s\right)\tilde{f}\left(\xi^2 - \eta, s\right)\ d\eta + \tilde{H}\left(\xi^2, s\right) \\
& \left[R\tilde{H}'\left(\xi_{tip}^2, s\right) + S\tilde{H}\left(\xi_{tip}^2, s\right)\right]^{-1}\left[\tilde{c} - \left(R\tilde{g}'\left(\xi_{tip}^2, s\right) + S\tilde{g}\left(\xi_{tip}^2, s\right)\right)\right]
\end{aligned}
\tag{7.238}
$$

It is worth to point out that, considering Eq. (7.238), the solution of the problem depends of the convolution integral of the external load (distributed along the span) with the transfer function of the system (H) and on the loads applied at the tip (c).

7.9   Numerical results

In this section the results concerning the aeroelastic response of a single-layered, uniform, rectangular, swept wing are presented and discussed. The results have been divided into two parts: one for the validation of the model and its features with respect to Goland's one;[48, 49, 58, 67] and another with regard to the aerothermoelastic response. In the first part, the dynamic characteristics of the Goland's wing in terms of Frequency Response Functions (FRFs), and, dynamic aeroelastic stability analysis are presented. This analysis is developed comparing the different behaviour of the FW and WR models respectively. In the second part, after an introduction on the hypotheses

and assumptions of the external heat flux, and of the assumed material properties, it is shown and discussed the effect on the laser beam on the aeroelasticity of the wing. Specifically, chosen as reference configuration that of the straight wing with warping restraint included, the time histories of the plunging and pitching degrees of freedom, due to the considered thermal excitation, are reported and discussed with special emphasis on the effects of the transverse isotropy of the material constituents, sweep angle, transverse shear flexibility, heat flux time variation and flight speed.

7.9.1   Model validation

The configuration, introduced by Goland in Ref. [48], has been considered as reference configuration for the validation of the present model. Consistently the following geometrical and dynamical characteristics have been assumed

$$
\begin{array}{lll}
l = 6.096\ m & b_n = 0.9144\ m & a = -1/3 \\
x_{cg} = .2b_n & \omega_{1,b} = 50\ rad/s & \omega_{1,t} = 87\ rad/s
\end{array}
\tag{7.239}
$$

where l is the mid-span, b_n the mid-chord measured normally to the trailing edge, a is the non-dimensional distance between the aerodynamic center and the elastic center, and x_{cg} is the distance between the center of gravity and the elastic center of the wing, whereas, $\omega_{1,h}$ and $\omega_{1,t}$ are respectively the first uncoupled bending and torsion angular frequencies of the wing. Using the previous numerical data, the dynamics and aeroelastic stability analysis of the free to warp and warping restraint models (FW and WR) considered in the theoretical section of this Chapter have been solved separately. Specifically, Fig. 7.3 shows the FRFs for the pitch and plunge degrees of freedom

(a) Pitch

(b) Plunge
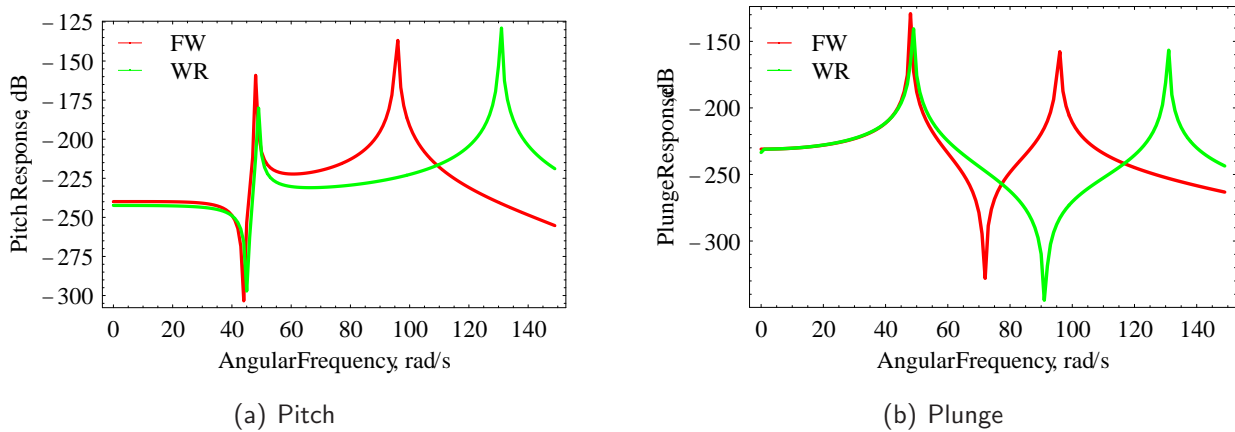
Figure 7.3: FRFs of the FW and WR models.

for the FW and WR models. It can be observed that the consideration of the warping restriction affects mainly the first torsion frequency, which is increased from the original 95.68 rad/s of the FW coupled model to the 130.75 rad/s of the WR coupled model, but not the bending one, which is slightly increased from the original 48.12 rad/s of the FW coupled model to the 48.78 rad/s of the

WR coupled model, a result which is expectable due to the constrained nature of this model. The effect of the transverse shear flexibility in terms of the first bending and torsion angular frequencies for the two models is reported in Tab. 7.1 The aeroelastic stability analysis is reported in Figs.

Table 7.1: Transverse shear flexibility effect on the first bending and torsional frequencies (rad/s).

$R\ (:= E/G')$	$\omega_{1,b}^{FW}$	$\omega_{1,b}^{WR}$	$\omega_{1,t}^{FW}$	$\omega_{1,t}^{WR}$
0.	48.12	48.78	95.68	130.75
20.	46.52	47.05	93.33	119.20
40.	45.05	45.49	91.14	110.58
60.	43.72	44.06	89.10	103.88
80.	42.47	42.75	87.21	98.52
100.	41.35	41.56	85.41	94.12

7.4-7.5 in terms of the frequency response functions and in Fig. 7.6 in terms of the determinant of

(a) Pitch (b) Plunge
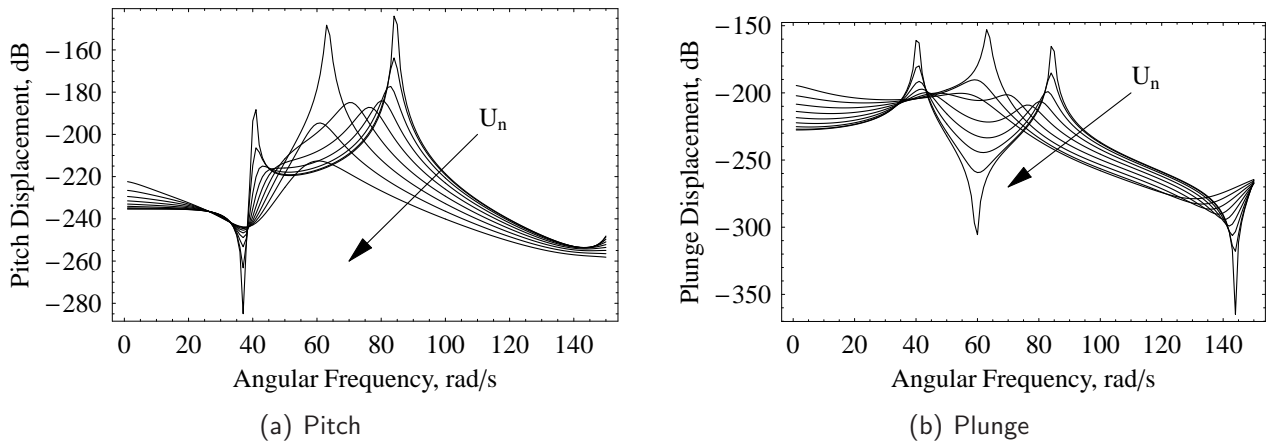
Figure 7.4: FRFs of the FW model for varying flight speeds.

(a) Pitch (b) Plunge
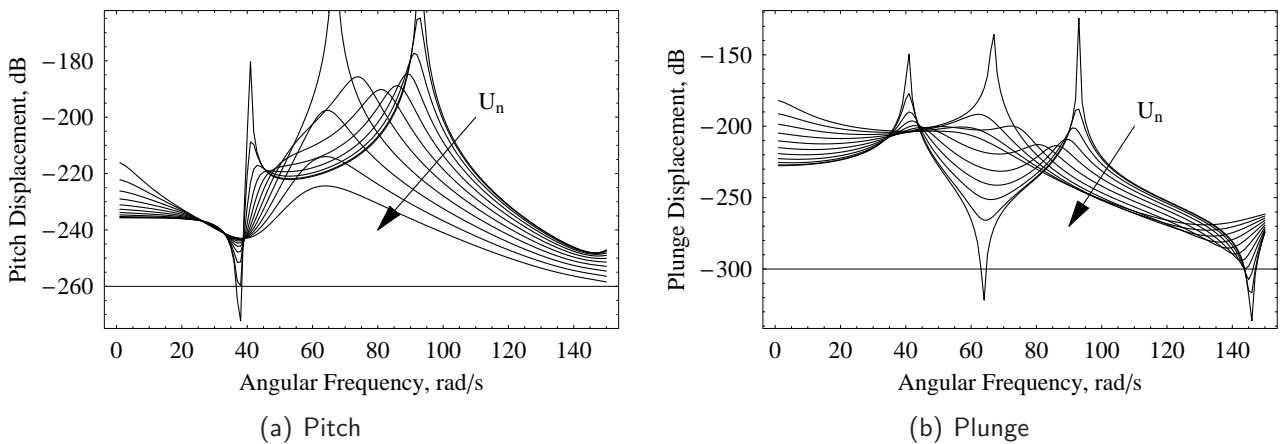
Figure 7.5: FRFs of the WR model for varying flight speeds.

29th May 2005

(a) Free warping model

(b) Warping restraint model
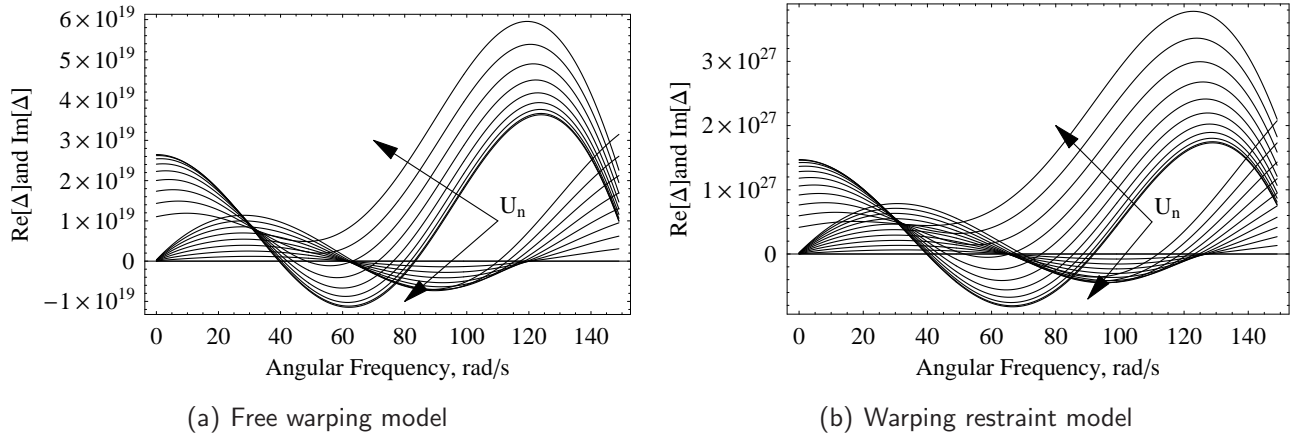
Figure 7.6: $\Re\left[\Delta\left(\omega\right)\right]$ and $\Im\left[\Delta\left(\omega\right)\right]$ for $0 \leq U_n \leq 240 \text{ m/s}$. Free warping model and warping model

the inverse of the aeroelastic operator (see Eq. 7.238) evaluated on the imaginary axis, that is

$$
\Delta\left(j\,\omega, U_n\right) \quad := \quad \text{Det}\left[\text{R}\tilde{\text{H}}'\left(\xi_{tip}^2, j\,\omega, U_n\right)\text{K} + \text{S}\tilde{\text{H}}\left(\xi_{tip}^2, j\,\omega, U_n\right)\text{K}\right] \tag{7.240}
$$

In particular, in Fig. 7.6 the real and imaginary parts of the Δ are plotted for several flight speed, accordingly, the flutter instability can be determined when $\Re\left[\Delta\right]$ and $\Im\left[\Delta\right]$ are simultaneously zero. It is worth noting that also the divergence speed (or static aeroelastic instability) can be identified from these graphs: specifically, in Figs. 7.4-7.5 the divergence corresponds to the flight speed at which the FRF tends to infinity at zero frequency, whereas in Fig. 7.6 the static instability can be found when the real and imaginary parts are equal to zero at zero frequency.

In order to evaluate the effect of the transverse shear flexibility on the aeroelastic behaviour of the two models in Tab. 7.2 the flutter speeds and angular frequencies of the FW and WR

Table 7.2: Transverse shear flexibility effect on the flutter speed (m/s) and angular frequency (rad/s).

$R\ (:= E/G')$	$U_{Flutter}^{FW}$	$U_{Flutter}^{WR}$	$\omega_{Flutter}^{FW}$	$\omega_{Flutter}^{WR}$
0.	136.0	204.9	70.08	86.17
20.	133.0	184.1	68.09	79.94
40.	129.5	168.7	66.47	75.18
60.	127.0	156.7	64.80	71.40
80.	124.5	147.3	63.22	68.31
100.	122.0	139.6	61.82	65.71

models for various transverse shear flexibility ratios are reported.[†] It is worth noting that the flutter instability appears, in both considered wing models, essentially in the torsional mode, and that the WR model is more stable than the FW one. This is due to the fact that the warping restraint on

---

[†] The present results are identical to those already obtained by Karpouzian and Librescu in Refs. [58, 59, 60] even using a different solution procedure.

the root cross-section introduces torsion stiffness into the model so that the wing becomes more rigid in twist. Opposite considerations apply with respect to the transverse shear flexibility effect; in particular, from Tabs. 7.1-7.2, it can be observed that the increase of the flexibility ratio yields an attenuation of the warping rigidity such that the WR model for $R = 100$ is almost aeroelastically equivalent to the FW unshareable (*i.e.*, for $R = 0$) model.

7.9.2   Aerothermoelastic response

In this subsection the aerothermoelastic response of the uniform rectangular wing, considered in the previous section, and exposed to a time-depending laser beam, is presented. It is worth noting that in our case the thermal excitation enters into the problem by means only of the boundary conditions due to the cancellations of the thermal moments in the equilibrium equations when an un-coupled formulation is considered and to the consideration of a uniform distribution of the external heat flux along the span-wise direction. Indeed, in spite of Eqs. 7.172-7.172, where the temperature field has been related to the Lagrangean variables of the system, here, the elastic feedback on the temperature field has not been considered. For this reason the only contribution to the temperature in the body is T_3 which can be re-expressed in the following form

$$T_3\left(\mathbf{x}, t\right) \;\; = \;\; \frac{8 q_{max}}{\rho c_t \bar{z}} \sum_{n=0}^{\infty} \left(-1\right)^n \cos \frac{n \pi z}{\bar{z}} \; e^{-\frac{k_1 n^2 \pi^2}{\rho c_t \bar{z}^2} t} \; \int_0^t e^{\frac{k_1 n^2 \pi^2}{\rho c_t \bar{z}^2} t^*} \; \hat{q}_3\left(t^*\right) \; dt^* \qquad (7.241)$$

where q_{max} is the maximum value of laser power intensity applied as a load (in the following it has been assumed equal to $10^7 \; W/m^2$), and $\hat{q}_3\left(t\right)$ is its time dependence, which in the present applications has been assumed equal to

$$\hat{q}\left(\tau\right) \;\; = \;\; \frac{1}{2}\left(1 - \cos \frac{\tau}{\tau_0}\right) \qquad (7.242)$$

Having in view the previous considerations several aeroelastic analyses have been performed. Specifically, chosen as reference configuration that of a uniform unswept wing incorporating the warping restraint feature (WR model) and the effect of the transverse shear flexibility ($R := E/G' = 100$[58]) the effect of the transverse isotropy of the material constituents, external heat period, flight speed, transverse shear flexibility ratio, and sweep angle has been analysed.

In particular, Fig. 7.7 shows the time and frequency content of the input signal for four different time periods ($\tau_0 = 0.05, 0.1, 0.25, 0.5$ s), whereas Fig. 7.8 shows the FRF of the pitch and plunge degrees of freedom in vacuo in the wide range of angular frequencies chosen to evaluate the time history of the aerothermoelastic response. It can be recognized that only for $\tau_0 = 0.05$ s the external input is capable to excite all the modes of the wing contained in the frequency range, this is not too much surprisingly because, as it is apparent from Fig. 7.7 for $\tau_0 = 0.05 s$ the heat flux is close to a Dirac in the origin.

(a) Time distribution

(b) Frequency spectrum
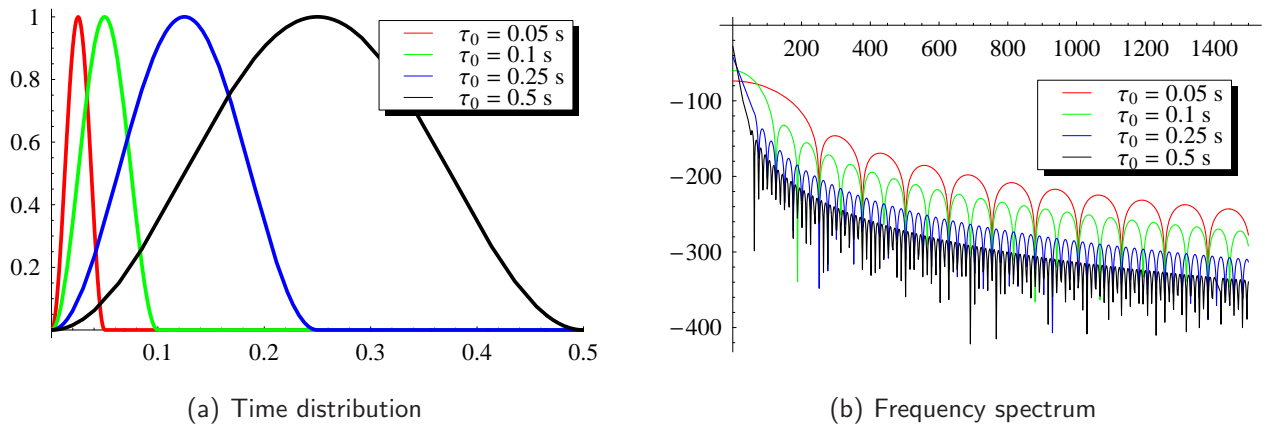
Figure 7.7: Time and Frequency content of the thermal excitation. Free warping model and Warping restraint model
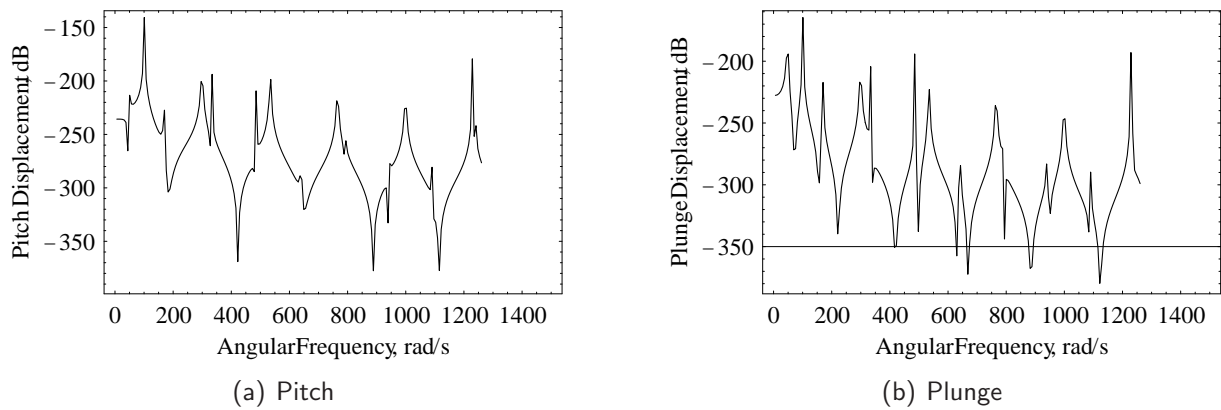
(a) Pitch

(b) Plunge

Figure 7.8: FRFs of the warping restraint model. Pitch and Plunge
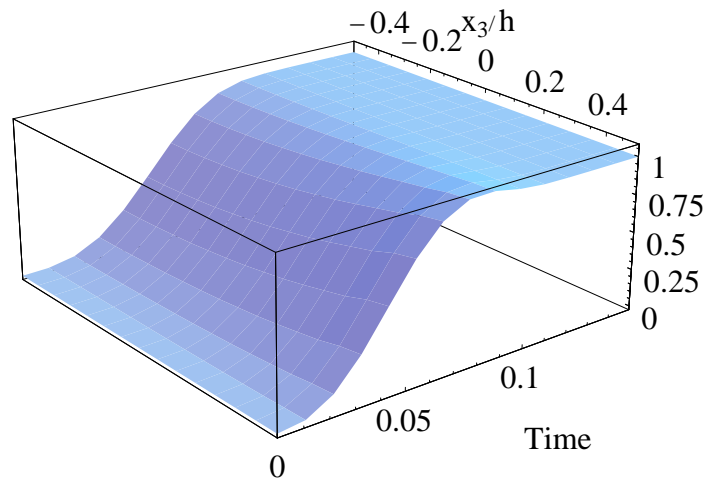
Figure 7.9: Temperature field.

In Fig. 7.9 a three-dimensional plot of the temperature field arising in the body due to the impact of the laser beam is shown for $\tau_0 = 0.1$ s. It can be observed that the temperature after a transient

arrives at a stationary value which is due to the imposition of impermeability conditions in Eq. 7.159 for the modeling of the thermal field.[†]

For reference purposes to the following results in Tab. 7.3 the reference values of the material

Table 7.3: Material and aerodynamic reference values.

R	100
ρ_∞	1.225 kg/m^3
U_n	100 m/s
τ_0	0.1 s
Λ	0°
k_3	300 kg m/s^3 K

and aerodynamic properties chosen in the analysis for the WR model are reported. Note that the reference value for the thermal conductivity is that of the pyrolytic graphite in the plane of transverse isotropy as reported in Ref. [41], whereas the specific heat is chosen such that the characteristic thermal time is equal to the characteristic structural one (*i.e.*, the first bending period).[‡]

In order to illustrate the effect of the anisotropy of the material constituents in Figs. 7.10 the
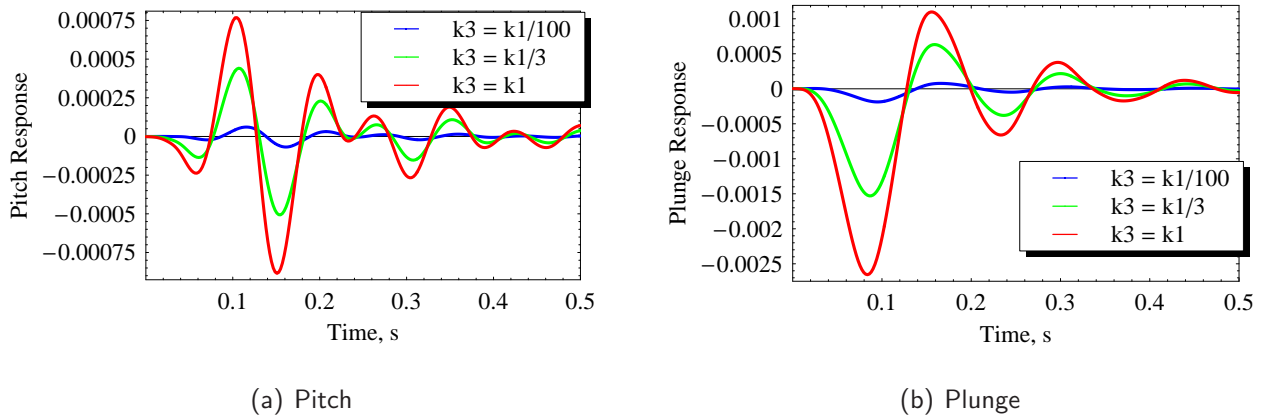
(a) Pitch

(b) Plunge

Figure 7.10: Effect of thermal transversal isotropy. Pitch and Plunge

time histories of the pitch and plunge displacements in the reference configuration are compared to those pertinent to other two different choices of thermal conductivity in the thickness direction. In particular, for $k_3 = k_1/100$ a condition typical of a pyrolytic graphite material is approached

---

[†] Indeed, more realistically, prescribed surface temperature or convection boundary conditions should be imposed accordingly to Ref. [17].

[‡] Although this choice could appear instrumental, it is particularly useful in evaluating the thermally induced vibrations of the wing as it is discussed in Ref. [17]. Indeed, the importance of the inertia effects increases as the ratio of these two characteristic times becomes smaller; on the other hand as this ratio increases the inertia forces disappear and the static solution alone remains.

29th May 2005

(see Ref. [41]). From this figure it is apparent that the consideration of a much smaller thermal conductivity in the thickness direction yields an attenuation of the response. This result is not surprising if compared with Eq. 7.156 where it was observed that the increase of the ratio k_1/k_3 corresponds to a virtual stretch of the space in the thickness direction.

(a) Pitch   (b) Plunge
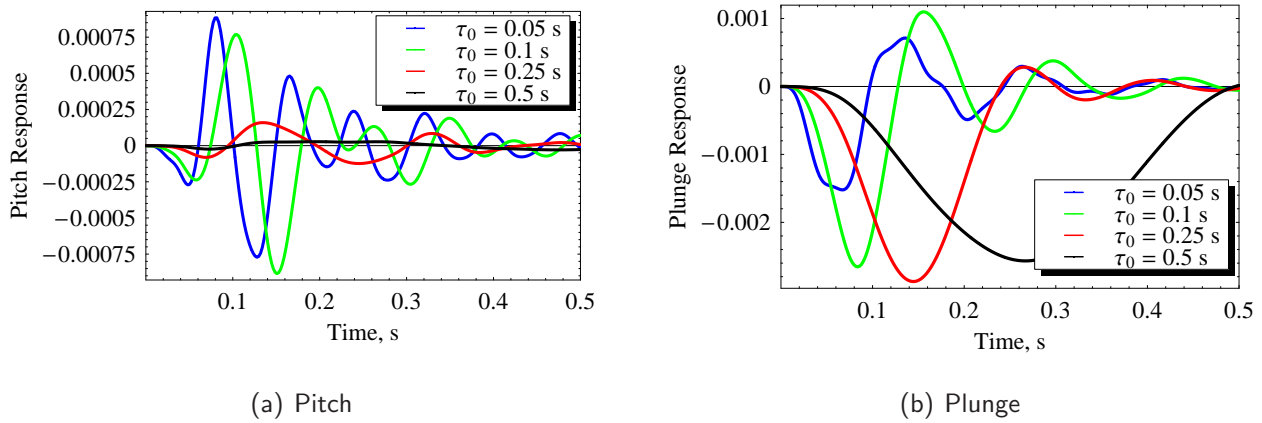
Figure 7.11: Effect of external heat flux period. Pitch and Plunge

(a) Pitch   (b) Plunge
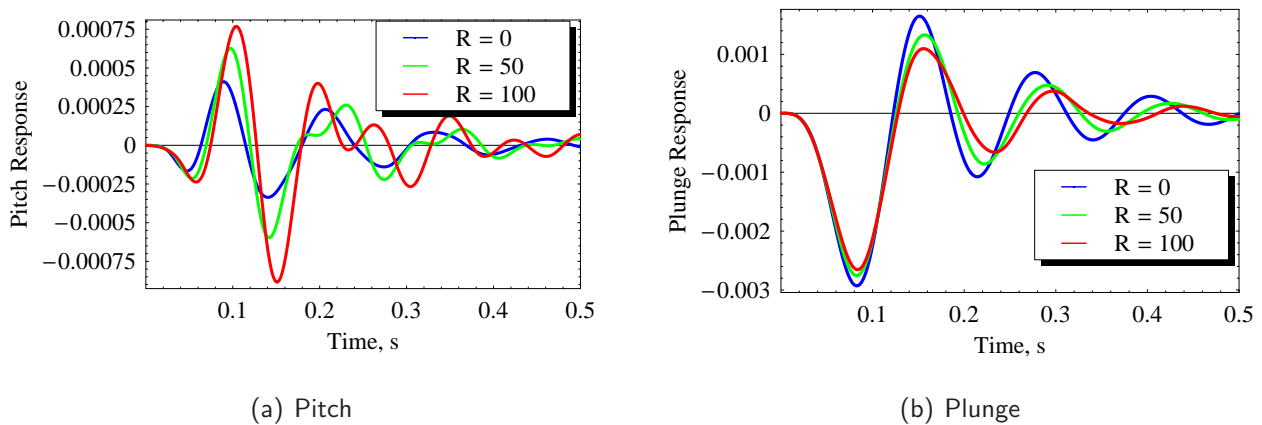
Figure 7.12: Effect of transverse shear. Pitch and Plunge

Figures 7.11-7.13 show the time histories of the pitch and plunge variables, for three different heat flux time periods, four flight speeds, three different transverse shear ratios and three different sweep angles. It is worth noting that in all the shown cases the plunge displacement starting from zero increases in the negative sense and features an oscillatory character. This is consistent with the assumption that the laser impacts the wing on its upper surface, thus extending the fibers of the upper surface and so determining, in the instant times immediately subsequent the application of the load, a negative deflection of the wing. In particular, the results presented in Figs. 7.12 deserve special attention. As said before, they represent the time histories of plunge and pitch for three different choices of the transverse shear flexibility ratio. Someone, led from the observation that an increasing of flexibility turns into a lowering of the natural frequencies, could expect that

(a) Pitch   (b) Plunge
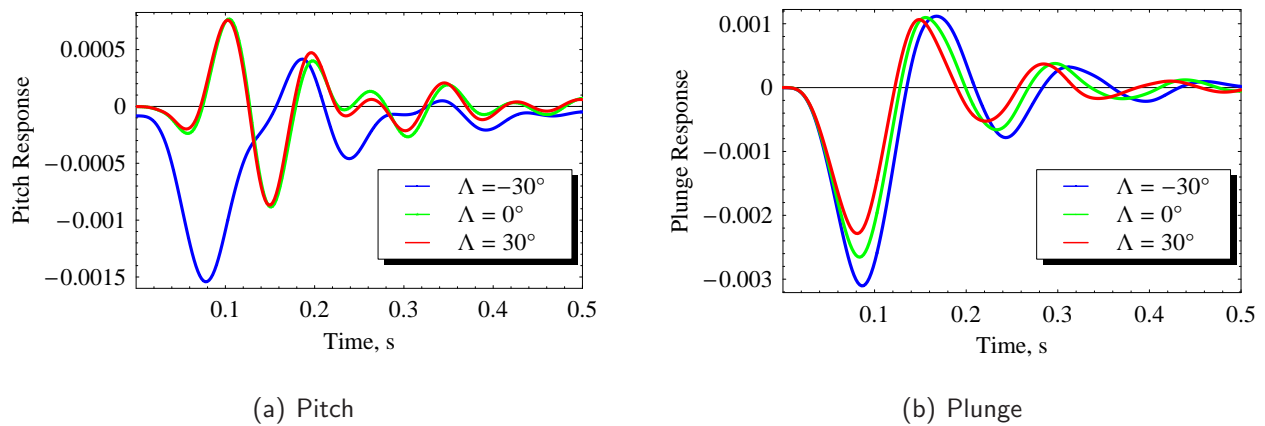
Figure 7.13: Effect of sweep angle. Pitch and Plunge

the increasing of the transverse flexibility would determine a generalized increment of the maximum displacement for both the pitch and the plunge. With the help of the following figures and of some physical considerations, it will be proved that this conclusion is wrong. Indeed, observe that, if the transverse flexibility is increased, this means that the normal does not remain normal after the deformation,[‡] and, this means that, during the motion, part of the energy that would be expended to curve the reference line of the beam, is, instead, expended to rotate the fibers with respect to the normal.[§] On the other hand the introduction of this type of flexibility, that, equivalently, can be interpreted as the relaxation of the Euler-Bernoulli material constraint, affects the torsional behaviour in an opposite way. Indeed, now each fiber (or section) of the wing receive less opposition to its torsional motion from the preceding and succeeding fibers. These considerations are clarified also by the following figures (Fig. 7.14–7.17). They represent the FRFs and time histories of the aeroelastic system excited by a unit pulse at the tip for two different frequency ranges. It might be noticed, in particular from the observation of the FRFs, that the natural frequencies of the pitch and plunge displacements lower increasing R. Moreover, it might be noticed, either in the frequency and time domains, that the increase of R yields a raising for the pitch and a lowering for the plunge of the maximum displacement in correspondence of their first natural frequencies. Hence, the behaviour of the aero-thermo-elastic analysis previously shown, where the thermal excitation operated as a low-pass filter, is confirmed.

Finally, note that in Fig. 7.18 the approach of the dynamic response in the time domain has been used to recognize the occurrence of the flutter instability. Indeed in this figure for $U_n = 150 \ m/s$ the forced oscillations, especially for the pitch displacement, exhibits a divergent behavior.

[‡] For a comprehensive analysis and theoretical presentation of the hypotheses underlying the definition of material constraints, such that just introduced (referred as Euler-Bernoulli hypothesis [constraint] in the current literature for the case of beams, and to Reissner-Mindlin hypothesis [constraint] in the case of shells) the reader is referred to Part II of this thesis, where these issues have been introduced and employed in the framework of shells' theory.

[§] Note that in order to properly model the rotation of the fiber a representation of the displacement field has been used that considers it as an independent variable (β), with the exception of releasing this independence as soon as the shear strain would have been zero due to the consideration of an infinity transverse rigidity (*i.e.*, null flexibility).

29th May 2005

(a) Broadband

(b) Narrow band
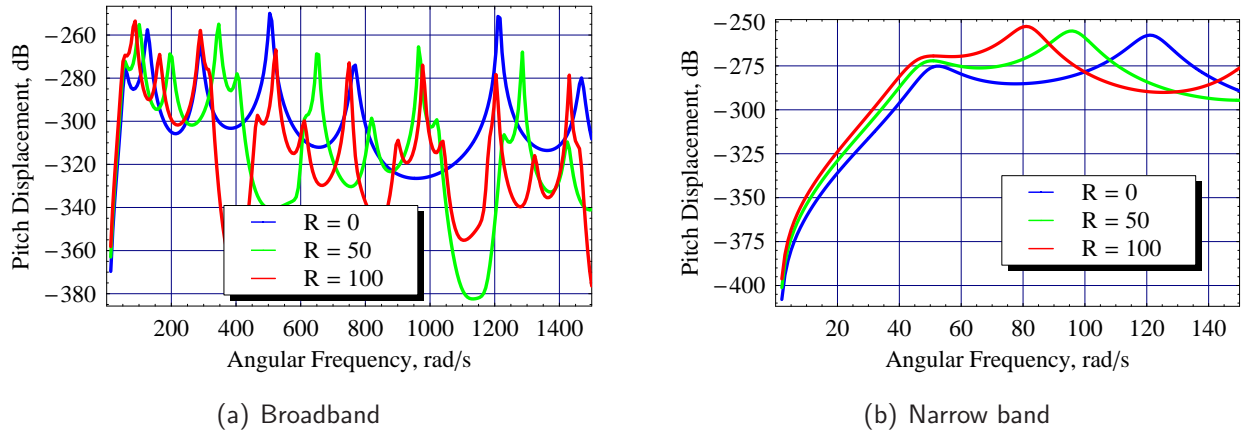
Figure 7.14: Effect of transverse shear: FRF of the Pitch DOF.

(a) Broadband

(b) Narrow band
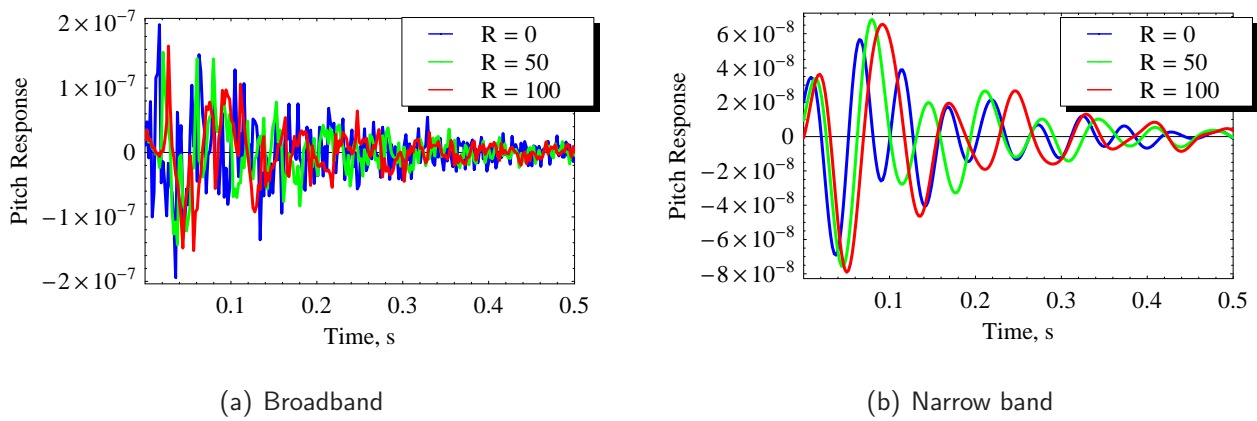
Figure 7.15: Effect of transverse shear: time histories of the Pitch DOF.
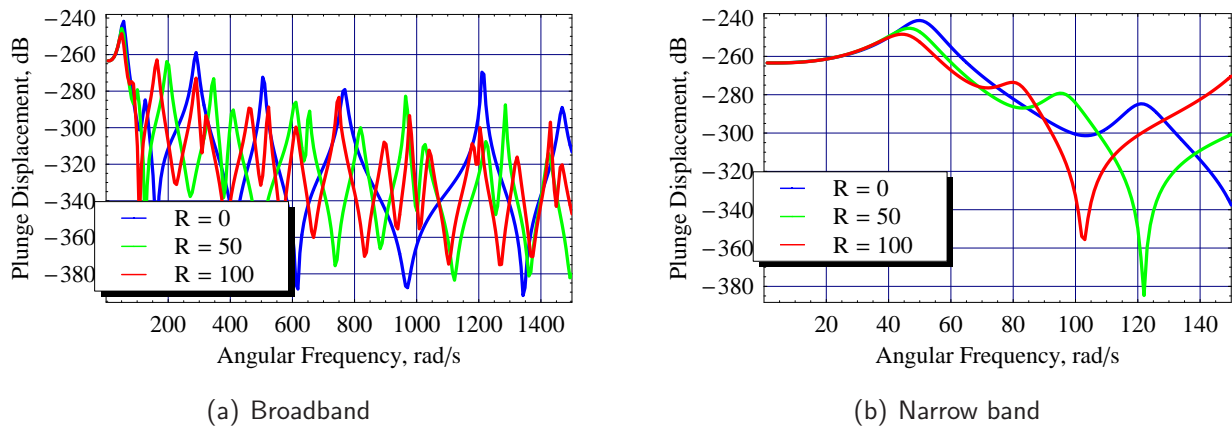

(a) Broadband

(b) Narrow band

Figure 7.16: Effect of transverse shear: FRF of the Plunge DOF.

7.10 Concluding remarks

In this chapter a study of the aero-thermo-elastic response of a solid rectangular wing impacted by a laser beam on its upper surface, made of advanced material, and featuring several non-classical effects

(a) Broadband

(b) Narrow band
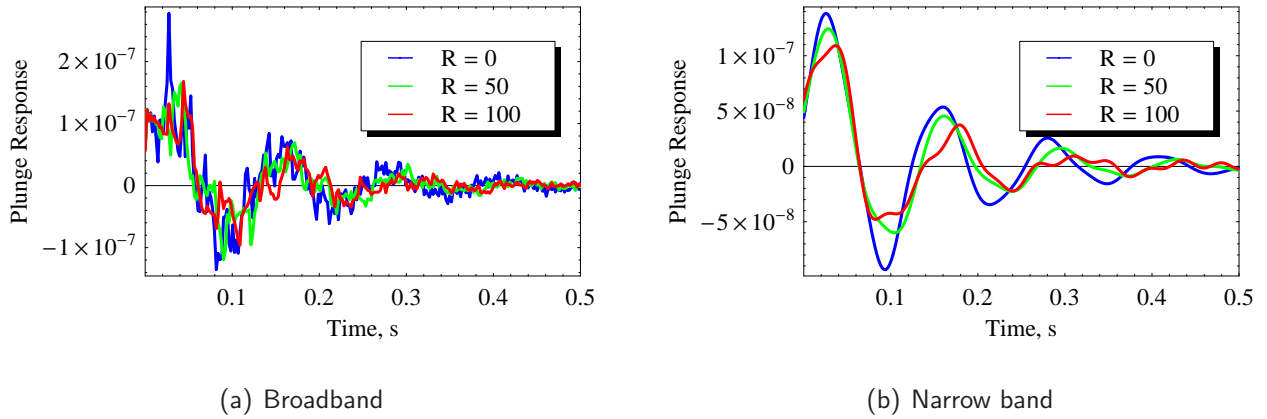
Figure 7.17: Effect of transverse shear: time histories of the Plunge DOF.
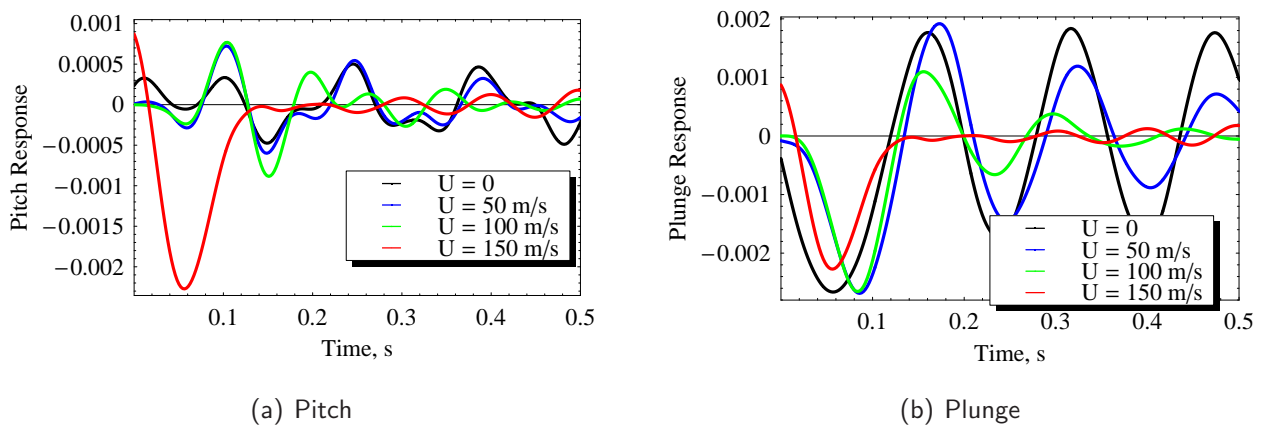
(a) Pitch

(b) Plunge

Figure 7.18: Effect of flight speed. Pitch and Plunge

has been presented and discussed. From the theoretical point of view several aspects have been addressed; in particular, it has been shown the presence of an elastic feedback in the determination of the temperature into the body due to the application of the external input which is expected to influence the aeroelasticity (and eventually stability) of the wing in the flight speed range. Moreover, an efficient and clean solution methodology has been developed, finally, several non-classical effects, such as the transverse shear flexibility and the warping restraint, have been considered and their influence on the aeroelastic characteristics of a simple model have been evaluated. Being the presented results limited to the simple configuration of a rectangular, uniform, single-layered wing (whose basic results have been tested and compared with those present in the existing literature), several enhancements and complexities can be expected to be presented in future works. In particular, the effect of the elastic feedback in the temperature field will be addressed also in the numerical analysis, and the effect of a multi-layer structure with as external layer thin coatings for thermal insulation will be put under consideration by the authors in future works.

29th May 2005

Chapter 8

Aeroelastic vibrations suppression by shunted piezo-electric patches

8.1 Introduction

Piezoelectric materials, with passive electrical loads, may be integrated into a host structure in order to increase damping and then to reduce the amplitude of vibrations [55]. As shown in literature, a resistive-inductive load forms, with the inherent capacity of the piezo element, a resonant circuit, which behaves, when bonded on a vibrating structure, as a vibration absorber. As a mechanical vibration absorber [55], the tuned electrical circuit provides a high damping in an almost flat frequency response function (FRF) around the mode of interest, on which the circuit were tuned. Obviously optimal parameters of the resistor and of the inductor must be adopted [55] in order to get the result mentioned above.

Home-made codes, based on a finite element (FE) description of the structure, were used in order to get the modal parameters, natural frequencies and damping ratios, for systems with piezo patches ideally bonded on them, and the possibility to use a FE commercial code (MSC.NASTRAN) were pointed out [8]. Recently, this passive damping technique has been adopted in the aeroelastic field [72], and a modal-based FE description of the piezo-host structure system with piezo elements shunted by resistive (R) and resistive-inductive ($R-L$) loads were proposed and applied on a small glider wing [5]. The modal-based FE approach were applied and extended to linear aeroelastic systems, with a semi-active control procedure function of the flight conditions (*i.e.*, flight speed, air density, and Mach number) [7].

Unfortunately, this type of device - as the mechanical vibration absorber - only affects the mode on which it is tuned [32]. Therefore, as it is usually necessary to damp the first two or three modes of a vibrating structure, some strategies were used to face this problem [7]. The first one used piezo patches tuned some on a mode and others on another mode. The second one adopted an external electrical circuit in the form of a ladder network, so as to damp more modes simultaneously [57, 18].

Numerical simulations of the circuit proposed in [57] with finite element models of simple vibrating structures were presented in [10], where the difficulties to get the proper capacitors in order to damp more than two modes were pointed out. Recently, a ladder network of the Foster type, using notch filters, was suggested in [118]. Nevertheless, if many modes have to be damped, the total number of the notch filters becomes too high.

In this thesis a different electrical circuit is presented. It uses notch filters, but in a ladder network of the Cauer type [14], this solution limits the number of the notch filters, even if its behavior is completely equivalent to the one in [118]. The electrical network, introduced into the FE commercial code (MSC.NASTRAN, [56, 93]), permitted – with the modal-based FE description – a numerical study of the dynamic and aeroelastic behavior of a small glider wing.

8.2 Theoretical Basis

Let us consider a laminar or piezo patch with e_3 indicating the normal direction to the middle plane of the element, and e_1 and e_2 two orthogonal directions in the plane. Supposing a linear electromechanical behavior for the piezo material, considering for it a small finite Cartesian element, and following [55], the local constitutive electro-mechanical equations in the Laplace domain are:

$$\begin{pmatrix} \mathsf{I} \\ \mathsf{S} \end{pmatrix} = \begin{bmatrix} s\mathsf{C}_p^T & s\mathsf{Ad} \\ \mathsf{d}'\mathsf{L}^{-1} & \mathsf{s}_{sc} \end{bmatrix} \begin{pmatrix} \mathsf{V} \\ \mathsf{T} \end{pmatrix} \tag{8.1}$$

where I represents the vector of electrical current flowing along the three directions, S the vector of internal deformations, V the vector of electrical potential applied on the element through the electrodes, and T the vector of internal stresses. If the inherent capacitance is shunted with a passive electric load, the overall admittance (Y_{sh}) is given by:

$$\mathsf{Y}_{sh} = \mathsf{Y}_{oc} + \mathsf{Y}_L \tag{8.2}$$

where Y_L is the admittance of the external circuit, and Y_{oc} is the admittance in open circuit condition. At the same time, the shunted piezoelectric compliance is written as:

$$\mathsf{s}_{sh} = \left[\mathsf{s}_{sc} - \mathsf{d}'\mathsf{L}^{-1}\mathsf{Z}_{sh}s\mathsf{Ad} \right] \tag{8.3}$$

where Z_{sh} is the overall electrical impedance, whose components are $Z_{sh_i} = Z_{oc_i}Z_{L_i}/\left(Z_{oc_i} + Z_{L_i}\right)$, i.e., the inverse of the relative components of the overall admittance Y_{sh}.

When the piezoelectric element is uniaxially loaded with either a normal or a shear stress in the plane orthogonal to the polarization direction (e_3) where the electrodes of the considered plane are present (e.g., loaded in the direction e_1 or e_2), the diagonal term of the compliance matrix relating

the stress in the $j - th$ direction with the strain in the same direction can be written as:

$$s_{sh_{jj}} = s_{sc_{jj}} \left[1 - \bar{Z}_{sh_3} k_{3j}^2 \right] \tag{8.4}$$

where $\bar{Z}_{sh_3}$ represents the nondimensional impedance of the shunted load with respect to the impedance of the piezo in open circuit condition ($\bar{Z}_{sh_3} = \frac{Z_{sh_i}}{Z_{oc_i}}$), and k_{3j} is the electromechanical coupling coefficient.

Thus the nondimensional mechanical stiffness ($\bar{K}_{sh_{jj}}$), normalized with respect to the one of the piezo in open circuit condition, is [55]:

$$\bar{K}_{sh_{jj}} = \frac{1 - k_{3j}^2}{1 - \bar{Z}_{sh_3} k_{3j}^2} \tag{8.5}$$

Since the current due to the piezo deformation flows along the direction 3, hereafter, for the sake of notation simplicity, the subscript 3 will be omitted.

8.3   Shunted electrical loads: Resistive and Resistive-Inductive

For a resistive electrical load (R), the nondimensional electrical impedance is equal to:

$$\bar{Z}_{sh}^R = \frac{sC_p^T}{1 + sRC_p^T} \tag{8.6}$$

where C_p^T is the piezo capacitance at constant stress. Substituting Eq. (8.6) into Eq. (8.5), one can obtain, in the Fourier domain, the mechanical shunted stiffness of the passive element:

$$K_{sh}^R(\omega) = K_{sc} \left\{ 1 + \bar{k}^2 \left[1 - \frac{1}{1 + (\omega RC_P^S)^2} + j \frac{\omega RC_P^S}{1 + (\omega RC_P^S)^2} \right] \right\} \tag{8.7}$$

where $\bar{k}^2 = k_{3j}^2 / \left(1 - k_{3j}^2 \right)$, and C_P^S is the inherent capacitance of the piezo device at constant strain. As one can see, the stiffness of the piezo element, with a resistive load, is frequency dependent and similar to the one of models of viscoelastic materials which can be represented either by the Zener–Biot or by a three–parameter model [3, 9]. As shown in [55], the maximum of the imaginary part of the complex stiffness, Eq. (8.7), is reached at $\omega_{max} = 1/(RC_P^S)$, whereas the maximum relative to the loss factor is $\omega_{max}^\eta = \sqrt{1 - k_{3j}^2}/(RC_P^S)$. Since k_{3j}^2 is generally much lower than 1, it is acceptable to assume that $\omega_{max}^\eta \simeq \omega_{max}$. Thus, a suitable choice of R would permit to get ω_{max} coincident with the natural frequency of the mode to be damped, ω_n.

It is worth noting that, although the mode of the host structure to be damped is known, the natural frequency of the overall shunted structure is unknown because it depends on the resistor which loads the piezo device. Therefore, in numerical tests the eigenvalues have to be achieved with an

iterative procedure, whereas in experimental tests several resistors should be used in order to get the frequency at which the maximum damping is gained. Actually, the desired natural angular frequency can be obtained from the natural angular frequencies relative to the short and to the open circuit ($\omega_{n_{sc}}$ and $\omega_{n_{oc}}$ respectively[1]) with the following relationship [8]:

$$\hat{\omega}_n = \sqrt{\frac{(\omega_{n_{sc}})^2 + (\omega_{n_{oc}})^2}{2}} \tag{8.8}$$

where $\omega_{n_{sc}}$ and $\omega_{n_{oc}}$ are the natural frequencies of the mode when the piezo circuit is short or open respectively. Once $\omega_{n_{sc}}$ and $\omega_{n_{oc}}$ are evaluated, it is straightforward to get the resistive load necessary to gain the maximum damping:

$$R = \frac{1}{\hat{\omega}_n C_P^S} \tag{8.9}$$

Moreover, Eq. (8.7) can be recast as:

$$K_{sh}^R(f) = K_{sc}\left[1 + \bar{k}^2\left(1 - \frac{1}{1 + (\alpha_0 f)^2} + j\frac{\alpha_0 f}{1 + (\alpha_0 f)^2}\right)\right] \tag{8.10}$$

where:

$$\alpha_0 = 2\pi R C_p^S \tag{8.11}$$

Note that, considering the optimal resistance given by Eq. (8.9), the optimal value of α_0 is equal to $2\pi/\hat{\omega}_n$. When resistors (R) and inductors (L) are used to shunt the piezoelectric electrodes, a resonant circuit is formed with the inherent capacitance of the piezo device. In this case the nondimensional overall electrical impedance can be written:

$$\bar{Z}_{sh}^{RL} = \frac{LC_P^T s^2 + RC_P^T s}{LC_P^T s^2 + RC_P^T s + 1}. \tag{8.12}$$

Substituting Eq. (8.12) into Eq. (8.5) one can easily obtain the complex stiffness of the shunted passive element in the Fourier domain:

$$K_{sh}^{RL} = K_{sc}\left\{1 + \bar{k}^2\left[1 - \frac{1 - \omega^2 LC_P^S - j\omega RC_P^S}{(1 - \omega^2 LC_P^S)^2 + (\omega RC_P^S)^2}\right]\right\} \tag{8.13}$$

As shown in [55], the behavior of the piezo material with its electrical circuit, when integrated with the host structure, is almost like a vibration absorber. Similarly to the mechanical case [32], if an almost flat frequency response curve of the overall structure around a natural frequency is desired, optimum parameters should be used. Considering the analogy of the dynamical absorbers,

---

[1] Note that in the technical literature the nomenclature ω_n^E and ω_n^D is also employed instead of $\omega_{n_{sc}}$ and $\omega_{n_{oc}}$.

the optimal value of the ratio between the electrical angular frequency and $\omega_{n_{sc}}$ ($\delta = \omega_{el}/\omega_{n_{sc}} = 1/\omega_{n_{sc}}\sqrt{LC_p^S}$) can be obtained [55], and expressed in function of the angular frequencies of the system in short and open circuit conditions [8, 5]:

$$\delta^{opt} = \sqrt{1 + K_{ij}^2} = \left(\frac{\omega_{n_{oc}}}{\omega_{n_{sc}}}\right). \tag{8.14}$$

where K_{ij} is the generalized electromechanical coupling factor [55]. Furthermore the dissipation tuning parameter ($r = RC_p^S\omega_{n_{sc}}$) is given by:

$$r^{opt} \simeq \sqrt{2}\frac{K_{ij}}{1 + K_{ij}^2} = \sqrt{2}\frac{\sqrt{(\omega_{n_{oc}})^2 - (\omega_{n_{sc}})^2}}{(\omega_{n_{oc}})^2}\omega_{n_{sc}}. \tag{8.15}$$

Equations (8.14) and (8.15) can be used to express the optimal inductance and resistance as functions of the natural frequencies of the system in open and short circuit conditions:

$$L_{opt} = \frac{1}{C_p^S(\omega_{n_{oc}})^2} \tag{8.16}$$

$$R_{opt} = \frac{\sqrt{2\left[(\omega_{n_{oc}})^2 - (\omega_{n_{sc}})^2\right]}}{C_p^S(\omega_{n_{oc}})^2} \tag{8.17}$$

Equation (8.13) can be rewritten as:

$$K_{sh}^{RL}(f) = K_{sc}\left[1 + \bar{k}^2\left(1 - \frac{1 - \alpha_1 f^2}{\beta(f)} + j\frac{\alpha_2 f}{\beta(f)}\right)\right] \tag{8.18}$$

where:

$$\beta(f) = \left(1 - \alpha_1 f^2\right)^2 + \left(\alpha_2 f\right)^2 \tag{8.19}$$

$$\alpha_1 = (2\pi)^2 LC_p^S \tag{8.20}$$

$$\alpha_2 = 2\pi RC_p^S \tag{8.21}$$

8.4 Modal coordinates approach

As discussed before, piezo devices, bonded on a structure, behave as a viscoelastic material or a vibration absorber (depending on the resistive or resistive–inductive load), so it would be possible to introduce them into a finite element model of a structure modeling them as *brick*-like elements or by introducing a complex mechanical stiffness matrix to get complex eigenvalues, [9, 8]. Nevertheless, some commercial finite element codes (*e.g.*, MSC.NASTRAN [56], ABAQUS [2, 1]) have also the possibility to consider viscoelastic finite elements in order to get the frequency response functions. These codes typically perform the viscoelastic description considering a frequency dependent func-

tion, given as a table of stiffness values versus frequency, to characterize the viscoelastic properties. In this way, the elastic characteristics of a piezo devices, resistively shunted, can be integrated with the structural FE description. Indeed, also the elastic properties of piezo patches shunted with RL loads, can be usefully employed in the same manner. Therefore, in spite of the type of the electrical load, the considered FE code provides the frequency response function of the whole system, when the stiffness frequency table is assigned. Thus, supposing the piezo-patches perfectly bonded on the structures, once the stiffness matrix is established, depending on the electrical loads, it is possible to introduce this passive devices in the physical co-ordinates of the structural system by using the equivalence with a viscoelastic material model. The stiffness matrix of a viscoelastic finite element, referring to the notation used in the MSC.NASTRAN code [56], can be written as:

$$\mathsf{K}(f) = \bar{\mathsf{K}}\frac{G'(f) + jG''(f)}{G_{ref}} \tag{8.22}$$

where $\bar{\mathsf{K}}$ is the mechanical stiffness matrix of a generic viscoelastic finite element, $G'(f)$ and $G''(f)$ are two real function of the frequency f. Therefore, once $\bar{\mathsf{K}}$, $G'(f)$, $G''(f)$ and G_{ref} have been derived from the equivalence with Eqs. (8.10) and (8.18), the equation of motion of the overall structure can be derived.

Specifically, for a transversely isotropic material , the flexibility matrix of a piezoelectric element can be written, assuming that the direction 3 is the axis of the transverse isotropy (or the polarization axis), as follows:

$$\mathsf{s}_{sh}^{(e)}(f) = \begin{bmatrix} s_{sc_{11}}^{(e)} & s_{sc_{12}}^{(e)} & s_{sc_{13}}^{(e)} & 0 & 0 & 0 \\ s_{sc_{12}}^{(e)} & s_{sc_{11}}^{(e)} & s_{sc_{13}}^{(e)} & 0 & 0 & 0 \\ s_{sc_{13}}^{(e)} & s_{sc_{13}}^{(e)} & s_{sc_{33}}^{(e)} & 0 & 0 & 0 \\ 0 & 0 & 0 & s_{sc_{55}}^{(e)} & 0 & 0 \\ 0 & 0 & 0 & 0 & s_{sc_{55}}^{(e)} & 0 \\ 0 & 0 & 0 & 0 & 0 & s_{sc_{66}}^{(e)} \end{bmatrix} \left[1 - \bar{Z}_{sh3}^{(e)}(f)k_{31}^2 \right] \tag{8.23}$$

Then the element stiffness matrix, for the principle of virtual work, becomes:

$$\mathsf{K}_p^{(e)}(f) = \int_{Vol^{(e)}} \mathbf{\Phi}^{(e),T}\mathsf{C}^{(e),T}\mathsf{s}_{sh}^{(e)^{-1}}\mathsf{C}^{(e)}\mathbf{\Phi}^{(e)}dV^{(e)} =$$
$$\left[\int_{Vol^{(e)}} \mathbf{\Phi}^{(e),T}\mathsf{C}^{(e),T}\mathsf{s}_{sh}^{(e)^{-1}}\mathsf{C}^{(e)}\mathbf{\Phi}^{(e)}dV^{(e)} \right] \left(1 - \bar{Z}_{sh3}^{(e)}(f)k_{31}^2 \right)^{-1} \tag{8.24}$$

where $\mathbf{\Phi}^{(e)}$ is the matrix of F.E. shape functions, $\mathsf{C}^{(e)}$ is the differential operator relating strains to displacements, and $Vol^{(e)}$ is the volume of the element.

Thus, from Eq. (8.57), Lagrange's equilibrium equations of a system with N_p piezoelectric passive

elements can be written, in the Fourier domain, as follows:

$$\left\{ -\omega^2(\mathsf{M}_s + \mathsf{M}_p) + \mathsf{K}_s + \sum_{e=1}^{N_p} \left(\mathsf{K}_{(p,sc)}^{(e)} \frac{G''^{(e)}(f) + jG'''^{(e)}(f)}{G_{ref}^{(e)}} \right) \right\} \tilde{\mathsf{x}} = \tilde{\mathsf{f}} \qquad (8.25)$$

where $\tilde{\mathsf{x}}$ is the vector of nodal displacement in the Fourier domain, M_s and K_s are the mass and stiffness matrices of the host structure, $\tilde{\mathsf{f}}$ is the vector of external loads, and M_p and K_p are the additive mass and stiffness matrix contributions of the piezo elements considered in the structure. The frequency functions $G''^{(e)}(f)$ and $G'''^{(e)}(f)$ may be different for each patch, if distinct electrical loads are considered, so a few modes can be affected. Thus, Eq. (8.25) permits to design the piezo devices as multimodal tuned dampers.

Firstly, let us compare the frequency dependent functions in Eq. (8.57) with the one relevant to resistive load, Eq. (8.10):

$$\frac{G'(f) + jG''(f)}{G_{ref}} = 1 + \bar{k}^2 \left[1 - \frac{1}{1 + j\alpha_0 f} \right] \qquad (8.26)$$

After, the case of $R - L$ load is considered:

$$\frac{G'(f) + jG''(f)}{G_{ref}} = 1 + \bar{k}^2 \left[1 - \frac{1}{1 - \alpha_1 f^2 + j\alpha_2 f} \right] \qquad (8.27)$$

In the Laplace domain Eq. (8.27) yields ($f = -j\frac{s}{2\pi}$):

$$\frac{G'(s) + jG''(s)}{G_{ref}} = 1 + \bar{k}^2 - \frac{\bar{k}^2}{\frac{\alpha_1}{4\pi^2}(s - s_1)(s - s_2)} \qquad (8.28)$$

where the poles s_1 and s_2 are:

$$s_{1,2} = \frac{-\dfrac{\alpha_2}{2\pi} \pm \sqrt{\dfrac{\alpha_2^2}{4\pi^2} - \dfrac{4\alpha_1}{4\pi^2}}}{\dfrac{\alpha_1}{2\pi^2}} \qquad (8.29)$$

In order to get the equivalence of the shunted piezo-patch device with a vibration absorber, $4\alpha_1$ must be greater than α_2^2 and, therefore, the previous equation becomes:

$$s_{1,2} = \frac{\pi}{\alpha_1} \left[-\alpha_2 \pm j\sqrt{4\alpha_1 - \alpha_2^2} \right] \qquad (8.30)$$

Using this analogy, it is possible to study the frequency behavior of complex structures assigning suitable frequency functions depending on the electrical loads. On the contrary, it is possible to solve the problem studying the whole structure in a modal basis. This approach, which seems particularly

efficient, has been used in the numerical tests performed in the present thesis. The method, besides reducing the FEM dimensions, permits not only to get a multimodal approach, but also to vary the damping introduced by the piezo devices if required by the operative conditions, as also stated in [72], where different flight parameters were considered in an iterative procedure to get the response of a typical section model.

Moreover, considering linear aeroelastic systems with the unsteady aerodynamic modeled via finite–state approach [78, 42, 71], it is possible to carry out response and stability analysis in a state–space representation. Therefore, it would be possible to design an appropriate control law of electric parameters for tuning the piezo-patches at each flight condition. Both multimodal analysis and aeroelastic considerations, when shunted piezo-patches are considered, are not usually allowed in commercial finite element codes; that is the reason to adopt the modal approach previously proposed for mechanical systems in [110, 109, 111].

The real eigenproblem associated to the system in short-circuit condition is written as follows:[2]

$$\left[-\omega_n^2 \mathsf{M} + \mathsf{K}_s + \sum_{e=1}^{N_p} \left[\mathsf{K}_{(p,sc)}^{(e)} \right] \right] \boldsymbol{\phi}^{(n)} = 0 \tag{8.31}$$

where $\boldsymbol{\phi}^{(n)}$ represents the n-th generic N-dimensional real eigenvector corresponding to the real angular eigenfrequency ω_n and normalized with respect to modal mass. Performing a variable change in modal coordinates:

$$\mathsf{x} = \boldsymbol{\Phi}\mathsf{q}, \tag{8.32}$$

if only the first M modes are retained in the spectral analysis, the matrix $\boldsymbol{\Phi}$ is a $N \times M$ rectangular transformation matrix. On the basis of the new modal coordinates, the input ($\tilde{\mathsf{e}}$)/output ($\tilde{\mathsf{q}}$) relationship in the Laplace domain is given by:

$$\left[s^2 \mathsf{I} + \Omega^2 + \sum_{e=1}^{N_p} \hat{\mathsf{K}}_{(p,sc)}^{(e)} \left(\bar{k}^{(e)2} - \frac{\bar{k}^{(e)2}}{\frac{\alpha_1^{(e)}}{4\pi^2}\left(s - s_1^{(e)}\right)\left(s - s_2^{(e)}\right)} \right) \right] \tilde{\mathsf{q}} = \tilde{\mathsf{e}} \tag{8.33}$$

where Ω^2 is the diagonal eigenvalue matrix of the system with piezo in short circuit conditions ($\Omega^2 = \boldsymbol{\Phi}^T \left[\mathsf{K}_s + \sum_{e=1}^{N_p} \left(\mathsf{K}_{(p,sc)}^{(e)} \right) \right] \boldsymbol{\Phi}$) and $\hat{\mathsf{K}}_{(p,sc)}^{(e)} = \boldsymbol{\Phi}^T \mathsf{K}_{(p,sc)}^{(e)} \boldsymbol{\Phi}$ is the stiffness matrix of a piezoelectric element written in modal coordinates, whereas $\tilde{\mathsf{e}} := \boldsymbol{\Phi}^T \tilde{\mathsf{f}}$ represent the generalized force vector. In the following aeroelastic application this vector will be splitted in two aerodynamic contributions,

---

[2] In Eq. (8.31), M is the overall structural mass of the system, sum of the host structure and the piezo masses:

$$\mathsf{M} = \mathsf{M}_s + \sum_{e=1}^{N_p} \mathsf{M}_p^{(e)}.$$

i.e.,

$$\tilde{e} = \tilde{e}_A + \tilde{e}_G \tag{8.34}$$

where $\tilde{e}_A$ represents the modal aerodynamic load due to the elastic deformation of the structure, whereas $\tilde{e}_G$ is the external modal load due to a gust.

8.5 Piezo modeling in linear Aeroelastic Analysis

In the linear modeling of the unsteady aerodynamic, the vector $\tilde{e}_A$ in Eq. (8.34) can be expressed as a linear combination of the lagrangean variables $\tilde{q}$, *i.e.*, , in the Laplace domain as:

$$\tilde{e}_A = q_D \mathsf{E}(s; U_\infty, M_\infty) \tilde{q} \tag{8.35}$$

where $q_D = \frac{1}{2} \varrho_\infty U_\infty^2$ is the dynamic pressure and E is the so-called generalized aerodynamic force (GAF) matrix. Let us consider the following approximated representation of the aerodynamic operator by means of a finite–state technique [78, 42, 71]: this consists on using the aerodynamic data, given by the aerodynamic panel codes (*i.e.*, the complex evaluation of the matrix E for prescribed values of $s_i = j\omega_i$), to determine a matrix polynomial approximation of such a matrix with respect to the Laplace variable s. The structure of such approximation is given by:

$$\mathsf{E}_{app}(s) = \mathsf{A}_0 + \mathsf{A}_1 \left(\frac{s\,c}{2\,U_\infty} \right) + \mathsf{A}_2 \left(\frac{s\,c}{2\,U_\infty} \right)^2 + \mathsf{C} \left(\mathsf{I} \frac{s\,c}{2\,U_\infty} - \mathsf{A} \right)^{-1} \mathsf{B} \tag{8.36}$$

where $\mathsf{A}_0, \mathsf{A}_1, \mathsf{A}_2, \mathsf{A}, \mathsf{B}, \mathsf{C}$ are matrices of interpolation in a specific range of flight speed depending on the Mach number. The unknown matrices are obtained with a minimization process of the global error between the sampled aerodynamic data in the frequency domain and the analytical function given by Eq. (8.36) [71]. It is also worth pointing out that the process shown before, basically consisting on substituting the aerodynamic matrix E (which originally is a transcendental function of s, [16]) with a rational polynomial approximation in s, corresponds in the time domain in approximating the aerodynamic time integral-differential operator with a purely differential one, but with more (aerodynamic) states included. Indeed, the first three matrices have the same modal model dimensions, while A has dimensions (N_{poles}, N_{poles}), B (N_{poles}, M), C (M, N_{poles}), where N_{poles} is the number of the mentioned aerodynamic poles added in the finite-state approximation process.

Referring to a condition with only one piezo ($N_p = 1$) and without any external gust force, Eq.

(8.33), considering Eqs. (8.34) and (8.36), yields:

$$\left[s^2 I + \Omega^2 + \left[\bar{k}^2 \hat{K}_{(p,sc)} - \frac{\bar{k}^2}{\frac{\alpha_1}{4\pi^2}(s - s_1)(s - s_2)} \hat{K}_{(p,sc)} \right] \right] \tilde{q} =$$

$$q_D \left[\frac{s^2 c^2}{4 U_\infty^2} A_2 + \frac{sc}{2 U_\infty} A_1 + A_0 + C \left(\frac{sc}{2 U_\infty} I - A \right)^{-1} B \right] \tilde{q} \tag{8.37}$$

Then, using the following positions:

$$\tilde{v} = s\tilde{q} \tag{8.38}$$

$$\tilde{g} = \frac{\bar{k}^2}{\frac{\alpha_1}{4\pi^2}(s - s_1)(s - s_2)} \hat{K}_{(p,sc)} \tilde{q} \tag{8.39}$$

$$\tilde{r} = \left(\frac{sc}{2 U_\infty} I - A \right)^{-1} B\tilde{q} \tag{8.40}$$

$$\tilde{h} = s\tilde{g} \tag{8.41}$$

(where v, g, h have the same dimensions of the modal model M, while r is N_{poles} dimensional) the problem can be written in a first order form by introducing the following state-space matrix $(4M + N_{poles}) \times (4M + N_{poles})$:

$$\hat{A} = \begin{bmatrix} 0 & I & 0 & 0 & 0 \\ V_1 & V_3 & V_4 & V_2 & 0 \\ \frac{2 U_\infty}{c} B & 0 & \frac{2 U_\infty}{c} A & 0 & 0 \\ 0 & 0 & 0 & 0 & I \\ \bar{k}^2 \frac{4\pi^2}{\alpha_1} \hat{K}_{(p,sc)} & 0 & 0 & -s_1 s_2 I & (s_1 + s_2) I \end{bmatrix} \tag{8.42}$$

where

$$V_1 = -\left[I - q_D \frac{c^2}{4 U_\infty^2} A_2 \right]^{-1} \left(\Omega^2 + \bar{k}^2 \hat{K}_{(p,sc)} - q_D A_0 \right) \tag{8.43}$$

$$V_2 = \left[I - q_D \frac{c^2}{4 U_\infty^2} A_2 \right]^{-1} \tag{8.44}$$

$$V_3 = -\left[I - q_D \frac{c^2}{4 U_\infty^2} A_2 \right]^{-1} \left(-q_D \frac{c}{2 U_\infty} A_1 \right) \tag{8.45}$$

$$V_4 = \left[I - q_D \frac{c^2}{4 U_\infty^2} A_2 \right]^{-1} C q_D \tag{8.46}$$

It is worth noting that the dynamics of the mechanical system takes essentially place in $\tilde{q}$ and $\tilde{v}$ subspaces, the aerodynamics in $\tilde{r}$, and the electro-dynamics of piezoelectric element in $\tilde{g}$ and $\tilde{h}$.

Thus, as a matter of fact, the problem can be written in the Laplace domain:

$$s\tilde{\mathsf{x}} = \hat{\mathsf{A}}\tilde{\mathsf{x}} \tag{8.47}$$

where $\tilde{\mathsf{x}} = \{\tilde{\mathsf{q}}, \tilde{\mathsf{v}}, \tilde{\mathsf{r}}, \tilde{\mathsf{g}}, \tilde{\mathsf{h}}\}^T$ is the state-space vector, $\hat{\mathsf{A}}$ is an explicit function of flight speed (U_∞) and air density (ϱ_∞), and an implicit function of Mach number (M_∞) through the matrices $\mathsf{A}_2, \mathsf{A}_1, \mathsf{A}_0, \mathsf{A}, \mathsf{B}, \mathsf{C}$; furthermore, $\hat{\mathsf{A}}$ is a function of the tuning parameters $(\alpha_0,\ \alpha_1,\ \text{and}\ \alpha_2)$ of the piezoelectrics devices, and of the electromechanical coupling coefficient (k_{31}). In order to study the system aeroelastic stability, problem (8.47) can be associated to a standard eigenproblem:

$$\left[s_n \mathsf{I} - \hat{\mathsf{A}}(U_\infty, \varrho_\infty, M_\infty, \alpha_1, \alpha_2, k_{31}) \right] \tilde{\mathsf{u}}^{(n)} = 0 \tag{8.48}$$

whose solutions, *e.g.*, at various U_∞, allow one to draw the locus of the roots s_n and then to make a stability analysis at fixed altitude (ϱ_∞) and Mach number (M_∞).

8.6   Optimal Tuning within the Flight Speed Range

Because of the dependence on velocity of the state-space matrix $\hat{\mathsf{A}}$, the choice of the optimal parameters α_0, α_1 and α_2 of piezoelectric devices must be done carefully. Indeed, poles and mode shapes of the aeroelastic system change with flight-parameters and the pole mobility in the Gauss plane can cause a loss of efficiency of piezo devices: then it should be appropriate to design a law defining the dependence of the tuning on the flight parameters (*e.g.*, the flight speed). This goal has been achieved with two different procedures. First, it should be possible to maximize the modal damping in the system parametrically varying the piezoelectric parameters for each airspeed. Otherwise, one could evaluate at each airspeed the natural frequencies of the system in open and short circuit conditions. Once these values are known, optimal parameters can be found from the following equations:

$$\alpha_0 = (2\pi) R_{opt} C_p^S = 2\pi \sqrt{\frac{2}{(f_{n_{oc}})^2 + (f_{n_{sc}})^2}} \tag{8.49}$$

$$\alpha_1 = (2\pi)^2 L_{opt} C_p^S = \frac{1}{(f_{n_{oc}})^2} \tag{8.50}$$

$$\alpha_2 = (2\pi) R_{opt} C_p^S = \frac{\sqrt{2\left[(f_{n_{oc}})^2 - (f_{n_{sc}})^2\right]}}{(f_{n_{oc}})^2} \tag{8.51}$$

Note that α_0 is directly derived from Eqs. (8.8) and (8.9), whilst the optimal values α_1 and α_2 are obtained by Eqs. (8.16) and (8.17) considering their relations with the resistance/inductance values. In the reported tests, the second procedure was adopted, because it seems to be quicker and more controllable, although approximated. Indeed, Equations (8.16) and (8.17) are based on the

hypothesis of undamped host systems even if they are successively applied in this thesis on damped (or aeroelastic) systems.

8.7   Multi-modal damping control strategies

There are two different strategies to realize a multi-modal passive control with piezoelectric patches Fig. (8.1). The first one consists of shunting each group of patches, bonded to the host structure, with a R-L circuit - which behaves as a resonant circuit with the inherent capacity of the piezo patch - tuned on a single natural frequency. A finite element modeling to represent the piezo-patch dynamics has been introduced in Ref. [7] for a the vibration control of a single mode: the essential issue of such approach are outlined in Appendix A.

The other method consists in using a single shunt network resonating at several natural frequencies [57, 18, 10]. The problem of mode–by–mode filtering, is obviously of relevant importance, and therefore notch filters have been adopted in [118]. On the other hand, it is remarkable that with this second approach it is possible to use all the patches bonded on the structure in order to transfer the vibrational energy into the electrical circuit and so to dissipate the energy associated to several vibrational modes.

a)   b)
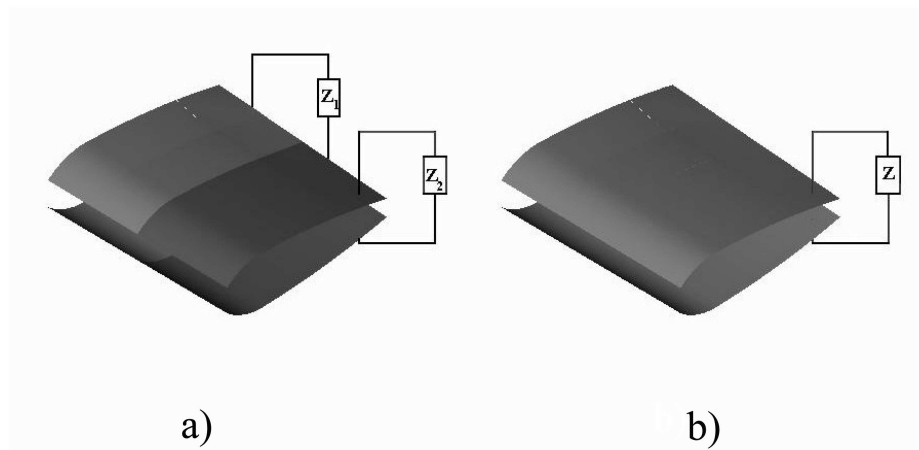
Figure 8.1: Multi-modal control strategies: 1a - A single group of piezo patch connected to a $R-L$ circuit; 1b - The whole piezo patches connected to a multi-modal network.

A ladder network of the Cauer type has been suggested in this thesis in order to reduce the number of notch filters needed for a multi-modal approach with the Foster network introduced in [118]. Obviously, the choice of the electrical elements of the network represents a crucial point

in the behavior of this passive damping system. In fact, the notch filter components influence the possibility of the multi-modal circuit to follow the mono-modal behavior close to the tuning frequencies. Starting from solutions available in literature [118], an enhancement of the reliability and robustness of such a technique, has been obtained employing the new shunt circuit mentioned above, which presents a less sensitive behavior towards the filter components.
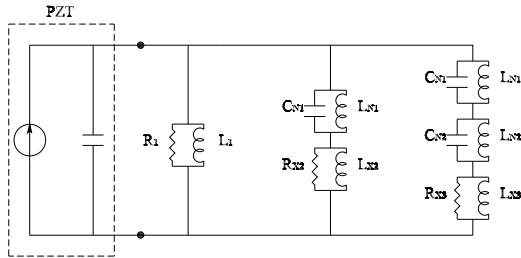
Figure 8.2: Wu's shunt network to damp three modes (Foster network)
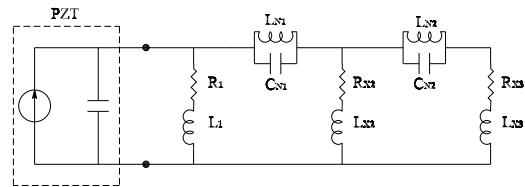
Figure 8.3: Proposed shunt network to damp three modes (Cauer network)

The layout of the Wu's circuit and of the one proposed - relative to the considered three modes - are reported in Figs. (8.2) and (8.3), respectively. In each mesh, a resistor and an inductor (R_{xi}, L_{xi}) have been inserted in order to tune the piezoelectric system on each of the selected frequencies. It is noteworthy that both the circuits use notch-filters ($C_N - L_N$) to filter one mode from another and then to let the electric current flow in the subsequent meshes. The number of notch filters in the two approaches is completely different as the modes to be damped increase. Nevertheless, only three modes are tuned in the example presented and so the difference is of only one notch filter, but for higher number of tuned modes, much less notch filters are necessary for the proposed circuit, as shown in Tab.(8.1). The electrical components for the network of Fig.(8.3) are reported hereafter

$no. of modes$	$no. filters\ (Wu)$	$no. filters\ (proposed)$
3	3	2
4	6	3
n	$\frac{1}{2}n(n-1)$	$n-1$

Table 8.1: Comparison between the number of notch filters versus the number of modes, which have to be damped, for the Wu's circuit and the one proposed

as function of the piezo capacitance at constant strain C_p^S and of the natural angular frequencies of the whole system when the piezo patches have their terminals connected in short (subscript SC) or open circuit (subscript OC). First, let us introduce the following quantity

$$\omega_{SHi} = \sqrt{\frac{\omega_{SCi}^2 + \omega_{OCi}^2}{2}} \tag{8.52}$$

which represents an estimation of the natural frequency of the $i - th$ mode selected in shunting

condition [7, 4].

Starting from the first mesh, the optimal values, L_1 and R_1, are given by [7]:

$$\begin{cases} R_1 = \dfrac{2}{C_p^S \left(\omega_{OC1}^2 + \omega_{SC1}^2\right)} \\[4mm] L_1 = \dfrac{2\omega_{SC1}}{C_p^S \omega_{OC1}^2} \sqrt{\dfrac{\omega_{OC1}^2 - \omega_{SC1}^2}{\omega_{OC1}^2 + \omega_{SC1}^2}} \end{cases} \tag{8.53}$$

It can be noted that these quantities are not affected by any other electrical components of the network because, at the first natural frequency, the first notch filter should be open ($Z_{N1} = \infty$). For the second mesh the following expressions are to be added to the previous ones:

$$\begin{cases} R_{X2} = Re\left[\dfrac{1}{Y_{opt2}(\omega_{SH2}) - Y_{opt1}(\omega_{SH2})} - Z_{N1}(\omega_{SH2})\right] \\[4mm] L_{X2} = Im\left[\dfrac{1}{Y_{opt2}(\omega_{SH2}) - Y_{opt1}(\omega_{SH2})} - Z_{N1}(\omega_{SH2})\right]\left(\dfrac{1}{\omega_{SH2}}\right) \end{cases} \tag{8.54}$$

Equations (8.54) guarantee that the parallel impedance of the first and second mesh equals the optimal one for the second mode, $Z_{opt2}(\omega_{SH2}) = 1/Y_{opt2}(\omega_{SH2})$. The last mesh is disconnected because $Z_{N2} = \infty$ at the frequency of the second mode. For the third mesh in Fig. (8.3) the unknown electrical components are given by:

$$\begin{cases} R_{X3} = Re\left[\dfrac{1}{\dfrac{1}{\dfrac{1}{Y_{opt3}(\omega_{SH3}) - Y_{opt1}(\omega_{SH3})} - Z_{N1}(\omega_{SH3})} - Y_{X2}(\omega_{SH3})} - Z_{N2}(\omega_{SH2})\right] \\[8mm] L_{X3} = Im\left[\dfrac{1}{\dfrac{1}{\dfrac{1}{Y_{opt3}(\omega_{SH3}) - Y_{opt1}(\omega_{SH3})} - Z_{N1}(\omega_{SH3})} - Y_{X2}(\omega_{SH3})} - Z_{N2}(\omega_{SH2})\right]\left(\dfrac{1}{\omega_{SH3}}\right) \end{cases} \tag{8.55}$$

Due to the peculiar structure of the network, the unknown impedances (R_{Xi}, L_{Xi}), relevant to further tuned modes, can be obtained generalizing Eqs. (8.55). As mentioned before, the parameters

of the notch filters have to be established in function of the natural shunting frequencies of the modes to be damped.

Let us now discuss the behavior of such a filter and its influence on the efficiency of the electrical network. The filter impedance (Z_N) is given by:

$$Z_N = \frac{j\omega L_N}{1 - \omega^2 L_N C_N} \tag{8.56}$$

where the filter inductance can be evaluated as function of the capacitance and of the electrical resonant frequency of the parallel circuit, coincident with the natural shunting frequency of the mode to filter out (ω_{SH}):

$$L_N = \frac{1}{C_N \omega_{SH}^2} \tag{8.57}$$

The filter behavior is represented in Fig. (8.4), where the magnitude of Z_N is depicted versus frequency for different $C_N's$. It is apparent that the choice of the filter capacitance influences the final behavior of the shunt circuit and in turn the efficiency of the passive damping control technique. For the sake of simplicity, let us consider a bi-modal shunt circuit. As one can see from Fig. (8.5), if the capacitance of the notch filter is very small, Z_N has a very high magnitude ($Z_N \to \infty$) for a broad frequency band astride the cut-off frequency, and therefore the filter can be practically consider as open for each frequency of interest. On the contrary, for C_N very high, as it is clear from Fig. (8.5), being $|Z_N|$ extremely low, it is possible to consider $Z_N \to 0$ except for a very narrow frequency band near the electrical resonant frequency of the filter.
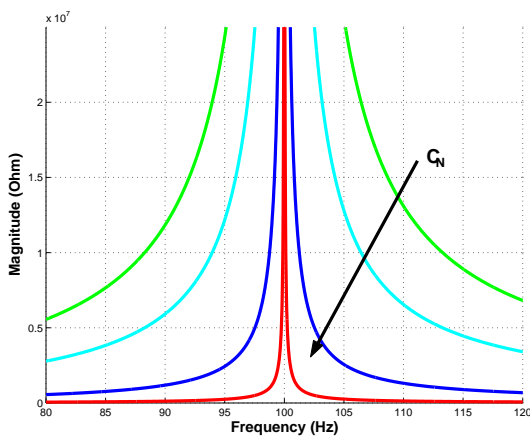
Figure 8.4: Impedance magnitude of the notch-filter versus frequency and in function of C_N
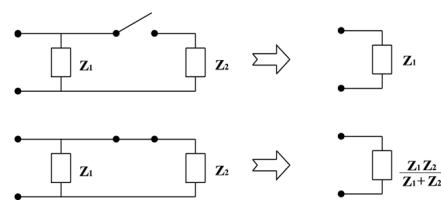
Figure 8.5: Practical shunt circuit behavior for two limit conditions of C_N

29th May 2005

8.8   Numerical results

The host structure for the piezo patches is an actual wing of a remote controlled unmanned glider. The wing has a fiber glass skin, two sandwiches spars in carbon fiber with glass fiber skin and spruce core. Wing structural analysis has been performed by the finite element (FE) MSC.NASTRAN code [56, 93], using quadrilateral elements to model the composite skin and the two composite spars. A belt of piezo patches, whose properties are summarized in Tab. (8.2), has been ideally bonded, in the FE model, to the glider surface near the root (Figs. (8.6)). In particular, 24 piezo patches have been bonded to the upper surface and 24 to the lower one. The width of the piezo belt is about 7% of the wing span.   The comparison between the technique presented in [118] and the proposed one,

(a) Wing model
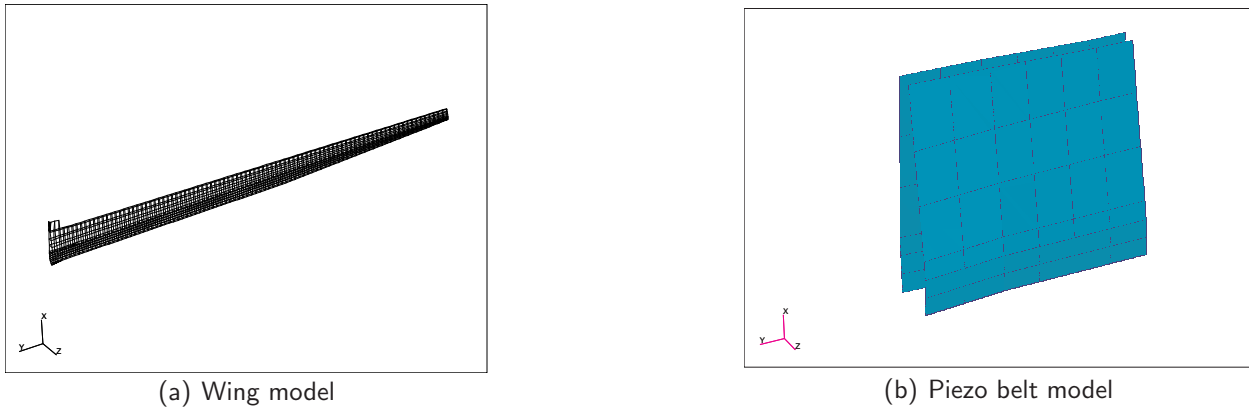
(b) Piezo belt model

Figure 8.6: Wing finite element model and layout of the piezo belt.

thickness (h)	0.38 mm
short-circuit Young modulus (E_{sc})	69. 10^9 Pa
open-circuit Young modulus (E_{oc})	86.52 10^9 Pa
Poisson modulus (ν)	0.33
mass density (ρ)	7700 kg/m^3
electromechanical coupling coefficient (k)	0.5

Table 8.2: Piezo patches properties

for a three-modal damping system, is based on the behavior of the overall shunt circuit impedances, in terms of magnitude and phase, and on the glider wing FRFs. The three natural frequencies to be controlled are: $f_n^I = 3.401$ Hz, $f_n^{II} = 34.455$ Hz and $f_n^{III} = 52.601$ Hz, corresponding to the $1st$, $4th$ and $6th$ mode respectively.

In Figs. (8.7) and (8.8) the magnitude and the phase of the shunt impedances, provided by the Wu's circuit (black line) and by the proposed one (red line), are depicted together with the mono-modal reference optimal values: lines blue for the $1st$, green for the $2nd$ and cyan for the $3rd$ mode respectively. It is noteworthy that in the multi-modal approach the shunt impedance, in order to tune the piezoelectric system on the different frequencies, must adapt itself, in the neighborhood
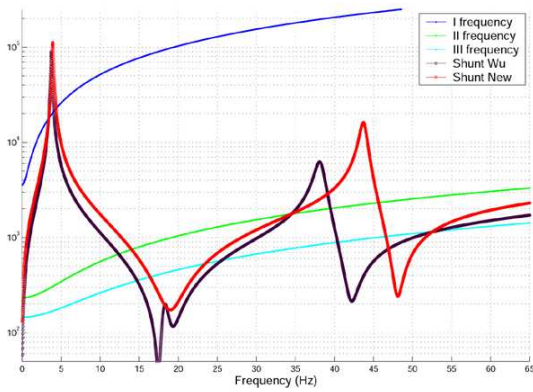
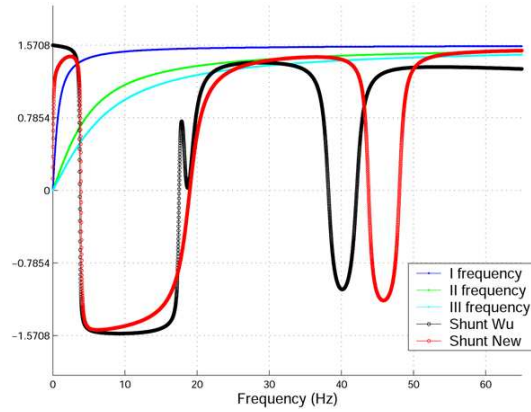Figure 8.7: Shunt impedance magnitude

Figure 8.8: Shunt impedance phase

of the mode natural frequencies, on the curve of the corresponding mono-modal impedances. It can be pointed out that some simplified hypotheses have been introduced in [118] and used in the examples. Specifically, the resistors and inductors have been obtained taking account not of the whole network components, but firstly considering a circuit with resistors only, and then deriving the reactive components from the circuit with only the inductors and the capacitors. These assumptions simplify the calculations of the unknown electrical components, but only permits to match the reference behavior of the $1st$ mode (both in magnitude and in phase), whereas for the $4th$ mode the magnitude is worse than the proposed network and for the $6th$ mode, although better in magnitude, the phase diverges from the reference curve. At any rate, the $FRF's$ in Figs. (8.9), (8.10),
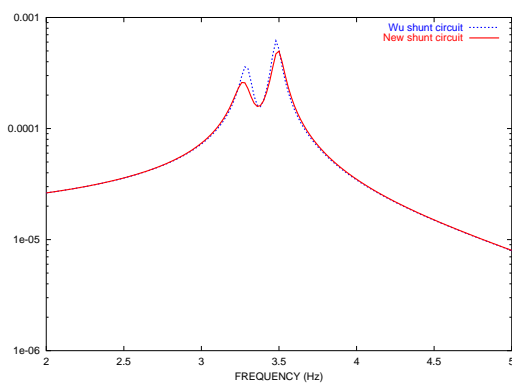
Figure 8.9: FRF in the neighborhood of the $1st$ natural frequency.
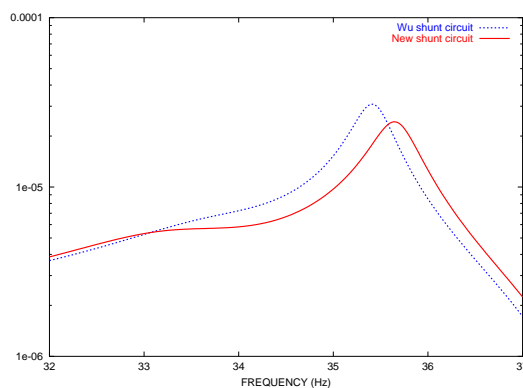
Figure 8.10: FRF in the neighborhood of the $4th$ natural frequency.

and (8.11), relative to the neighborhood of the three considered natural frequencies, reveal the correctness of the considerations presented above. In fact, the proposed network always behaves a bit better, although the two curves – the blue one achieved with the Wu's circuit and the red one gained with the proposed network – are practically the same. Therefore, the advantages of the proposed circuit consists on its greater simplicity, more robustness and reliability, and to a lower number of notch filter used. The results obtained till now were referred to the elastic vibrations of the wing, that is without considering any aerodynamic load. From the aeroelastic point of view –
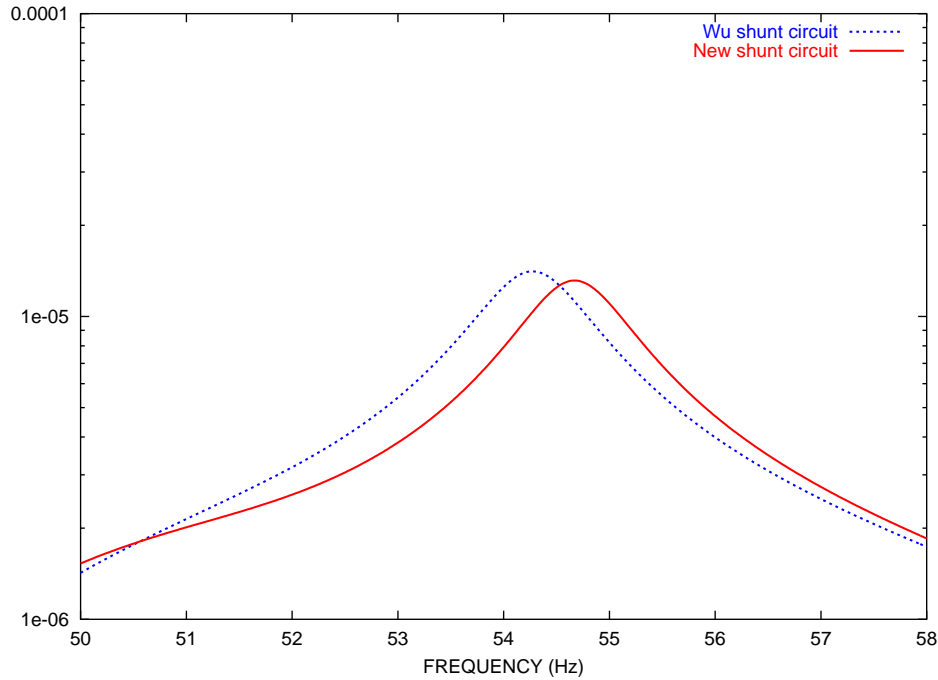
Figure 8.11: FRF in the neighborhood of the $6th$ natural frequency.

because of the dependence of the state-space on velocity, air density and Mach number [42, 71] – the choice of the optimal shunt parameters (L_1, R_1, L_{X2}, R_{X2}... etc.) must be carefully done. A concise presentation of the used aeroelastic modeling in a state-space form has been reported in Appendix B. Indeed, poles and modes of the aeroelastic system change with flight conditions and that may cause a loss of effectiveness of piezo devices. In order to guarantee, in all flight conditions, a correct coupling between the dynamics of the flow/structure system and the electric network, shunted with the piezoelectric elements, a semi-active control could be used, [7, 15, 115]. Actually, this approach would need to evaluate, at each operating condition, the actual aeroelastic poles and thus the optimal shunt parameters to use during the flight. Therefore, resistors and inductors should be changed according to the flight conditions, leaving unchanged the capacitances of the notch filters fixed from the natural frequencies derived by the ground dynamical tests of the system. In other words, the electrical components of the notch filter are determined by the actual natural frequency, then L_N is derived from Eq.(8.57). As example, the root locus function versus the airspeed, at fixed Mach number ($M = 0$) and air density ($\rho = 1.181 \ Kg/m^3$), is presented in Fig. (8.12). The green lines show the root loci of the host structure alone, whereas the red lines represent the root loci for the three-modal semi-active damping control. It is apparent the coupling between the dynamics of the structure and that one introduced by the piezo patches in the region relevant to the controlled poles ($1st$, $4th$ and $6th$). Nevertheless, it is worth noting that in the multi-modal approach, reported in Fig. (8.13), a loss of interaction is observed, in a restricted range of the flight conditions of the $4th$ pole, due to the partial updating of the shunt circuit parameters. Indeed, the optimal tuning should be carried out with respect both the resonance frequencies of the shunt
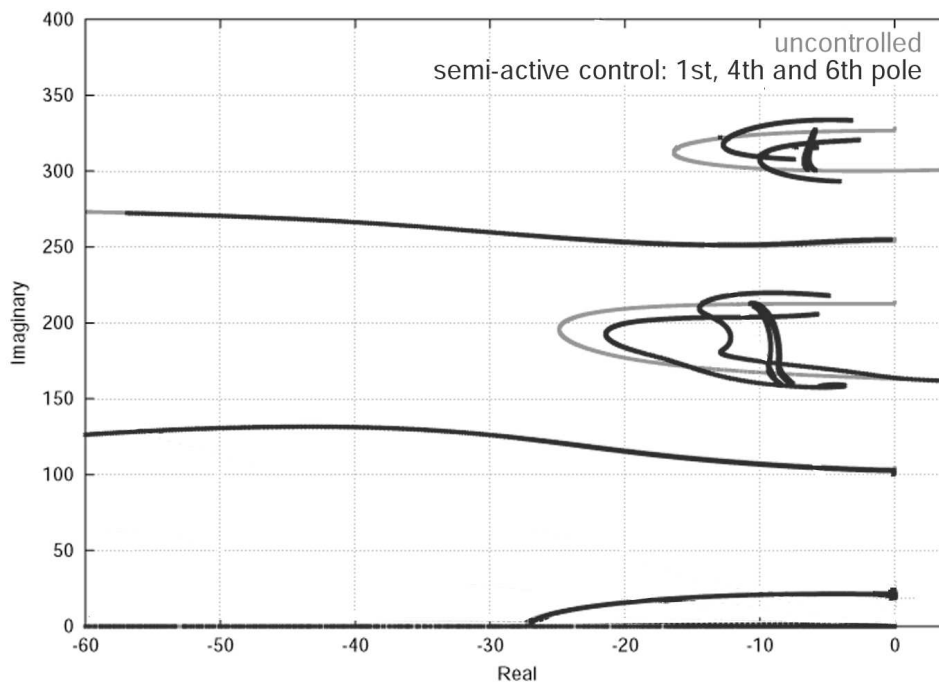
Figure 8.12: Roots loci: the $1st$, $4th$ and the $6th$ poles are controlled

circuit and the filter behavior out of design conditions. However in this thesis, the semi-active control considers only the pole variation, while the filter behavior is not updated to the actual circuit. In other words, although the notch filter is upgraded with the flight conditions, C_N remains fixed, and therefore it is possible to meet with the troubles presented in Fig. (8.56).

Finally, let us note that, because of the first pole stability, the dynamics of the piezoelectric devices is capable to influence the aeroelastic dynamics of this mode in a limited range of flight conditions, as shown in Fig. (8.15).

It is noteworthy that the bonded piezoelectric belt enhances the flutter limit. A comparison between mono-modal and three-modal damping controls, applied on the $4th$ pole, which is the first to reach the aeroelastic instability, is reported in Tab.(8.3).

	$mono-modal$	$three-modal$
$U_F \ m/s$	113.40	112.90
$Gain$	3.94 %	3.57 %

Table 8.3: Comparison of the flutter limit velocities between the mono-modal and the multi-modal techniques. The flutter velocity for the wing without piezo patches is $U_F = 109.0 \ m/s$

The control strategy adopted for the $1st$ pole has been realized using a semi-active approach until the airflow velocity of $55 \ m/s$, then a *static* control has been used, because the pole becomes purely real at $U_\infty = 59 \ m/s$. For this reason, it is not possible to determine the tuning circuit parameters, relevant to the first shunt mesh, by using Eqs. (8.53).

Although the enhancement in the flutter limit provided by the multi-modal approach is practically the
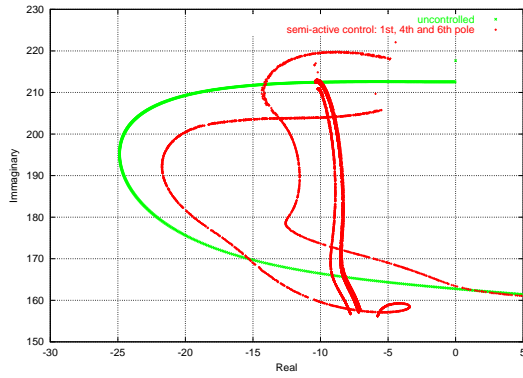
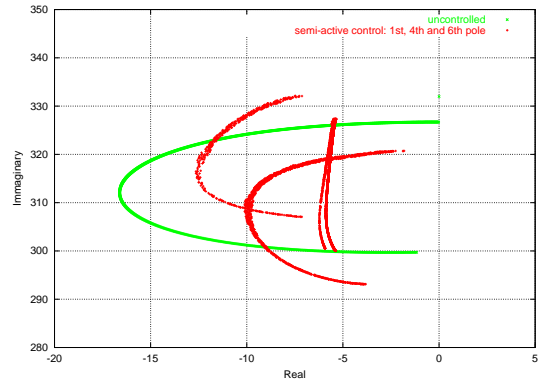Figure 8.13: Roots locus: zoom in the $4th$ pole neighborhood.

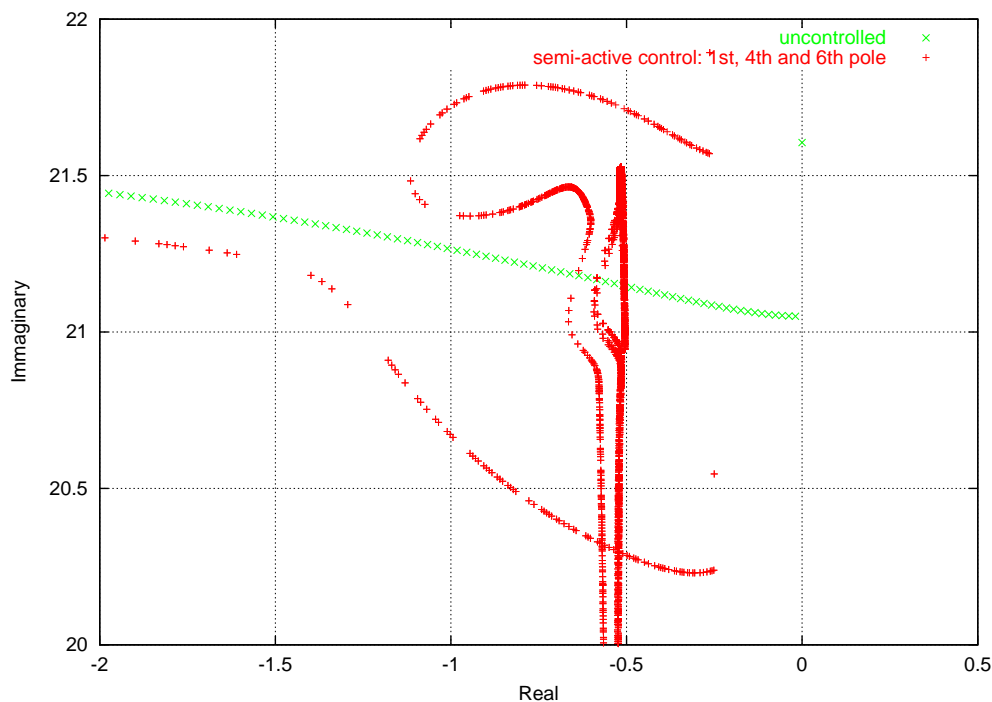Figure 8.14: Roots locus: zoom in the $6th$ pole neighborhood.

Figure 8.15: Roots locus: zoom in the $1st$ pole neighborhood.

same as the mono-modal one, nevertheless the multi-modal technique could be preferred because, from the point of view of the damping introduced by the piezo patches with respect to a gust response, the multi-modal technique results to be more efficient, because more modes are damped. In fact, for a flight speed equal to $U_\infty = 109 \ m/s$ (that is a velocity very close to the flutter margin when no control is considered) and a gust input with constant unitary spectrum, the amplitudes of the output spectra (in the semi-log plane) are as presented in Fig.(8.16). As one can see, both the $4th$ and the $6th$ aeroelastic modes are affected by the piezo circuit, in particular it is evident (for each mode) the behavior like vibration absorbers, which consists in splitting the original natural frequency in two close modes. Figure (8.16), relative to the $4th$ modal co-ordinate, is actually representative of the other co-ordinates, for which the spectral magnitudes have a similar behavior. It is apparent that the piezo effect introduces damping only on the II and the III controlled poles.
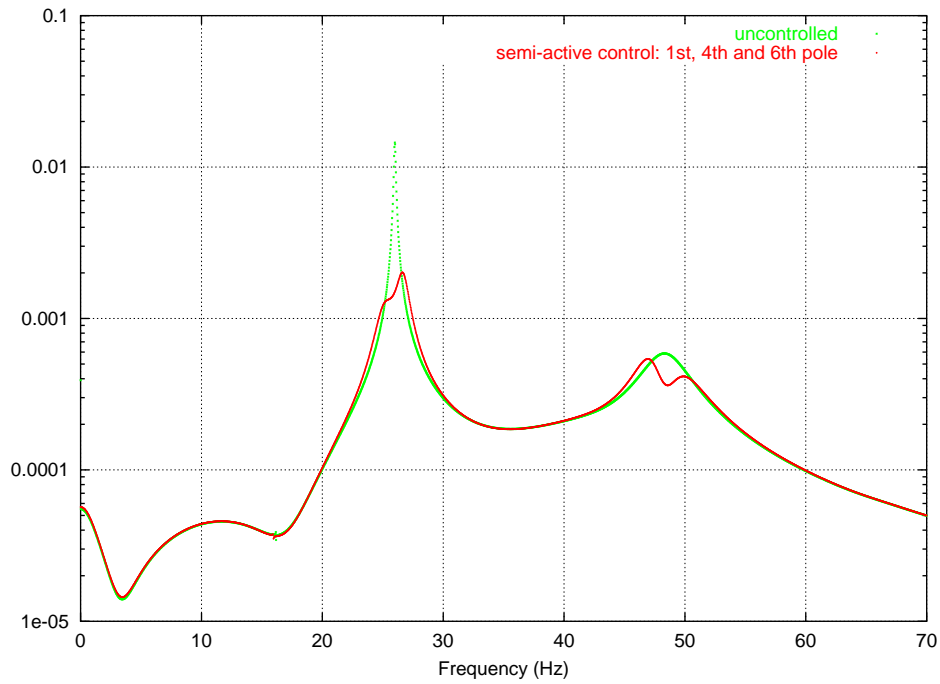
Figure 8.16: Gust response of the IV modal coordinate at $U_\infty = 109 \ m/s$

Indeed, the I aeroelastic mode does not contribute to the instability.

In the following Figure (8.17) is reported the gust response as function of time, obtained by the inverse Fourier transform of the function in Fig.(8.16). In this Figure, the damping introduced by
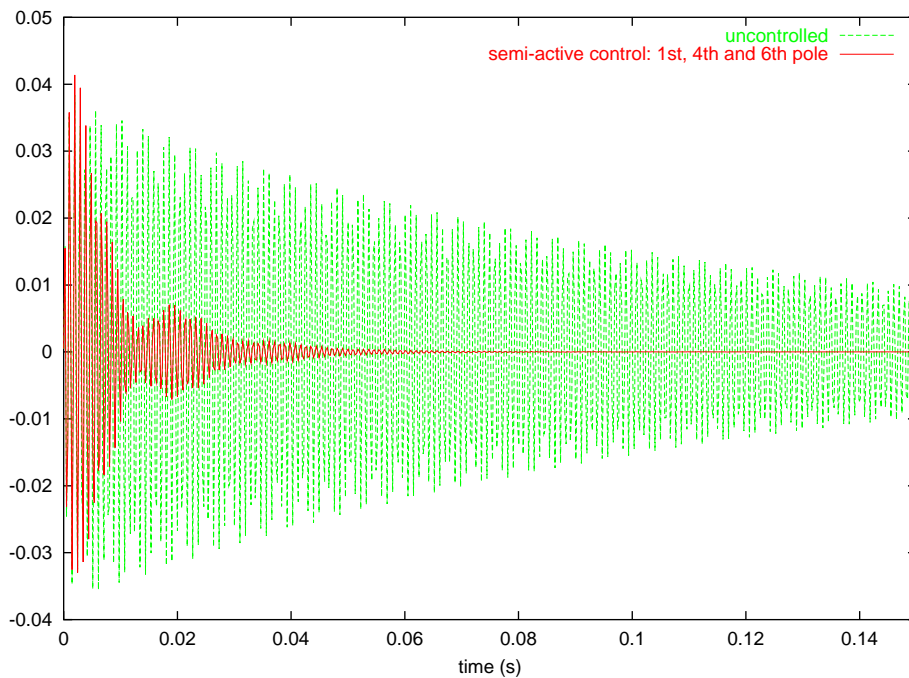

Figure 8.17: Gust response in the time domain with and without piezo patches

the piezoelectric patches is clearly shown. This result confirms that the energy of the structural

vibration is reduced, being possible to transform the mechanical energy into the electrical one and to dissipate it in the piezo shunt system.

It is worth noting that the results shown – in terms of roots loci and gust response – are obtained using a semi-active control, in other words, the actual parametric dependence of the state-space representation on aerodynamics has been considered. Consequently, for each flight condition, the piezoelectric patches are shunted to an adequate electrical load.

Hereafter, in order to show the robustness of the presented network, a comparison between the Wu and the proposed shunted circuit – relative to the gust response – but out of the design conditions, has been realized. Indeed, using shunted circuit components designed for the ground conditions ($U_\infty = 0 \ m/s$, and $\rho = 1.1826 \ kg/m^3$), the numerical tests have been carried out in two different flight situations. The tests conditions – in terms of airflow velocity and altitude (*i.e.*, air density) – are presented in Tab. (8.4).

	$U_\infty = 0 \ m/s \quad h = 0 \ m$	$U_\infty = 15 \ m/s \quad h = 150 \ m$	$U_\infty = 50 \quad m/s \ h = 1500 \ m$
$f_{1st} \ (Hz)$	3.401	3.371	2.734
$f_{4th} \ (Hz)$	34.455	33.71	34.47
$f_{6th} \ (Hz)$	52.601	51.63	49.58

Table 8.4: Comparison between natural frequencies in two different flight and design conditions.

The system poles change for different operative conditions, as shown in the previous table for the natural frequencies, and for this reason the circuit parameters should be re-designed to tune the piezoelectric system.
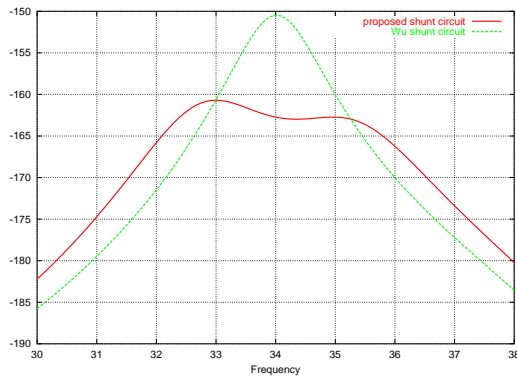

Figure 8.18: Gust response at $U_\infty = 15 \ m/s$, $h = 150 \ m$: zoom in the $4th$ pole neighborhood.

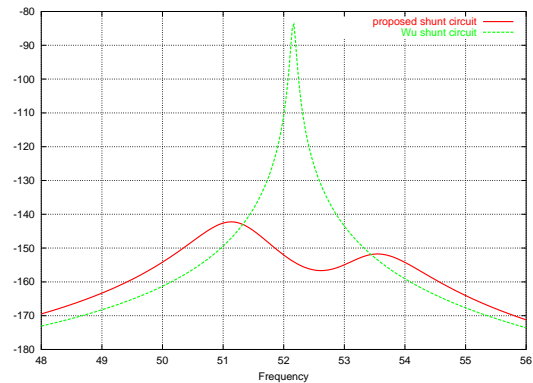Figure 8.19: Gust response at $U_\infty = 15 \ m/s$, $h = 150 \ m$: zoom in the $6th$ pole neighborhood.

The gust responses of the glider wing, relative to the first test conditions and with the piezo devices shunted to the proposed circuit (red line) and Wu's circuit (green line), are depicted in Figs. (8.18), (8.19), and (8.20). It can be pointed out that the response, obtained using the proposed network, presents the typical dynamic damper behavior for each controlled pole. On the contrary, although the application of Wu's technique introduces some damping (less than the one obtained with the
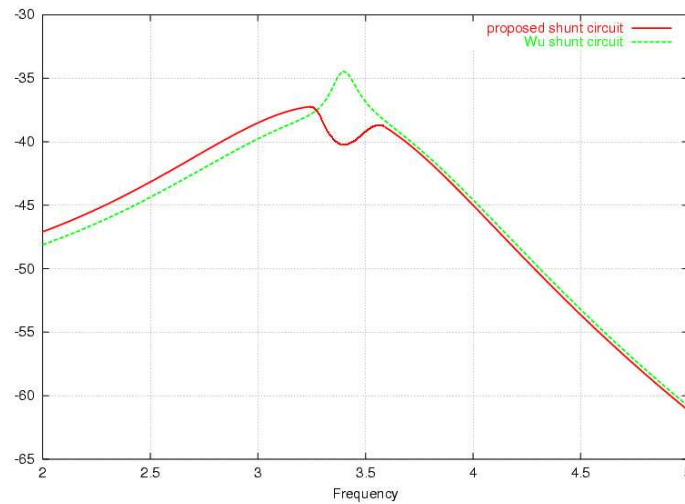
Figure 8.20: Gust response at $U_\infty = 15\ m/s$, $h = 150\ m$: zoom in the $1st$ pole neighborhood.

proposed approach), it does not assure the tuning of the shunt circuit.

The response relative to the second flight conditions is shown in Figs. (8.21) and (8.22). The
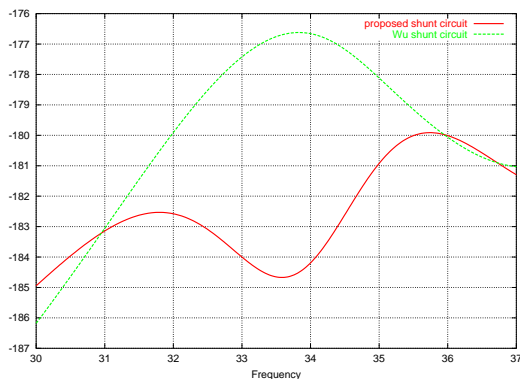

Figure 8.21: Gust response at $U_\infty = 50\ m/s$, $h = 1500\ m$: zoom in the $4th$ pole neighborhood.

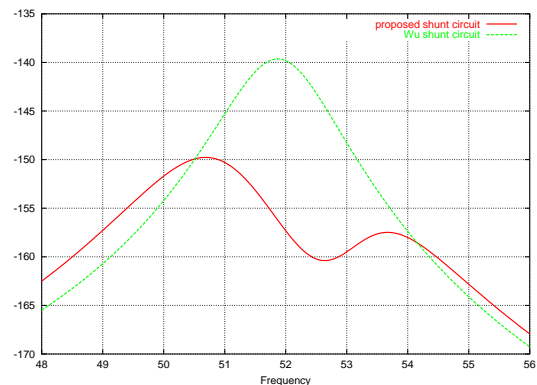
Figure 8.22: Gust response at $U_\infty = 50\ m/s$, $h = 1500\ m$: zoom in the $6th$ pole neighborhood.

response in the neighborhood of the $1st$ pole is not depicted because, in the considered conditions, the $1st$ frequency is very close to zero. Therefore, since the first aeroelastic mode is almost static, practically it does not exist a dynamical response in the $1st$ pole neighborhood. These final tests ensure that it is possible to use the proposed shunt circuit out of the design conditions, that is out of tuning, although in a limited range of flight situations. Moreover, the examples have emphasized the issues associated to the use of the notch-filters. Indeed, the comparison, between the Wu's approach and the proposed one, has underlined how the reliability and the robustness of a piezoelectric passive control are strictly connected to the simplicity of shunt network, *i.e.*, to the notch filter number.

8.9   Concluding remarks

In this chapter a multi-modal passive piezoelectric approach consisting in shunting the piezoelectric patches, bonded to the host structure, to an electrical circuit tuned on the aeroelastic frequency of vibrations has been presented. The point of view adopted is substantially systematic, in the sense that the piezoelectric coupling is integrated in a state-space representation of the aeroelastic system (constructed on the basis of the approximated natural modes of the structure), without entering in the details of the structural model, and of the finite element procedure employed to arrive at the state-space representation. The state-space representation, in terms of the modal co-ordinates, has permitted to recognize a number of coupling effects between the structural, aerodynamical, and piezoelectrical degrees of freedom, and, in particular, to analyze how the vibration energy flows in the piezoelectric systems, and how the aeroelastic systems evolve under the effect of the piezoelectric coupling. In particular, the possibility to damp different modes by a network of the Cauer type, with notch filters, has been considered. This network permits to use less notch filters with respect to other networks proposed in literature. The impedances are simple to derive, being the circuit a ladder network. The proposed circuit is also more robust with regard to the out of tuning, as shown in the thesis. For this reason, it was possible to synthesize the external circuit of the piezo elements by using the data derived from the on ground tests of the glider wing, presented as example. It has been shown that, the presented circuit behave as vibration absorbers also in flight conditions. The numerical examples, presented in this Chapter, have demonstrated the usefulness of the proposed circuit also in the aeroelastic field. The aeroelastic applications on an actual wing of a fully composite glider have revealed the weak capability of these passive devices in improving the stability margin of an actual aeroelastic configuration (the wing of a remote controlled unmanned glider), either by using a mono or three-modal aeroelastic control. Nevertheless, it has also shown that these devices are able to reduce the gust response amplitude, in the parametric range of working of the system, whenever it is in the neighborhood of the controlled poles.

In conclusion, multimodal damping with some piezo devices, each with its electrical load, can be obtained by suitable programs, which allow one to introduce the different electrical circuits or the electrical networks into the stiffness matrix of the piezo devices. Therefore the dynamic behavior of simple structures can be achieved and used in a pre-design program. The positive results obtained press to investigate the possibility to introduce the presented methodologies (or similar), into those mechanical finite element codes, which are commonly used in modelling aerospace structures.

Concluding remarks

This thesis presents a novel mathematical model for micro-structured continuum bodies. Indeed, continua with micro-structure have been considered as best candidate for the analysis and description of structural systems featuring an interaction between different disciplines (*e.g.*, aero-elasticity, thermo-elasticity, electro-elasticity). This attitude has been recognized to be an essential issue in the development of the mathematical model as well as in the applicative examples considered, when dealing with materials that show preferential directions in their constitutive nature.

In a first part, exploiting the potentialities of tensorial algebra and treating bodies as continua with micro-structure, the equilibrium equations have been obtained, in the deformed configuration in terms of the integral stress resultants, by means of the Virtual Work Principle. Therefore, the resulting system of equilibrium equations has been recognized capable of describing non-linear elasticity issues in presence of large displacement and/or large deformations. The use of the Virtual Work Principle permitted to decompose the solution in two contributions. One associated to the motion of the body in presence of a material constraint on the micro-structure, or fiber, of the continuum, and the other expressing the difference between the exact solution in absence of that constraint and of the constrained solution. One chapter has been dedicated to the presentation and discussion of this constraint and, in order to illustrate the purposes and potentialities of the followed approach, a simple applicative example (relevant to a rectilinear homogeneous and transversely isotropic beam) has been considered, where the advantages contained in treating separately the two contributions are apparent, from the computational and modelling points of view. The material constraint chosen falls in the class of the Kirchhoff-Love-type, for shells, and Euler-Bernoulli-type, for beams, and compared to it the Reissner-Mindlin model, regarding to shells, and the Timoshenko model, regarding to beams, have been considered. In both cases, the constraint is kinematically equivalent to a rigidity condition of the fiber to the support (mid-surface for shells, mid-axis for beams) that prevents the fiber from rotating during the motion. In an attempt to apply these models to an innovative structure made with piezo-elastic fibers not normal to the support in the undeformed configuration, the previous constraints have been extended to the case of fibers inclined with respect to the normal. Furthermore, in order to achieve the most formal simplification of the resulting equilibrium equations, three distinct approaches have been analysed to express the virtual displacement field. The first approach, denoted *natural*, employs the intrinsic reference frame, associated to the support in any point; the second approach, employs a triad made of the

tangent vectors to the mid-surface and the unit vector along the fiber; the third approach has been characterized by the consideration of an orthogonal frame made of vectors orthogonal to the fiber and of the unit vector along the fiber.

In the second part, following a conceptual continuity with the previous considerations, three different problems of aerospace interest have been faced: the formal equivalence of the operators describing the equilibrium and, consequently, of the modelling nature of the three problems, has been clearly recognized in these applications. In particular, the first problem has regarded the study of the static response of a shell, reduced to a one-dimensional continuum under appropriate modelling hypothesis, whose fibers, inclined respect to the normal to the mid-surface, have been assumed made of piezo-electric material with principal direction of polarization coherently oriented with the chosen fiber direction. Via the imposition of an electric voltage difference at the edges of each fiber reduced from a modelling point of view to an external load in the structural problem, it has been possible to deform elastically the body and consequently to recognize this application - developed within the line of the considerations exposed in the first part - as a possible candidate for the description of the behaviour of possible future morphing structures capable of deforming up to a desired configuration. The second problem regarded the analysis of the aeroelastic response of a swept wing under the effect of a thermal excitation, reduced, also in this case, to an external load acting on the structural system. The wing structure has been assumed made of homogeneous and transversely isotropic material, with isotropy direction coincident with the fiber direction, this time assumed normal to the mid-plane, both elastically and thermally. Finally, the third problem regarded the presentation of a semi-passive damping technique for aeroelastic vibrations via the use of piezoelectric patches properly shunted on an electrical load resonant a the frequencies of the host aeroelastic system. The approach, exclusively of a systematic nature, permitted the integration of the dynamics of the shunted piezoelectric system with that structural and aeroelastic, and it has permitted to recognize how, from the point of view of the poles of the resulting system, these dynamics interact and influence each other. The resulting damping of the aeroelastic vibrations has been said semi-passive because in any flight condition the shunt circuit parameters have been tuned to optimise the transfer of energy between the aeroelastic and piezoelectric systems and the thus to enhance the vibration suppression.

It is worth noting that, in addition to the formal equivalence of the operators that describe the equilibrium, another element of continuity among the applications presented is represented by the presence of distinct phenomenological physical couplings. These multi-disciplinary couplings (electro-elasticity, thermo-elasticity, aero-elasticity and their combinations) have been faced assuming that the coupling was one-directional, or, in other words, that, the elasticity was influenced by the other discipline (electricity or temperature) but the latter was not influenced by the first, except for the case of the aeroelastic coupling. The principal reason inherent this choice is represented by the request of a modelling simplification that justifies itself with the fact that the previous application were intended more to the presentation of the qualities of the structural model than to description

of the coupling itself. At this regard, it should not be forgot that the choice of assume the body to be a continuum with micro-structure, has been done in order to describe coherently the behaviour of materials and thus structures made of those materials, having a preferential direction.

Either the first and the second part are supplied of a bibliographic documentation that has permitted to underline the innovative feature proposed.

It is now appropriate to discuss some of the enhancements that will be included in the future, either from the theoretical and from the applicative side. In particular, from the theoretical side, the importance of the decomposition of the motion in a part associated to the constraint and in a part expressing the difference between the constrained and the unconstrained solutions has been pointed out in the illustrative example contained in the first part, either from a conceptual (to show how the unconstrained equations reduce in the limit to the constrained equations) and computational point of view. These considerations should be evaluated in general, moreover, the consequences associated to the three different strategies that can be followed adopting this decomposition will be evaluated and compared. Indeed, the decomposition of the displacement field may be assumed: (i) on the virtual displacement and coherently on the effective displacements in the final equilibrium equations; (ii) on the virtual displacement but not in the final equations; (iii) on the final equations but not on the virtual displacements. It is worthy to anticipate that whilst the first approach ensures that the resulting structural operator be self-adjoint, the mixed approaches yield to a problem not symmetric from the point of view of the equilibrium equations but potentially easier to be solved because partially uncoupled. From the applicative side, in addition to expand the presented problems to the considerations of a bi-directional coupling, the first application would deserve of an analysis for determination of the fiber distribution capable of the best actuation performance for an assigned final configuration to be reached by the structure.

29th May 2005

Appendix A

Tensors analysis and operations on tensors

A.1 Vectors and tensors

Following Refs. [87, 23], let $\mathscr{E}$ be a 3-dimensional Euclidean space, let $\mathscr{V}$ be the vector space associated with $\mathscr{E}$ and denote with $\mathcal{U} := \{\mathbf{v} \in \mathscr{V} | \; \|\mathbf{v}\| = 1\}$ the sphere of all vectors having unit length. One may think of $\mathscr{E}$ as equipped with a Cartesian frame $\{\mathcal{O}; \mathbf{e}_1, \mathbf{e}_2, \mathbf{e}_3\}$ with orthogonal basis vectors $\mathbf{e}_i \in \mathcal{U}$ (i= 1, 2, 3); the Cartesian components of a vector $\mathbf{v} \in \mathscr{V}$ are then $v_i := \mathbf{v} \cdot \mathbf{e}_i$ and, in particular, the triplet $(p_1, p_2, p_3) \in \Re^3$, $p_i := \mathbf{p}\,(p) \cdot \mathbf{c}_i$, of components of the position vector are the Cartesian coordinates of a point $p \in \mathscr{E}$.

Now a vector field $\mathbf{w}$ on a domain $\mathscr{W} \in \mathscr{V}$ can be defined as a map

$$\mathbf{w} : \mathscr{W} \mapsto \mathscr{V} \tag{A.1}$$

meaning that in every point $p \in \mathscr{E}$ there exists a rule (*i.e.*, a map) which associates to p a vector $\mathbf{w} \in \mathscr{V}$ (examples of vector fields that will be considered later are the displacement field, the velocity field, the acceleration field, *etc*).

Let us now introduce a general (or convected, or material) curvilinear co-ordinate system $\{\xi^k\}$ as a one-to-one smooth map that maps an open set $\mathscr{U} \subseteq \mathscr{E}$ to $\Re^3$ according to

$$\left(x^1, x^2, x^3\right) \mapsto \left(\xi^1\left(x^i\right), \xi^2\left(x^i\right), \xi^3\left(x^i\right)\right) \tag{A.2}$$

Taking the partial derivatives of the position vector with respect to ξ^k one has

$$\mathbf{g}_k \quad := \quad \frac{\partial x^i}{\partial \xi^k}\, \mathbf{e}_i = x^i_{,k}\, \mathbf{e}_i \tag{A.3}$$

These vectors, known as covariant volume basis vectors, are the tangent vectors to the material co-ordinates and constitute a triplet of independent vectors in terms of which any vector field can be represented. Note that, the $\{\mathbf{g}_k\}$ have a local definition in the sense that they represent the tangents

to the material co-ordinates in a particular point $p \in \mathscr{U}$; moreover, they are linearly independent due to the one-to-one correspondence between the ξ^k and the points $p \in \mathscr{U}$, in fact the Jacobian of the transformation $x^i \mapsto \xi^k (x^i)$ is not vanishing, so the $\{\mathbf{g}_k\}$ are a basis for each (ξ^1, ξ^2, ξ^3). Together with the covariant basis vectors $\{\mathbf{g}_k\}$ one can introduce also the contravariant basis vectors defined as

$$\mathbf{g}_h \cdot \mathbf{g}^k = \delta_h^k \tag{A.4}$$

where δ_h^k is the Kronecker's delta, or

$$\mathbf{g}^1 = \frac{\mathbf{g}_2 \times \mathbf{g}_3}{\sqrt{g}} \tag{A.5}$$

$$\mathbf{g}^2 = \frac{\mathbf{g}_3 \times \mathbf{g}_1}{\sqrt{g}} \tag{A.6}$$

$$\mathbf{g}^3 = \frac{\mathbf{g}_1 \times \mathbf{g}_2}{\sqrt{g}} \tag{A.7}$$

with

$$\sqrt{g} = \mathbf{g}_1 \times \mathbf{g}_2 \cdot \mathbf{g}_3 \tag{A.8}$$

the metrics in p associated to (ξ^k). Similarly, one can introduce a tensorial quantity, known as metric tensor and its own inverse (both symmetric positive definite second rank tensors whose determinant is given by Eq. (A.8)), defined by

$$\mathbf{G} \quad := \quad \mathbf{g}_h \cdot \mathbf{g}_k \; \mathbf{g}^h \otimes \mathbf{g}^k = g_{hk} \; \mathbf{g}^h \otimes \mathbf{g}^k \tag{A.9}$$

and its inverse

$$\mathbf{G}^{-1} \quad := \quad \mathbf{g}^h \cdot \mathbf{g}^k \; \mathbf{g}_h \otimes \mathbf{g}_k = g^{hk} \; \mathbf{g}_h \otimes \mathbf{g}_k \tag{A.10}$$

Thus, any vector field $\mathbf{v} \in \mathscr{V}$ can be written

$$\mathbf{v} \quad := \quad v^k \; \mathbf{g}_k = v^k \; x^i_{,k} \; \mathbf{e}_i \tag{A.11}$$

where

$$v^k \quad := \quad \mathbf{v} \cdot \mathbf{g}^k \tag{A.12}$$

or in terms of the contravariant basis vectors

$$\mathbf{v} \quad := \quad v_k \; \mathbf{g}^k \tag{A.13}$$

where

$$v_k \quad := \quad \mathbf{v} \cdot \mathbf{g}_k \tag{A.14}$$

Similarly, any tensor field $\mathbf{T} \in \mathscr{V}$ has a unique representation in the basis of covariant, contravariant or mixed basis vectors, given by[*]

$$\mathbf{T} \quad := \quad t^{hk} \; \mathbf{g}_h \otimes \mathbf{g}_k = t_{hk} \; \mathbf{g}^h \otimes \mathbf{g}^k = t_k^h \; \mathbf{g}_h \otimes \mathbf{g}^k = t_h^k \; \mathbf{g}^h \otimes \mathbf{g}_k \tag{A.15}$$

where

$$t^{hk} \quad := \quad \mathbf{T} \cdot \mathbf{g}^h \otimes \mathbf{g}^k \tag{A.16}$$

and similar definitions hold with respect to the remaining contravariant and mixed components in Eq. (A.15).

A.2   Gradient, divergence, curl

From *"Tensor Analysis and Continuum Mechanics"*, Ref. [37], Chapter 1.

It is assumed that the reader is familiar with the representation of vectors by arrows, with their addition and their resolution into components, i.e., with the vector parallelogram and its extension to three dimensions. We also assume familiarity with the dot product and later (p.36) with the cross product. Vectors subjected to this special kind of algebra will be called Gibbs type vectors and will be denoted by bold face letters.

In this and the following sections the reader will learn a completely different means of describing the same physical quantities, called tensor algebra. Each of the competing formulations has its advantages and its drawbacks. The Gibbs form of vector algebra is independent of a coordinate system, appeals strongly to visualization and leads easily into graphical methods, while tensor algebra is tied to coordinates, is abstract and very formal. This puts the tensor formulation of physical problems at a clear disadvantage as long as one deals with simple objects, but makes it a powerful tool in situations too complicated to permit visualization. The Gibbs formalism can be extended to physical quantities more complicated than a vector (moments of inertia, stress, strain), but this extension is rather cumbersome and rarely used. On the other hand, the vector appears as a special case of a more general concept, which includes stress and inertia tensors but it is easily extended beyond them.

In order to prove the previous statements and to introduce some useful concepts and operations

---

[*] Extensions to tensors of higher rank can be easily made considering the definition of Eq. (A.15), nonetheless, in Appendix (A) some additional consideration on tensor fields of any order and the operations between tensors are reported.

on tensors, a parallel definition of Gradient, Curl and Divergence of a vector field will be presented. The definition of these operators in Gibbs' notation will be made using Ref. [12], whereas the tensor's counterpart will be addressed using Ref. [94].

Specifically, it will be showed how it is tortuous to express a consistent definition of the Curl within the Gibbs' notation for quantities different from scalars and vectors, compared to the elegance and straightforwardness of the tensorial one. Indeed, very often a mixed definition of these operators can be found in the existing literature, where tensors and Gibbs' notation are used together leading to unavoidable inconsistencies which bring misunderstandings and approximations.

Gradient

Gibbs'

The Gradient of a vector field can be defined as the linear transformation which, applied on an arbitrary vector, gives the variation of the vector field in the direction of the vector on which it is applied, *i.e.*,

$$\operatorname{Grad} \mathbf{f} : \qquad \frac{\partial \mathbf{f}}{\partial \mathbf{v}} = (\operatorname{Grad} \mathbf{f}) \, \mathbf{v} \tag{A.17}$$

Tensors'

The Gradient of a tensor of order *n* can be defined as a tensor of order *n+1* which is obtained multiplying tensorially the derivatives of the tensor, with respect to the covariant coordinates, with the corresponding contravariant base vectors, *i.e.*,

$$\operatorname{Grad} \mathbf{f} : \qquad \operatorname{Grad} \mathbf{f} := \frac{\partial \mathbf{f}}{\partial \xi^j} \otimes \mathbf{g}^j \qquad\qquad for \; j = 1, 2, .. \tag{A.18}$$

Curl

Gibbs'

The curl of a vector field is two times the axial vector of the skew-symmetric part of the Gradient (Ref. [12, p. 149, note 21], where the axial vector is defined as the unique vector $(\mathbf{w})$ associated to any skew-symmetric tensor $(\mathbf{W})$such that $\mathbf{W}\mathbf{v} = \mathbf{w} \times \mathbf{v}$ for any $\mathbf{v}$.

$$\operatorname{Curl} \mathbf{f} : \qquad (\operatorname{Grad} \mathbf{f}) - (\operatorname{Grad} \mathbf{f})^T \, \mathbf{v} = \operatorname{Curl} \mathbf{f} \times \mathbf{v} \qquad\qquad \forall \mathbf{v} \tag{A.19}$$

Alternatively, another definition which makes use of the Stokes' theorem can be casted

$$\operatorname{Curl} \mathbf{f} := \lim_{\Delta S \to 0} \oint_{\mathcal{L}} (\mathbf{f} \cdot d\mathbf{s}) \; \mathbf{n} \tag{A.20}$$

where S is a generic surface which has $\mathcal{L}$ as contour line, and $\mathbf{n}$ is the unit normal (coherently chosen with the orientation defined in the space) to that surface. The above expression permits to interpret the Curl operator as a measure of the infinitesimal circulation experienced by the vector field in space, and in this sense the axial vector helps to identify the direction in which the field rotates (or circulates).

Tensors'

The Curl of a tensor of order n can be defined as a tensor of the same order n which is obtained multiplying vectorially the derivatives of the tensor, with respect to the covariant coordinates, with the corresponding contravariant base vectors, *i.e.*,

$$\mathrm{Curl}\,\mathbf{f}: \qquad \mathrm{Curl}\,\mathbf{f} := -\frac{\partial \mathbf{f}}{\partial \xi^j} \times \mathbf{g}^j \qquad \textit{for } j = 1, 2, .. \qquad (A.21)$$

Divergence

Gibbs'

The divergence of a vector field can be defined as the trace of the gradient of that field.

$$\mathrm{Div}\,\mathbf{f}: \qquad \mathrm{Div}\,\mathbf{f} := \mathrm{tr}\,(\mathrm{Grad}\,\mathbf{f}) \qquad (A.22)$$

Alternatively, or geometrically, the divergence can be intepreted as a mean value of the variation of the field along the three principal directions, in this sense the Green-Gauss theorem which is often used to introduce this operator is very useful. Indeed, from this theorem one can interpret, more correctly, the divergence as the infinitesimal flux outgoing a certain closed surface, or

$$\mathrm{Div}\,\mathbf{f} := \lim_{\Delta S \to 0} \oint \mathbf{f} \cdot d\mathbf{s} \qquad (A.23)$$

Tensors'

The divergence of a tensor of order n can be defined as a tensor of order *n-1* which is obtained dot-producting the derivatives of the tensor, with respect to the covariant coordinates, with the corresponding contravariant base vectors, *i.e.*,

$$\mathrm{Div}\,\mathbf{f}: \qquad \mathrm{Div}\,\mathbf{f} := -\frac{\partial \mathbf{f}}{\partial \xi^j} \cdot \mathbf{g}^j \qquad \textit{for } j = 1, 2, .. \qquad (A.24)$$

Remarks

It is worth to point out that in the previous tensorial definitions of the differential operators, no limit has been placed on the order of the tensor. This means that an easy generalization of these

definitions can be obtained starting from the simple case of a vector field. On the other hand, as it is apparent, for instance, in Ref. [12, page 149, note 48], an analogous generalization is not always possible and other considerations have to be brought for the definition of a Curl of a linear transformation. Moreover, because the scalar fields are tensors of order zero, it is clear that the curl of a scalar has no meaning, involving the cross product of two tensors which can be defined starting from its definition in vectorial notation; eventually, also the divergence could appear meaningless involving the dot product between a scalar and a vector, nonetheless, this operation can still be performed substituting the derivative with the gradient. Similarly, the tensor product of a scalar with a vector can appear meaningless, and so the gradient. Nonetheless, it can be reduced to the scalar multiplication of a vector.

Note also that, previously, attention has been placed in order to not use the word tensor in the definition of the operators within the Gibbs' formulation, unfortunately, often, in the present literature it can be found a mixed and very confusing use of these two expressions.

A.3   On the divergence of a vector

In this appendix useful expressions for the divergence of a vector in three-dimensional and two-dimensional spaces are obtained. Let us first introduce the Christoffel symbols, Γ_{kp}^{h}, defined by

$$\Gamma_{kp}^{h} := \frac{\partial \mathbf{g}_p}{\partial \xi^k} \cdot \mathbf{g}^h = \frac{\partial^2 \mathbf{x}}{\partial \xi^k \partial \xi^p} \cdot \mathbf{g}^h = \Gamma_{pk}^{h} \qquad (A.25)$$

Then, the covariant derivative of a vector

$$\frac{\partial \mathbf{g}_p}{\partial \xi^k} = \Gamma_{kp}^{h} \ \mathbf{g}_h \qquad (A.26)$$

Hence, one has

$$\frac{\partial}{\partial \xi^k} \left(c^p \mathbf{g}_p \right) = \frac{\partial c^p}{\partial \xi^k} \mathbf{g}_p + c^r \ \Gamma_{rk}^{p} \ \mathbf{g}_p = c^p{}_{/k} \ \mathbf{g}_p \qquad (A.27)$$

where, $c^p{}_{/k}$, is given by

$$c^p{}_{/k} := \frac{\partial c^p}{\partial \xi^k} + c^r \ \Gamma_{rk}^{p} \qquad (A.28)$$

The divergence of a vector $\mathbf{c}$ in a three-dimensional space is defined by

$$\text{div} \ \mathbf{c} := c^k{}_{/k} \qquad (A.29)$$

Recalling the invariant nature of tensors, the above is the appropriate generalization of the definition in cartesian coordinates; using Eq. (A.27), one obtains

$$c^p{}_{/p} = \frac{\partial c^p}{\partial \xi^p} + c^r \; \Gamma^p_{rp} = \frac{1}{\sqrt{g}} \frac{\partial}{\partial \xi^p} \left(\sqrt{g} \; c^p \right) \tag{A.30}$$

where the following relation has been used

$$\Gamma^p_{rp} = \frac{1}{\sqrt{g}} \frac{\partial \sqrt{g}}{\partial \xi^r} \tag{A.31}$$

For, using Eqs. (3.35)-(3.38)

$$
\begin{aligned}
\frac{\partial \sqrt{g}}{\partial \xi^r} &= \frac{\partial}{\partial \xi^r} \left(\mathbf{g}_1 \times \mathbf{g}_2 \cdot \mathbf{g}_3 \right) = \\
&= \frac{\partial \mathbf{g}_1}{\partial \xi^r} \cdot \mathbf{g}_2 \times \mathbf{g}_3 + \frac{\partial \mathbf{g}_2}{\partial \xi^r} \cdot \mathbf{g}_3 \times \mathbf{g}_1 + \frac{\partial \mathbf{g}_3}{\partial \xi^r} \cdot \mathbf{g}_1 \times \mathbf{g}_2 \\
&= \sqrt{g} \, \frac{\partial \mathbf{g}_k}{\partial \xi^r} \cdot \mathbf{g}^k = \sqrt{g} \, \Gamma^k_{rk}
\end{aligned}
\tag{A.32}
$$

Similarly, for two-dimensional spaces one has

$$\text{div } \mathbf{c} := c^\alpha{}_{/\alpha} = \frac{\partial c^\alpha}{\partial \xi^\alpha} + c^\beta \; \Gamma^\alpha_{\beta\alpha} \tag{A.33}$$

Note that

$$\Gamma^\alpha_{\alpha\gamma} = \frac{1}{\sqrt{a}} \frac{\partial \sqrt{a}}{\partial \xi^\gamma} \tag{A.34}$$

For, using Eqs. (3.21), (3.26), (3.15) and (3.17)-(3.20) we have

$$
\begin{aligned}
\frac{\partial \sqrt{a}}{\partial \xi^\gamma} &= \frac{\partial}{\partial \xi^\gamma} \left(\mathbf{a}_1 \times \mathbf{a}_2 \cdot \mathbf{n} \right) = \\
&= \frac{\partial \mathbf{a}_1}{\partial \xi^\gamma} \cdot \mathbf{a}_2 \times \mathbf{n} + \frac{\partial \mathbf{a}_2}{\partial \xi^\gamma} \cdot \mathbf{n} \times \mathbf{a}_1 + \frac{\partial \mathbf{n}}{\partial \xi^\gamma} \cdot \mathbf{a}_1 \times \mathbf{a}_2 \\
&= \sqrt{a} \, \Gamma^\beta_{1\gamma} \, \mathbf{a}_\beta \cdot \mathbf{a}^1 + \sqrt{a} \, \Gamma^\beta_{2\gamma} \, \mathbf{a}_\beta \cdot \mathbf{a}^2 = \sqrt{a} \, \Gamma^\alpha_{\alpha\gamma}
\end{aligned}
\tag{A.35}
$$

Hence

$$\text{div } \mathbf{c} := \frac{1}{\sqrt{a}} \frac{\partial}{\partial \xi^\alpha} \left(\sqrt{a} \; c^\alpha \right) = c^\alpha{}_{/\alpha} \tag{A.36}$$

Finally, note that using Eqs. (3.25) and (A.36) one has

$$\frac{\partial}{\partial \xi^\alpha} \left(\sqrt{a} \; c^\alpha \; \mathbf{n} \right) = \frac{\partial}{\partial \xi^\alpha} \left(\sqrt{a} \; c^\alpha \right) \mathbf{n} - \sqrt{a} \; c^\alpha \; b^\beta_\alpha \; \mathbf{a}_\beta = \sqrt{a} \left[c^\alpha{}_{/\alpha} \mathbf{n} - c^\alpha \; b^\beta_\alpha \; \mathbf{a}_\beta \right] \tag{A.37}$$

29th May 2005

A.4   On the divergence of a tensor

In this appendix a convenient expression for the divergence of a (second order) tensor is obtained.

Note that it is valid for an N-dimensional space. In particular, it is valid if the Latin indices are replaced by Greek ones (used in the main body of this work for two-dimensional spaces).

Let us first introduce the covariant derivative of a tensor. Using Eq. (A.26)

$$\frac{\partial}{\partial \xi^k} \left(c^{pq} \, \mathbf{g}_p \otimes \mathbf{g}_q \right) = \frac{\partial c^{pq}}{\partial \xi^k} \, \mathbf{g}_p \otimes \mathbf{g}_q + c^{rq} \, \Gamma^p_{rk} \, \mathbf{g}_p \otimes \mathbf{g}_q + c^{pr} \, \Gamma^q_{rk} \, \mathbf{g}_p \otimes \mathbf{g}_q = c^{pq}{}_{/k} \, \mathbf{g}_p \otimes \mathbf{g}_q \quad \text{(A.38)}$$

where

$$c^{pq}{}_{/k} := \frac{\partial c^{pq}}{\partial \xi^k} + c^{pq} \, \Gamma^p_{rk} + c^{pr} \, \Gamma^q_{rk} \quad \text{(A.39)}$$

In a three-dimensional space, the divergence of a second order tensor $\mathbf{C} = c^{pq} \, \mathbf{g}_p \otimes \mathbf{g}_q$ is a vector defined by

$$\operatorname{Div} \mathbf{C} := c^{pq}{}_{/p} \, \mathbf{g}_p \quad \text{(A.40)}$$

or, using Eqs. (A.32) and (A.38)

$$
\begin{aligned}
\operatorname{Div} \mathbf{C} \quad &:= \quad \frac{\partial c^{pq}}{\partial \xi^p} \, \mathbf{g}_q + c^{rq} \, \Gamma^p_{rp} \, \mathbf{g}_q + c^{pr} \, \Gamma^q_{rp} \, \mathbf{g}_q \\
&= \quad \frac{\partial c^{pq}}{\partial \xi^p} \, \mathbf{g}_q + \frac{1}{\sqrt{g}} \, \frac{\partial \sqrt{g}}{\partial \xi^r} \, c^{rq} \, \mathbf{g}_q + c^{pr} \, \frac{\partial \mathbf{g}_p}{\partial \xi^r} \\
&= \quad \frac{1}{\sqrt{g}} \, \frac{\partial}{\partial \xi^p} \left(\sqrt{g} \, c^{pq} \, \mathbf{g}_q \right) \quad \text{(A.41)}
\end{aligned}
$$

Similarly, in two-dimensional spaces, using the convention on Greek symbols, one may define

$$\operatorname{Div} \mathbf{C} := c^{\alpha\beta}{}_{/\alpha} \, \mathbf{a}_\beta \quad \text{(A.42)}$$

or using Eq. (A.39) specialized to the two-dimensional case, i.e.,

$$c^{\alpha\beta}{}_{/\alpha} := \left(\frac{\partial c^{\alpha\beta}}{\partial \xi^\alpha} + c^{\gamma\beta} \, \Gamma^\alpha_{\alpha\gamma} + c^{\alpha\gamma} \, \Gamma^\beta_{\alpha\gamma} \right) \quad \text{(A.43)}$$

one has

$$
\begin{aligned}
c^{\alpha\beta}{}_{/\alpha}\,\mathbf{a}_\beta &= \frac{\partial c^{\alpha\beta}}{\partial \xi^\alpha}\,\mathbf{a}_\beta + c^{\gamma\beta}\,\Gamma^\alpha_{\gamma\alpha}\,\mathbf{a}_\beta + c^{\alpha\gamma}\,\Gamma^\beta_{\gamma\alpha}\,\mathbf{a}_\beta \\
&= \frac{\partial c^{\alpha\beta}}{\partial \xi^\alpha}\,\mathbf{a}_\beta + \frac{1}{\sqrt{a}}\,\frac{\partial \sqrt{a}}{\partial \xi^\gamma}\,c^{\gamma\beta}\,\mathbf{a}_\beta + c^{\alpha\gamma}\left(\frac{\partial \mathbf{a}_\gamma}{\partial \xi^\alpha} - b_{\alpha\gamma}\,\mathbf{n}\right) \\
&= \frac{1}{\sqrt{a}}\frac{\partial}{\partial \xi^\alpha}\left(\sqrt{a}\,c^{\alpha\beta}\mathbf{a}_\beta\right) - b_{\alpha\gamma}\,c^{\alpha\gamma}\,\mathbf{n}
\end{aligned} \tag{A.44}
$$

where Eqs. (3.21) and (A.35) have been used.

A.5   Operations on Tensors

In this Section some basic properties of the operations on tensors, that have been used extensively in the main body of this thesis, are reported. In particularly, these notes are an extract of the extensive appendix on this matter that can be found in Ref. [94].

Let us start, recalling that scalars (or real numbers) are referred to as tensors of order zero, and vectors are referred to as tensors of order one. Higher order tensors can thus be defined inductively starting from the notion of a vector. In particular, one may state that the quantity $\mathbf{T}$ is a tensor of order two if it is a linear operator whose domain is the space of all vectors $\mathbf{v}$ and whose range $\mathbf{Tv}$ is a vector. Consequently, by induction, the quantity $\mathbf{T}$ is called a tensor of order M $(M \geq 1)$ if it is a linear operator whose domain is the space of all vectors $\mathbf{v}$ and whose range $\mathbf{Tv}$ is a tensor of order $M - 1$.

In order to define the operations of tensor product, dot product, and juxtaposition for tensors, one may refer to special tensors as it is reported also in Ref. [94].

Tensor Product

The tensor product operation is denoted by the symbol $\otimes$ and it is defined so that for an arbitrary vector $\mathbf{v}$, the quantity $(\mathbf{a}_1 \otimes \mathbf{a}_2)$ is a second order tensor satisfying the following relations

$$
(\mathbf{a}_1 \otimes \mathbf{a}_2)\,\mathbf{v} = \mathbf{a}_1\,(\mathbf{a}_2 \cdot \mathbf{v}) \tag{A.45}
$$

In generalizing these ideas, let $\mathbf{A}$ be a special tensor of order M which is formed by the tensor product of a string of M $(M \geq 2)$ vectors $(\mathbf{a}_1, \mathbf{a}_2, ..., \mathbf{a}_M)$, and let $\mathbf{B}$ be a special tensor of order N formed by a string of N $(N \geq 2)$ vectors $(\mathbf{b}_1, \mathbf{b}_2, ..., \mathbf{b}_M)$. It then follows that $\mathbf{A}$ satisfies the relations

$$
\begin{aligned}
\mathbf{A}\mathbf{v} &= (\mathbf{a}_1 \otimes \mathbf{a}_2 \otimes ... \otimes \mathbf{a}_{M-1})\,(\mathbf{a}_M \cdot \mathbf{v}) \\
\mathbf{v}\mathbf{A} &= (\mathbf{a}_1 \cdot \mathbf{v})\,(\mathbf{a}_2 \otimes \mathbf{a}_3 \otimes ... \otimes \mathbf{a}_M)
\end{aligned} \tag{A.46}
$$

29th May 2005

Therefore, when $\mathbf{v}$ operates either on the right or the left side of $\mathbf{A}$ it has the effect of forming the scalar product with the vector in the string closest to it, and it causes the result $\mathbf{Av}$ or $\mathbf{vA}$ to have order one less than the order of $\mathbf{A}$ since one of the tensor products is removed.

Dot Product

The dot product operation between two vectors can be generalized to an operation between two tensors of any order. For example, the dot product between a second order tensor and a third order tensor can be written as

$$
\begin{aligned}
(\mathbf{a}_1 \otimes \mathbf{a}_2) \cdot (\mathbf{b}_1 \otimes \mathbf{b}_2 \otimes \mathbf{b}_3) &= (\mathbf{a}_1 \cdot \mathbf{b}_1)(\mathbf{a}_2 \cdot \mathbf{b}_2)\,\mathbf{b}_3 \\
(\mathbf{b}_1 \otimes \mathbf{b}_2 \otimes \mathbf{b}_3) \cdot (\mathbf{a}_1 \otimes \mathbf{a}_2) &= \mathbf{b}_1\,(\mathbf{b}_2 \cdot \mathbf{a}_1)(\mathbf{b}_3 \cdot \mathbf{a}_2)
\end{aligned}
\tag{A.47}
$$

From the previous example it is apparent that the dot product between tensors of different order does not necessarily commute, moreover, it can be seen that the tensor of smallest order controls the outcome of the dot product operation. Finally, in general, the dot product $\mathbf{A} \cdot \mathbf{B}$ of the tensors defined before is a tensor of order $|M - N|$.

Cross Product

The dot product operation between two vectors can be generalized to an operation between two tensors of any order. For example, the dot product between a second order tensor and a third order tensor can be written as

$$
\begin{aligned}
(\mathbf{a}_1 \otimes \mathbf{a}_2) \times (\mathbf{b}_1 \otimes \mathbf{b}_2 \otimes \mathbf{b}_3) &= (\mathbf{a}_1 \times \mathbf{b}_1) \otimes (\mathbf{a}_2 \times \mathbf{b}_2) \otimes \mathbf{b}_3 \\
(\mathbf{b}_1 \otimes \mathbf{b}_2 \otimes \mathbf{b}_3) \times (\mathbf{a}_1 \otimes \mathbf{a}_2) &= \mathbf{b}_1 \otimes (\mathbf{b}_2 \times \mathbf{a}_1) \otimes (\mathbf{b}_3 \times \mathbf{a}_2)
\end{aligned}
\tag{A.48}
$$

From the previous example it is apparent that the cross product between tensors of different order does not necessarily commute, moreover, it can be seen that the tensor of smallest order controls the outcome of the cross product operation. Finally, in general, the dot product $\mathbf{A} \cdot \mathbf{B}$ of the tensors defined before is a tensor of order $|N|$ which is equal to the highest order tensor $\mathbf{B}$.

Juxtaposition

The operation of juxtaposition is indicated when two tensors are placed next to each other without an operator between. In particular, the juxtaposition operation causes only one of the vectors in each tensor (the vector closest to each other) to be connected by the inner product. The remaining vectors form a string of vectors connected by tensor products. The sorting of these vectors in the string is the same as their sorting in the juxtaposition operation. The order of the resulting tensor is the sum of the orders of the two tensors placed in juxtaposition minus two.

In general, the juxtaposition $\mathbf{A}\mathbf{B}$ of the special tensors defined before is a tensor of order $(M + N - 2)$ which is given by

$$
\begin{aligned}
\mathbf{A}\mathbf{B} &= (\mathbf{a}_1 \otimes \mathbf{a}_2 \otimes ... \otimes \mathbf{a}_M)(\mathbf{b}_1 \otimes \mathbf{b}_2 \otimes ... \otimes \mathbf{b}_N) \\
&= (\mathbf{a}_M \cdot \mathbf{b}_1)(\mathbf{a}_2 \otimes ... \otimes \mathbf{a}_{M-1}) \otimes (\mathbf{b}_2 \otimes ... \otimes \mathbf{b}_N)
\end{aligned}
\tag{A.49}
$$

From the previous example it is apparent that the juxtaposition operation is not commutative. Furthermore, since only the closest vectors are connected by the inner product, it follows that the juxtaposition of any order tensor $\mathbf{A}$ with a vector $\mathbf{v}$, is the same as the dot product of the two tensors

$$
\mathbf{A}\mathbf{v} = \mathbf{A} \cdot \mathbf{v} \,, \qquad \mathbf{v}\mathbf{A} = \mathbf{v} \cdot \mathbf{A}
\tag{A.50}
$$

Appendix B

Gradient vs Divergence approach: a comparison

In this chapter a comparison between the so-called "gradient approach" and the "divergence approach" is presented. Both the two approaches have been used in the main body of the thesis to obtain the equilibrium equations and the related boundary conditions[‡] for shell-like bodies. In particular, these notes are limited to the consideration of the "Surface Convected Frame" approach (preferred to the other ones for its generality), and discuss the obtainment of both the equilibrium equations and of the related boundary conditions.

B.1 Equilibrium equations

In this Section the equilibrium equations (Eqs. (4.76)-(4.77)) using the gradient and the divergence approach respectively, starting from the expression of the inner virtual work already employed in the main body of the thesis, are derived.

B.1.1 Gradient approach

It has been denoted with this name the approach that permit to obtain the equilibrium equations by expressing the Gradient operator on the basis of the $\overset{o}{g}{}^{k}$ vectors and then performing an integration by parts.

[‡] Recall, in particular, that in Chapter 2 the second has been used, whereas in the subsequent chapters the first one has been preferred.

Let us recall Eq. (4.57)

$$
\begin{aligned}
\delta \mathcal{W}_i &= \iiint_{\mathcal{V}} \mathbf{T} \cdot \operatorname{Grad} \mathbf{v} \, d\mathcal{V} = \iiint_{\mathcal{V}_0} \mathbf{T} \cdot \operatorname{Grad} \mathbf{v} \, \sqrt{g} \, d\xi^1 d\xi^2 d\zeta \\
&= \iiint_{\mathcal{V}_0} \sqrt{\mathring{g}} \left\{ \mathring{\mathbf{S}} \cdot \left(\mathring{\nabla} \otimes \mathring{\mathbf{u}} - \mathring{u}_3 \mathbf{C} \right) + \mathring{r} \, \mathring{u}_3' + \mathring{\mathbf{p}} \cdot \mathring{\mathbf{u}}' \right. \\
&\quad + \left. \mathring{\mathbf{q}} \cdot \left[\mathring{\nabla} \mathring{u}_3 - \mathbf{d} \, \mathring{u}_3 + \mathbf{C}^T \mathring{\mathbf{u}} \right] \right\} d\xi^1 d\xi^2 d\zeta
\end{aligned}
\tag{B.1}
$$

Focusing on the first term in the previous equation, one has

$$
\begin{aligned}
\iiint_{\mathcal{V}_0} \sqrt{\mathring{g}} \, \mathring{\mathbf{S}} \cdot \mathring{\nabla} \otimes \mathring{\mathbf{u}} \, d\xi^1 d\xi^2 d\zeta &= \iiint_{\mathcal{V}_0} \sqrt{\mathring{g}} \, \mathring{\sigma}^{\beta\alpha} \left(\frac{\partial \mathring{u}_\alpha}{\partial \xi^\beta} - \mathring{u}_\gamma \, \mathring{\Gamma}^\gamma_{\alpha\beta} \right) d\xi^1 d\xi^2 d\zeta \\
&= \iiint_{\mathcal{V}_0} \left[\frac{\partial}{\partial \xi^\beta} \left(\sqrt{\mathring{g}} \, \mathring{\sigma}^{\beta\alpha} \, \mathring{u}_\alpha \right) - \sqrt{\mathring{g}} \, \mathring{\Gamma}^k_{\beta k} \, \mathring{\sigma}^{\beta\alpha} \, \mathring{u}_\alpha - \sqrt{\mathring{g}} \, \frac{\partial \mathring{\sigma}^{\beta\alpha}}{\partial \xi^\beta} \, \mathring{u}_\alpha \right. \\
&\quad \left. - \sqrt{\mathring{g}} \, \mathring{\sigma}^{\beta\alpha} \mathring{\Gamma}^\gamma_{\alpha\beta} \, \mathring{u}_\gamma \right] d\xi^1 d\xi^2 d\zeta \\
&= \iiint_{\mathcal{V}_0} \left[\frac{\partial}{\partial \xi^\beta} \left(\sqrt{\mathring{g}} \, \mathring{\sigma}^{\beta\alpha} \, \mathring{u}_\alpha \right) - \left(\mathring{\nabla} \cdot \mathring{\mathbf{S}} \right) \cdot \mathring{\mathbf{u}} \right] d\xi^1 d\xi^2 d\zeta
\end{aligned}
\tag{B.2}
$$

where the 2-D divergence of the tensor $\mathring{\mathbf{S}}$, with respect to the metrics of the $\mathring{\mathbf{g}}^k$ vectors, is defined as

$$
\mathring{\nabla} \cdot \mathring{\mathbf{S}} = \mathring{\sigma}^{\beta\alpha}_{\angle\beta} \, \mathring{\mathbf{g}}_\alpha := \left(\frac{\partial \mathring{\sigma}^{\beta\alpha}}{\partial \xi^\beta} + \mathring{\Gamma}^k_{\beta k} \, \mathring{\sigma}^{\beta\alpha} + \mathring{\sigma}^{\beta\gamma} \mathring{\Gamma}^\alpha_{\gamma\beta} \right) \mathring{\mathbf{g}}_\alpha
\tag{B.3}
$$

Similarly, for the fifth term in Eq. (B.1) one has

$$
\begin{aligned}
\iiint_{\mathcal{V}_0} \sqrt{\mathring{g}} \, \mathring{\mathbf{q}} \cdot \mathring{\nabla} \mathring{u}_3 \, d\xi^1 d\xi^2 d\zeta &= \iiint_{\mathcal{V}_0} \sqrt{\mathring{g}} \, \mathring{\sigma}^{\beta3} \, \frac{\partial \mathring{u}_3}{\partial \xi^\beta} \, d\xi^1 d\xi^2 d\zeta \\
&= \iiint_{\mathcal{V}_0} \left[\frac{\partial}{\partial \xi^\beta} \left(\sqrt{\mathring{g}} \, \mathring{\sigma}^{\beta3} \, \mathring{u}_3 \right) - \sqrt{\mathring{g}} \, \mathring{\Gamma}^k_{\beta k} \, \mathring{\sigma}^{\beta3} \, \mathring{u}_3 - \sqrt{\mathring{g}} \, \frac{\partial \mathring{\sigma}^{\beta3}}{\partial \xi^\beta} \, \mathring{u}_3 \right] d\xi^1 d\xi^2 d\zeta \\
&= \iiint_{\mathcal{V}_0} \left[\frac{\partial}{\partial \xi^\beta} \left(\sqrt{\mathring{g}} \, \mathring{\sigma}^{\beta3} \, \mathring{u}_3 \right) - \left(\mathring{\nabla} \cdot \mathring{\mathbf{q}} \right) \mathring{u}_3 \right] d\xi^1 d\xi^2 d\zeta
\end{aligned}
\tag{B.4}
$$

where the 2-D divergence of the vector $\mathring{\mathbf{q}}$, with respect to the metrics of the $\mathring{\mathbf{g}}^k$ vectors, is defined as

$$
\mathring{\nabla} \cdot \mathring{\mathbf{q}} = \mathring{\sigma}^{\beta3}_{\angle\beta} := \frac{\partial \mathring{\sigma}^{\beta3}}{\partial \xi^\beta} + \mathring{\Gamma}^k_{\beta k} \, \mathring{\sigma}^{\beta3} = \frac{1}{\sqrt{\mathring{g}}} \frac{\partial}{\partial \xi^\beta} \left(\frac{\mathring{g}}{\mathring{\sigma}} \right)^{\beta3}
\tag{B.5}
$$

It is now apparent that the application of the previous relations (that may be regarded as an extension of the Green-Gauss theorem) in Eq. (B.1) leads to the equilibrium equations reported in Eqs. (4.76)-(4.77).

B.1.2 Divergence approach

It has been denoted with this name the approach consisting in applying first the Green-Guass theroem in the 3-D body manifold, and then decomposing the 3-D Divergence operator in the 2-D and 1-D manifolds that concur to the definition of the micro-structure of the body.

Recall the expression of the virtual work in the 3-D metrics

$$
\begin{aligned}
\delta \mathcal{W}_i &= \iiint_{\mathcal{V}} \mathbf{T} \cdot \operatorname{Grad} \mathbf{v} \; d\mathcal{V} = \iiint_{\mathcal{V}_0} \tau^{hk} \; \mathbf{u}_{k\|h} \; \sqrt{g} \; d\xi^1 d\xi^2 d\zeta \\
&= \iiint_{\mathcal{V}_0} \tau^{hk} \left(\frac{\partial \hat{u}_k}{\partial \xi^h} - \hat{\Gamma}^r_{kh} \; \hat{u}_r \right) \sqrt{g} \; d\xi^1 d\xi^2 d\zeta \\
&= \iiint_{\mathcal{V}_0} \left[\frac{\partial}{\partial \xi^h} \left(\sqrt{g} \; \tau^{hk} \; \hat{u}_k \right) - \sqrt{g} \; \operatorname{Div} \mathbf{T} \cdot \mathbf{u} \right] d\xi^1 d\xi^2 d\zeta
\end{aligned}
\tag{B.6}
$$

where the following definition for the 3-D Divergence operator has been used

$$
\operatorname{Div} \mathbf{T} = \tau^{hk}_{\|h} \; \mathbf{g}_k := \left(\frac{\partial \tau^{hk}}{\partial \xi^h} + \hat{\Gamma}^r_{hr} \; \tau^{hk} + \tau^{hr} \hat{\Gamma}^k_{rh} \right) \mathbf{g}_k = \frac{1}{\sqrt{g}} \; \frac{\partial}{\partial \xi^h} \left(\sqrt{g} \; \tau^{hk} \; \mathbf{g}_k \right)
\tag{B.7}
$$

Thus, using the definitions of the shifters (cfr. Eqs. (3.52)-(3.55)) and the definition of the stress terms on the surface conveted frame (cfr. Eqs. (4.58)-(4.61)), one has

$$
\begin{aligned}
\operatorname{Div} \mathbf{T} &= \frac{1}{\sqrt{g}} \; \frac{\partial}{\partial \xi^\beta} \left[\sqrt{\overset{\circ}{g}} \left(\overset{\circ}{\sigma}{}^{\beta\alpha} \; \overset{\circ}{\mathbf{g}}_\alpha + \overset{\circ}{\sigma}{}^{\beta 3} \; \overset{\circ}{\mathbf{g}}_3 \right) \right] \\
&+ \frac{1}{\sqrt{g}} \; \frac{\partial}{\partial \zeta} \left[\sqrt{\overset{\circ}{g}} \left(\overset{\circ}{\sigma}{}^{3\alpha} \; \overset{\circ}{\mathbf{g}}_\alpha + \overset{\circ}{\sigma}{}^{33} \; \overset{\circ}{\mathbf{g}}_3 \right) \right]
\end{aligned}
\tag{B.8}
$$

With reference to the first term in the previous equation, one has

$$
\begin{aligned}
\iiint_{\mathcal{V}_0} \frac{\partial}{\partial \xi^\beta} \left(\sqrt{\overset{\circ}{g}} \; \overset{\circ}{\sigma}{}^{\beta\alpha} \; \overset{\circ}{\mathbf{g}}_\alpha \right) \cdot \mathbf{u} \; d\xi^1 \; d\xi^2 \; d\zeta &= \\
= \iiint_{\mathcal{V}_0} \sqrt{\overset{\circ}{g}} \left(\overset{\circ}{\sigma}{}^{\beta\alpha}_{\angle\beta} \; \overset{\circ}{\mathbf{g}}_\alpha + \overset{\circ}{\sigma}{}^{\beta\alpha} \; c_{\alpha\beta} \; \overset{\circ}{\mathbf{g}}_3 \right) \cdot \mathbf{u} \; d\xi^1 \; d\xi^2 \; d\zeta & \\
= \iiint_{\mathcal{V}_0} \sqrt{\overset{\circ}{g}} \left[\left(\overset{\circ}{\nabla} \cdot \overset{\circ}{\mathbf{S}} \right) \cdot \overset{\circ}{\mathbf{u}} + \overset{\circ}{\mathbf{S}} \cdot \mathbf{C}^T \overset{\circ}{u}_3 \right] d\xi^1 \; d\xi^2 \; d\zeta &
\end{aligned}
\tag{B.9}
$$

where Eq. (B.3) has been used to express the 3-D divergence operator on the 2-D manifold.

29th May 2005

With reference to the second term in Eq. (B.8), one has

$$
\iiint_{\mathcal{V}_0} \frac{\partial}{\partial \xi^\beta} \left(\sqrt{\mathring{g}} \, \mathring{\sigma}^{\beta 3} \, \mathring{\mathbf{g}}_3 \right) \cdot \mathbf{u} \, d\xi^1 \, d\xi^2 \, d\zeta =
$$

$$
= \iiint_{\mathcal{V}_0} \sqrt{\mathring{g}} \left[\left(\mathring{\sigma}^{\beta 3}_{\angle \beta} + \mathring{\sigma}^{\beta 3} \, d_\beta \right) \mathring{\mathbf{g}}_3 - \mathring{\sigma}^{\beta 3} \, c^\gamma_\beta \, \mathring{u}_\gamma \right] d\xi^1 \, d\xi^2 \, d\zeta
$$

$$
= \iiint_{\mathcal{V}_0} \sqrt{\mathring{g}} \left[\left(\mathring{\nabla} \cdot \mathring{\mathbf{q}} \right) \mathring{u}_3 + \mathbf{C}^T \, \mathring{\mathbf{q}} \cdot \mathring{\mathbf{u}} \right] d\xi^1 \, d\xi^2 \, d\zeta \tag{B.10}
$$

where the definition of the divergence operator of $\mathring{\mathbf{q}}$ in Eq. (B.5) has been used.

It is still apparent that the equilibrium equations, Eqs. (4.76)-(4.77), could be also obtained by means of this second approach.

B.2 Boundary conditions

In this Section the boundary conditions (Eqs. (4.75) and (5.97)) are derived using the gradient and the divergence approach respectively, starting from the expression of the inner virtual work already employed in the previous Section. The analysis has been divided into two parts: the first related to the work exerted on the upper and lower surfaces (that will enter the equilibrium equations for the shell model), and the second related to the work on the contour (that represent the actual boundary conditions for the shell model).

B.2.1 Upper and Lower Surfaces

In this section the expression of the boundary terms (from the point of view of 3-D elasticity) are developed on the upper and lower surfaces, and it will be shown how they re-enter the equilibrium equations of the shell model.

Gradient approach

Recalling Eqs. (4.67)-(4.68), from the third and fourth terms in Eq. (B.1) one has

$$
\iiint_{\mathcal{V}_0} \sqrt{\mathring{g}} \left(\mathring{r} \, \mathring{u}'_3 + \mathring{\mathbf{p}} \cdot \mathring{\mathbf{u}}' \right) d\xi^1 \, d\xi^2 \, d\zeta
$$

$$
= \sum_{k=0}^{N} k \int_{\mathcal{S}_0} \sqrt{\mathring{g}} \left(\mathring{r}_{(k-1)} \mathring{u}_{3_k} + \mathring{\mathbf{p}}_{(k-1)} \cdot \mathring{\mathbf{u}}_{(k)} \right) d\xi^1 \, d\xi^2 \tag{B.11}
$$

From the previous Equation it is apparent that the virtual work on the upper and lower surfaces contributes to the equilibrium in the domain of integration of the shell model, or, in other words, that these terms enter the equilibrium equations and not the boundary conditions for the shell model.

Divergence approach

In this case let us start from Eq. (B.6) and, in particular, let us concentrate on the first term in that Equation for $h = 3$ (*i.e.*, the derivative along the thickness).

$$\iiint_{\mathcal{V}_0} \frac{\partial}{\partial \zeta} \left(\sqrt{g}\ \tau^{3k}\ \hat{u}_k \right)\ d\xi^1\ d\xi^2\ d\zeta = \int_{\mathcal{S}_0} \left[\sqrt{g}\ \tau^{3k}\ \hat{u}_k \right]_{-1}^{+1}\ d\xi^1\ d\xi^2 \qquad \text{(B.12)}$$

Recalling that

$$\sqrt{g}\ \tau^{3k}\ \hat{u}_k \;\; = \;\; \sqrt{g}\ \tau^{3k}\ \mathbf{g}_k \cdot \mathbf{u} = \sqrt{g}\ \tau^{3k}\ \overset{\circ}{\mathscr{T}}{}^{\,p}_k\ \overset{\circ}{\mathbf{g}}_p \cdot \mathbf{u} = \sqrt{\overset{\circ}{g}} \left(\overset{\circ}{\sigma}{}^{3\alpha}\ \overset{\circ}{u}_\alpha + \overset{\circ}{\sigma}{}^{33}\ \overset{\circ}{u}_3 \right) \qquad \text{(B.13)}$$

thus substituting Eq. (B.13) in Eq. (B.12) yields

$$\iiint_{\mathcal{V}_0} \frac{\partial}{\partial \zeta} \left(\sqrt{g}\ \tau^{3k}\ \hat{u}_k \right)\ d\xi^1\ d\xi^2\ d\zeta = \sum_{k=0}^{N} \int_{\mathcal{S}_0} \sqrt{\overset{\circ}{g}} \left(\overset{\circ}{\mathbf{P}}_{(k-1)} \cdot \overset{\circ}{\mathbf{u}} + \overset{\circ}{r}_{(k-1)}\ \overset{\circ}{u}_{3_{(k)}} \right)\ d\xi^1\ d\xi^2 \quad \text{(B.14)}$$

Again the previous result confirms the equivalence of the two approaches.[†]

B.2.2   Contour Surface

In this section the expression of the boundary terms coming from the virtual work on the contour surface of the shell is developed.

Gradient approach

From the first term in Eqs. (B.2) and (B.4) one has

$$\iiint_{\mathcal{V}_0} \frac{\partial}{\partial \xi^\beta} \left[\sqrt{\overset{\circ}{g}} \left(\overset{\circ}{\sigma}{}^{\beta\alpha}\ \overset{\circ}{u}_\alpha + \overset{\circ}{\sigma}{}^{\beta 3}\ \overset{\circ}{u}_3 \right) \right]\ d\xi^1 d\xi^2 d\zeta$$

$$= \sum_{k=0}^{N} \int_{\mathcal{S}_0} \frac{\partial}{\partial \xi^\beta} \left[\sqrt{\overset{\circ}{g}} \left(\overset{\circ}{n}{}^{\beta\alpha}_{(k)}\ \overset{\circ}{u}_{\alpha_{(k)}} + \overset{\circ}{q}{}^{\beta}\ \overset{\circ}{u}_{3_{(k)}} \right) \right]\ d\xi^1\ d\xi^2 \qquad \text{(B.15)}$$

Now, recall that (see Section 2.2.3 for comparison) on the contour surface one has

$$d\xi^2 \;\; = \;\; \sqrt{a_c}\ n_{c_1}\ d\gamma \qquad \text{(B.16)}$$

$$d\xi^1 \;\; = \;\; -\sqrt{a_c}\ n_{c_2}\ d\gamma \qquad \text{(B.17)}$$

[†] As a matter of fact let us observe that the previous proofs could also be obtained (as it was done in Chapter 2) starting from the expression of the normal to the upper and lower surfaces in terms of the covariant and contravariant base vectors of the SCF. In particular, let us observe that, being ζ a material coordinate, the upper and lower surfaces (respectively $\zeta = +1$ and $\zeta = -1$) are also co-ordinate surfaces and thus the normal to these surfaces is parallel to $\mathbf{g}^3$.

thus, substituting the previous relations in Eq. (B.15) one has

$$
\iiint_{\mathcal{V}_0} \frac{\partial}{\partial \xi^\beta} \left[\sqrt{\mathring{g}} \left(\mathring{\sigma}^{\beta\alpha} \, \mathring{u}_\alpha + \mathring{\sigma}^{\beta 3} \, \mathring{u}_3 \right) \right] \, d\xi^1 d\xi^2 d\zeta = \sum_{k=0}^{N} \oint_\Gamma \left(\mathring{\mathbf{N}}_{(k)}^T \boldsymbol{\nu} \cdot \mathring{\mathbf{u}} + \mathring{\mathbf{q}}_{(k)} \cdot \boldsymbol{\nu} \, \mathring{u}_{3_{(k)}} \right) \, d\gamma \quad \text{(B.18)}
$$

where $\boldsymbol{\nu} = \mathbf{n}_c \sqrt{a_c \mathring{g}}$ is a vector parallel to outer normal to the contour line of the main surface.

Divergence approach

From Eq. (B.6) and, in particular, from the first term in that Equation for $h = \alpha$, one has

$$
\iiint_{\mathcal{V}_0} \frac{\partial}{\partial \xi^\alpha} \left(\sqrt{g} \, \tau^{\alpha k} \, \hat{u}_k \right) \, d\xi^1 \, d\xi^2 \, d\zeta
$$
$$
= \int_{\xi^2} \int_{-1}^{+1} \left[\sqrt{g} \, \tau^{\alpha k} \, \hat{u}_k \right]_{\xi^1} \, d\zeta \, d\xi^2 + \int_{\xi^1} \int_{-1}^{+1} \left[\sqrt{g} \, \tau^{\alpha k} \, \hat{u}_k \right]_{\xi^2} \, d\zeta \, d\xi^1 \quad \text{(B.19)}
$$

Using again Eqs. (B.16) and (B.17), and recalling the expression of the stress terms on the SCF in terms of the stress terms in the volume frame, one has

$$
\iiint_{\mathcal{V}_0} \frac{\partial}{\partial \xi^\alpha} \left(\sqrt{g} \, \tau^{\alpha k} \, \hat{u}_k \right) \, d\xi^1 \, d\xi^2 \, d\zeta = \sum_{k=0}^{N} \oint_\Gamma \left(\mathring{\mathbf{N}}_{(k)}^T \boldsymbol{\nu} \cdot \mathring{\mathbf{u}} + \mathring{\mathbf{q}}_{(k)} \cdot \boldsymbol{\nu} \, \mathring{u}_{3_{(k)}} \right) \, d\gamma \quad \text{(B.20)}
$$

So it is proved the complete equivalence between the two approaches.[‡]

[‡] Also with respect to the virtual work on the contour surface, note that one could alternatively (as it has been done in Chapter 2) start from the virtual work on the contour surface, then express the normal to this surface in terms of the base vectors of the Surface Convected Frame and finally obtain the same relations previously developed.

Appendix C

Model matrices for aero-thermo-elastic analysis

In the following the expressions of the matricial operators introduced in Eq. 7.221 are reported (for a definition of the coefficients used refer to the list of symbols reported in the nomenclature section)

$$
M \ = \ \begin{bmatrix}
-I^{(0,0)} & 0 & 0 & 0 & 0 \\
0 & -I^{(0,2)} & 0 & 0 & 0 \\
0 & 0 & -I^{(2,2)} & 0 & 0 \\
0 & 0 & 0 & -I^{(0,2)} - I^{(2,0)} - I^{(0,0)} {x_0}^2 & -I^{(0,0)} x_0 \\
0 & 0 & 0 & -I^{(0,0)} x_0 & I^{(0,0)}
\end{bmatrix}
$$

$$
K \ = \ \begin{bmatrix}
-\dfrac{A\,E}{1-\nu^2} & 0 & 0 & 0 & 0 \\
0 & -\dfrac{C_1\,E}{1-\nu^2} & 0 & 0 & 0 \\
0 & 0 & -\dfrac{D\,E}{1-\nu^2} & 0 & 0 \\
0 & 0 & 0 & -\dfrac{C_1\,E}{2\,(1+\nu)} - C_2\,G' & 0 \\
0 & 0 & 0 & 0 & -A\,G'
\end{bmatrix}
$$

$$
L \ = \ \begin{bmatrix}
0 & 0 & 0 & 0 & 0 \\
0 & 0 & 0 & 0 & -A\,G' \\
0 & 0 & 0 & \dfrac{C_1\,E}{2\,(1+\nu)} - C_2\,G' & 0 \\
0 & 0 & -\dfrac{C_1\,E}{2\,(1+\nu)} + C_2\,G' & 0 & 0 \\
0 & A\,G' & 0 & 0 & 0
\end{bmatrix}
$$

$$
\mathsf{P} = \begin{bmatrix} 0 & 0 & 0 & 0 & 0 \\ 0 & A\,G' & 0 & 0 & 0 \\ 0 & 0 & \dfrac{C_1\,E}{2\,(1+\nu)} + C_2\,G' & 0 & 0 \\ 0 & 0 & 0 & 0 & 0 \\ 0 & 0 & 0 & 0 & 0 \end{bmatrix}
\qquad
\mathsf{c} = \left\{ \begin{array}{c} \Theta_{22}^{(0,0)} \\ \Theta_{22}^{(0,1)} \\ 0 \\ 0 \\ 0 \end{array} \right\}
$$

$$
\mathsf{R} = \begin{bmatrix} \dfrac{A\,E}{1-\nu^2} & 0 & 0 & 0 & 0 \\ 0 & \dfrac{C_1\,E}{1-\nu^2} & 0 & 0 & 0 \\ 0 & 0 & \dfrac{D\,E}{1-\nu^2} & 0 & 0 \\ 0 & 0 & 0 & \dfrac{C_1\,E}{2\,(1+\nu)} + C_2\,G' & 0 \\ 0 & 0 & 0 & 0 & A\,G' \end{bmatrix}
$$

$$
\mathsf{S} = \begin{bmatrix} 0 & 0 & 0 & 0 & 0 \\ 0 & 0 & 0 & 0 & 0 \\ 0 & 0 & 0 & 0 & 0 \\ 0 & 0 & \dfrac{C_1\,E}{2\,(1+\nu)} - C_2\,G' & 0 & 0 \\ 0 & -A\,G' & 0 & 0 & 0 \end{bmatrix}
$$

$$
\mathsf{A} = \begin{bmatrix} 0 & 0 & 0 & 0 & 0 \\ 0 & 0 & 0 & 0 & 0 \\ 0 & 0 & 0 & 0 & 0 \\ 0 & 0 & 0 & -\left(\tfrac{1}{8}+a^2\right) b_n{}^4\,\pi\,\rho_\infty & -a\,b_n{}^3\,\pi\,\rho_\infty \\ 0 & 0 & 0 & -a\,b_n{}^3\,\pi\,\rho_\infty & -b_n{}^2\,\pi\,\rho_\infty \end{bmatrix}
$$

$$
\mathsf{B} = \begin{bmatrix} 0 & 0 & 0 & 0 & 0 \\ 0 & 0 & 0 & 0 & 0 \\ 0 & 0 & 0 & 0 & 0 \\ 0 & 0 & 0 & -\tfrac{1}{2}\,(1-2\,a)\,b_n{}^3\,\pi\,\rho_\infty\,U_n & 0 \\ 0 & 0 & 0 & b_n{}^2\,\pi\,\rho_\infty\,U_n & 0 \end{bmatrix}
\qquad
\mathsf{C} = \begin{bmatrix} 0 & 0 & 0 & 0 & 0 \\ 0 & 0 & 0 & 0 & 0 \\ 0 & 0 & 0 & 0 & 0 \\ 0 & 0 & 0 & -\tfrac{1}{2}\,b_n{}^3\,\pi\,\rho_\infty\,U_n{}^2\,\tan\Lambda & 0 \\ 0 & 0 & 0 & 0 & 0 \end{bmatrix}
$$

$$
D \;=\; \begin{bmatrix} 0 & 0 & 0 & 0 & 0 \\ 0 & 0 & 0 & 0 & 0 \\ 0 & 0 & 0 & 0 & 0 \\ 0 & 0 & 0 & -\left(\tfrac{1}{8}+a^2\right) b_n{}^4 \pi \rho_\infty U_n \tan\Lambda & -a\, b_n{}^3 \pi \rho_\infty U_n \tan\Lambda \\ 0 & 0 & 0 & -a\, b_n{}^3 \pi \rho_\infty U_n \tan\Lambda & -b_n{}^2 \pi \rho_\infty U_n \tan\Lambda \end{bmatrix}
$$

$$
E \;=\; \begin{bmatrix} 0 & 0 & 0 & 0 & 0 \\ 0 & 0 & 0 & 0 & 0 \\ 0 & 0 & 0 & 0 & 0 \\ 0 & 0 & 0 & 2\left(\tfrac{1}{4}-a^2\right) b_n{}^3 \pi \rho_\infty U_n & -\left(1+2\,a\right) b_n{}^2 \pi \rho_\infty U_n \\ 0 & 0 & 0 & \left(1-2\,a\right) b_n{}^2 \pi \rho_\infty U_n & -2\, b_n \pi \rho_\infty U_n \end{bmatrix}
$$

$$
F \;=\; \begin{bmatrix} 0 & 0 & 0 & 0 & 0 \\ 0 & 0 & 0 & 0 & 0 \\ 0 & 0 & 0 & 0 & 0 \\ 0 & 0 & 0 & \left(1+2\,a\right) b_n{}^2 \pi \rho_\infty U_n{}^2 & 0 \\ 0 & 0 & 0 & 2\, b_n \pi \rho_\infty U_n{}^2 & 0 \end{bmatrix}
$$

$$
G \;=\; \begin{bmatrix} 0 & 0 & 0 & 0 & 0 \\ 0 & 0 & 0 & 0 & 0 \\ 0 & 0 & 0 & 0 & 0 \\ 0 & 0 & 0 & 2\left(\tfrac{1}{4}-a^2\right) b_n{}^3 \pi \rho_\infty U_n{}^2 \tan\Lambda & -\left(1+2\,a\right) b_n{}^2 \pi \rho_\infty U_n{}^2 \tan\Lambda \\ 0 & 0 & 0 & \left(1-2\,a\right) b_n{}^2 \pi \rho_\infty U_n{}^2 \tan\Lambda & -2\, b_n \pi \rho_\infty U_n{}^2 \tan\Lambda \end{bmatrix}
$$

Bibliography

[1] ABAQUS. *ABAQUS/Standard Theory Manual*. Hibbitt, Karlsson & Sorensen Inc., 5.6 edition, 1996.

[2] ABAQUS. *ABAQUS/Standard User's Manual*. Hibbitt, Karlsson & Sorensen Inc., 5.6 edition, 1996.

[3] A. Agneni, L. Balis-Crema, and S. Sgubini. Complex stiffness identification for shunted piezo-electric absorbers. In *IAF - 50th International Astronautical Congress*, 1999.

[4] A. Agneni and G. Coppotelli. Technical note: Modal parameter prediction for structure with resistive loaded piezoelectric devices. *Experimental Mechanics*, 44:97–100, February 2004.

[5] A. Agneni, G. Coppotelli, F. Mastroddi, and S. Sgubini. Damping aeroelastic vibrations by shunted piezoelectric devices. In *International Forum on Aeroelasticity and Structural Dynamics*, 2001.

[6] A. Agneni, M. Del Sorbo, F. Mastroddi, and G. M. Polli. Multimodal damping by shunted piezo-paches: Possible aeroelastic applications. *submitted to International Journal of Applied Electromagnetics and Mechanics*, 2003.

[7] A. Agneni, F. Mastroddi, and G. M. Polli. Shunted piezoelectric patches in elastic and aeroelastic vibrations. *Computers & Structures*, 81:91–105, 2003.

[8] A. Agneni and A. Paolozzi. On the use of finite element codes for structures with passive piezoceramic devices. In *SPIE'S Smart Materials and MEMS*, 2000.

[9] A. Agneni and S. Sgubini. Piezoceramic devices as viscoelastic systems. In *XV Congresso Nazionale A.I.D.A.A.*, 1999.

[10] A. Agneni and S. Sgubini. Multimodal damping by piezoceramic devices with passive loads. In *XVI Congresso Nazionale A.I.D.A.A.*, 2001.

[11] J. D. Anderson. *Fundamentals of Aerodynamics*. McGraw Hill, 1984.

[12] U. Andreaus, N. Rizzi, and G. Ruta. *Appunti di Scienza delle Costruzioni*. ESAGRAFICA, 1st edition, 1997.

[13] I. Arias and J. D. Achenbach. Thermoelastic generation of ultrasound by line-focused laser irradiation. *International Journal of Solids and Structures*, 40:6917–6935, 2003.

[14] S. I. Baskakov. *Signals and Circuits*. MIR, 1986.

[15] R. C. Batra. Engineering and designing smart structures. Lecture notes, Virginia Tech, December 2001.

[16] R. L. Bisplinghoff, H. Ashley, and R. L. Halfman. *Aeroelasticity*. Dover, 1996.

[17] B. A. Boley and J. H. Weiner. *Theory of Thermal Stresses*. John Wiley and Sons, 1960.

[18] D. R. Browning and W. D. Wynn. Multiple-mode piezoelectric passive damping experiments for an elastic plate. In *SPIE 11th International Modal Analysis Conference*, volume 1923, pages 1520–1526, 1993.

[19] F. W. Byron and R. W. Fuller. *Mathematics of Classical and Quantum Physics*. Dover, 2d edition, 1992.

[20] D. E. Carlson. Linear thermoelasticity. In C. Truesdell, editor, *Encyclopedia of Physics*, volume VIa/2, pages 297–345, Berlin, 1972. Springer-Verlag.

[21] D. E. Carlson, E. Fried, and D. A. Tortorelli. Geometrically-based consequences of internal constraints. *Journal of Elasticity*, 70:101–109, 2003.

[22] H. S. Carslaw and J. C. Jaeger. *Conduction of Heat in Solids*. Oxford University press, 1959.

[23] K. Chau Le. *Vibrations of Shells and Rods*. Springer-Verlag, 1999.

[24] P. G. Ciarlet and V. Lods. Asymptotic analysis of linearly elastic shells. I. justification of membrane shell equations. *Archive for Rational Mechanics and Analysis*, 136(2):119–161, 1996.

[25] P. G. Ciarlet and V. Lods. Asymptotic analysis of linearly elastic shells. III. justification of Koiter's shell equations. *Archive for Rational Mechanics and Analysis*, 136(2):191–200, 1996.

[26] P. G. Ciarlet, V. Lods, and B. Miara. Asymptotic analysis of linearly elastic shells. II. justification of flexural shell equations. *Archive for Rational Mechanics and Analysis*, 136(2):163–190, 1996.

[27] E. Cosserat and F. Cosserat. *Theory of deformable bodies*. Number 11561 in NASA-TT-F. NASA Center for Aerospace Information (CASI), 1968. Translated from French "Theorie des corps deformable" (1909).

[28] F. Daví. The theory of Kirchhoff rods as an exact consequence of three-dimensional elasticity. *Journal of Elasticity*, 29:243–262, 1992.

[29] F. Daví. Dynamics of linear anisotropic rods. *International Journal of Solids and Structures*, 33(7):917–929, 1996.

[30] F. Daví. Dynamics of linear piezoelectric rods. *Journal of Elasticity*, 46:181–198, 1997.

[31] F. dell'Isola, M. Porfiri, and S. Vidoli. Piezo-electro-mechanical (PEM) structures: passive vibration control using distributed piezoelectric transducers. *Comptes Rendus Mecanique*, 331(1):69–76, 2003.

[32] J. P. den Hartog. *Mechanical Vibrations*. Dover, 2 edition, 1985.

[33] A. Di Carlo, P. Podio-Guidugli, and W. O. Williams. Shells with thickness distension. *International Journal of Solids and Structures*, 38(6-7):1201–1225, 2001.

[34] P. Duhem. Le potentiel thermodynamic et la pression hydrostatique. *Ann. Ecole Normale*, 10(3):187–230, 1893.

[35] M. Epstein and M. De León. On uniformity of shells. *International Journal of Solids and Structures*, 35(17):2173–2182, 1998.

[36] M. Epstein and Y. Tene. A linear theory of thin elastic shells, based on conservation of a non-normal straight line. *International Journal of Solids and Structures*, 9(2):257–268, 1973.

[37] W. Flugge. *Tensor Analysis and Continuum Mechanics*. Springer-Verlag, 1972.

[38] A. M. Garber. Pyrolytic materials for thermal protection systems. *Aerospace Engineering*, pages 126–137, January 1963.

[39] P. Gaudenzi. Exact higher order solutions for a simple adaptive structures. *International Journal of Solids and Structures*, 35(26-27):3595–3610, 1998.

[40] P. Gaudenzi and K.-J. Bathe. An iterative finite element procedure for the analysis of piezoelectric continua. *Journal of Intelligent Material Systems and Structures*, 6:266–273, 1995.

[41] GE Advanced Ceramics. Pyrolytic graphite brochure, 2004.

[42] M. Gennaretti and P. Lisandrin. Flap-lag rotor dynamics and aeroelastic stability using finite-state aerodynamics. In *24th European Rotorcraft Forum*, Marseilles, France, 1998.

[43] P. Germain. The method of virtual power in continuum mechanics. part 2: Microstructure. *SIAM Journal of Applied Mathematics*, 25(3):556–575, November 1973.

[44] F. H. Gern and L. Librescu. Effects of externally mounted stores on aeroelasticity of advanced swept cantilevered aircraft wings. *Aerospace Science and Technology*, 5:321–333, 1998.

[45] F. H. Gern and L. Librescu. Static and dynamic aeroelasticty of advanced aircraft wings carrying external stores. *AIAA Journal*, 36(7):1121–1129, 1998.

[46] F. H. Gern and L. Librescu. Aeroelastic tailoring of advanced aircraft wings carrying external stores. *Quaderni dell'Accademia delle Scienze di Torino*, 9:201–219, 1999.

[47] F. H. Gern and L. Librescu. Aeroelastic tailoring of composite aircraft wings exhibiting non-classical effects and carrying external stores. *Journal of Aircraft*, 37(6):1097–1104, 2000.

[48] M. Goland. The flutter of a uniform cantilever wing. *Journal of Applied Mechanics*, 12(4):A197–A208, 1945.

[49] M. Goland and Y. L. Luke. The flutter of a uniform wing with tip weights. *Journal of Applied Mechanics*, 15(1):13–20, 1948.

[50] A. E. Green and P. M. Naghdi. On electromagnetic effects in the theory of shells and plates. *Phil. Trans. R. Soc. Lond. A*, 309(1510):559–610, November 1983.

[51] A. E. Green and P. M. Naghdi. A unified procedure for construction of theories of deformable media. II. generalized continua. *Proceedings: Mathematical and Physical Sciences*, 448(1934):357–377, March 1995.

[52] A. E. Green, P. M. Naghdi, and M. L. Wenner. On the theory of rods. II. developments by direct approach. *Phil. Trans. R. Soc. Lond. A*, 337(1611):485–507, April 1974.

[53] A.E. Green and W. Zerna. *Theoretical Elasticity*. Oxford University Press, 2d edition, 1968.

[54] M.E. Gurtin and P. Podio-Guidugli. The thermodynamics of constrained materials. *Archives of Rational Mechanics and Analysis*, 51:192–208, 1973.

[55] N.W. Hagood and A. von Flotow. Damping of structural vibrations with piezoelectric materials and passive electrical networks. *Journal of Sound and Vibrations*, 146:243–268, 1991.

[56] D.N. Herting. *MSC.NASTRAN - Advanced Dynamics Analysis User's Guide*. The MacNeal-Schwendler Corporation, 70 edition, 1997.

[57] J. J. Hollkamp. Multimodal passive vibration suppression with piezoelectric materials and resonant shunts. *Journal of Intelligent Material Systems and Structures*, 5:49–57, January 1994.

[58] G. Karpouzian and L. Librescu. Comprehensive model of anisotropic composite aircraft wings suitable for aeroelastic analyses. *Journal of Aircraft*, 31(3):703–712, 1994.

[59] G. Karpouzian and L. Librescu. Exact flutter solution of advanced composite swept wings in various flight speed regimes. In *36th AIAA/ASME/ASCE/AHS/ASC Structures, Structural Dynamics and Material Conference*, 1995. AIAA-95-1382.

[60] G. Karpouzian and L. Librescu. Nonclassical effects on divergence and flutter of anisotropic swept aircraft wings. *AIAA Journal*, 34(4):768–794, 1996.

[61] H. K. Khalil. *Nonlinear Systems*. Prentice Hall, 2nd edition, 1996.

[62] W. B. Kratzig and D. Jun. On 'best' shell models - from classical shells, degenerated and multi-layered concepts to 3d. *Archive of Applied Mechanics*, 73(1-2):1–25, 2003.

[63] P.-S. Lee and K.-J. Bathe. Insight into finite shell discretizations by use of the "Basic Shell Mathematical Model". *Computers & Structures*, 83:69–90, 2005.

[64] J.W. Leech, E.A. Witmer, and L. Morino. Dynamically-induced large deformations of multi-layer, variable thickness shells. *AIAA Journal*, 11(8):1189–1191, August 1973.

[65] M. Lembo and P. Podio-Guidugli. Plate theory as an exact consequence of three-dimensional linear elasticity. *European Journal of Mechanics, A/Solids*, 10(5):485–516, 1991.

[66] L. Librescu and A. A. Khdeir. Aeroelastic divergence of swept-forward composite wings including warping restraint effect. *AIAA Journal*, 26(11):1373–1377, 1988.

[67] I. Lottati. Flutter and divergence aeroelastic characteristics for composite forward swept cantilevered wing. *AIAA Journal*, 22(11):1001–1007, 1985.

[68] A. E. H. Love. *A Treatise on the Mathematical Theory of Elasticity*. Dover, 4-th edition, 1944.

[69] J. E. Marsden and T. J. R. Hughes. *Mathematical Foundations of Elasticity*. Prentice-Hall, 1983.

[70] P. Marzocca, L. Librescu, and W. A. Silva. Aeroelastic response and flutter of swept aircraft wings. *AIAA Journal*, 40(5):801–812, 2002.

[71] F. Mastroddi and M. Gennaretti. An investigation about finite-state models for aeroelastic analysis of fixed wings. In *International Forum on Aeroelasticity and Structural Dynamics*, 2001.

[72] A.M. Rivas McGowan. An examination of applying shunted piezoelectrics to reduce aeroelastic response. In *CEAS/AIAA/ICASE/NASA Langley International Forum on Aeroelasticity and Structural Dynamics*, pages 553–571, 1999.

[73] R. D. Mindlin. High frequency vibrations of piezoelectric crystal plates. *International Journal of Solids and Structures*, 8(7):895–906, 1972.

[74] R. D. Mindlin. Equations of high frequency vibrations of thermopiezoelectric crystal plates. *International Journal of Solids and Structures*, 10(6):625–637, 1974.

[75] L. Morino, J.W. Leech, and E.A. Witmer. An improved numerical calculation technique for large elastic-plastic transient deformations of thin shells, part 1 – background and theoretical formulation. *Journal of Applied Mechanics*, 38(2):423–428, June 1971.

[76] L. Morino, J.W. Leech, and E.A. Witmer. An improved numerical calculation technique for large elastic-plastic transient deformations of thin shells, part 2 – evaluations and applications. *Journal of Applied Mechanics*, 38(2):429–436, June 1971.

[77] L. Morino and F. Mastroddi. *Introduction to Theoretical Aeroelasticity for Aircraft Designers*. In Preparation, 2003.

[78] L. Morino, F. Mastroddi, R. De Troia, G.L. Ghiringhelli, and P. Mantegazza. Matrix fraction approach for finite-state aerodynamic modeling. *AIAA Journal*, 33(4):703–711, April 1995.

[79] P. M. Naghdi. The theory of shells and plates. In C. Truesdell, editor, *Encyclopedia of Physics*, volume VIa/2, pages 425–640, Berlin, 1972. Springer-Verlag.

[80] P. M. Naghdi. Finite deformations of elastic rods and shells. In D. E. Carlson and R. T. Shield, editors, *Proceedings of the IUTAM Symposium on Finite Elasticity*, pages 47–103, Lehigh University, 1980. Martinus Nijhoff.

[81] P. M. Naghdi and A. R. Srinivasa. A dynamical theory of structured solids. i. basic developments. *Philosophical Transactions: Physical Sciences and Engineering*, 345(1677):425–458, December 1993.

[82] P. M. Naghdi and A. R. Srinivasa. A dynamical theory of structured solids. II. special constitutive equations and special cases of the theory. *Philosophical Transactions: Physical Sciences and Engineering*, 345(1677):459–476, December 1993.

[83] V. Nicotra and P. Podio-Guidugli. Piezoelectric plates with changing thickness. *Journal of Structural Control*, 5(2):73–86, December 1998.

[84] E. J. Nolan and S. M. Scala. Aerothermodynamic behavior of pyrolytic graphite during sustained hypersonic flight. *ARS Journal*, 32(1):26–35, January 1962.

[85] A. K. Noor. Structures technology for future aerospace systems. In P. Zarchan, editor, *Progress in Astronautics and Aeronautics*, volume 188. American Institute of Aeronautics and Astronautics, 2000.

[86] A. D. Pierce. *Acoustics : an introduction to its physical principles and applications*. McGraw-Hill, 1981.

[87] P. Podio-Guidugli. A primer in elasticity. *Journal of Elasticity*, 58:1–104, 2000.

[88] P. Podio-Guidugli and G. Tomassetti. Thickness waves in electroelastic plates. *Wave Motion*, 34:175–191, 2001.

[89] P. Podio-Guidugli and M. Vianello. The representation problem of constrained linear elasticity. *Journal of Elasticity*, 28:271–276, 1992.

[90] G. M. Polli, L. Morino, and F. Mastroddi. Shells with thickness distension and bent fiber: a modified Kirchhoff-Love and Reissner-Mindlin model. Technical notes, University of Rome "*La Sapienza*", 2003.

[91] M. Rahmoune, A. Benjeddou, R. Ohayon, and D. Osmont. New thin piezoelectric plate models. *Journal of Intelligent Material Systems and Structures*, 9(12):1017–1029, 1998.

[92] S. Roccella and P. Gaudenzi. On the formulation of a piezoelectric plate model. *Journal of Intelligent Material Systems and Structures*, 16(4):285–290, 2005.

[93] W.P. Rodden and E.H. Johnson. *MSC.NASTRAN - Aeroelastic Analysis User's Guide*. The MacNeal-Schwendler Corporation, 68 edition, 1994.

[94] M. B. Rubin. *Cosserat Theories: Shells, Rods and Points*. Kluwer Academic Publisher, 2000.

[95] G.C. Ruta. On inner constraint in plane circular arches. *Archive of Applied Mechanics*, 74(3-4):212–222, 2004.

[96] J. G. Simmonds. Some comments on the status of shell theory at the end of the 20th century: Complaints and correctives. *AIAA Paper*, 1074:1912–1921, 1997.

[97] J. C. Simo and D. D. Fox. On stress resultant geometrically exact shell model. Part I: formulation and optimal parametrization. *Comput. Methods Appl. Mech. Eng.*, 72(3):267–304, 1989.

[98] J. C. Simo, D. D. Fox, and M. S. Rifai. On a stress resultant geometrically exact shell model. Part II: the linear theory; computational aspects. *Comput. Methods Appl. Mech. Eng.*, 73(1):53–92, 1989.

[99] J. C. Simo, D. D. Fox, and M. S. Rifai. Formulation and computational aspects of a stress resultant geometrically exact shell model. In *Computational mechanics of nonlinear response of shells*, pages 31–55. Springer-Verlag, 1990.

[100] J. C. Simo, D. D. Fox, and M. S. Rifai. On a stress resultant geometrically exact shell model. Part III: computational aspects of the nonlinear theory. *Comput. Methods Appl. Mech. Eng.*, 79(1):21–70, 1990.

[101] J. C. Simo, M. S. Rifai, and D. D. Fox. On a stress resultant geometrically exact shell model. Part IV: variable thickness shells with through-the-thickness stretching. *Comput. Methods Appl. Mech. Eng.*, 81(1):91–126, 1990.

[102] J.C. Simo and L. Vu-Quoc. A geometrically-exact rod model incorporating shear and torsion-warping deformation. *International Journal of Solids and Structures*, 27(3):371–393, 1991.

[103] A. V. Srinivasan. Smart biological systems as models for engineered structures. *Materials Science and Engineering C*, 4:19–26, 1996.

[104] S. Thangjitham and L. Librescu. Analytical studies on static aeroelastic behavior of forward-swept composite wing structures. *Journal of Aircraft*, 28(2):151–157, 1991.

[105] T. Theodorsen. General theory of aerodynamic instability and the mechanism of flutter. Technical report, NACA Report 496, 1935.

[106] S. P. Timoshenko and S. Woinosky-Kreiger. *Theory of Plates and Shells*. McGraw-Hill, 2nd edition, 1970.

[107] R. A. Toupin. Stress tensor in elastic dielectrics. *Journal of Rational Mechanics and Analysis*, pages 440–452, 1960.

[108] R. A. Toupin. Theory of elasticity with couple-stress. *Archives of Rational Mechanics and Analysis*, 17:85–112, 1964.

[109] M.A. Trindade and A. Benjeddou. Modeling of frequency-dependent viscoelastic materials for active-passive vibration damping. *Transactions of ASME*, 2000.

[110] M.A. Trindade, A. Benjeddou, and R. Ohayon. Finite element analysis of frequency- and temperature-dependent hybrid active-passive vibration damping. *European Journal of Finite Elements*, 9, 1999.

[111] M.A. Trindade, A. Benjeddou, and R. Ohayon. Finite element analysis of of hybrid active-passive vibration damping: a unified approach. *ICAST 99*, 1999.

[112] C. A. Truesdell and W. Noll. The non-linear field theories of mechanics. In C. A. Truesdell, editor, *Encyclopedia of Physics*, volume III/3, Berlin, 1965. Springer-Verlag.

[113] S. Vidoli and R. C. Batra. Derivation of plate and rod equations for a piezoelectric body from a mixed three-dimensional variational principle. *Journal of Elasticity*, 59:23–50, 2000.

[114] S. Vidoli and F. dell'Isola. Vibration control in plates by uniformly distributed pzt actuators interconnected via electric networks. *European Journal of Mechanics - A/Solids*, 20(3):435–456, 2001.

[115] K.W. Wang. Structural vibration suppression via parametric control actions – piezoelectric materials with real-time semi-active networks. In A. Guran and D. J. Inman, editors, *Wave Motion, Intelligent Structures and Nonlinear Mechanics*, pages 112–134. World Scientific Publishing Company, 1995.

[116] Z. G. Wei and R. C. Batra. Deformations of an axially loaded thermoviscoplastic bar due to laser heating. *Journal of Thermal Stresses*, 26:701–712, 2003.

[117] G. Wempner and D. Talaslidis. *Mechanics of Solids and Shells: Theories and Approximations*. CRC Press, 2003.

[118] S.-Y. Wu. Method for multiple mode piezoelectric shunting with single pzt transducer for vibration control. *Journal of Intelligent Material Systems and Structures*, 9:991–998, 1998.